STEVIOSIDE

TECHNOLOGY, APPLICATIONS AND HEALTH

Sirshendu De, Sourav Mondal
and Suvrajit Banerjee

WILEY Blackwell

Stevioside

Stevioside

Technology, Applications and Health

Sirshendu De, Sourav Mondal and Suvrajit Banerjee

Indian Institute of Technology (IIT) Kharagpur
Kharagpur, India

WILEY Blackwell

This edition first published 2013 © 2013 by John Wiley & Sons, Ltd.

Registered Office
John Wiley & Sons, Ltd., The Atrium, Southern Gate, Chichester, West Sussex, PO19 8SQ, UK

Editorial Offices
9600 Garsington Road, Oxford, OX4 2DQ, UK
The Atrium, Southern Gate, Chichester, West Sussex, PO19 8SQ, UK
111 River Street, Hoboken, NJ 07030-5774, USA

For details of our global editorial offices, for customer services and for information about how to apply for permission to reuse the copyright material in this book please see our website at www.wiley.com/wiley-blackwell.

Library of Congress Cataloging-in-Publication Data

De, Sirshendu.
Stevioside : technology, applications, and health / Sirshendu De, Sourav Mondal and Suvrajit Banerjee, IIT Kharagpur.
pages cm
Includes bibliographical references and index.
ISBN 978-1-118-35066-9 (cloth : alk. paper) 1. Stevioside. I. Mondal, Sourav. II. Banerjee, Suvrajit. III. Title.
TP425.D427 2013
664′.5–dc23
2013027961

A catalogue record for this book is available from the British Library.

Wiley also publishes its books in a variety of electronic formats. Some content that appears in print may not be available in electronic books.

Cover images: Stevia plant © iStockphoto.com/Olivier Le Moal; Sugar background © iStockphoto.com/fotek; Stevia © iStockphoto.com/MonaMakela
Cover design by Steve Thompson

Set in 10.5/12.5pt Times by SPi Publisher Services, Pondicherry, India

1 2013

Contents

Authors' biographies

Dr Sirshendu De is a professor in the Department of Chemical Engineering, at the Indian Institute of Technology (IIT) Kharagpur, India. He obtained his Bachelor of Technology (1990), Master of Technology (1992) and PhD (1997) degrees from the Indian Institute of Technology Kanpur. His major field of interest is membrane-based separation processes: design, modelling and fabrication of flat-sheet and hollow-fibre membranes. He has already authored six books, ten book chapters, five patents and more than 190 publications in national and international journals of repute. He has also transferred two technologies for commercialisation. His other fields of research are adsorption, transport phenomena, modelling of flow through microchannel, etc. He has been the recipient of several prestigious awards, including the Shanti Swarup Bhatnagar Award in 2011 for fundamental contribution and innovation in basic science and technology (Engineering Science category). He also received the Herdillia Award in 2010 for excellence in basic research in chemical engineering, the VNMM Award in 2009 for excellence in innovative applied research, the Young Engineer Award from the Indian National Academy of Engineering in 2001 for excellence in engineering research, and the Amar Dye Chem Award in 2000 for excellence in chemical engineering research. He is a fellow of the Indian National Academy of Engineering, New Delhi, and the Indian National Academy of Science, Allahabad, for his contribution to engineering and research.

Sourav Mondal received his undergraduate degree in chemical engineering from Jadavpur University in 2010 and a Master's degree in chemical engineering from the Indian Institute of Technology Kharagpur. Currently he is pursuing doctoral research in the Department of Chemical Engineering at the Indian Institute of Technology Kharagpur. He has co-authored one book, one book chapter and 18 publications in international journals of repute, and presented four papers in national and international conferences. He is also involved in a project for computer simulation of a magnesium reactor, development of a ceramic membrane module and molecular dynamics-based simulation of self-assembled structures in an aqueous environment.

Suvrajit Banerjee obtained his Bachelor of Technology in chemical engineering from West Bengal University of Technology, India, in 2010. He gained his Master of Technology in chemical engineering in 2012 from the Indian Institute of Technology Kharagpur, India, where he worked extensively in the field of membrane

separation processes. Suvrajit Banerjee is a novel separations enthusiast. Presently, he is a PhD student in chemical and biological engineering and graduate research assistant at the Center for Biotechnology and Interdisciplinary Studies at Rensselaer Polytechnic Institute, Troy, NY, USA. His present research focuses on the use of molecular dynamics simulations to gain insights into protein–ligand binding during chromatographic separation processes and the role of water molecules and mobile phase modifiers in these processes.

Preface

Stevioside is one of the naturally occurring sweeteners, belonging to the diterpene glycoside family, which can be widely applied in food as a dietary supplement, in soft drinks, medicine and daily chemicals. It is a good dietary supplement, non-calorific, thermally stable and non-toxic, with a sugar-like taste profile and suitable for diabetic and phenylketonuria patients and obese persons. It is also non-fermentable and exhibits anticarcinogenic, antioxidant, antihyperglycaemic, antihypertensive, antidiarrhoeal, anti-inflammatory and anticariogenic properties.

Stevioside tastes about 300 times sweeter than 0.4% sucrose solution. Thus, extraction and purification of stevioside is an area of active research. Stevioside has a greater presence in the extract of *Stevia rebaudiana* leaves compared to the other glycosides, namely rebaudioside A, B, D and E, dulcoside A and B. Current sweetener extraction techniques involve many unit operations, including solvent extraction (methanol and ethanol), ion exchange, etc. Solvent extraction may not be suitable for human consumption and ion exchange is not economic. In this regard, membrane-based processes can offer an attractive alternative. This book provides a detailed understanding of the design and modelling characteristics at various levels of processing using membranes.

With the rapid increase in popularity of stevioside as a sugar substitute and its associated health benefits, there is need for an efficient and feasible extraction process for stevioside in the near future. Since no other book exists on this topic, the proposed book covers the state of the art of stevioside extraction with an emphasis on membrane technology. Thus, it is envisaged that the significance of this book will be remarkably high in this context. Apart from extraction aspects, the book also presents an account of the history, medicinal values and other applications in some detail.

Composition, source, various physical and chemical properties and methods of analysis are covered in Chapter 1. Steviol glycosides have numerous health benefits. Various facets of this aspect are presented in Chapter 2. Applications of stevioside in different sectors, therapeutics, food, drink, etc., are discussed in Chapter 3. The conventional extraction process of stevioside includes a number of unit operations and the state of the art of these conventional extraction processes is presented in Chapter 4. The fundamentals of membrane-based processes, including advantages, features, classifications, modelling approaches, modules, limitations and applications, have been outlined in Chapter 5. Chapter 6 deals with the development of

applications of membrane-based operations for stevioside processing in different steps: clarification, purification, concentration, etc. A description of membrane processes for extraction of stevioside is presented in Chapter 7. In this chapter, optimisation of water extraction, comparison between centrifuge and microfiltration as the primary clarification, use of ultrafiltration for main clarification, optimised selection of membranes and operating conditions, identification of flux decline mechanism, various modes of ultrafiltration (unstirred, stirred and cross-flow) and concentration by nanofiltration are discussed in detail. Relevant modelling for scaling up of membrane-based systems is covered with full details in Chapter 8. Enhancement of stevioside purity by using diafiltration is discussed in Chapter 9 and the economics of the process is presented in Chapter 10.

We believe this book will have two fold impacts. First, its academic value is high, since it deals with extraction of an upcoming bioproduct using membrane-based processes. Second, it will have a substantial impact on the scaling up of such systems in actual industrial scale from laboratory data. This book can be used as a reference for courses involving membrane and food technology and food processing taught in postgraduate level. And of course, it would be an extremely useful reference book for students and professionals in the fields of chemical engineering, food technology, biotechnology, bioengineering, agricultural engineering, industrial engineering and pharmaceutical engineering.

We have tried our best to make this book comprehensive and hope that it will ignite further research interest and industrial development in the relevant and associated fields of engineering. We hope that readers will benefit from the applicability and significance of membrane-based technology for food processing in general presented through this book. Although we have put our best efforts into organising all possible information regarding processing of Stevia extract, readers' comments and suggestions for improvement will be gratefully acknowledged.

Sirshendu De
Sourav Mondal
Suvrajit Banerjee

Acknowledgements

We extend our gratitude to Mr Dhruba Sakha, Department of Chemical Engineering, Indian Institute of Technology Kharagpur, for his invaluable efforts in helping us to determine the concentration of steviol glycosides by high-performance liquid chromatography. We also express our thanks to Dr Chhaya for her co-operation in conducting the membrane separation experiments.

Finally, it is our pleasure to thank all those who made this book possible, and to acknowledge the good wishes, blessings and whole-hearted support of our near and dear ones, to whom we are really indebted.

List of figures

List of tables

1

Introduction to stevioside

In the past couple of decades, use of sweeteners as food additives has attracted considerable interest. The global market for high-potency sweeteners during 2010 was reported to be $1.146 billion (Leatherhead Food Research 2011). The market demand for stevioside in comparison to other sweeteners is presented in Figure 1.1. Among the sugar substitutes, artificial sweeteners saccharin and aspartame are quite popular because of their high sweetness potency (Mitchell 2006; Nabors 2011; Wilson 2007). However, the sweet herb *Stevia rebaudiana* Bertoni, belonging to the family Asteraceae within the tribe Eupatoricae (King and Robinson 1987), has sweet-tasting diterpenoid glycosides in its leaves (Bertoni 1905; Gosling 1901), which have high sweetness potency (Geuns 2003), with the added advantage that Stevia sweeteners are natural plant products (Kim and Dubois 1991). Stevia sweeteners are unique in having zero Glycaemic Index effect, zero carbohydrate and zero calories (O'Donnell and Kearsley 2012), compared to other conventional sweeteners. It is the world's only natural sweetener in this category. The sweet part of the Stevia herb is extracted and then blended with other all-natural ingredients to create a delicious and healthy sweetener.

Stevia rebaudiana is native to Paraguay and is widespread in its country of origin. The natural habitat of *Stevia rebaudiana* is subtropical grasslands (mesothermal-humid climatic zone) at altitudes of about 200–600 m above sea level, in the Amambay Cordillera, a mountain range of north-eastern Paraguay (Katayama et al. 1976). It usually grows in semi-dry mountainous terrain, and its habitat ranges from grasslands, scrub forests, forested mountain slopes and conifer forests to subalpine vegetation (Kinghorn 2001).

Stevia rebaudiana is a New World genus distributed from the South American Andes to the southern United States, through Argentina, the Brazilian highlands and Central Mexico (Grashoff 1972). It is a 30–60 cm tall herbaceous plant with perennial rhizomes, simple, opposite and narrowly elliptic to oblanceolate leaves,

Stevioside: Technology, Applications and Health, First Edition.
Sirshendu De, Sourav Mondal and Suvrajit Banerjee.

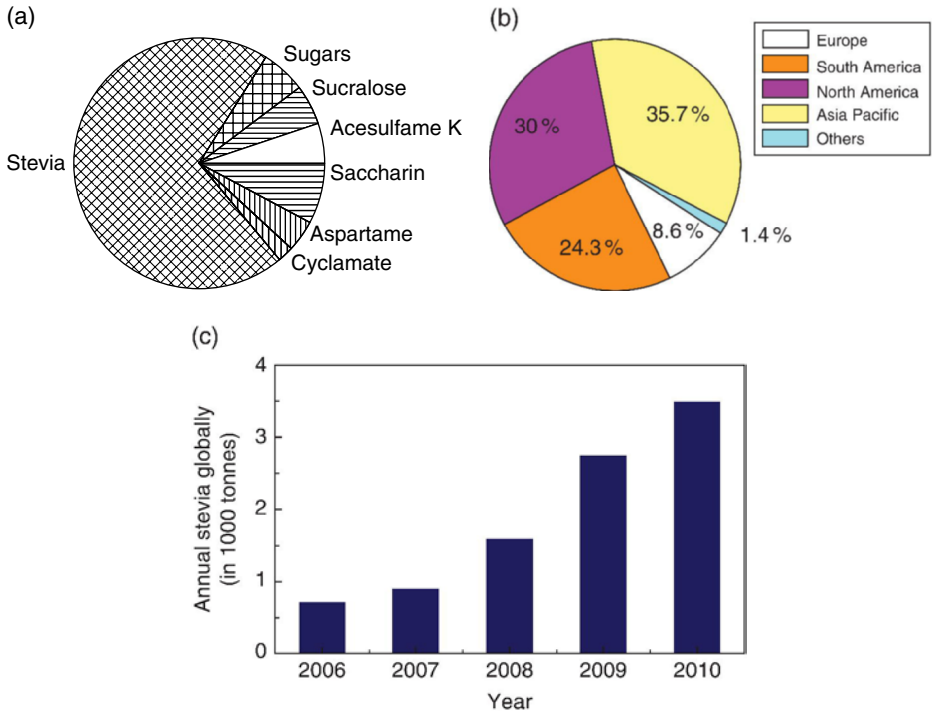

Figure 1.1 Market potential of Stevia and related products in the world. (a) Percentage compound annual growth rate (CAGR) of different sweeteners in the projected years 2011–15. (b) Global Stevia market in different regions of the world in 2010. (c) Annual global Stevia production in the last 5 years. For a colour version of this figure, see Plate 1.1.

trinerved venation, paniculate-corymbose inflorescences with white flowers, and achenes bearing numerous, equally long pappus awns (Robinson 1930). A picture of the plant is shown in Figure 1.2.

The following chemical description of steviol glycoside is taken from the original JECFA monograph (WHO 2000):

> 'Stevioside is a glycoside of the diterpene derivative steviol (ent-1 3-hydroxykaur-1 6-en-19-oic acid). Steviol glycosides are natural constituents of the plant *Stevia rebaudiana* Bertoni. The leaves of *S. rebaudiana* Bertoni contain eight different steviol glycosides, the major constituent being stevioside (triglucosylated steviol), constituting about 5–10% in dry leaves. Other main constituents are rebaudioside A (tetraglucosylated steviol), rebaudioside C, and dulcoside A. *S. rebaudiana* is native to South America and has been used to sweeten beverages and food for several centuries. The plant has also been distributed to South-east Asia. Stevioside has a sweetening potency 250–300 times that of sucrose and is stable to heat. In a 62-year-old sample from a

Figure 1.2 *Stevia rebaudiana* Bertoni plant. For a colour version of this figure, see Plate 1.2.

herbarium, the intense sweetness of *S. rebaudiana* was conserved, indicating the stability of stevioside to drying, preservation, and storage (Soejarto et al. 1982; Hanson and de Oliveira 1993).'

1.1 History of Stevia

Stevia rebaudiana Bertoni is one of 154 members of the genus *Stevia* and one of only two that produces sweet steviol glycosides (Robinson 1930; Soejarto et al. 1982, 1983). Stevia was first brought to the attention of Europeans in 1887 (Bertoni 1899) when M.S. Bertoni learned of its unique properties from the Paraguayan Indians and Mestizos (Lewis 1992). Various reports cited by Lewis (1992) indicate that it was long known to the Guarani Indians of the Paraguayan highlands who called it caá-êhê, meaning 'sweet herb'. Stevioside, the most abundant sweet constituent present in the leaves of *Stevia rebaudiana*, was first isolated in impure form

in the first decade of the 20th century (Bertoni 1905, 1918) but the final chemical structure was determined 60 years later by Mosettig et al. (1963). The second major sweet diterpene glycoside from *S. rebaudiana* was identified around 1970 (Kohda et al. 1976). Further, six less abundant sweet component glycosides were isolated from the species, namely rebaudioside B–E, dulcoside A and steviolbioside (Kobayashi et al. 1977; Tanaka 1982; Yamasaki et al. 1976).

The first reports of commercial cultivation in Paraguay were in 1964 (Katayama et al. 1976; Lewis 1992). A large effort aimed at establishing Stevia as a crop in Japan was begun by Sumida (1980). Since then, Stevia has been introduced as a crop in a number of countries including Brazil, Korea, Mexico, United States, Indonesia, Tanzania and, since 1990, Canada (Brandle and Rosa 1992; Donalisio et al. 1982; Fors 1995; Goenadi 1983; Lee et al. 1979; Saxena and Ming 1988; Schock 1982). Currently, Stevia production is centred in China and the major market is in Japan (Kinghorn and Soejarto 1985). Milestones of discovery and various uses of stevioside are presented in Table 1.1.

In 1999, the Joint Food and Agriculture Organisation (FAO)/World Health Organisation (WHO) Expert Committee on Food Additives (JECFA) and the EU Scientific Committee for Food reviewed stevioside and concluded that it was unacceptable for use as a sweetener, on the basis of the data available at that time. In 2004, the JECFA reviewed stevioside again and granted a temporary maximum usage level of 2 mg/kg body weight for steviol glycosides.

In June 2008, the JECFA concluded that steviol glycosides are safe for use in foods and beverages and established an acceptable daily intake (ADI) of 4 mg/kg body weight (FAO 2008; FAO/WHO 2009). The JECFA established specifications for the identity and purity of steviol glycosides, requesting a minimum content of 95% of the sum of the seven steviol glycosides, which are stevioside, rebaudioside A, rebaudioside C, dulcoside A, rubusoside, steviolbioside and rebaudioside B (WHO 2008; 2009).

Food Standards Australia New Zealand (FSANZ) completed its evaluation of the use of steviol glycosides in foods in 2008 and recommended that the Australia and New Zealand Food Regulation Ministerial Council allow the use of steviol glycosides in food (FSANZ 2008). In 2008, Switzerland approved the use of Stevia as a sweetener, citing the favourable actions of the JECFA. Subsequently, France published its approval for the food uses of rebaudioside A with a purity of 97% (AFSSA 2009). In December 2008, the US Food and Drug Administration (FDA) stated it had no objection to the conclusion of expert panels that Stevia containing a minimum of 95% rebaudioside A is generally recognised as safe (GRAS) for use as a general-purpose sweetener in foods and beverages.

In September 2009, based on a review of the international regulation of *Stevia rebaudiana* and the clinical evidence for safety and efficacy, the Natural Health Products Directorate, Health Canada recommended an acceptable daily intake of 4 mg steviol/kg body weight established by WHO (2008), for consumption of *Stevia* and steviol glycosides in natural health products (NHPs). In Japan, China,

Table 1.1 Major historical developments in the discovery and use of stevioside as a sweetener and dietary supplement

Chronological sequence of events	Reference
Report of sweetness of *S. Rebaudiana* leaves from Paraguay published in a major scientific paper	Gosling 1901
First chemical report on the sweet constituents of Stevia	Bertoni 1905
Realisation that stevioside is a form of glycoside	Dieterich 1908
Production of steviolbioside from stevioside	Wood et al. 1955
Evidence that stevioside is a sophoroside	Vis and Fletcher 1956
Final structures of steviol and isosteviol confirmed	Mosetigg et al. 1963
Steviol chemically synthesised	Cook and Knox, 1970; Mori and Matsui 1970
S. rebaudiana from Brazil cultivated experimentally in Japan	Sumida 1973
Isolation and characterisation of rebaudioside A	Kohda et al. 1976
Minor *S. rebaudiana* leaf diterpene glycosides obtained	Yamasaki et al. 1976; Kobayashi et al. 1977
Advent of extensive use of *S. rebaudiana* extracts for sweetening and flavouring of foods and beverages in Japan	Abe and Sonobe 1977; Akashi 1977
From 1982 onwards, large-scale cultivation of *S. rebaudiana* in mainland China and nearby islands	Kinghorn and Soejarto 1991
Demonstration of mutagenic activity of metabolically activated steviol in a forward mutation test	Pezzuto et al. 1985
First approval of *S. rebaudiana* products in Brazil	Schwontkowski 1995
During the 1980s, *S. rebaudiana* leaves become a popular herbal tea in the USA	Blumenthal 1995
First approval of stevioside in South Korea	Korea National Institute of Health 1996
Import ban on *S. rebaudiana* into USA by FDA (1991)	Blumenthal 1995
FDA import ban on *S. rebaudiana* leaves rescinded in 1995	Blumenthal 1995
Long-term toxicity test, showing lack of any carcinogenic effects by stevioside, conducted in rats of both sexes in Japan	Toyoda et al. 1997
In USA, rebaudioside A and stevioside are considered as generally recognised as safe (GRAS) products	Curry 2010
Steviol glycosides are permitted as food additive by European Union in December 2011	Stones 2011

Korea, Brazil, Paraguay and several other countries worldwide, steviol glycosides are considered natural food constituents and, as such, are implicitly accepted for food use.

In Europe, steviol glycosides have recently been approved for use as a sweetener. The European Food Safety Authority (EFSA) has conducted a general safety assessment for the approval of steviol glycosides as a sweetener in foodstuffs and for use as a flavour enhancer. A positive scientific opinion from the EFSA is a prerequisite to the European Commission proposing legislation for the

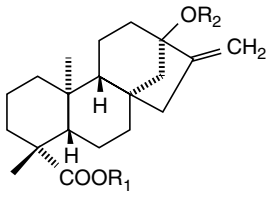

	R_1	R_2
Stevioside	Glc	Glc-Glc (2→1)
Rebaudioside A	Glc	Glc-Glc (2→1) | Glc (3→1)
Rebaudioside C (= Dulcoside B)	Glc	Glc-Rha (2→1) | Glc (3→1)
Rebaudioside D	Glc-Glc (2→1)	Glc-Glc (2→1) | Glc (3→1)
Rebaudioside E	Glc-Glc (2→1)	Glc-Glc (2→1)
Dulcoside B	Glc	Glc-Rha (2→1)

Glc = β – *D* – glucopyransosyl; rha = α – *L* – rhamnopyranosyl

Figure 1.3 Structures of the sweet-tasting glycosides isolated from *S. rebaudiana*.

authorisation and marketing of this substance in the EU. In light of the JECFA's 2008 findings and in response to a June 2008 request by the European Commission regarding the safety of steviol glycosides as a sweetener for use in the food, the EFSA re-examined the safety of steviol glycosides (EFSA 2010). After careful consideration of the data on stability, degradation products, metabolism and toxicology, the EFSA panel established an acceptable daily intake for steviol glycosides, which is similar to the JECFA's determination.

1.2 Composition of Stevia

A number of natural products can be derived from the plant *Stevia rebaudiana*. However, the best known are the diterpenoid glycosides, comprising stevioside, rebaudioside A and C–E and dulcoside A. The structures of the sweet-tasting components are illustrated in Figure 1.3.

The yield of stevioside from the dried leaves of *S. rebaudiana* can vary from 5% to 20%, depending upon the cultivation (Kim and Dubois 1991). In addition to the

Table 1.2 List of all the chemical constituents of *S. rebaudiana* leaves (excluding oil)

Compound lass	Constituent	% (w/w) Yield	Reference
Diterpenoid	Dulcoside A	0.03	Kobayashi et al. 1977
ent-Kaurene	Rebaudioside A	1.43	Kohda et al. 1976
	Rebaudioside B	0.44	Kohda et al. 1976
	Rebaudioside C (= dulcoside B)	0.4	Sakamoto et al. 1977a
	Rebaudioside D	0.03	Sakamoto et al. 1977b
	Rebaudioside E	0.03	Sakamoto et al. 1977b
	Steviolbioside	0.04	Kohda et al. 1976
	Stevioside	2.18	Kohda et al. 1976
Labdane	Austroinulin	0.06	Sholichin et al. 1980
	6-*O*-Acetylaustroinulin	0.15	Sholichin et al. 1980
	Jhanol	0.006	Sholichin et al. 1980
	Sterebin A	0.001	Oshima et al. 1986
	Sterebin B	0.0009	Oshima et al. 1986
	Sterebin C	0.0003	Oshima et al. 1986
	Sterebin D	0.0004	Oshima et al. 1988
	Sterebin E	0.002	Oshima et al. 1988
	Sterebin F	0.003	Oshima et al. 1988
	Sterebin G	0.0002	Oshima et al. 1988
	Sterebin H	0.0002	Oshima et al. 1988
Flavonoid	Apigenin 4′-*O*-glucoside	0.01	Rajbhandari and Roberts 1983
	Kaempferol 3-*O*-rhamnoside	0.008	Rajbhandari and Roberts 1983
	Luteolin 7-*O*-glucoside	0.009	Rajbhandari and Roberts 1983
	5,7,3′-Trihydroxy 3,6,4′-trimethoxyflavone	0.01	Rajbhandari and Roberts 1983
Sterol	Stigmasterol	Trace	Nabeta et al. 1976
	Stigmasterol $\beta-D-$ glucoside	Trace	Matsuo et al. 1986
Triterpenoid	β- Amyrin acetate	Trace	Sholichin et al. 1980
	Lupeol	Trace	Sholichin et al. 1980
	Lupeol esters	Trace	Sholichin et al. 1980
Other organic components	Chlorophyll A	0.00041	Abou-Arab et al. 2010
	Chlorophyll A	0.00027	
	Carotenoids	0.00007	
	Total pigments	0.00075	
	Tannins	7.8	Rasenack 1908

diterpenoid glycosides, several other components such as flavonoids, labdane, oils, etc., are present in varied amounts. A complete list of the components (except the volatile oils) is presented in Table 1.2.

A number of labdane-type diterpenes can also be identified from *S. rebaudiana*, along with the glycosides (see Figure 1.4). Besides jhanol and asutroinulin

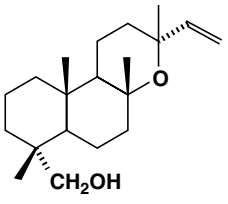

Jhanol

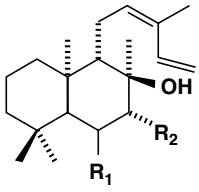

	R_1	R_2
Austroinulin	OH	OH
6-*O*-Acetyl-austroinulin	OAc	OH
7-*O*-Acetyl-austroinulin	OH	OAc

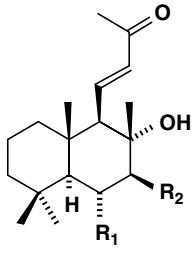

	R_1	R_2
Sterebin A	OH	OH
Sterebin B	OAc	OH
Sterebin C	OH	OAc
Sterebin D	H	OH

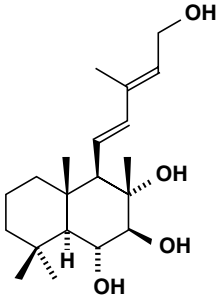

Sterebin E

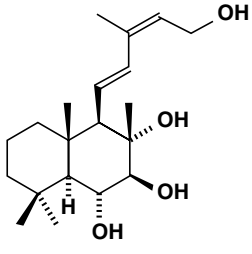

Sterebin F

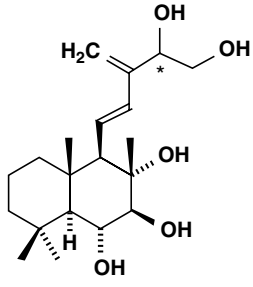

Sterebin G

Sterebin H

(*Sterebin G and H are C-14 epimers)

Figure 1.4 Structures of different labdane type glycosides isolated from *S. rebaudiana*.

which were isolated using methanol extraction (Sholichin et al. 1980), eight novel labdane type diterpenoids, sterebins A–H, have been identified using spectroscopic and nuclear magnetic resonance (NMR) techniques (Oshima et al. 1986, 1988).

The triterpenoids and sterols primarily constitute β-sitosterol (39.4%) and sigmasterol (45.8%) of the total sterol fraction (D'Agostino et al. 1984). A lupeol ester, lupeol 3-palmitate and β-amyrin acetate were obtained from methanolic extraction by gas chromatography-mas spectrometry (GC-MS) (Sholichin et al. 1980; Yasukawa et al. 1993), as shown in Figure 1.5.

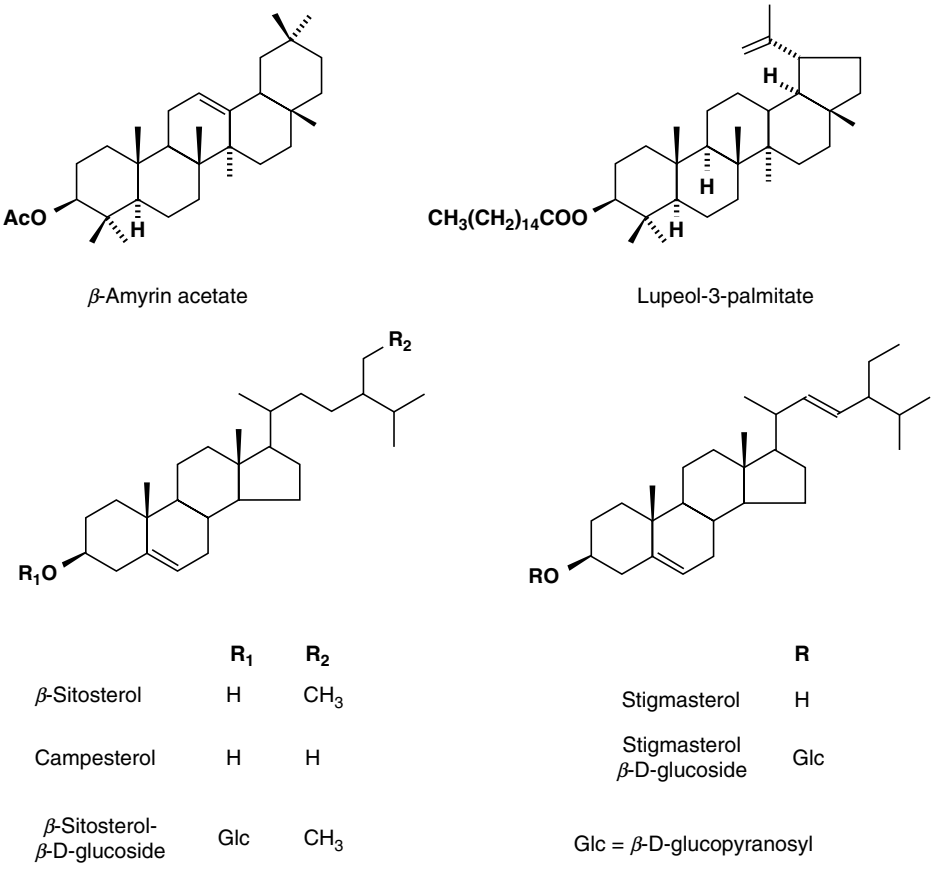

	R_1	R_2
β-Sitosterol	H	CH_3
Campesterol	H	H
β-Sitosterol-β-D-glucoside	Glc	CH_3

	R
Stigmasterol	H
Stigmasterol β-D-glucoside	Glc

Glc = β-D-glucopyranosyl

Figure 1.5 Structures of different triterpenoids and sterols from *S. rebaudiana*.

In the estimation of flavonoid constituents, six standard flavonoids were extracted in ethyl acetate fraction and two from chloroform as shown in Figure 1.6 (Rajbhandari and Roberts 1983). These compounds were determined using a combination of ultraviolet (UV) and proton nuclear magnetic resonance (^{1}H-NMR) spectroscopy, and mass spectroscopy.

The essential oil components include a number of alkanols, aldehydes, aromatic alcohols, monoterpenes and sesquiterpenes (Fujita et al. 1977; Martelli et al. 1985). Apart from this, other phytochemicals such as chlorophylls, β-carotene, organic acids, etc. are also present (Cheng and Chang 1983). Among the minerals, potassium is the major proportion, while other metals such as zinc, calcium, iron, etc. are also present in trace amounts.

The protein content represented by amino acids in Stevia leaves (Abou-Arab et al. 2010; Mohammad et al. 2007), water-soluble vitamins (Kim et al. 2011) and fatty acids (Tadhani and Subhash 2006) are reported in Table 1.3.

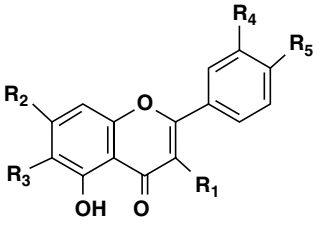

Compound	R_1	R_2	R_3	R_4	R_5
Apigenin 4′-*O*-glucoside	H	H	OH	H	Glc
Kaempferol 3-*O*-rhamnoside	Rha	H	OH	H	OH
Luteolin 7-*O*-glucoside	H	H	Glc	OH	OH
Quercetin 3-*O*-arabinoside	Ara	H	OH	OH	OH
Quercetin 3-*O*-glucoside	Glc	H	OH	OH	OH
Quercetin 3-*O*-rhamnoside	Rha	H	OH	OH	OH
Centaureidin	OMe	OMe	OH	OH	OMe
Apigenin 7-*O*-glucoside	H	H	Glc	H	OH
Quercetin 3-*O*-rutinoside	Rut	H	OH	OH	OH

Glc = O-β-D-glucopyranosyl; rha = O-α-L-rhamnopyranosyl;
ara = O-α-L-arabinopyranosyl; rut = 6-O-α-L-rhamnopyranosyl-D-glucopyranosyl

Figure 1.6 Flavonoids structures isolated from *S. rebaudiana*.

1.3 Source of stevioside

The sweet-tasting glycosides have been reported to be present in the leaves, flowers and stems but not in the roots of *S. rebaudiana* (Tanaka 1982).The primary source of stevioside and rebaudioside A is the leaves (5–20% w/w). They are also found in the flowers at lower concentrations, around 0.9–1% (w/w) (Darise et al. 1983). Because of the economic importance of steviol glycosides, synthetic methods of synthesis have also been attempted (Mori and Matsui 1965, 1966, 1970; Mori et al. 1970a,b; Nakahara 1982; Nakahara et al. 1971; Ziegler and Kloek 1971, 1977). Conversion of steviol glycosides to stevioside and rebaudioside A was also reported (Kaneda et al. 1977; Ogawa et al. 1978, 1980). However, extraction of glycosides using solvent (refer to Chapter 4) and membrane separation (Chapter 6–9) is feasible for large-scale production of stevioside as a dietary supplement and sweetener.

Table 1.3 Amino acid, vitamin and fatty acid contents of Stevia leaves

Amino acids			
Essential amino acids		Non-essential amino acids	
Amino acid	Amount % (w/w)	Amino acid	Amount % (w/w)
Arginin	0.45	Aspartate	0.37
Lysine	0.7	Serine	0.46
Histidine	1.13	Glutamic	0.43
Phenylalanine	0.77	Proline	0.17
Leucine	0.98	Glycine	0.25
Methionine	1.45	Alanine	0.56
Valine	0.64	Cystine	0.4
Therionine	1.13	Tyrosine	1.08
Isolucine	0.42		
Minerals		Fatty acids composition	
Element	Mineral content (mg/g)	Fatty acids	Amount (% w/w)
Potassium	0.211	Palmitic acid (C16)	0.2751
Calcium	0.177	Palmitoleic acid (C16-1)	0.0127
Sodium	0.149	Stearic acid (C18)	0.0118
Magnesium	0.032	Oleic acid (C18-1)	0.0436
Manganese	0.029	Linoleic acid (C18-2)	0.124
Iron	0.059	Linolenic acid (C18-3)	0.2159
Zinc	0.013		
Water-soluble vitamins			
Vitamin		Content (mg/g)	
Vitamin C		0.15	
Vitamin B2		0.0043	
Vitamin B6		0.0	
Folic acid		0.522	
Niacin		0.0	
Thiamin		0.0	

Steviol glycosides were first commercialised as a sweetener in 1971 by the Japanese firm Morita Kagaku Kogyo, a leading Stevia extract producer in Japan. It has been cultivated and manufactured by several companies in different parts of the globe. Some of the leading companies making stevioside products are mentioned in Table 1.4. Currently, China is the largest exporter of stevioside in the world.

Since the first commercialisation, the demand for Stevia for sweetening and flavouring purposes has increased enormously in Japan (Kinghorn et al. 2001). Cultivation of *S. rebaudiana* for the Japanese market mainly occurs in China, Taiwan, Thailand and some parts of Malaysia (Kinghorn and Soejarto 1991). Stevioside has also been consumed in Korea since 1995, with the majority of its use being in the sweetening of the beverage, soju (Kinghorn et al. 2001). Stevioside extract, containing

Table 1.4 World's leading stevioside manufacturing companies in different countries

China	Korea	Japan	India	Brazil
Shandong Shengwang Group Pharmaceutical Ganzhou Julong High-tech Industrial Co. GLG Life Tech Corp. Ministry of Ningbo Dekang Biochem Co. and more than 400 other companies	KOTRA Daepyung Ginseng Korea Macrocare Tech	Morita Kagaku Kogyo Co. Tokiwa Phytochemical Co. Tama Biochemical Co.	Golden Trees Bio Tech Pvt. Ltd. Biosweet Ventures GoGreen Pvt. Ltd.	Stevia Comercial Exportadora
Canada	Cameroon	Hong-Kong	Taiwan	South Africa
Ferlow Brothers	Che and Sons	Yurui (Shanghai) Chemical Co. Sunrise Health Co.	Kasmac Industries Co.	Globaltrade
Paraguay	Argentina	USA	Australia	Singapore
SteviaLand International Agrolife	QuFu Natural Green Project Co.	NuSci Institute Daimoku Power PharmBrand USA LLC Stevia	Lancer Biomed Pvt. Ltd. Herbin Biotech Inc.	Allspices (SG) pte Jal Innovation (s)
Germany	Belgium	Poland		
B&S Naturwelten UG Mangostan-Gold Eco-Nature	Plant and Warmth	PHZ Libra Trade Lukasz Kirzynski Agrol		

Table 1.5 Current status of usage of stevioside in different countries

Country	Status
Japan	Widely used as a sweetener since 1970
South Korea	Consumption as sweetener in beverages from 1990 (presently constitutes more than 50% of the sweetener market in Korea)
Australia and New Zealand	All steviol glycosides are approved for use as food additives from 2008
Brazil	Approved in 1986 for use as sweetener and food additive
Mexico	Mixed steviol glycoside extracts as food additives, not as individual products (2009)
Hong Kong	Steviol glycosides as food additives from 2010
Israel	Steviol glycosides as food additives in 2012
Paraguay	Currently available in liquid form, for use in herbal tea
Russian Federation	Allowed in minimal dosage limit as food additive (2008)
Norway	Steviol glycoside as food additive in 2012, but the plant itself is banned
Singapore	Steviol glycoside is a permitted sweetening agent in certain foods, since 2005
Canada	Available as dietary supplement
European Union (Europe)	Permitted use as food additive in 2011
United States	Stevia leaf and extracts available as dietary supplements in 1995. Rebaudioside available as dietary supplement in 2008
China	Currently, the largest exporter of stevioside in the world. Cultivated and produced in large scale from 1990
Argentina, Chile, Malaysia, Vietnam, Thailand, Indonesia, Uruguay, UAE, Taiwan, Peru, Philippines, Turkey, Columbia and India	Steviol glycosides were approved for use as sweetener in food after the FDA's approval in 2008

60% stevioside and free from steviol and isosteviol, is approved for use in foods, beverages, medicines, soft drinks, etc., in Brazil. In Brazil, production occurs in the southern province of the country for the local market (Oliveira Ferro 1997, personal communication). Significant amounts of cultivation and stevioside processing are also done in Canada (Brandle et al. 1998), the Czech Republic (Nepovim et al. 1998), India (Chalapathi et al. 1997) and Russia (Dzyuba and Vseross 1998). The current status of stevioside use in different countries is reported in Table 1.5.

1.4 Physicochemical and biological properties of steviol glycosides

The sweetness potency of stevioside has been rated to be 300 times the relative sweetness intensity of 0.4% sucrose solution. The compound exhibits a slightly

Table 1.6 Physical properties of steviol glycosides present in *S. rebaudiana*

Compound	CAS number	Molecular weight	Melting point (°C)	Solubility in water (%)
Stevioside	57817-89-7	804	196–198	0.13
Rebaudioside A	58543-16-1	966	242–244	0.80
Rebaudioside B	58543-17-2	804	193–195	0.10
Rebaudioside C	63550-99-2	958	215–217	0.21
Rebaudioside D	63279-13-0	1128	283–286	1.00
Rebaudioside E	63279-14-1	966	205–207	1.70
Steviolbioside	41093-60-1	642	188–192	0.03
Dulcoside A	64432-06-0	788	193–195	0.58

menthol-like bitter after-taste (Bakal and Nabors 1986). The sweetness intensities (i.e. sweetening power relative to sucrose, which is taken as 1) of the other *S. rebaudiana* sweet components have been determined as: dulcoside A, 50–120; rebaudioside A, 250–450; rebaudioside B, 300–350; rebaudioside C (previously known as dulcoside B), 50–120; rebaudioside D, 250–450; rebaudioside E, 150–300; and steviolbioside, 100–125 (Crammer and Ikan 1987). Also, stevioside has been found to be synergistic with aspartame, acesulfame-K and cyclamate, but not with saccharin (Bakal and Nabors 1986).

The solubility of stevioside in aqueous systems is fairly low but the second most abundant component in *S. rebaudiana* leaves, rebaudioside A, which has a more pleasant taste than stevioside, is 6–7 times more soluble in water, since it contains an additional glucose unit in its molecule (Kinghorn and Soejarto 1991; Kohda et al. 1976). Table 1.6 details the physical properties and chemical index for all the glycosides.

Other physical properties of stevioside include bulk density of 0.443 g/mL, water-holding capacity of 4.7 mL/g, fat absorption capacity of 4.5 mL/g, emulsification value of 5.0 mL/g and swelling index of 5.01 g/g (Mishra et al. 2010).The true density of Stevia leaf powder is low in comparison to protein-rich pulses. Higher bulk densities are usually desirable for reducing paste thickness, a factor in child feeding where bulk is of concern. Unfortunately, Stevia leaf powder lacks this property. The increased water-holding capacity of Stevia leaf powder is due to its high protein content. This enhances the swelling ability, an important property of protein for preparation of viscous foods such as soups, gravies, dough and baked products. Formation and stabilisation of emulsion are aided by the protein content and are critical in many food applications, such as cake, batters, coffee whiteners, milk, frozen desserts and others. This property depends heavily on composition and the stress to which the product is subjected during processing (Savita et al. 2004). Fat absorption capacity has been attributed to the physical entrapment of oil. Stevioside also possesses a reasonable fat absorption capacity, which plays an important role in food processing, as fat acts on flavour retainers and increases the mouthfeel of foods.

Table 1.7 Proximate analysis of dry *S. rebaudiana* leaves

Component	% (w/w) of dry weight basis
Moisture	4.2–6.5
Protein	6.2–20.42
Fat	2.5–5.6
Crude fibre	13.6–18.5
Ash	8.5–13.1
Carbohydrates	35.2–52.8
Reducing sugar	5.6–6.1
Non-reducing sugar	9.6–9.9

Stevioside is a thermally stable molecule upto 100 °C, in the pH range 3–9. However, it decomposes rapidly at higher alkaline pH levels (Kinghorn and Soejarto 1985). Both stevioside and rebaudioside A have been found to be stable when formulated in acidulated beverages at room temperatures for a minimum of 3 months (Chang and Cook 1983). Solid stevioside is stable for 1 h at 120 °C, and does not undergo browning or caramelisation (Abou-Arab et al. 2010), but decomposes when temperatures exceed 140 °C (Kroyer 1999). The chemical composition of Stevia leaves is listed in Table 1.7 (Abou-Arab et al. 2010; Anish and Rema 2006; Savita et al. 2004).

Stevia leaf extract exhibits a high degree of antioxidant activity and has been reported to inhibit hydroperoxide formation in sardine oil with potency greater than that of either DL-α-tocopherol or green tea extract. The antioxidant activity of Stevia leaf extract has been attributed to the scavenging of free radical electrons and superoxides (Thomas and Glade 2010). A recent study assessing the *in vitro* potential of ethanolic leaf extract of *S. rebaudiana* indicates that it has significant potential for use as a natural antioxidant (Shukla et al. 2009). Stevia is thought to inhibit the growth of certain bacteria and other infectious organisms (Patil et al. 1996; Sivaram and Mukundam 2003). It has also been reported in the literature that the bactericidal activity of *Escherichia coli* (and other food-borne pathogenic bacteria), other microorganisms like *Salmonella typhimurium*, *B. subtilis* and *Staph. aureus* is also inhibited by the fermented Stevia leaf extract (Debnath 2008; Ghosh et al. 2008; Tomita et al. 1997).

Steady consumption of glycoside brings down the level of sugar radionuclides and cholesterol in blood (Atteh et al. 2008), facilitates generation of cells and coagulation of blood, reinforces blood vessels and reduces the probability of growth of cancerous cells (Barriocanal et al. 2008; Jeppesen et al. 2003; Maki et al. 2008; Wingard et al. 1980). Glycoside exhibits anti-inflammatory (Jayaraman et al. 2008; Sehar et al. 2008), diuretic and chloretic properties (Kochikyan et al. 2006). It is known to arrest ulcer formation in the gastrointestinal canal (Kochikyan et al. 2006) and therefore it is useful in the treatment of diarrhoea (Chatsudthipong and Muanprasat 2009). It decreases hypertension and obesity (Chan et al. 2000; Goyal et al. 2010; Hsieh et al. 2003; Jeppesen et al. 2002; Lee et al. 2001; Pól et al. 2007),

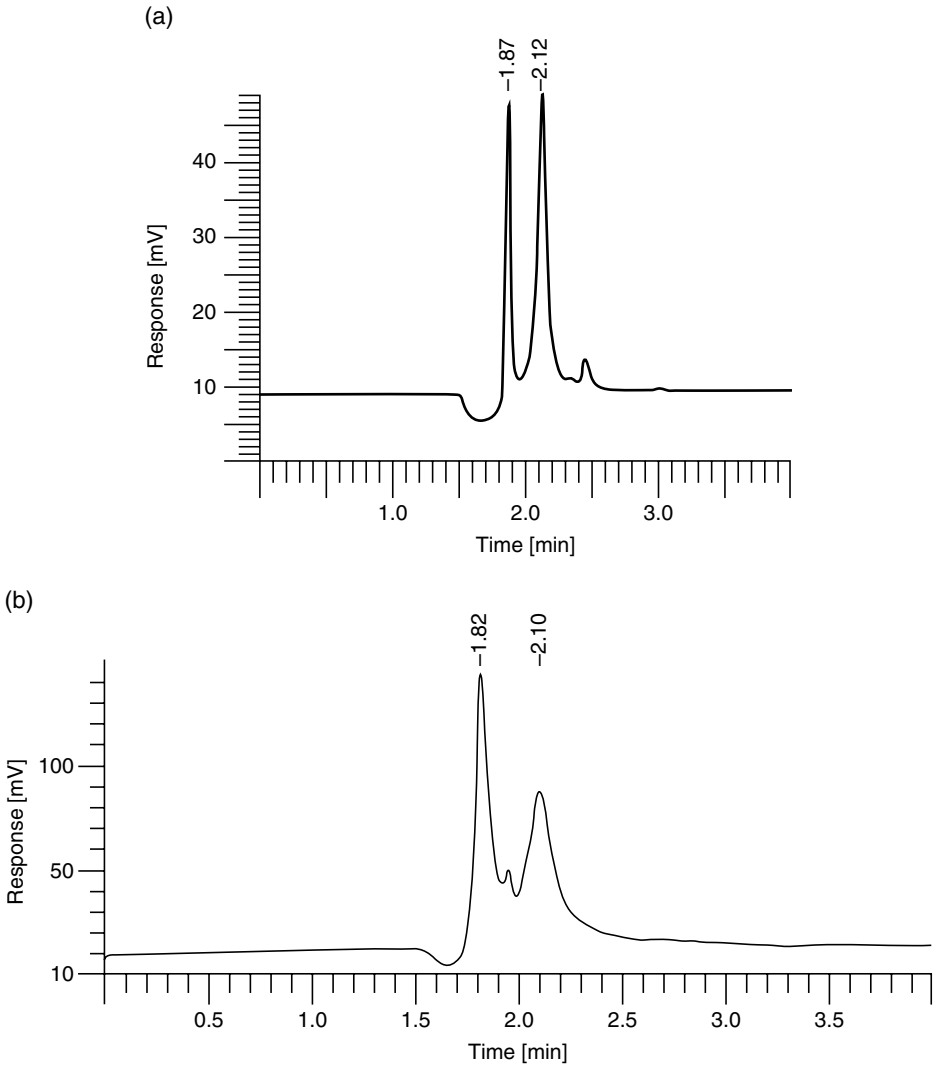

Figure 1.7 Chromatogram showing the response of (a) pure stevioside in water and (b) stevia extract using a C-18 column.

diabetes (Chen et al. 2006; Jeppesen et al. 2000, 2006) and activities of human rotavirus (Suanarunsawat and Chaiyabutr 1997; Takahashi et al. 2001). It also enhances glucose metabolism (Suanarunsawat and Chaiyabutr 1997; Toskulkao et al. 1995) and rejuvenates renal function (Jutabha et al. 2000). Glycosides are proven to be useful for treatment of gingivitis (Blauth de Slavutzky 2010) and caries effects (Blauth de Slavutzky 2010; Das et al. 1992; Suanarunsawat and Chaiyabutr 1997).

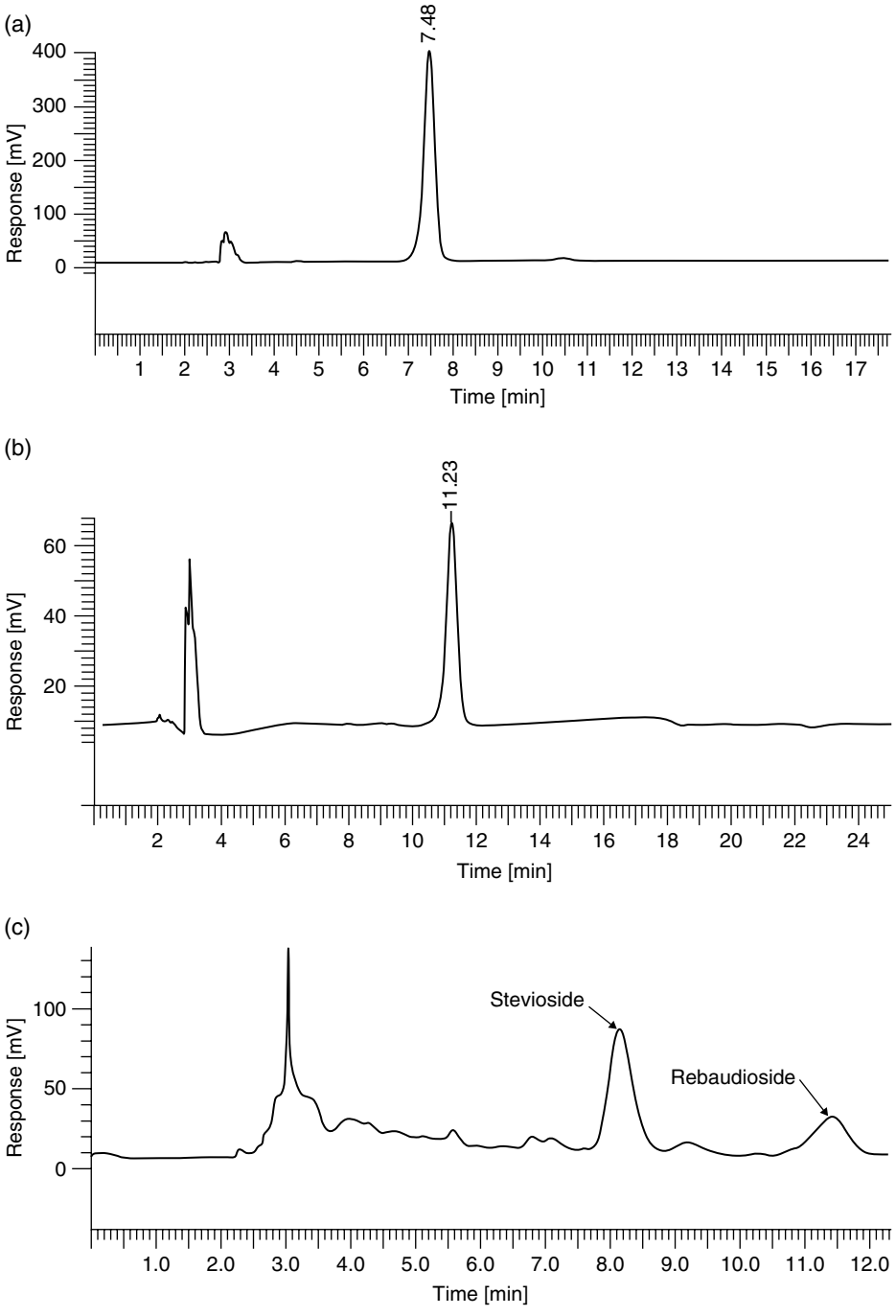

Figure 1.8 High-pressure liquid chromatogram response of (a) pure stevioside in water, (b) pure rebaudioside A in water and (c) Stevia extract using an amino (NH_2) column.

1.5 Analysis of stevioside (steviol glycosides) and Stevia extract

Stevioside (or rather total steviol glycosides) concentration in the extract is analysed using high-performance liquid chromatography (HPLC). The sample is injected into a C-18 reverse-phase HPLC column (4.6 mm ID, 250 mm length and 5 μm particle size). Acetonitrile and water mixture (80:20, v/v) is used as a mobile phase at a flow rate of 1 mL/min. Stevioside concentration is demonstrated by UV detector at a wavelength of 210 nm. A typical chromatogram using C-18 column is presented in Figure 1.7.

The differential quantification of stevioside, rebaudioside A, C, dulcoside A, etc. can be determined using amino (NH_2) reverse-phase HPLC column (4.6 mm ID, 250 mm length and 5 μm particle size). The mobile phase is a mixture of acetonitrile and water at a ratio of 80:20 (volume basis) and the flow rate is 1 mL/min. A UV detector is used for detection of stevioside present in the sample at a wavelength of 210 nm. A typical chromatogram using amino column is shown in Figure 1.8. The experimental procedure for plotting a standard curve is as follows. Initially a crude sample, of some specific concentration, is prepared using standard stevioside (98% pure) and methanol. Then standard solutions of varying concentrations (ranging from 10 to 100 ppm) are prepared by diluting the crude sample using acetonitrile and water (80:20, v/v) solution. This represents the calibration curve which is essential for determination of stevioside concentration of an unknown sample.

Colour is measured in order to analyse its concentration in different samples. Colour of the extract is measured in terms of optical absorbance (A_{420}) at a wavelength of 420 nm using a spectrophotometer. Clarity of the extract is measured in terms of percentage of transmittance (%T) using a spectrophotometer. This is given by the equation $\%T = 100 \times 10^{-A}$, where, A is optical absorbance at a wavelength of 660 nm. The total solids of the sample are measured gravimetrically by heating the extract in a hot air oven at $104 \pm 2\,^{\circ}C$ until the difference in the weight of the extract becomes constant at successive intervals.

References

Abe, K., Sonobe, M. (1977) Use of Stevioside in the food industry. New Food Industry 19, 67–72.

Abou-Arab, A., Abou-Arab, A., Abu-Salem, M.F. (2010) Physico-chemical assessment of natural sweeteners Steviosides produced from Stevia Rebaudiana Bertoni plant. Africa J Food Sci 4, 269–281.

AFSSA (Agence Francais De Securite Sanitaire Des Aliments) (2009) http://www.afssa.fr/Documents/AAAT2009sa0119.pdf.

Akashi, H. (1977) Present status and prospect for Stevioside for utilization. Shokuhin Kogyo 20, 20–26.

Anish, T., Rema, S. (2006). Preliminary studies on Stevia rebaudianci leaves: proximal composition, mineral analysis and phytochemical screening. J Med Sci 6, 321–326.

Atteh, J., Onagbesan, O., Tona, K., Decuypere, E., Geuns, J., Buyse, J. (2008) Evaluation of supplementary Stevia (Stevia Rebaudiana, bertoni) leaves and Stevioside in broiler diets: effects on feed intake, nutrient metabolism, blood parameters and growth performance. J Anim Physiol Anim Nutr (Berl) 92, 640–649.

Bakal, A.I., Nabors, L. (1986) Stevioside. In: Nabors, L., Gelardi, R.C. (eds) *Alternative Sweeteners*. New York: Marcel Dekker, pp295–307.

Barriocanal, L., Palacios, M., Benitez, G., et al. (2008) Apparent lack of pharmacological effect of Steviol glycosides used as sweeteners in humans: a pilot study of repeated exposures in some normatensive and hypotensive individuals and in type 1 and type 2 diabetics. Regul Toxicol Pharmacol 51, 37–41.

Bertoni, M.S. (1899) El caá-ehê (Eupatorium rebaudianum, Species Novas). J Agron 1, 35–37.

Bertoni, M.S. (1905) Le Kaá hê-é: sa nature et ses propriétés. Paraguay Sci Annu Series I 5, 1–14.

Bertoni, M.S. (1918) La Stevia Rebaudiana Bertoni. La estevina y la rebaudina, neuvas substancias edulcorantes. Paraguay Sci Annu Series II 6, 29–134.

Blauth de Slavutzky, S. (2010) Stevia and sucrose effect on plaque formation. J Consum Prot Food Saf 5, 213–216.

Blumenthal, M. (1995) FDA lifts import ban on Stevia. Herb can be imported as a dietary supplement: future use as a sweetener is still unclear. Herbal Gram 35, 17–18.

Brandle, J.E., Rosa, N. (1992) Heritability for yield, leaf, stem ratio and Stevioside content estimated from a landrace cultivar of Stevia Rebaudiana. Can J Plant Sci 72, 1263–1266.

Brandle, J.E., Starratt, A.N., Gizjen, M. (1998) Stevia Rebaudiana: its agricultural, biological, and chemical properties. Can J Plant Sci 78, 527–536.

Chalapathi, M.V., Thimmegowda, S., Sridhara, S., Parama,V.R.R., Prasad, T.G. (1997) Natural noncalorie sweetener Stevia (Stevia Rebaudiana Bertoni) – a future crop of India. Crop Res 14, 347–350.

Chang, S.S., Cook, J.M. (1983) Stability studies of Stevioside and rebaudioside A in carbonated beverages. J Agri Food Chem 31, 409–412.

Chatsudthipong, V., Muanprasat, C. (2009) Stevioside and related compounds: therapeutic benefits beyond sweetness. Pharmacol Ther 121, 41–54.

Chen, J., Jeppesen, P., Abudula, R., Dyrskog, S., Colombo, M., Hermansen, K. (2006) Stevioside does not cause increased basal insulin secretion or b-cell desensitization as does the sulphonylurea, glibenclamide: studies in vitro. Life Sci 78, 1748–1753.

Cheng, T.F., Chang, W.H. (1983) Studies on the non-Stevioside components of Stevia extracts. Nat Sci Council Monthly Taipei 11, 96–108.

Cook, I.F., Knox, J.R. (1970) A synthesis of Steviol. Tetrahedron Lett 11, 4091–4093.

Crammer, B., Ikan, R. (1987) Progress in the chemistry and properties of the rebaudiosides. In: Grenby, T.H. (ed) *Developments in Sweeteners – 3*. London: Elsevier Applied Science, pp45–64.

Curry, L.L. (2010) *Agency Response Letter GRAS Notice No. GRN 000287*. Washington, DC: Food and Drug Administration. http://www.accessdata.fda.gov/scripts/fcn/gras_notices/grn000287.pdf

D'Agostino, M., de Simone, F., Pizza, C., Aquino, R. (1984) Sterols from Stevia Rebaudiana Bertoni. Bull Ital J Exper Biol 60, 2237–2240.

Darise, M., Kohda, H., Mizutani, K., Kasai, R.,Tanaka, O. (1983) Chemical constituents of flowers of Stevia Rebaudiana Bertoni. Agri Biol Chem 47, 133–135.

Das, S., Das, A., Murphy, R., Punwani, I., Nasution, M., Kinghorn, A. (1992) Evaluation of the cariogenic potential of the intense natural sweeteners Stevioside and rebaudioside A. Caries Res 26, 363–366.

Debnath, M. (2008) Clonal propagation and antimicrobial activity of an endemic medicinal plant Stevia Rebaudiana. J Med Plants Res 2, 45–51.

Dieterich, K. (1908) The constituents of Eupatorium rebaudianum, 'Kaa-he-e', and their pharmaceutical value. Pharmaceut Central Hall 50, 435–458.

Donalisio, M.G.R., Duarte, F.R., Pinto, A.J.D.A., Souza, C.J. (1982) Stevia Rebaudiana. Agronomics 34, 65–68.

Dzyuba, O., Vseross, O. (1998) Stevia Rebaudiana (Bertoni) Hemsley – a new source of natural sweetener for Russia. Plant Resources 34, 86–95.

EFSA (European Food Standards Agency) (2010) Scientific opinion on the safety of Steviol glycosides for the proposed uses as a food additive. EFSA Panel on Food Additives and Nutrient Sources added to Food (ANS). EFSA J 8(1537), 1–84.

FAO (Food and Agriculture Organisation) (2008) *Steviol Glycosides. FAO JECFA Monographs 5*. Rome: Food and Agriculture Organisation.

FAO/WHO (Food and Agriculture Organisation/World Health Organisation) (2009) *List of Substances Scheduled for Evaluation and Request for Data*. Joint FAO/WHO Expert Committee on Food Additives, Seventy-Third Meeting, Food Additives and Contaminants. Geneva June 8–17. Accessed at: http://www.who.int/ipcs/food/jecfa/jecfa73.pdf.

Fors, A. (1995) A new character in the sweetener scenario. Sugar J 58, 30.

FSANZ (Food Standards Australia New Zealand) (2008) *Final Assessment Report, Application A540, Steviol Glycosides as Intense Sweeteners*. Canberra: Food Standards Australia New Zealand.

Fujita, S.I., Taka, K., Fujita, Y. (1977) Miscellaneous contributions to the essential oils of plants from various territories. XLI. On the components of the essential oil of Stevia Rebaudiana Bertoni. Yakugaku Zasshi 97, 692–694.

Geuns, J.M.C. (2003) Molecules of interest: Stevioside. Phytochemistry 64, 913–921.

Ghosh, S., Subudhi, E., Nayak, S. (2008) Antimicrobial assay of Stevia Rebaudiana Bertoni leaf extracts against 10 pathogens. Int J Integr Biol 2, 27–31.

Goenadi, D.H. (1983) Water tension and fertilization of Stevia Rebaudiana Bertoni on Oxic Tropudalf. Menara Perkebunam 51, 85–90.

Gosling, C. (1901) Caá-êhê or azuca-caá. Kew Bull, 183–194.

Goyal, S.K., Samsher, Goyal, R.K. (2010) Stevia (Stevia Rebaudiana), a bio-sweetener: a review. Int J Food Sci Nutr 61, 1–10. http://informahealthcare.com/doi/abs/10.3109/09637480903193049

Grashoff, J.E. (1972) A systematic study of the North and Central American species of Stevia. PhD dissertation, University of Texas. University of Michigan Microfilm 73–7556, pp1–608.

Hanson, J.R., de Oliveira, B.H. (1993) Stevioside and related sweet diterpenoid glycosides. Natur Prod Report 10, 301–309.

Hsieh, M., Chan, P., Sue, Y., et al. (2003). Efficacy and tolerability of oral Stevioside in patients with mild essential hypertension: a two-year, randomized, placebo-controlled study. Clin Ther 25, 2797–2808.

Jayaraman, S., Manoharan, M., Illanchezian, S. (2008) In-vitro antimicrobial and antitumor activities of Stevia Rebaudiana (Asteraceae) leaf extracts. Trop J Pharmaceut Res 7, 1143–1149.

Jeppesen, P., Gregersen, S., Poulsen, C., Hermansen, K. (2000) Stevioside acts directly on pancreatic a cells to secrete insulin: actions independent of cyclic adenosine monophosphate and adenosine triphosphate-sensitive K+channel activity. Metabolism 49, 208–214.

Jeppesen, P.B., Gregersen, S., Alstrup, K.K., Hermansen, K. (2002) Stevioside induces antihyperglycaemic, insulinotropic and glucagonostatic effects in vivo: studies in the diabetic Goto-Kakizaki (GK) rats. Phytomedicine 9, 9–14.

Jeppesen, P., Gregersen, S., Rolfsen, S., et al. (2003) Antihyperglycemic and blood pressure-reducing effects of Stevioside in the diabetic Goto-Kakizaki rat. Metabolism 52, 372–378.

Jeppesen, P.B., Kyrskog, S.E., Aggersen, X.J., Hermansen, K. (2006) Can stevioside in combination with a soy based dietary supplement be a new useful treatment of type 2 diabetes? An in vivo study in the diabetic Goto-Kakizaki rat. Rev Diabet Stud 3, 189–199.

Jutabha, P., Toskulkao, C., Chatsudthipong, V. (2000) Effect of Stevioside on PAH transport by isolated perfused rabbit renal proximal tubule. Can J Physiol Pharmacol 78, 737–744.

Kaneda, N., Kasai, R., Yamasaki, K., Tanaka, O. (1977) Chemical studies on sweet diterpene-glycosides of Stevia Rebaudiana: conversion of Stevioside into Rebaudioside-A. Chem Pharmaceut Bull 25, 2466–2467.

Katayama, O., Sumida, T., Hayashi, H., Mitsuhashi, H. (1976) *The Practical Application of Stevia and Research and Development Data (English translation)*. Japan: ISU Company, p747.

Kim, I., Yang, M., Lee, O., Kang, S. (2011) The antioxidant activity and the bioactive compound content of Stevia Rebaudiana water extracts. LWT Food Sci Technol 44, 1328–1332.

Kim, S.H., Dubois, G.E. (1991) Natural high potency sweeteners. In: Marie, A., Piggott, J.R. (eds) *Handbook of Sweeteners*. New York: Springer, pp116–185.

King, R.M., Robinson, H. (1987) *The Genera of the Eupatorieae (Asteraceae*). *Monographs in Systematic Botany*. St Louis, MO: Missouri Botanical Garden.

Kinghorn, A.D. (2001) *Stevia: The Genus Stevia*. London: Taylor and Francis.

Kinghorn, A.D., Soejarto, D.D. (1985) Current status of Stevioside as a sweetening agent for human use. In: Wagner, H., Hikino, H., Farnsworth, R. (eds) *Economic and Medicinal Plant Research*. London: Academic Press, pp1–52.

Kinghorn, A.D., Soejarto, D.D. (1991) Stevioside. In: Nabors, L.B., Gelardi, R.C. (eds) *Alternative Sweeteners*. New York: Marcel Dekker, pp157–171.

Kinghorn, A.D., Wu, C.D., Soejarto, D.D. (2001) Stevioside. In: Nabors, L.B., Gelardi, R.C. (eds) *Alternative Sweeteners*, 2nd edn. New York: Marcel Dekker, pp167–183.

Kobayashi, M., Horikawa, S., Degrandi, I.H., Ueno, J., Mitsuhashi, H. (1977) Dulcosides A and B, new diterpene glycosides from Stevia Rebaudiana. Phytochemistry 16, 1405–1408.

Kochikyan, V., Markosyan, A., Abelyan, L., Balayan, A., Abelyan, V. (2006) Combined enzymatic modification of Stevioside and rebaudioside A. Appl Biochem Microbiol 42, 31–37.

Kohda, H., Kasai, R., Yamasaki, K., Murakami, K., Tanaka, O. (1976) New sweet diterpene glycosides from Stevia Rebaudiana. Phytochemistry 15, 981–983.

Korea National Institute of Health (1996) *Report on the Safety of Stevioside*. Seoul: Korea National Institute of Health, pp1–5.

Kroyer, G.T. (1999) The low calorie sweetener Stevioside: stability and interaction with food ingredients. Food Sci Technol 32, 509–512.

Leatherhead Food Research (2011) *The Global Food Additives Market*, 5th edn. Leatherhead, UK: Leatherhead Food Research.

Lee, C.N., Wong, K., Liu, J., Chen, Y., Chan, P. (2001) Inhibitory effect of Stevioside on calcium influx to produce antihypertension. Planta Med 67, 796–799.

Lee, J.I., Kang, K.K., Lee, E.U. (1979) Studies on new sweetening resource plant Stevia (Stevia Rebaudiana Bert.) in Korea. I, effects of transplanting date shifting by cutting and seeding dates on argonomic characteristics and dry leaf yields of Stevia Res. Rep ORD 21, 171–179.

Lewis, W.H. (1992) Early uses of Stevia Rebaudiana (Asteraceae) leaves as a sweetener in Paraguay. Econ Bot 46, 336–337.

Maki, K., Curry, L., Reeves, M., et al. (2008) Chronic consumption of rebaudioside A, a Steviol glycoside, in men and women with type 2 diabetes mellitus. Food Chem Toxicol 46, 47–53.

Martelli, A., Frattini, C., Chialva, F. (1985) Unusual essential oils with aromatic properties. I. Volatile components of Stevia Rebaudiana Bertoni. Flavour Fragr J 1, 3–7.

Matsuo,T., Kanamori, H., Sakamoto, I. (1986) Nonsweet glucosides in the leaves of Stevia Rebaudiana. Hiroshima-ken Eisei Kenkyusho Kenkyu Hokoku 33, 25–29.

Mishra, P., Singh, R., Kumar, U., Prakash, V. (2010) Stevia Rebaudiana – a magical sweetener. Global J Biotechnol Biochem 5, 62–74.

Mitchell, H. (ed) (2006) *Sweeteners and Sugar Alternatives in Food Technology*. Oxford: Blackwell Publishing Ltd.

Mohammad, M., Mohammad, U., Sher, M., Habib, A., Iqbal, A. (2007) In vitro clonal propagation and biochemical analysis of field established Stevia Rebaudiana Bertoni. Pak J Botany 39, 2467–2474.

Mori, K., Matsui, M. (1965) Total synthesis of methyl (±)-8α-carboxymethylpodocarpan-13-one-4-β-carboxylate, a degradation product of Steviol. Tetrahedron Lett 6, 2347–2350.

Mori, K., Matsui, M. (1966) Diterpenoid total synthesis-II. An alternative route to methyl (±)-7-oxopodocarp-8-en-16-oate. Tetrahedron 22, 879–884.

Mori, K., Matsui, M. (1970) Synthesis of erythroxydiol A (hydroxymonogynol). Tetrahedron Lett 37, 3287–8288.

Mori, K., Matsui, M., Sumiki,Y. (1970a) A new method for the construction of a bicyclo [3.2.1] octane ring system with a bridgehead hydroxyl group. A partial synthesis of (–)-epiallogibberellic acid. Tetrahedron Lett 11, 429–432.

Mori, K., Nakahara, Y., Matsui, M. (1970b) Total synthesis of (±)-Steviol. Tetrahedron Lett 11, 2411–2414.

Mosettig, E., Beglinger, U., Dolder, F., Lichti, H., Quitt, P., Waters, J.A. (1963) The absolute configuration of Steviol and isosteviol. J Am Chem Soc 85, 2305–2309.

Nabeta, K., Kasai, T., Sugisawa, H. (1976) Phytosterol from the callus of Stevia Rebaudiana Bertoni. Agri Biol Chem 40, 2103–2104.

Nabors, L.B. (ed) (2011) *Alternative Sweeteners*. Boca Raton, FL: CRC Press.

Nakahara, Y. (1982) Synthetic studies of physiologically active natural products with characteristic ring structures. Nippon Nogeikagaku Kaishi 56, 943–955.

Nakahara, Y., Mori, K., Matsui, M. (1971) Diterpenoid total synthesis. Part XVI. Alternative synthetic routes to (±)-Steviol and (±)-kaur-16-en-19-oic acid. Agri Biol Chem 35, 918–928.

Nepovim, A., Drahosova, H.,Valicek, P., Vanek, T. (1998) The effect of cultivation conditions on the content of Stevioside in Stevia Rebaudiana plants cultivated in the Czech Republic. Pharma Pharmacol Lett 8, 19–21.

O'Donnell, K., Kearsley, M. (2012) *Sweeteners and Sugar Alternatives in Food Technology*. Oxford: Wiley Blackwell.

Ogawa, T., Nozaki, M., Matsui, M. (1978) A stereocontrolled approach to the synthesis of glycosyl esters. Partial synthesis of Stevioside from steviobioside. Carbohydrate Res 60, C7–C10.

Ogawa, T., Nozaki, M., Matsui, M. (1980) Total synthesis of Stevioside. Tetrahedron 36, 2641–2648.

Oshima, Y., Saito, J.I., Hikino, H. (1986) Sterebins A, B, C and D, bisnorditerpenoids of Stevia Rebaudiana leaves. Tetrahedron 42, 6443–6446.

Oshima,Y., Saito, J.I., Hikino, H. (1988) Sterebins E, F, G and H, diterpenoids of Stevia Rebaudiana leaves. Phytochemistry 27, 624–626.

Patil, V., Ashwini, K., Reddy, P., Purushotham, M., Prasad, T., Udaykumar, M. (1996) In vitro multiplication of Stevia Rebaudiana. Curr Sci 70, 960.

Pezzuto, J.M., Compadre, C.M., Swanson, S.M., Nanayakkara, N.P.D., Kinghorn, A.D. (1985) Metabolically activated Steviol, the aglycone of Stevioside, is mutagenic. Proc Natl Acad Sci USA 82, 2478–2482.

Pól, J., Hohnová, B., Hyötyläinen, T. (2007) Characterization of Stevia Rebaudiana by comprehensive two-dimensional liquid chromatography time-of-flight mass spectrometry. J Chromatogr A 1150, 85–92.

Rajbhandari, A., Roberts, M.F. (1983) The flavonoids of Stevia Rebaudiana. J Natur Prod 46, 194–195.

Rasenack, P. (1908) *Sweet Substances of Eupatorium Rebaudianum and of Licorice*. Federal Biological Research Centre for Agriculture and Forestry. Berlin: German Health Authority 28, 420–423.

Robinson, B.L. (1930) Observations on the genus Stevia. Contributions of the Gray Herbarium of Harvard University 90, 36–58.

Sakamoto, I., Yamasaki, K., Tanaka, O. (1977a) Application of 13C NMR spectroscopy to chemistry of natural glycosides: rebaudioside-C, a new sweet diterpene glycoside of Stevia Rebaudiana. Chem Pharmaceut Bull 25, 844–846.

Sakamoto, I., Yamasaki, K., Tanaka, O. (1977b) Application of 13CNMR spectroscopy to chemistry of plant glycosides: rebaudiosides-D and -E, new sweet diterpene-glucosides of Stevia Rebaudiana Bertoni. Chem Pharmaceut Bull 25, 3437–3439.

Savita, S., Sheela, K., Sunanda, S., Shankar, A., Ramakrishna, P. (2004) Stevia Rebaudiana – a functional component for food industry. J Human Eco 15, 261–264.

Saxena, N.C., Ming, L.S. (1988) Preliminary harvesting characteristics of Stevia. Phys. Prop Agri Mat Prod 3, 299–303.

Schock, C.C. (1982) *Experimental Cultivation of Rebaudi's Stevia in California*. University of California Agronomy Progress Report No. 122. Davis, CA: University of California.

Schwontkowski, D. (1995) *Herbs of the Amazon: Common and Traditional Uses*. Utah: Science Student Brain Trust Publishing.

Sehar, I., Kaul, A., Bani, S., Pal, H., Saxena, A. (2008) Immune up regulatory response of a non-caloric natural sweetener, Stevioside. Chemio-Biol Interact 173, 115–121.

Sholichin, M., Yamasaki, K., Miyama, R., Yahara, S., Tanaka, O. (1980) Labdane-type diterpenes from Stevia Rebaudiana. Phytochemistry 19, 326–327.

Shukla, S., Mehta, A., Bajpai, V., Shukla, S. (2009) In vitro antioxidant activity and total phenolic content of ethanolic leaf extract of Stevia Rebaudiana Bert. Food Chem Toxicol 47, 2338–2343.

Sivaram, L., Mukundam, U. (2003) In vitro culture studies on Stevia Rebaudiana. In Vitro Cell Dev Biol Plant 39, 520–523.

Soejarto, D.D., Kinghorn, A.D., Farnsworth, N.R. (1982) Potential sweetening agents of plant origin. III. Organoleptic evaluation of Stevia leaf herbarium samples for sweetness. J Natur Prod 45, 590–599.

Soejarto, D.D., Compadre, C.M., Medon, P.J., Kamath, S.K., Kinghorn, A.D. (1983) Potential sweetening agents of plant origin II. Field search for sweet-tasting Stevia species. Econ Bot 37, 71–78.

Stones, M. (2011) Stevia wins final EU approval. 22 November 2011. www.foodmanufacture.co.uk.

Suanarunsawat, T., Chaiyabutr, N. (1997) The effect of Steviosides on glucose metabolism in rat. Can J Physiol Pharmacol 75, 976–982.

Sumida, T. (1973) Reports on Stevia Rebaudiana Bertoni M. introduced from Brazil as a new sweetness resource in Japan. Misc Pub Hokkaido Nat Agri Exp Station 2, 69–83.

Sumida, T. (1980) Studies on Stevia Rebaudiana Bertoni as a possible new crop for sweetening resource in Japan. J Central Agri Exp Station 31, 1–71.

Tadhani, M., Subhash, R. (2006) Preliminary studies on Stevia Rebaudiana leaves: proximal composition, mineral analysis and phytochemical screening. J Med Sci 6, 321–326.

Takahashi, K., Matsuda, M., Oashi, K., et al. (2001) Analysis of anti-rotavirus activity of extract from Stevia Rebaudiana. Antiviral Res 49, 15–24.

Tanaka, O. (1982) Steviol-glycosides: new natural sweetener. Trend Anal Chem 1, 246–248.

Thomas, J., Glade, M. (2010) Stevia: it's not just about calories. Open Obes J 2, 101–109.

Tomita, T., Sato, N., Arai, T., et al. (1997) Bactericidal activity of a fermented hot-water extract from Stevia Rebaudiana Bertoni and other food-borne pathogenic bacteria. Microbiol Immunol 41, 1005–1009.

Toskulkao, C., Sutheerawatananon, M., Wanichanon, C., Saitongdee, P., Suttagit, M. (1995) Effect of Stevioside and Steviol on intestinal glucose absorption hamsters. J Nutr Sci Vitaminol 41, 105–113.

Toyoda, K., Matsui, H., Shoda, T., Uneyama, C., Takada, K., Takahashi, M. (1997) Assessment of the carcinogenicity of Stevioside in F344 rats. Food Chem Toxicol 35, 597–603.

Vis, E., Fletcher, H.G. Jr (1956) Stevioside. IV. Evidence that Stevioside is a sophoroside. J Am Chem Soc 75, 4709–4710.

WHO (World Health Organisation) (2000) *Safety Evaluation of Certain Food Additives. Stevioside*. Joint FAO/WHO Expert Committee on Food Additives. WHO Food Additive Series No. 42. Geneva: WHO.

WHO (World Health Organisation) (2008) *Summary and Conclusions, Steviol Glycosides*. Joint FAO/WHO Expert Committee on Food Additives. Geneva: WHO.

WHO (World Health Organisation) (2009) *Safety Evaluation of Certain Food Additives. Steviol Glycosides (Addendum)*. Joint FAO/WHO Expert Committee on Food Additives. WHO Food Additive Series No. 60. Geneva: WHO.

Wilson, R. (2007) *Sweeteners*. New York: John Wiley & Sons Inc.

Wingard, R., Brown, J., Enderlin, F., Dale, J., Hale, R., Seitz, C. (1980) Intestinal degradation and absorption of the glycosidic sweeteners Stevioside and rebaudioside A. Cell Molec Life Sci 36, 519–520.

Wood, H.B. Jr, Allerton, R., Diehl, H.W., Fletcher, H.G. Jr (1955) Stevioside. I. The structure of the glucose moieties. J Organ Chem 20, 875–883.

Yamasaki, K., Kohda, H., Kobayashi, T., Kasai, R., Tanaka, O. (1976) Structures of Stevia diterpene-glucosides: applications of ^{13}C NMR. Tetrahedron Lett 17, 1005–1008.

Yasukawa, K., Yamaguchi, A., Arita, J., Sakurai, S., Ikeda, A., Takido, M. (1993) Inhibitory effect of edible plant extracts on 12-O-tetradecanoyphorbol-13-acetate-induced ear oedema in mice. Phytother Res 7, 185–189.

Ziegler, F.E., Kloek, J.A. (1971) 1-Hydroxy-7-methylene bicyclo[3.2.1]octane: a gibbane-steviolC/D ring model. Tetrahedron Lett 12, 2201–2203.

Ziegler, F.E., Kloek, J.A. (1977) The stereocontrolled photoaddition of allene to cyclopent-1-ene-1-carboxaldehydes. A total synthesis of (±)-Steviol methyl ester and isosteviol methyl ester. Tetrahedron 33, 373–380.

2

Health benefits and pharmacological effects of steviol glycosides

Stevioside, which is well known for its sweetness and its potential use as a low-calorie natural sweetener, also has therapeutic effects on human physiology. Some of the potential health benefits of stevioside are outlined in Table 2.1.

2.1 Effect of stevioside in absorption, distribution, metabolism and excretion

The mechanism of transport of stevioside in living organisms in terms of absorption, distribution, metabolism and excretion (ADME) is of paramount importance as it provides an understanding of the extent and kinetics of systemic exposure to stevioside or its metabolic products. It has been observed that stevioside absorption is relatively low in the intestine, owing to its molecular weight (Geuns et al. 2003). Moreover, stevioside has been found to be resistant to degradation by the action of digestive enzymes of mouth, stomach and small intestine (Hutapea et al. 1997; Koyama et al. 2003a; Wingard et al. 1980). On the other hand, the bacterial microflora in the lower gastrointestinal tract (colon) of humans has been shown to hydrolyse both stevioside and rebaudioside A to agylone steviol (Gardana et al. 2003; Koyama et al. 2003a) via successive removal of the glucose units (Geuns 2007; Geuns et al. 2003) and this hydrolysis is essential for absorption of steviol glycosides.

Bacteroides sp. is primarily responsible for this conversion in the human intestine (Gardana et al. 2003). Experimental studies indicate that no measurable amount of stevioside is present in the faeces, whereas free steviol is present when relatively high doses of stevioside are administered to human subjects (Geuns 2007; Renwick and Tarka 2008). Stevioside and rebaudioside A were completely degraded to its

Stevioside: Technology, Applications and Health, First Edition.
Sirshendu De, Sourav Mondal and Suvrajit Banerjee.

Table 2.1 Different physiological effects of stevioside consumption

Health effects	Reference
Antihyperglycaemic effect (reduction in blood glucose level in both type 1 and type 2 diabetes)	Jeppesen et al. 2000, 2002, 2003
Anticarcinogenic effects (can be used in treatment of cancer)	Mizushina et al. 2005
Natural antioxidant	Shukla et al. 2009; Ghanta et al. 2007
Enhances glucose metabolism	Suanarunsawat and Chaiyabutr, 1997; Toskulkao et al. 1995
Antidiarrhoeal therapeutics	Tomita et al. 1997; Pariwat et al. 2008
Ulceration in the gastrointestinal tract	Kochikyan et al. 2006
Decreases the sugar content, radionuclides, cholesterol, triglyceride and low-density lipoprotein cholesterol in the blood	Atteh et al. 2008
Improves cell regeneration and blood coagulation, suppresses neoplastic growth and strengthens blood vessels	Barriocanal et al. 2008; Jeppesen et al. 2003; Maki et al. 2008
Anti-inflammatory effect	Jayaraman et al. 2008; Sehar et al. 2008
Prevents bradycardia and hypotension	Humboldt and Boech 1977
Antimicrobial effect	Puri and Sharma 2011; Takahashi et al. 2001
Anticariogenic	Blauth de Slavutzky 2010; Suanarunsawat and Chaiyabutr 1997
Antigingivitis activity	Blauth de Slavutzky 2010
Substitutes for saccharose in the treatment of obesity and hypertension	Chan et al. 2000; Goyal et al. 2010; Hsieh et al. 2003; Lee et al. 2001; Pól et al. 2007
Anti human rotavirus activities	Takahashi et al. 2001
Diuretic	Melis 1995
Vasodilatory properties	Melis 1992a; Melis and Sainati 1991a; Lee et al. 2001

aglycone steviol after 10-h and 24-h incubation, respectively, with human intestinal microflora. Hydrolysis progressed through formation of steviolbioside, with its concentration peaking after 2–4 h of incubation for stevioside and 12–15 h for rebaudioside A, and then decreasing rapidly to zero. After 3–4 h of incubation, steviol was detected and its concentration increased rapidly thereafter. The final microbial metabolite of stevioside and rebaudioside A remained unchanged during a 72-h incubation period with the action of human microflora, which implies that bacterial enzymes failed to degrade the steviol structure (Renwick and Tarka 2008).

It has been suggested by Koyama et al. (2003b) that oral administration of steviol to rats results in increasing steviol concentration in the portal venous blood, reaching a peak within 15 min of ingestion. In addition, experimental investigations

suggest that the rate of hydrolysis of stevioside is slightly greater than that of rebaudioside A (Koyama et al. 2003b; Wingard et al. 1980), and the rate of steviol transport is in favour of absorptive direction involving both passive diffusion and carrier-mediated transport through a monocarboxylic transporter, compared to stevioside (Chatsudthipong and Muanprasat 2009).

The distribution of stevioside takes place after hydrolysis of stevioside to steviol. It has been found that accumulation of steviol is maximal in the liver, kidney and intestine (Cardoso et al. 1996). High-performance liquid chromatography (HPLC) analysis of bile showed that steviol is the major metabolite present in rats. However, analysis of urine revealed the presence of steviol glucuronide in humans (Geuns et al. 2006) and no stevioside or steviol was detected.

The metabolic conversion of stevioside to steviol occurs in the liver. The metabolic pathway of steviol involves phase I metabolism of steviol by cytochrome P450 and phase II metabolism in which steviol is conjugated with glucuronide (Roberts and Renwick 2008). There are two probable routes of stevioside excretion, via bile and urine. Steviol glucuronide is the common major metabolite found in circulation of both humans and rats. Biliary and urinary tracts appear to be the major routes for steviol glucuronide excretion. However, the extent to which this metabolite is excreted via these two routes differs between humans and rats. In the latter, the principal route is through faeces via biliary excretion of steviol glucuronide (Nakayama et al. 1986; Roberts and Renwick, 2008; Wingard et al. 1980). In humans, steviol glucuronide is predominantly excreted via the urine (Cardoso et al. 1996; Geuns 2007; Geuns et al. 2006; Wheeler et al. 2008). This is due to different molecular weight (MW) thresholds for human and rat biliary excretion of organic anions (Kwon et al. 2002). In the rat, anions with molecular weight less than 325 Da are excreted in urine and in humans, anions less than 500–600 Da are excreted in urine (Renwick 2008).

Stevioside and rebaudioside A undergo similar metabolic and elimination pathways in humans, with steviol glucuronide being excreted primarily in the urine and steviol through the faeces which account for 62% and 5.2%, respectively, of the total administered stevioside dose in a 72-h period (Wheeler et al. 2008). The excretory process probably involves renal organic anion transporters (Srimaroeng et al. 2005).

2.2 Antihyperglycaemic effect

There has been a sharp increase in the incidence of type 2 diabetes mellitus among the developing and industrialised nations, due to ageing, dietary habits and reduced physical activities. Diabetes is a chronic metabolic disorder resulting from insulin abnormalities, insulin secretion from islet β-cells, pancreatic α-cell dysfunction and relative imbalance of insulin and glucagon levels. It has been found that stevioside and Stevia extract can be used for treatment of diabetic patients (both type 1 and type 2) as it significantly decreases the plasma glucose levels (Renwick and Molinary 2010).

Stevioside and steviol both enhance insulin secretion and insulin sensitivity of the islet cells but only in presence of elevated glucose levels (Jeppesen et al. 2000, 2003; Lailerd et al. 2004). Both have a long-lasting and apparently reversible insulinotropic effect via direct action on the β-cells to stimulate insulin secretion (Jeppesen et al. 2000). Preliminary experiments in rats reveal that in STZ-induced diabetic rats, the hypoglycaemic effect of oral intake of stevioside (1, 2 or 10 mg/kg body weight(BW)/day for 15 days) is mediated via its effect on phosphoenol pyruvate carboxy kinase (PEPCK), a rate-limiting enzyme for gluconeogenesis controlling glucose production in the liver (Chen et al. 2005). Stevioside slows down gluconeogenesis in the liver via suppression of PEPCK gene expression, leading to a decrease in plasma glucose levels in diabetic rats (Giffin et al. 1993). Injection of stevioside along with glucose provokes insulin secretion, suppresses glucagon level in the plasma and decreases blood glucose response to glucose tolerance test in anaesthetised type 2 diabetic rats, which supports the fact that stevioside possesses antihyperglycaemic, insulinotropic and glucagonostatic effects in type 2 diabetic situations (Jeppesen et al. 2002).

Excessive oral intake of stevioside (500 mg/kg BW) in diabetic rats increases the insulin sensitivity of the body, as determined by the glucose-insulin index, which indicates the degree of insulin sensitivity or insulin action on glucose disposal rate followed by glucose loading (Chang et al. 2005; Lailerd et al. 2004).

Stevioside shows a direct effect on glucagon secretion as well (Hong et al. 2006), by decreasing the release of glucagon, probably by enhancing mRNA expressions of carnitine palmitoyltransferase, peroxisome proliferator-activated receptor gamma (PPARγ) and stearoyl-CoA desaturase. However, rebaudioside A affects insulin secretion stimulation in the presence of extracellular Ca^{2+}, i.e. insulin stimulation at high glucose levels disappears in the absence of extracellular Ca^{2+} (Abudula et al. 2004, 2008). Rebaudioside A stimulates insulin secretion from pancreatic β-cells via inhibition of K_{ATP}, thereby allowing β-cells to depolarise and activate Ca^{2+} channels. This inhibition of K_{ATP} is possible in the presence of a high glucose level, underscoring the glucose dependency of rebaudioside A action. However, the signalling pathway through which high plasma glucose triggers the action of rebaudioside A is still not known. Long-term consumption of rebaudioside A shows no effect on glucose homeostasis, lipid profile or blood pressure (Maki et al. 2008) and exhibits good tolerance properties.

In addition to stevioside and steviol, isosteviol, a metabolic compound of stevioside, improves lipid profile and regulates the expression of key β-cell genes, including insulin regulatory transcription factors, thereby improving glucose homeostasis, enhancing insulin sensitivity, lowering plasma triglyceride and decreasing weight of diabetic KKAy mice (Nordentoft et al. 2008). Chronic type 2 diabetes is normally accompanied by hypertension and dyslipidaemia (UKPDS Group 1998a,b). Thus, the ideal pharmacological intervention in type 2 diabetes should be aimed at lowering blood pressure, lipid and glucose concentration in the plasma. As stevioside possesses blood pressure-lowering and hypoglycaemic effects (Jeppesen et al. 2003), it has a high potential to be used clinically for the treatment of these patients. It is interesting to note that the effect of stevioside is dependent largely on

the plasma glucose level, being observed only when plasma glucose level is elevated. Hence, it seems to be safe for normal healthy individuals. However, the mechanism of this effect is still not known.

2.3 Antihypertensive effect

Studies in animals as well as humans have established that stevioside and Stevia extract decrease mean arterial blood pressure by inducing vasodilation (decreased total peripheral resistance – TPR) and diuresis as well as natriuresis, which leads to a subsequent decrease in plasma volume (Melis 1995; Melis and Sainati 1991a,b). This antihypertensive effect of Stevia extract is more prominent with prolonged oral intake (Jeppesen et al. 2003; Melis 1996). Stevioside has been found to cause bradycardia and hypotension in humans (Humboldt and Boech 1977). It has been considered to have an inotropic effect by decreasing systole duration which ultimately reduces stroke volume and pressure. Long-term ingestion of stevioside in humans significantly reduces systolic and diastolic blood pressure in those with mild to moderate hypertension, without affecting the body mass index, blood biochemistry values or left ventricular mass index (Hsieh et al. 2003). Moreover, overall quality of life improved significantly with stevioside treatment compared to placebo, and there has been no report of major adverse clinical effects. This supports the fact that stevioside is well tolerated during long-term use.

Intracellular Ca^{2+} is important for myocardial contraction and vasoconstriction, which determine peripheral vascular resistance. Melis and Sainati (1991a) have reported that intravenous infusion of stevioside produces a significant hypotensive effect in a dose-dependent manner, which probably occurs via a vasodilating effect acting through Ca^{2+} pathways. Verapamil, a known Ca^{2+} channel blocker of cardiac and vascular smooth muscles, enhances the systemic effect of stevioside, whereas $CaCl_2$ infusion suppresses the vasodilating response of stevioside (Melis 1992a; Melis and Sainati 1991a). Results using isolated aortic rings supported the notion that stevioside causes vasorelaxation via inhibition of Ca^{2+} influx into the vascular smooth muscle and is not effective in inhibiting intracellular Ca^{2+} release (Lee et al. 2001). This phenomenon was observed in the absence of endothelium (denuded vessel), showing that the vasorelaxation effect of stevioside is not related to nitric oxide. However, the precise mechanism of stevioside antihypertensive action still remains unclear. Indomethacin, a potent prostaglandin inhibitor, is able to abolish stevioside action on blood pressure (Melis and Sainati 1991b), implying that the mechanism also involves prostaglandin interference. In addition, stevioside antihypertensive action occurs without changes in serum dopamine, norepinephrine and epinephrine levels, ruling out changes of sympathetic tone (Chan et al. 1998).

The antihypertensive effects of stevioside and Stevia extract could be partly due to their effects on plasma volume. Intravenous infusion of stevioside in rats induces natriuresis, diuresis and increased renal plasma flow (RPF), but does not affect glomerular filtration rate (GFR) (Melis and Maciel 1986). As these phenomena are

abolished by indomethacin, it was suggested that stevioside may cause vasodilation of both afferent and efferent arterioles, leading to increased RPF with no change in GFR (Melis and Sainati 1991b). The increased urine flow rate or diuresis might have been due to decreased fluid and sodium reabsorption in the proximal tubule. This is supported by the finding of increased glucose clearance following administration of stevioside in rats, indicating a drop in glucose reabsorption by proximal renal tubular cells (Melis 1992b). A diuretic effect of crude extract of *S. rebaudiana* has also been observed following oral administration in rat (Melis 1995, 1996). Furthermore, steviol induces diuresis and natriuresis with no significant changes in RPF and GFR after intravenous injection into rats (Melis 1997).

Both chronic oral intake and acute intravenous administration of stevioside and steviol to rats produce diuresis and natriuresis leading to decreased plasma volume. However, those studies did not allow discrimination of the systemic effect from the direct effect on kidney function. Chatsudthipong and Thongouppakarn (1995) infused stevioside directly into the renal artery of rats and observed diuresis, which occurs as a consequence of decreased proximal tubular reabsorption as indicated by lithium clearance. Stevioside appears not to have any significant impact on blood pressure in humans with normal and low-normal resting blood pressure. The blood pressure-lowering capacity of stevioside is only observed in hypertensive subjects.

2.4 Anti-inflammatory effect

Inflammation can be defined as an early host immune reaction, mediated via immune cells and their cytokines. Inflammation is typically associated with a variety of disorders, such as autoimmune diseases (Atassi and Casali 2008), inflammatory bowel disease (Bamias and Cominelli 2007; Cho 2008), atherosclerosis (Niessner et al. 2007) and cancer (Niessner et al. 2007). The proinflammatory cytokines tumour necrosis factor (TNF)-R and interleukin (IL)-1β, and the reactive free radical nitric oxide (NO) synthesised by inducible NO synthase (iNOS) are the important inflammatory mediators reported to be involved in the development of a number of such inflammatory diseases (Freeman and Natanson 2000). The release of these inflammatory cytokines is essential for host survival from infection and also is required for repair of tissue injury (Glauser 1996). Toll-like receptor 4 (TLR4) is the principal receptor for lipopolysaccharide (LPS) and plays a key role in intracellular signal transduction (Aderem and Ulevitch 2000). Stimulation of monocytes by LPS leads to the phosphorylation of the inhibitor of the transcription nuclear factor kappa B(NF-κB), IκBs, by IκB kinase (IKKs), resulting in the rapid translocation of NF-κB to the nucleus (May and Ghosh 1999). NF-κB activation is involved in expression of cytokine genes, such as TNF-R and IL-1β. Stimulation by LPS is required for NF-κB-dependent expression of TNF-R in human monocytes and Tamm-Horsfall protein (THP)-1 cells.

Stevioside alone can directly activate THP-1, especially at the dose of 1 mM, to release TNF-R and NO. The magnitude of induction of inflammatory mediator is

consistently less than that of LPS stimulation. In LPS-stimulated THP1 cells, stevioside suppresses the release of TNF-α, IL-1β and NO by interfering with the signalling pathway of NF-κB, a transcription factor that controls the expression of inflammatory cytokines in these immune cells (Bunprajun et al. 2012; Fengyang et al. 2012). Stevioside induces TNF-R, IL-1β and NO production in unstimulated human monocytic THP-1 cells. The induction of TNF-R, IL-1β and NO may augment macrophage function and thus contribute to the enhancement of innate immunity. On the other hand, inhibited release of TNF-R, IL-1β and NO in LPS-stimulated THP-1 cells could be of benefit in circumstances where there is a pathological effect resulting from excessive TNF-R, IL-1β and NO production, which may indicate an anti-inflammatory effect of stevioside. Thus, in the case of an infected host, stevioside may be useful due to its ability to prevent undesirable effects of inflammatory response, and in healthy individuals it may offer an immune-related benefit as it can boost monocyte activity (Boonkaewwan et al. 2006, 2008).

2.5 Anticarcinogenic antitumour effects

There is evidence to show that stevioside or Stevia extracts inhibit growth of different types of cancer cells in humans. Isosteviol, one of the components in Stevia extract, inhibits DNA polymerases and human DNA topoisomerase II, cellular targets for pharmacotherapy of cancer as well as inflammatory diseases (Mizushina et al. 2005). Isosteviol acts non-competitively with the DNA template-primer and nucleotide substrate. The compound also reduces 12-O-tetradecanoylphorbol-13-acetate (TPA)-induced inflammation (Yasukawa et al. 2002) known to promote cancer in mammalian cells.

Several studies investigating the effect of stevioside or Stevia extract on tumour development in animals initiated with carcinogens are summarised here.

In vitro screening studies that assessed Epstein–Barr virus activation by treatment of Raji cells with TPA demonstrated no tumour-promoting effects of stevioside or steviol (Konoshima and Takasaki 2002; Okamoto et al. 1983).

Rebaudioside A administered orally (20 mg/kg BW/day; 6.58 mg steviol equivalents/kg BW/day) had no effect on development of colonic aberrant crypt foci in male F344 rats initiated with azoxymethane (Kawamori et al. 1995).

Stevioside at a dietary concentration of 5% (equivalent to 2500 mg/kg BW) had no effect on urinary bladder tumour development in male F344 rats initiated with *N*-butyl-*N*-(hydroxybutyl)nitrosamine (Hagiwara et al. 1984; Ito et al. 1984).

Stevioside or Stevia extract administered topically decreased skin tumour formation in female ICR mice initiated with 7,12-dimethylbenz[a]anthracene and TPA (Konoshima and Takasaki 2002; Yasukawa et al. 2002).

Stevioside induces apoptosis of human breast cancer cells and inhibits cell proliferation through overexpression of Bax in MCF-7. It exhibits antitumour properties which are mediated through G1 arrest and involve signalling pathways, with reactive oxygen species (ROS) being a prime initiating signalling compound (Paul et al. 2012).

2.6 Antioxidant activity

Antioxidants are free radicals that protect the body from oxidative stress due to the effects of oxygen-centred free radicals and ROS (Halliwell and Gutteridge 1999). ROS include the superoxide anion, hydrogen peroxide, hydroxyl radicals and singlet oxygen which cause degenerative human diseases such as cancer (Ames 1983), heart disease (Diaz et al. 1997) and cerebrovascular disease through multiple mechanisms (Huang et al. 2005). Stevioside, along with steviolbioside, isosteviol and steviol, caused inhibition of oxidative phosphorylation including adenosine triphosphate (ATP)ase, nicotinamide adenine dinucleotide (NADH)-oxidase, succinate dehydrogenase, succinate oxidase and glutamate dehydrogenase activity (Kelmer et al. 1985). It has been reported that Stevia leaf extract contains high level of total phenolic compounds and is capable of inhibiting, quenching free radicals to terminate the radical chain reaction, and acting as a reducing agent (Kim et al. 2011; Phansawan and Poungbangpho 2007).

The constituents of *S. rebaudiana* leaves showed strong antioxidant activity by inhibiting 2-diphenyl-1-picrylhydrazyl (DPPH), hydroxyl radical, nitric oxide, superoxide anion scavenging and hydrogen peroxide scavenging activities when compared with standard ascorbic acid (Xi et al. 1998). The percentage inhibition of DPPH radicals of various extracts of Stevia leaves ranges from 33% to 57% (Tadhani et al. 2007). The radical scavenging activity of plant extracts depends on the amount of polyphenolic compounds in the extracts (Shukla et al. 2009). Stevia extract are reported to be a rich source of flavonoid, which has the capacity to scavenge harmful ROS and other free radicals that originate from various cellular activities. The mechanism of action of flavonoids is multifold: it includes the inhibition of enzymes that are involved in ROS generation, chelating of trace metals such as free iron and copper, and the ability to reduce highly oxidising free radicals by donation of hydrogen atoms, thus protecting humans from various serious diseases such as heart attack, stroke and even cancer. Among the flavonoids, quercetin, in its glycosylated form (quercetin-3-O-arabinoside), quercitrin, kaempferol-3-O-rhamnoside, apigenin, luteolin and apigenin-4-O-glucoside are present. The strong radical scavenging activity and oxidative DNA damage-preventing activity of Stevia extract may be correlated with its rich content of flavonoids (Ghanta et al. 2007).

2.7 Antimicrobial and antidiarrhoeal effects

Stevia rebaudiana leaf extracts demonstrate antibacterial, antifungal, anti-yeast and antitumour activity. Stevia extract inhibits the food-related pathogens *Serratia marcescens*, *Klebsiella pneumoniae*, *Bacillus cereus*, *Pseudomonas aeruginosa*, *B. subtilis*, *Alcaligenes denitrificans* and *Salmonella typhimurium* (Puri and Sharma 2011). Tadhani and Subhash (2006) have reported that the antibacterial activity of Stevia extract is lower than the standard agent (ciproflaxcin). However, in cases of fungal organisms, the activity is significantly higher than the standard

(amphotericin-B in this case). Stevia extracted by organic solvents seems to have more bactericidal property than the aqueous extract (Jayaraman et al. 2008). Stevia extracts show potential inhibitory effects for all four serotypes of human rotavirus (HRV) (Takahashi et al. 2000). The inhibitory mechanism is blocking of the binding of anti-VP7 monoclonal antibodies to HRV-infected MA104 cells. The inhibitory components of the extract are heterogeneous anionic polysaccharides having different ion charges. The Stevia extract binds to VP7 and interferes with the binding of VP7 to the cellular receptors by steric hindrance, resulting in blockage of the virus attachment to the cells (Takahashi et al. 2001).

Diarrhoea can be categorised into four types: secretory, osmotic, motility related and exudative (Binder 1990). Currently, the mainstay of diarrhoeal therapy is rehydration therapy and antibiotic treatment. As stevioside is known to exert a bactericidal effect on a broad range of food-borne pathogens, including enterohaemorrhagic *Escherichia coli*, known to cause severe haemorrhagic/exudative diarrhoea, it may be a potential drug for treatment of diarrhoea (Tomita et al. 1997). Stevioside shows an inhibitory effect on intestinal smooth muscle contraction, stimulation of which results in hypermotility-associated diarrhoea (Shiozaki et al. 2006).

Pariwat et al. (2008) have shown that stevioside and other glycosides present in Stevia extract have a potential in the treatment of secretory diarrhoea. Stimulation of active chloride secretion followed by paracellular transport of sodium and water due to the release of enterotoxin by bacteria and subsequent enterotoxin-mediated hypersecretory response in the intestine leads to massive bodily fluid loss and dehydration in secretory diarrhoea. Steviol and dihydroisosteviol (but not stevioside) inhibit the cAMP-activated chloride signal channel, responsible for chloride secretion in the specific intestinal cells (Pariwat et al. 2008). Steviol-related compounds perform comparatively well in contrast to other cAMP-activated chloride channel inhibitors (Muanprasat et al. 2007; Sonawane et al. 2007, 2008), hence, they are potential candidates for diarrhoeal therapy.

2.8 Effect on renal function

Probably the most complex role of stevioside and steviol, so far, is their interaction with renal ion transporters in the body. Excessive (more than the acceptable daily intake – ADI) oral administration to rats of an aqueous extract induces systemic and renal vasodilation, causing hypotension, diuresis and natriuresis per milliliter of glomerular filtration rate (Melis 1995; Melis and Sainati 1991b). Stevioside and its aglycone metabolite steviol have been shown to inhibit the transepithelial transport of para-aminohippurate (PAH) in the renal proximal tubules of rabbits by interfering with the basolateral entry (Toskulkao et al. 1994). The precise mechanism by which stevioside and steviol inhibit PAH transepithelial transport still remains unclear, but some findings indicate a role in inhibiting or interfering with basolateral organic anion transporters (OATs) (Chatsudthipong and Jutabha 2001;

Jutabha et al. 2000). The interaction of stevioside and steviol with OATs in PAH transport is very much species selective, dose dependent and time varying (Burckhardt et al. 2001; Dantzler and Wright 2003).

The interaction of stevioside and steviol with organic cation transporters (OCTs) has been studied in Chinese hamster ovary cells (Chatsudthipong et al. 2003). The results reveal that steviol but not stevioside inhibits organic cation uptake via these transporters in a dose-dependent manner. The inhibitory effect of steviol has been reported to be more than significant and the latter is restricted to its function only in the intact renal tubules. At the level of maximum allowable intake of Stevia extract specified for human consumption, neither stevioside nor Stevia has any effect on the renal transport system. Renal proximal tubules serve an important function in elimination of various compounds and xenobiotics via the organic anion and cation secretory systems (Pritchard and Miller 1993). Hence, interference or inhibition of these secretory transport systems reduces clearance of xenobiotics and therapeutic drugs, potentially leading to altered therapeutic efficacy of such drugs. This particular feature can be exploited in future to delay clearance of drugs, leading to enhanced efficacy.

There are several other beneficial effects of stevioside and Stevia extract intake, including inhibitory effect of stevioside in skin tumour promotion (Yasukawa et al. 2002), antituberculosis effects (Sharipova et al. 2011), inhibition of arteriosclerosis (Geeraert et al. 2010), gastroprotective activity (Shiozaki et al. 2006), antiamnesic effects (Sharma et al. 2010) and immunomodulatory activities (Boonkaewwan et al. 2006; Sehar et al. 2008).

Several safety evaluations of stevioside and Stevia extract have been undertaken to verify toxicity levels, mutagenicity, carcinogenicity, genotoxicity and fertility issues, all of which were found to be negative (Curry 2010; EFSA, 2010; FAO 2010; FSANZ 2008; Geuns 2002; WHO 2009). These results confirm that stevioside, and other glycosides present in Stevia extract, are potentially safe for human consumption and do not imply any health hazard on prolonged usage.

References

Abudula, R., Jeppesen, P.B., Rolfsen, S.E.D., Xiao, J., Hermansen, K. (2004) Rebaudioside A potently stimulates insulin secretion from isolated mouse islets: studies on the dose-, glucose-, calcium-dependency. Metabolism 53, 1378 – 1381.

Abudula, R., Matchkov, V.V., Jeppesen, P.B., Nilsson, H., Aalkjær, C., Hermansen, K. (2008) Rebaudioside A directly stimulates insulin secretion from pancreatic beta cells: a glucose-dependent action via inhibition of ATP-sensitive K + -channels. Diabetes Obes Metab 10, 1074 – 1085.

Aderem, S., Ulevitch, R.J. (2000) Toll-like receptors in the induction of the innate immune response. Nature 406, 782–787.

Ames, B.N. (1983) Dietary carcinogens and anticarcinogens: oxygen radicals and degenerative diseases. Science 221, 1256–1264.

Atassi, M.Z., Casali, P. (2008) Molecular mechanisms of autoimmunity. Autoimmunity 41, 123 – 132.

Atteh, J., Onagbesan, O., Tona, K., Decuypere, E., Geuns, J., Buyse, J. (2008) Evaluation of supplementary Stevia (Stevia Rebaudiana, bertoni) leaves and Stevioside in broiler diets: effects on feed intake, nutrient metabolism, blood parameters and growth performance. J Anim Physiol Anim Nutr (Berl) 92, 640–649.

Bamias, G., Cominelli, F. (2007) Immunopathogenesis of inflammatory bowel disease: current concepts. Curr Opin Gastroenterol 23, 365 – 369.

Barriocanal, L.A., Palacios, M., Benitez, G., et al. (2008) Apparent lack of pharmacological effect of Steviol glycosides used as sweeteners in humans. A pilot study of repeated exposures in some normotensive and hypotensive individuals and in Type 1 and Type 2 diabetics. Regul Toxicol Pharmacol 51, 37 – 41.

Binder, H.J. (1990) Pathophysiology of acute diarrhea. Am J Med 88, 2S – 4S.

Blauth de Slavutzky, S.M. (2010) Stevia and sucrose effect on plaque formation. J Consum Prot Food Saf 5, 213–216.

Boonkaewwan, C., Toskulkao, C., Vongsakul, M. (2006) Anti-inflammatory and immunomodulatory activities of Stevioside and its metabolite Steviol on THP-1 cells. J Agri Food Chem 54, 785 – 789.

Boonkaewwan, C., Ao, M., Toskulkao, C., Rao, M.C. (2008) Specific immunomodulatory and secretory activities of Stevioside and Steviol in intestinal cells. J Agri Food Chem 56, 3777 – 3784.

Bunprajun, T., Yimlamai, T., Soodvilai, S., Muanprasat, C., Chatsudthipong, V. (2012) Stevioside enhances satellite cell activation by inhibiting of NF-κB signaling pathway in regenerating muscle after cardiotoxin-induced injury. J Agri Food Chem 60, 2844 – 2851.

Burckhardt, G., Bahn, A., Wolff, N.A. (2001) Molecular physiology of renal p-aminohippurate secretion. News Physiol Sci 16, 114 – 118.

Cardoso, V.N., Barbosa, M.F., Muramoto, E., Mesquita, C.H., Almeida, M.A. (1996) Pharmacokinetic studies of 131I-Stevioside and its metabolites. Nucl Med Biol 23, 97 – 100.

Chan, P., Xu, D.Y., Liu, J.C., et al. (1998) The effect of Stevioside on blood pressure and plasma catecholamines in spontaneously hypertensive rats. Life Sci 63, 1679 – 1684.

Chan, P., Linson, B., Chen, Y., Liu, J., Hsieh, M., Cheng, J. (2000) A double blind placebo-controlled study of the effectiveness and tolerability of oral Stevioside in human hypertension. Br J Clin Pharmacol 50, 215–220.

Chang, J.C., Wu, M.C., Liu, I. M., Cheng, J.T. (2005) Increase of insulin sensitivity by Stevioside in fructose-rich chow-fed rats. Horm Metab Res 37, 610 – 616.

Chatsudthipong,V., Jutabha, P. (2001) Effect of Steviol on para-aminohippurate transport by isolated perfused rabbit renal proximal tubule. J Pharmacol Exp Ther 298, 1120 – 1127.

Chatsudthipong, V., Muanprasat, C. (2009) Stevioside and related compounds: therapeutic benefits beyond sweetness. Pharmacol Therapeut 121, 41–54.

Chatsudthipong, V., Thongouppakarn, P. (1995) Effects and mechanism of Stevioside on rat renal function. FASEB J 9, A917.

Chatsudthipong, V., Lungkaphin, A., Kaewmokul, S. (2003) The interaction of Steviol with rabbit OCT1 and OCT2. FASEB J 17, A476.

Chen, T.H., Chen, S.C., Chan, P., Chu, Y.L., Yang, H.Y., Cheng, J.T. (2005) Mechanism of the hypoglycemic effect of Stevioside, a glycoside of Stevia Rebaudiana. Planta Med 71, 108 – 113.

Cho, J.H. (2008) The genetics and immunopathogenesis of inflammatory bowel disease. Nat Rev Immunol 8, 458 – 466.

Curry, L.L. (2010) *Agency Response Letter GRAS Notice No. GRN 000287*. Washington, DC: Food and Drug Administration. http://www.accessdata.fda.gov/scripts/fcn/gras_notices/grn000287.pdf

Dantzler, W.H., Wright, S.H. (2003) The molecular and cellular physiology of basolateral organic anion transport in mammalian renal tubules. Biochim Biophys Acta 1618, 185 – 193.

Diaz, M.N., Frei, B., Vita, J.A., Keaney, J.F. (1997) Antioxidants and atherosclerotic heart disease. N Engl J Med 337, 408–416.

EFSA (European Food Safety Authority) (2010) Scientific opinion on the safety of Steviol glycosides for the proposed uses as a food additive. EFSA Panel on Food Additives and Nutrient Sources added to Food (ANS). EFSA J 8, 1537.

FAO (Food and Agriculture Organisation) (2010) *Steviol Glycosides*. FAO JECFA Monographs 10. Rome: Food and Agriculture Organisation.

Fengyang, L., Yunhe, F., Bo, L., et al. (2012) Stevioside suppressed inflammatory cytokine secretion by downregulation of NF-κB and MAPK signaling pathways in LPS-stimulated RAW264.7 cells. Inflammation 35, 1669–1675.

Freeman, B.D., Natanson, C. (2000) Anti-inflammatory therapies in sepsis and septic shock. Expert Opin V Drugs 9, 1651–1663.

FSANZ (Food Standards Australia New Zealand) (2008) *Final Assessment Report, Application A540, Steviol Glycosides as Intense Sweeteners*. Canberra: Food Standards Australia New Zealand.

Gardana, C., Simonetti, P., Canzi, E., Zanchi, R., Pieta, P. (2003) Metabolism of Stevioside and rebaudioside A from Stevia Rebaudiana extracts by human microflora. J Agri Food Chem 51, 6618–6622.

Geeraert, B., Crombe, F., Hulsmans, M., Benhabile, N., Geuns, J.M.C., Holvoet, P. (2010) Stevioside inhibits atherosclerosis by improving insulin signaling and antioxidant defense in obese insulin-resistant mice. Int J Obes 34, 569–577.

Geuns, J.M.C. (2002) Safety evaluation of Stevia and Stevioside. Studies Nat Prod Chem 27, 299–319.

Geuns, J.M.C. (2007) Letter to the Editor: Comments to the paper by Nunes et al. (2007), Analysis of genotoxic potentiality of Stevioside by comet assay. Food Chem Toxicol 45, 662–666.

Geuns, J.M.C., Augustijns, P., Mols, R., Buyse, J.G., Driessen, B. (2003) Metabolism of Stevioside in pigs and intestinal absorption characteristics of Stevioside, rebaudioside A and Steviol. Food Chem Toxicol 41, 1599–1607.

Geuns, J.M.C., Buyse, J., Vankeirsbilck, A., Temme, E.H.M., Compernolle, F., Toppet, S. (2006) Identification of Steviol glucuronide in human urine. J Agri Food Chem 54, 2794 – 2798.

Ghanta, S. Banerjee, A., Poddar, A., Chattopadhyay, S. (2007) Oxidative DNA damage preventive activity and antioxidant potential of Stevia Rebaudiana (Bertoni) Bertoni, a natural sweetener. J Agri Food Chem 55, 10962–10967.

Giffin, B.F., Drake, R.L., Morris, R.E., Cardell, R.R. (1993) Hepatic lobular patterns of phosphoenolpyruvate carboxykinase, glycogen synthase, glycogen phosphorylase in fasted and fed rats. J. Histochem Cytochem 41, 1849 – 1862.

Glauser, M.P. (1996) The inflammatory cytokines: new developments in the pathophysiology and treatment of septic shock. Drugs 52, 9–17.

Goyal, S.K., Samsher, Goyal, R.K. (2010) Stevia (Stevia Rebaudiana), a bio-sweetener: a review. Int J Food Sci Nutr 61, 1–10. http://informahealthcare.com/doi/abs/10.3109/09637480903193049

Hagiwara, A., Fukushima, S., Kitaori, M., Shibata, M., Ito, N. (1984) Effects of three sweeteners on rat urinary bladder carcinogenesis initiated by N-butyl-N-(4-hydroxybutyl) nitrosamine. Gann 75, 763–768.

Halliwell, B., Gutteridge, J.M.C. (1999) *Free Radicals in Biology and Medicine*. Oxford: Oxford University Press.

Hong, J., Chen, L., Jeppesen, P. B., Nordentoft, I., Hermansen, K. (2006) Stevioside counteracts the α-cell hypersecretion caused by long-term palmitate exposure. Am J Physiol Endocrinol Metab 290, E416 – E422.

Hsieh, M.H., Chan, P., Sue, Y.M., et al. (2003) Efficacy and tolerability of oral Stevioside in patients with mild essential hypertension: a two-year, randomized, placebo-controlled study. Clin Ther 25, 2797 – 2808.

Huang, D., Ou, B., Priop, R. L. (2005) The chemistry behind antioxidant capacity assays. J Agri Food Chem 53, 1841–1856.

Humboldt, G., Boech, E.M. (1977) Efeito do edulcorante natural (Stevioside) e sinte' tico (sacarina) sobre o ritmo cardiaco em ratos. Arq Bras Cardiol 30, 257 – 277.

Hutapea, A.M., Toskulkao, C., Buddhasukh, D., Wilairat, P., Glinsukon, T. (1997) Digestion of Stevioside, a natural sweetener, by various digestive enzymes. J Clin Biochem Nutr 23, 177 – 186.

Ito, N., Fukushima, S., Shirai, T., Hagiwara, A., Imaida, K. (1984) Drugs, food additives and natural products as promoters in rat urinary bladder carcinogenesis. In: Börzsönyi, M., Day, N.E., Lapis, K., Yamasaki, H. (eds) *Models, Mechanisms and Etiology of Tumour Promotion*. IARC Scientific Publication No. 56. Lyon: International Agency for Research on Cancer, pp399–407.

Jayaraman, S., Manoharan, M.S., Illanchezian, S. (2008) In-vitro antimicrobial and antitumor activities of Stevia Rebaudiana (Asteraceae) leaf extracts. Trop J Pharmaceut Res 7, 1143–1149.

Jeppesen, P.B., Gregersen, S., Poulsen, C.R., Hermansen, K. (2000) Stevioside acts directly on pancreatic β cells to secrete insulin: actions independent of cyclic adenosine monophosphate and adenosine triphosphate-sensitive K^+-channel activity. Metabolism 49, 208 – 214.

Jeppesen, P.B., Gregersen, S., Alstrup, K.K., Hermansen, K. (2002) Stevioside induces antihyperglycaemic, insulinotropic and glucagonostatic effects in vivo: studies in the diabetic Goto-Kakizaki (GK) rats. Phytomedicine 9, 9 – 14.

Jeppesen, P.B., Gregersen, S., Rolfsen, S.E.D., et al. (2003) Antihyperglycemic and blood pressure-reducing effects of Stevioside in the diabetic Goto-Kakizaki rat. Metabolism 52, 372 – 378.

Jutabha, P., Toskulkao, C., Chatsudthipong, V. (2000) Effect of Stevioside on PAH transport by isolated perfused rabbit renal proximal tubule. Can J Physiol Pharmacol 78, 737 – 744.

Kawamori, T., Tanaka, T., Hara, A., Yamahara, J., Mori, H. (1995) Modifying effects of naturally occurring products on the development of colonic aberrant crypt foci induced by azoxymethane in F344 rats. Cancer Res 55, 1277–1282.

Kelmer, B.A., Alvarez, M., Brancht, A. (1985) Effects of Stevia Rebaudiana natural products on rat liver mitochondria. Biochem Pharmacol 34, 873–882.

Kim, I.S., Yang, M., Lee, O.H., Kang, S.K. (2011) The antioxidant activity and the bioactive compound content of Stevia Rebaudiana water extracts. LWT Food Sci Technol 44, 1328–1332.

Kochikyan, V., Markosyan, A., Abelyan, L., Balayan, A., Abelyan, V. (2006) Combined enzymatic modification of Stevioside and rebaudioside A. Appl Biochem Microbiol 42, 31–37.

Konoshima, T., Takasaki, M. (2002) Cancer-chemopreventive effects of natural sweeteners and related compounds. Pure Appl Chem 74, 1309–1316.

Koyama, E., Sakai, N., Ohori, Y. et al. (2003a) Absorption and metabolism of glycosidic sweeteners of Stevia mixture and their aglycone, Steviol in rats and humans. Food Chem Toxicol 41, 875–883.

Koyama, E., Kitazawa, K., Ohori, Y. et al. (2003b) In vitro metabolism of the glycosidic sweeteners, Stevia mixture and enzymatically modified Stevia in human intestinal microflora. Food Chem Toxicol 41, 359 – 374.

Kwon, T.H., Fulton, C., Wang, W. et al. (2002) Chronic metabolic acidosis upregulates rat kidney Na-HCO_3^- cotransporters NBCn1 and NBC3 but not NBC1. Am J Physiol Renal Physiol 282, F341–F351.

Lailerd, N., Saengsirisuwan, V., Sloniger, J.A., Toskulkao, C., Henriksen, E.J. (2004) Effects of Stevioside on glucose transport activity in insulin-sensitive and insulin resistant rat skeletal muscle. Metabolism 53, 101 – 107.

Lee, C.N., Wong, K.L., Liu, J.C., Chen, Y.J., Cheng, J.T., Chan, P. (2001) Inhibitory effect of Stevioside on calcium influx to produce antihypertension. Planta Med 67, 796 – 799.

Maki, K.C., Curry, L.L., Reeves, M.S., et al. (2008) Chronic consumption of rebaudioside A, a Steviol glycoside, in men and women with type 2 diabetes mellitus. Food Chem Toxicol 46, S47 – 53.

May, M.J., Ghosh, S. (1999) IκB kinases: kinsmen with different crafts. Science 284, 271–273.

Melis, E. (1997) Effects of Steviol on renal function and mean arterial pressure in rats. Phytomedicine 3, 349 – 352.

Melis, M.S. (1992a) Influence of calcium on the blood pressure and renal effects of Stevioside. Braz J Med Biol Res 25, 943 – 949.

Melis, M.S. (1992b) Renal excretion of Stevioside in rats. J Nat Prod 55(5), 688 – 690.

Melis, M.S. (1995) Chronic administration of aqueous extract of Stevia Rebaudiana in rats: renal effects. J. Ethnopharmacol 47, 129 – 134.

Melis, M.S. (1996) A crude extract of Stevia Rebaudiana increases the renal plasma flow of normal and hypertensive rats. Braz J Med Biol Res 29, 669 – 675.

Melis, M.S., Maciel, R.E. (1986) Participaçäo das prostaglandinas no mecanismo da açäo renal do verapamil (Effect of prostaglandins on the renal mechanisms of action of verapamil). Ciênc Cult 38, 154–159.

Melis, M.S., Sainati, A.R. (1991a) Effect of calcium and verapamil on renal function of rats during treatment with Stevioside. J. Ethnopharmacol 33, 257 – 262.

Melis, M.S., Sainati, A.R. (1991b) Participation of prostaglandins in the effect of Stevioside on rat renal function and arterial pressure. Braz J Med Biol Res 24, 1269 – 1276.

Mizushina, Y., Akihisa, T., Ukiya, M. et al. (2005) Structural analysis of isosteviol and related compounds as DNA polymerase and DNA topoisomerase inhibitors. Life Sci 77, 2127 – 2140.

Muanprasat, C., Kaewmokul, S., Chatsudthipong, V. (2007) Identification of new small molecule inhibitors of cystic fibrosis transmembrane conductance regulator protein: in vitro and in vivo studies. Biol Pharm Bull 30, 502 – 507.

Nakayama, K., Kasahara, D., Yamamoto, F. (1986) Absorption, distribution, metabolism and excretion in rats. J Food Hyg Soc Jpn 27, 1 – 8.

Niessner, A., Goronzy, J.J., Weyand, C.M. (2007) Immune-mediated mechanisms in atherosclerosis: prevention and treatment of clinical manifestations. Curr Pharm Des 13, 3701 – 3710.

Nordentoft, I., Jeppesen, P.B., Hong, J., Abudula, R., Hermansen, K. (2008) Isosteviol increases insulin sensitivity and changes gene expression of key insulin regulatory genes and transcription factors in islets of the diabetic KKAy mouse. Diabetes Obes Metab 10, 939 – 949.

Okamoto, H., Yoshida, D., Mizusaki, S. (1983) Inhibition of 12-O-tetradecanoylphorbol-13-acetateinduced induction in Epstein–Barr virus early antigen in Raji cells. Cancer Lett 19, 47–53.

Pariwat, P., Homvisasevongsa, S., Muanprasat, C., Chatsudthipong, V. (2008) A natural plant-derived dihydroisosteviol prevents cholera toxin-induced intestinal fluid secretion. J Pharmacol Exp Ther 324, 798 – 805.

Paul, S., Sengupta, S., Bandyopadhay, T.K., Bhattacharyya, A. (2012) Stevioside induced ROS-mediated apoptosis through mitochondrial pathway in human breast cancer cell line MCF-7. Nutr Cancer 64, 1087–1094.

Phansawan, B., Poungbangpho, S. (2007) Antioxidant capacities of Pueraria mirifica, Stevia Rebaudiana Bertoni, Curcuma longa Linn., Andrographis paniculata (Burm.f.) Nees. and Cassia alata Linn. for the development of dietary supplement. Kasetsart J (Nat Sci) 41, 548–554.

Pól, J., Hohnová, B., Hyötyläinen, T. (2007) Characterization of Stevia Rebaudiana by comprehensive two-dimensional liquid chromatography time-of-flight mass spectrometry. J Chromatogr A 1150, 85–92.

Pritchard, J.B., Miller, D.S. (1993) Mechanisms mediating renal secretion of organic anions and cations. Physiol Rev 73, 765 – 796.

Puri, M., Sharma, D. (2011) Antibacterial activity of Stevioside towards food-borne pathogenic bacteria. Eng Life Sci 11, 326–329.

Renwick, A.G. (2008). Toxicokinetics [section on elimination: excretion via the gut]. In: Hayes, W. (ed) *Principles and Methods of Toxicology*, 5th edn. Philadelphia: Taylor and Francis/CRC Press, p188.

Renwick, A.G., Molinary, S.V. (2010) Sweet-taste receptors, low-energy sweeteners, glucose absorption and insulin release. Br J Nutr 104, 1415–1420.

Renwick, A.G., Tarka, S.M. (2008) Microbial hydrolysis of Steviol glycosides. Food Chem Toxicol 46, S70–S74.

Roberts, A., Renwick, A.G. (2008) Comparative toxicokinetics and metabolism of rebaudioside A, Stevioside, and Steviol in rats. Food Chem Toxicol 46, S31 – 39.

Sehar, I., Kaul, A., Bani, S., Pal, H.C., Saxena, A.K. (2008) Immune up regulatory response of a non-caloric natural sweetener, Stevioside. Chem Biol Interact 173, 115 – 121.

Sharipova, R.R., Strobykina, I.Y., Mordovskoi, G.G., Chestnova, R.V., Mironov, V.F., Kataev, V.E. (2011) Antituberculosis activity of glycosides from Stevia Rebaudiana and hybrid compounds of steviolbioside and pyridinecarboxylic acid hydrazides. Chem Natur Compound 46(6), 902–905.

Sharma, A., Puri, M., Tiwary, A.K., Singh, N., Jaggi, A.S. (2010) Antiamnesic effect of Stevioside in scopolamine-treated rats. Ind J Pharmacol 42, 164–167.

Shiozaki, K., Fujii, A., Nakano, T., Yamaguchi, T., Sato, M. (2006) Inhibitory effects of hot water extract of the Stevia stem on the contractile response of the smooth muscle of the guinea pig ileum. Biosci Biotechnol Biochem 70, 489 – 494.

Shukla, S., Mehta, A., Bajpai, V.K., Shukla, S. (2009) In vitro antioxidant activity and total phenolic content of ethanolic leaf extract of Stevia Rebaudiana Bert. Food Chem Toxicol 47, 2338–2343.

Sonawane, N.D., Zhao, D., Zegarra-Moran, O., Galietta, L.J., Verkman, A.S. (2007) Lectin conjugates as potent, nonabsorbable CFTR inhibitors for reducing intestinal fluid secretion in cholera. Gastroenterology 132, 1234 – 1244.

Sonawane, N.D., Zhao, D., Zegarra-Moran, O., Galietta, L.J., Verkman, A.S. (2008) Nanomolar CFTR inhibition by pore-occluding divalent polyethylene glycolmalonic acid hydrazides. Chem Biol 15, 718 – 728.

Srimaroeng, C., Chatsudthipong, V., Aslamkhan, A.G., Pritchard, J.B. (2005). Transport of the natural sweetener Stevioside and its aglycone Steviol by human organic anion transporter (hOAT1; SLC22A6) and hOAT3 (SLC22A8). J Pharmacol Exp Ther 313, 621 – 628.

Suanarunsawat, T., Chaiyabutr, N. (1997) The effect of Steviosides on glucose metabolism in rat. Can J Physiol Pharmacol 75, 976–982.

Tadhani, M.B., Subhash, R. (2006) In vitro antimicrobial activity of Stevia Rebaudiana Bertoni leaves. Trop J Pharmaceut Res 5, 557–560.

Tadhani, M.B., Patel, V.H., Subhash, R. (2007) In vitro antioxidant activities of Stevia Rebaudiana leaves and callus. J Food Comp Anal 20, 323–329.

Takahashi, K., Mori, S., Sato, N., Shigeta, S. (2000) Extract of Stevia rebaudiana is a potent anti-rotavirus inhibitor in vitro and in vivo. Antiviral Res 46, A67.

Takahashi, K., Matsuda, M., Ohashi, K. et al. (2001) Analysis of anti-rota virus activity of extract from Stevia Rebaudiana. Antiviral Res 49, 15–24.

Tomita, T., Sato, N., Arai, T. et al. (1997) Bactericidal activity of a fermented hot-water extract from Stevia Rebaudiana Bertoni towards enterohemorrhagic Escherichia coli O157:H7 and other food-borne pathogenic bacteria. Microbiol Immunol 41, 1005 – 1009.

Toskulkao, C., Deechakawan, W., Leardkamolkarn, V., Glinsukon, T., Buddhasukh, D. (1994) The low calorie natural sweetener Stevioside: nephrotoxicity and its relationship to urinary enzyme excretion in the rat. Phytother Res 8, 281 – 286.

UKPDS Group (UK Prospective Diabetes Study Group) (1998a) Intensive blood-glucose control with sulphonylureas or insulin compared with conventional treatment and risk of complications in patients with type 2 diabetes (UKPDS 33). Lancet 352, 837 – 853.

UKPDS Group (UK Prospective Diabetes Study Group) (1998b) Tight blood pressure control and risk of macrovascular and microvascular complications in type 2 diabetes: UKPDS 38. BMJ 317, 703 – 713.

Wheeler, A., Boileau, A.C., Winkler, P.C. et al. (2008) Pharmacokinetics of rebaudioside A and Stevioside after single oral doses in healthy men. Food Chem Toxicol 46, S54 – S60.

WHO (World Health Organisation) (2009) *Safety Evaluation of Certain Food Additives. Steviol Glycosides (Addendum)*. Joint FAO/WHO Expert Committee on Food Additives. WHO Food Additive Series No. 60. Geneva: WHO.

Wingard, R.E., Brown, J.P., Enderlin, F.E., Dale, J.A., Hale, R.L., Seitz, C.T. (1980) Intestinal degradation and absorption of the glycosidic sweeteners Stevioside and rebaudioside A. Experientia 36, 519–520.

Yasukawa, K., Kitanaka, S., Seo, S. (2002) Inhibitory effect of Stevioside on tumor promotion by 12-O-tetradecanoylphorbol-13-acetate in two-stage carcinogenesis in mouse skin. Biol Pharm Bull 25, 1488 – 1490.

Xi, Y., Yamaguchi, T., Sato, M., Takeuchi, M. (1998) Antioxidant mechanism of Stevia Rebaudiana extract and antioxidant activity of inorganic salts. Nippon Kagaku Kaishi 45, 317–322.

3
Applications of stevioside

Stevia-based sweeteners offer a combination of favourable attributes for a dietary supplement: low calorie and high intensity. They can be specifically used for diabetic patients as a low-calorie/dietetic population and by others as an alternative to traditional sugar (i.e. corn syrup, fructose, glucose, sucrose, etc.).

The major application of Stevia extracts and stevioside is their use as a sweetener and dietary supplement; this covers all aspects of artificial sweeteners (non-sucrose) such as saccharin, aspartame, etc., as well as where sugar is used (Lemus-Mondaca et al. 2012). Steviol glycosides as a food additive significantly enhance the palatability of food and drinks. However, other uses beyond sweetness, including therapeutic benefits and medicinal value, have also been reported (Chatsudthipong and Muanprasat 2009). In addition, stevioside can also be used in chewing gum, toothpaste and some cosmetics. This low-calorie natural sweetener is used extensively in various food products such as biscuits, jams, chocolates, ice-creams, baked foods, soft drinks and fruit drinks (Goyal et al. 2010; Jayaraman et al. 2008; Tadhani and Subhash 2006; Wallin 2007), sauces, sweet corn, delicacies, pickles (Koyama et al. 2003), yoghurt (Amzad-Hossain et al. 2010; Tadhani and Subhash 2006; Wallin 2007), candies (Goyal et al. 2010; Koyama et al. 2003), soju, soy sauce (Amzad-Hossain et al. 2010; Tadhani and Subhash 2006), sea foods (Goyal et al. 2010; Koyama et al. 2003) and the common beverages like diptea, coffee and herbal tea, as it is heat-stable up to 200 °C, acid stable and not fermentable.

Although Stevia sweeteners possess a slightly latent sweetness compared to sucrose, their use has been expanding steadily, due to various characteristics including the following:

1. Approximately 300 times sweeter than sucrose and costing comparatively less than sugar with the development of economic technology.
2. Sweetness quality is superior to sucrose in mildness and refreshment.

Stevioside: Technology, Applications and Health, First Edition.
Sirshendu De, Sourav Mondal and Suvrajit Banerjee.

3. Sweetness is intensified by combining with salts and organic acids.
4. Latent sweetness is improved slightly with the addition of sugars.
5. 'Salt-softening' property is evident and this effect is improved with glycyrrhizin.
6. Stable at high temperature and across a wide pH range.
7. Substantially non-nutritive and non-cariogenic.
8. Fermentation and spoiling in soy sauce, soybean paste, pickles, etc.
9. Burning in bread, biscuits, fried foods, etc.
10. Colouring in foods containing amino acids through the Maillard reaction.
11. Hardening in baking of bread, biscuits, etc.
12. Absorption of moisture in dried foods and baked foods such as biscuits.
13. Depression of freezing point in ice creams, sherbets and frozen foods.

While Stevia sweeteners can be used in a wide variety of products, it is first necessary to identify the purpose for using them, i.e. as a sweetener, taste modifier, sugar defect eliminator or calorie reducer, before deciding on the type and amount of sweetener to be used (EFSA 2010). The level of use of Stevia and other artificial sweeteners in different dietary products is presented in Table 3.1.

The confectionery industry has yet to reap the benefit of Stevia, which can replace sugar as a sweetener. Stevia can be used in chocolates and candies, not only to meet market demand by diabetics but also to harvest the added advantage of this herb's actions against tooth decay. Stevia possesses an antimicrobial property which can be of great benefit to children, as it does not enhance the growth of pathogenic bacteria in the teeth, unlike sugar. Use of stevioside in various food formulations, i.e. herbal tea, bakery, confectionery, toothpaste, mouth refreshers, candies, chewing gums, etc., may protect from pathogenic bacteria such as *Bacillus cereus*, *Klebsiella pneumoniae* and *Pseudomonas aeruginosa*. These are the root causes of many food-borne diseases such as enteric fever, diarrhoea, etc. (Puri and Sharma 2011). Cargill, one of the world's largest agribusiness and trading companies, markets stevioside for its use in food such as yoghurt, cereals, ice cream and sweets (Lindsay 2007).

The leaves of Stevia impart a pleasant flavour apart from increasing the sweetness of the product. Fresh fruit juice can be enhanced by the addition of this natural sweetener, instead of cane sugar. Sweet-deprived diabetics can relish their favourite sweets with Stevia, in addition to the health-restoring activity of this herb. Different practical applications of Stevia extract in various forms are reported in Table 3.1.

The bakery industry may also benefit from the use of Stevia. All cooked and baked food items such as puddings and cakes can be sweetened with only very

Table 3.1 Maximum level of usage of different sweeteners in food products

Food stuff	Maximum use levels		
	Aspartame	Steviol glycosides	Steviol equivalents
Non-alcoholic drinks			
Water-based flavoured drinks, energy reduced or with no added sugar	600 mg/L	600 mg/L	198 mg/L
Milk- and milk derivative-based or fruit juice-based drinks, energy reduced or with no added sugar	600 mg/L	1000 mg/L	330 mg/L
Desserts and similar products			
Water-based flavoured desserts, energy reduced or with no added sugar	1000 mg/kg	1000 mg/kg	330 mg/kg
Milk- and milk derivate-based preparations, energy reduced or with no added sugar	1000 mg/kg	1000 mg/kg	330 mg/kg
Fruit- and vegetable-based desserts, energy reduced or with no added sugar	1000 mg/kg	1000 mg/kg	330 mg/kg
Egg-based desserts, energy reduced or with no added sugar	1000 mg/kg	1000 mg/kg	330 mg/kg
Cereal-based desserts, energy reduced or with no added sugar	1000 mg/kg	1000 mg/kg	330 mg/kg
Fat-based desserts, energy reduced or with no added sugar	1000 mg/kg	1000 mg/kg	330 mg/kg
'Snacks': certain flavours of ready-to-eat, prepacked, dry, savoury starch products and coated nuts	500 mg/kg	500 mg/kg	165 mg/kg
Confectionery			
Confectionery with no added sugar	1000 mg/kg	1000/1500 mg/kg (hard/soft candy)	330/495 mg/kg (hard/soft candy)
Cocoa- or dried fruit-based confectionery, energy reduced or with no added sugar	2000 mg/kg	2000 mg/kg	660 mg/kg
Starch-based confectionery, energy reduced or with no added sugar	2000 mg/kg	2000 mg/kg	660 mg/kg
Cocoa-, milk-, dried fruit- or fat-based sandwich spreads, energy reduced or with no added sugar	1000 mg/kg	1000 mg/kg	330 mg/kg
Chewing gum with no added sugar	5500 mg/kg	10 000 mg/kg	3300 mg/kg
Cider and perry	600 mg/L	600 mg/L	198 mg/L
Alcohol-free beer or with an alcohol content not exceeding 1.2% vol	600 mg/L	600 mg/L	198 mg/L
Beers with a minimum acidity of 30 milli-equivalents expressed as NaOH	600 mg/L	600 mg/L	198 mg/L
Brown beers of the 'oud bruin' type	600 mg/L	600 mg/L	198 mg/L
Edible ices, energy reduced or with no added sugar	800 mg/L	800 mg/L	264 mg/L

(*Continued*)

Table 3.1 (Continued)

Food stuff	Maximum use levels		
	Aspartame	Steviol glycosides	Steviol equivalents
Canned or bottled fruit, energy reduced or with no added sugar	1000 mg/kg	1000 mg/kg	330 mg/kg
Energy-reduced jams, jellies and marmalades	1000 mg/kg	1000 mg/kg	330 mg/kg
Energy-reduced fruit and vegetable preparations	1000 mg/kg	1000 mg/kg	330 mg/kg
Sweet-sour preserves of fruit and vegetables	300 mg/kg	600 mg/kg	198 mg/kg
Sweet-sour preserves and semi-preserves of fish and marinades of fish, crustaceans and molluscs	300 mg/kg	600 mg/kg	198 mg/kg
Sauces	350 mg/kg	350 mg/kg	115.5 mg/kg
Mustard	350 mg/kg	350 mg/kg	115.5 mg/kg
Fine bakery products for special nutritional uses	1700 mg/kg	1000 mg/kg	330 mg/kg
Complete formulae for weight control intended to replace total daily food intake or an individual meal	800 mg/kg	800 mg/kg	264 mg/kg
Complete formulae and nutritional supplements for use under medical supervision	1000 mg/kg	1000 mg/kg	330 mg/kg
Liquid food supplements/dietary integrators	600 mg/kg	600 mg/kg	198 mg/kg
Solid food supplements/dietary integrators	2000 mg/kg	2000 mg/kg	660 mg/kg
Essoblatten (a type of wafer)	1000 mg/kg	1000 mg/kg	330 mg/kg
Food supplements/diet integrators based on vitamin and/or mineral elements, syrup-type or chewable	5500 mg/kg	5500 mg/kg	1815 mg/kg
Breakfast cereals with a fibre content >15% and containing at least 20% bran, energy reduced or with no added sugar	1000 mg/kg	1000 mg/kg	330 mg/kg
Energy-reduced soups	110 mg/L	110 mg/L	36.3 mg/L
Breath-freshening micro-sweets with no added sugar	6000 mg/kg	10 000 mg/kg	3300 mg/kg
Strongly flavoured freshening throat pastilles with no added sugar	2000 mg/kg	2000 mg/kg	660 mg/kg
Drinks consisting of a mixture of a non-alcoholic drink and beer, cider, perry, spirits or wine	600 mg/L	600 mg/L	198 mg/L
Spirit drinks containing <15% alcohol by volume	600 mg/kg	600 mg/L	198 mg/L
Feinkostsalat (delicatessen salads)	350 mg/kg	350 mg/kg	115.5 mg/kg
Soy-based beverages		600 mg/L	198 mg/L

Table 3.2 Ethnomedical uses of Stevia in different countries (Taylor 2005)

Country/region	Ethnomedical uses
Brazil	Usually used for cavities in teeth, depression, diabetes, fatigue, heart support, hypertension, hyperglycaemia, infections, obesity, sweet cravings, urinary insufficiency, wounds, and as a tonic
Paraguay	Diabetes
South America	Diabetes, hypertension, infections, obesity
United States	Candida, diabetes, hypertension, hyperglycaemia, infections, and as a vasodilator

small quantities of Stevia leaf powder compared to table sugar. Stevioside is non-fermentable and it does not undergo browning reaction while cooking. This further widens its area of application in baking, enhancing the quality and safety of usage with a longer shelf-life. Breads made with Stevia as an ingredient for diabetic customers have demonstrated improvement in the texture and softness and increased shelf-life. A mere fragment of the leaf is enough to sweeten the mouth for an hour so fresh Stevia leaves are more than a chewing gum, although Stevia can be used in the making of chewing gums, mints and mouth refreshers.

Soft drink manufacturers have introduced health drinks and food supplementary beverages especially for diabetics. The majority of food supplementary products for diabetics emphasise the fibre and protein content, etc. The addition of dried Stevia leaves or powder to such products would not only naturally increase sweetness naturally but also help in invigorating the pancreatic gland (Geuns 2008). Further, no significant photodegradation on exposure to light in acidic beverages containing rebaudioside A or stevioside has been reported (Clos et al. 2008).

Stevia leaves are also blended with tea and coffee (Prakash and Upreti 2009; Prakash et al. 2010). Stevia leaves can be included in tea bags for diabetics, and lemonade can be prepared. Stevioside showed good stability up to 120 °C for 1 h. In aqueous solution, stevioside is remarkably stable in the pH range of 2–10 (Kroyer 2010). Stevia contains 5–20% of stevioside and rebaudioside. It can be extracted as a liquid concentrate that can be used directly in soft drinks, beverages, chocolates, etc.

Following FDA approval for use of steviol glycosides in food additives and GRAS notification of rebaudioside A, a major sweet-tasting component in *S. rebaudiana*, two Stevia-based low-calorie sugar substitutes have been marketed: Truvia, jointly developed by the Coca-Cola Company and Cargill, and Purevia, developed jointly by PepsiCo and the Whole Earth Sweetener Company. These products have been available in selected parts of the world (mainly in USA and UK) since 2011.

Apart from the sweet content, *S. rebaudiana* constituents also offer therapeutic benefits, having antihyperglycaemic, antihypertensive, anti-inflammatory, antitumour, antidiarrhoeal, diuretic and immunomodulatory effects (most of these have been discussed in detail in the previous chapter). Some of the ethnomedical uses of Stevia in different parts of the world are listed in Table 3.2.

References

Amzad-Hossain, M., Siddique, A., Mizanur-Rahman, S., Amzad-Hossain, M. (2010) Chemical composition of the essential oils of Stevia Rebaudiana Bertoni leaves. Asia J Trad Med 5, 56–61.

Chatsudthipong, V., Muanprasat, C. (2009) Stevioside and related compounds: therapeutic benefits beyond sweetness. Pharmacol Ther 121, 41–54.

Clos, J.F., DuBois, G.E., Prakash, I. (2008) Photostability of rebaudioside A and stevioside in beverages. J Agri Food Chem 56, 8507–13.

EFSA (European Food Standards Agency) (2010) Scientific opinion on the safety of Steviol glycosides for the proposed uses as a food additive. EFSA Panel on Food Additives and Nutrient Sources added to Food (ANS). EFSA J 8(1537), 1–84.

Geuns, J.M.C. (2008) Stevioside: a safe sweetener and possible new drug for the treatment of the metabolic syndrome. In: Weerasinghe, D.K., DuBois, G.E. (eds) *Sweetness and Sweeteners*. Washington, DC: American Chemical Society, pp.596–614.

Goyal, S.K., Samsher, Goyal, R.K. (2010) Stevia (Stevia Rebaudiana), a bio-sweetener: a review. Int J Food Sci Nutr 61, 1–10. http://informahealthcare.com/doi/abs/10.3109/09637480903193049

Jayaraman, S., Manoharan, M., Illanchezian, S. (2008) In-vitro antimicrobial and anti-tumor activities of Stevia Rebaudiana (Asteraceae) leaf extracts. Trop J Pharmaceut Res 7, 1143–1149

Koyama, E., Kitazawa, K., Ohori, Y. et al. (2003) In vitro metabolism of the glycosidic sweeteners, Stevia mixture and enzymatically modified Stevia in human intestinal microflora. Food Chem Toxicol 41, 359–374.

Kroyer, G. (2010) Stevioside and Stevia-sweetener in food: application, stability and interaction with food ingredients. J Consum Food Saf 5, 225–229.

Lemus-Mondaca, R., Vega-Gálvez, A., Zura-Bravo, L., Ah-Hen, K. (2012) Stevia Rebaudiana Bertoni, source of a high-potency natural sweetener: a comprehensive review on the biochemical, nutritional and functional aspects. Food Chem 132, 1121–1132

Lindsay, R. (2007) *Coke teams up with Cargill to launch new sweetener*. Times online, May 31.

Prakash, I., Upreti, M. (2009) *Stevioside Polymorphic and Amorphous Forms, Methods for Their Formulation, And Uses*. US Patent 8, 030, 481 B2.

Prakash, I., Upreti, M., Dubois, G.E., et al. (2010) *Sweetness Enhancers, Sweetness Enhanced Sweetener Compositions, Methods for Their Formulation, and Uses*. US Patent CN101742925 (A).

Puri, M., Sharma, D. (2011) Antibacterial activity of stevioside towards food borne pathogenic bacteria. Eng Life Sci 11, 326–329.

Tadhani, M., Subhash, R. (2006) Preliminary studies on Stevia Rebaudiana leaves: proximal composition, mineral analysis and phytochemical screening. J Med Sci 6, 321–326.

Taylor, L. (2005) *The Healing Power of Natural Herbs*. New York: Square One Publishers.

Wallin, H. (2007) *Steviol Glycosides*. 63rd Joint FAO/WHO Expert Committee on Food Additives (JECFA). Chemical and Technical Assessment (CTA). Rome: Food and Agriculture Association, pp1–8.

4

Conventional extraction processes of stevioside

Extraction of stevioside from Stevia leaves has been a field of active research since the early 1970s. The extraction process involves various operations in order to obtain high-purity stevioside powder. However, in all these processes, one step is key. Based on this criterion, the conventional extraction processes are divided into the following categories.

4.1 Ion exchange

Ion exchange is a process in which positively and negatively charged impurities are removed from an aqueous stream by oppositely charged resins (Wankat 2007).

Persinos (1973) filed a patent on stevioside production from the Stevia plant. The air-dried and pulverised stems and leaves were mixed with calcium carbonate and water and the mixture was kept at room temperature for about 20 h. Then the residue was filtered and pressurised to remove excess water and the process was repeated twice. The combined filtrate was mixed with Amberlite IR-120 ion exchange resin. The precipitate including the resin was filtered. The filtrate was deionised by passing it through two ion exchange resins (Amberlite IR-120 and Duolite A4). The effluent was then concentrated at about 50 °C overnight. The resultant syrup was dissolved in methanol and cooled to 5 °C to obtain stevioside crystals. Further enhancement in purity could be achieved by recrystallisation.

Adduci et al. (1987) reported isolation of stevioside using three main steps: hot water extraction and decolouration by electrolysis followed by ion exchange. The purity of stevioside attained was 70–80% and yield about 10%. Water extraction temperature was 90–100 °C. Electrolysis was carried out using a 30 ampere direct current for 2 h by adding 0.02 M hydrochloric acid per liter of the extract. The mixture was filtered and a second electrolysis was carried out for 20–30 min under the

Stevioside: Technology, Applications and Health, First Edition.
Sirshendu De, Sourav Mondal and Suvrajit Banerjee.

above operating conditions. A pale yellow solution resulted after another filtration, which was then allowed to pass through a column of mixed ion exchange resin consisting of Amberlite MB-1 (Amberlite IR-120 and Amberlite IRA-401). In the effluent, a clear solution was obtained with conductivity less than 50 μS. The solution was evaporated to powder which had a non-bitter taste.

A Korean patent (Won et al. 1990a) includes a method in which the extract is passed through a positively charged ion exchange resin (Diaion SKIB) and thereafter through a negatively charged resin (Amberlite IRA-904). In this method, a mixture of sweeteners is obtained. Another process patented by the same company (Won et al. 1990b) includes treatment of aqueous extract with calcium chloride and then passage through an Amberlite XAD-7 resin bed. Adsorbed stevioside in the bed was eluted with methanol and purified by column chromatography. Stevioside was further purified by crystallisation with methanol. However, in this method, both the chemicals, calcium chloride and methanol, were toxic. Column chromatography was also not commercially viable. In another patent (Susumu 1980), aqueous extract was treated with anionic resin leading to low purity of stevioside. Extract was optionally treated with ion exchange resins in another Japanese patent (Toyoshige 1984).

Payzant et al. (1999) proposed a two-step ion exchange resin process for purification of glycoside from Stevia leaves. The striking feature of this method was separation of individual glycosides from their mixture. In the first step of this method, sweet glycosides were extracted in aqueous solution. The solution was passed through a series of ion exchange resins to remove organic acids, inorganic salts, phenolic substances, proteins, etc. The resultant solution contained a mixture of 70% sweet glycosides. The dried powder was dissolved in water and was passed through an Amberlite XAD-7 resin bed. Sweet glycosides and bitter oil were adsorbed in the resin bed and non-sweet glycosides and carbohydrate impurities were not adsorbed. The adsorbed sweeteners were eluted by methanol solution that was dried to produce 95% sweet glycosides. The dried solid was mixed with anhydrous methanol and refluxed. Stevioside was precipitated by cooling and was recovered by filtration. The liquid filtrate was heated and cooled thereafter to precipitate rebaudioside A. This was further purified by mixing it with methanol and subjecting it to a series of heating and cooling steps so that the final purity of rebaudioside A was up to 95%.

Kumar et al. (2006) developed a process for production of stevioside from Stevia leaves. In this process, pulverised powder of Stevia leaves was extracted with demineralised water at 50–120 °C for 0.25–4 h under pressure of 1–8 bar. The extract was then mixed with calcium hydroxide to pH 9.2 and a precipitate was formed that was removed by filtration. The clear filtrate was fed through a strong cation exchange resin followed by a weak anion exchange resin. The eluant from anion exchange resin was 65% pure stevioside.

Yang et al. (2011) developed a process to recover 99% pure rebaudioside A from Stevia leaves. The leaves were extracted in water or ethanol or a mixture of two at 50–80 °C for about 30 min under high pressure in the range 200–3000 MPa. The liquid

extract was concentrated by evaporation at elevated temperature, filtered and passed through a bed of selective polar resin, causing adsorption of glycosides. Ethanol-water mixture was eluted to recover the adsorbed sweeteners and rebaudioside A was further purified by crystallisation to obtain purified rebaudioside A crystals of 85% purity. Further recrystallisation resulted in about 99% pure rebaudioside A.

A method of achieving high-purity stevioside and rebaudioside A was proposed by Purakayastha et al. (2010) and Magomet et al. (2011). In this method, the leaves of plants were heated at 45–75 °C using water (the proportion of leaves to water was 1 kg to 10 L) for about 1–6 h. The filtered extract was heated to about 50 °C for 0.5–1.0 h by adding calcium hydroxide up to a pH of about 10. The precipitate was removed and the supernatant was neutralised by ferric chloride solution for about 10–15 min. The resulting solution was passed through celite (a resin bed) for deionisation, and through three Amberlite beds for decolourisation. The solution was spray dried and contained about 65% stevioside and 25% rebaudioside A. The powder was extracted in methanol (at 20–25 °C for 0.5–1.0 h with agitation, about 1:5 (w/v) of powder to solvent ratio). The filtered precipitate was dried and analysed to obtain about 90% stevioside. The remaining solution was evaporated to remove methanol and after filtration, it was spray dried. The resulting powder was dissolved in ethanol (at 1:5 w/v solid to solvent, 40–45 °C for about 30 min with slow agitation). The precipitate was filtered and dried to obtain about 90% rebaudioside A.

Morita et al. (2011) developed a technology-based biotechnological route (cross-linking) to produce a Stevia variety that contained lower amounts of rebaudioside A so that high-purity stevioside was obtained quite easily, preferably in one step of crystallisation. The dried leaves were mixed with water and the extract was passed through an anion exchange resin and activated carbon. The eluate was fed to an adsorption resin where the glycoside components were adsorbed. The column was eluted by methanol and the eluate was concentrated under vacuum and dried to produce pale yellow powder. The powder was dissolved in methanol and then cooled to 4 °C to obtain crystals of stevioside of extremely high purity (90–98% depending on seasonal variation).

4.2 Solvent extraction

Organic solvents are quite commonly used for extraction of phytochemicals from plants, due to their selectivity for organic components. Water-immiscible solvents, methanol, chloroform, n-butanol, ethanol and fatty alcohols have been used for extraction of stevioside from Stevia leaves (Fumio 1980; Jackson et al. 2006; Pol et al. 2007; Shigeji 1980; Tadaaki et al. 1976; Tadashi and Masato 1995; Toyoshige and Usei 2002). Stevioside and rebaudioside A were further purified by crystallisation and recrystallisation from the solvent. However, the major drawback of these methods is utilisation of toxic chemicals which may be deleterious to health. Thus, the majority of studies use water as a solvent for extraction medium. The use of water and methanol as extraction media under pressurised conditions was studied by Pol et al. (2007).

In a recent study, Chhaya et al. (2012) used a systematic approach to evaluate the optimum conditions for water extraction of stevioside from Stevia leaves using response surface methodology. The optimum conditions of extraction were: temperature 78 °C; time of heating, 56 min; leaf to water ratio 1:14 (w/v). Under these conditions, extracted stevioside was 10.5 g per 100 g of dry Stevia leaves. It should be noted that the above conditions relate to the Indian variety of the plant.

4.3 Extraction by chelating agents

In order to overcome the use of toxic chemicals and slow, specialised and expensive equipment such as ion exchangers and chromatographs, chelating agents are sometimes used so that undesired/desired components form complexes with these chemicals, leading to easier separation. Kumar (1986) proposed a chelating agent-assisted extraction process of stevioside, in which the leaves were pulverised to a desired size and extracted with hot water at 60–80 °C for 2–5 h. The aqueous extract was chelated with carboxylic acid, such as citric acid, to remove metallic, protein- or colour-forming materials at pH range 2–4. The mixture was stirred for about 1–2 h at 30–80 °C and filtered through celite (diatomaceous earth). The pH of the resultant solution was raised to 10–13 by using calcium oxide or hydroxide and heated between 35–80 °C for 1–2 h and cooled to room temperature with slow stirring. The solution was again filtered through diatomaceous earth to remove proteins, pigments, etc. The resultant colourless solution was then neutralised by organic carboxylic acid such as citric acid. The filtrate was mixed with a solvent such as n-butanol. The aqueous layer was then cooled to 5–12 °C for 8–14 h to obtain the stevioside crystals which were filtered and dried. The process yield was 7.5%.

Giovanetto (1990) revealed a method in which hot water extraction of dry Stevia plant was carried out at 65 °C. Calcium hydroxide was added to the filtered extract to remove unwanted plant material. The resultant solution was fine filtered and almost colourless solution was passed through strongly acidic ion exchange resin and the eluate obtained was treated with a weakly basic ion exchange resin. Several such passes of acidic–basic resins were performed. The final eluate was filtered and dried to powder with an average purity of about 75%.

Deji (2009) invented an improved method for extraction of stevioside consisting of the following steps:

1. extraction by continuous countercurrent, suspended scum juice processing in a natural zeolite;
2. flocculation by modified bentonite;
3. microporous filtration;
4. adsorption by ADS-4 and -7 resins;
5. eluted liquid was concentrated by continuous vacuum drying.

The advantages of this process are: high speed and recovery (up to 90%); heat-sensitive materials are not destroyed; high throughput, and can be made a continuous process.

Weiping and Zhou (1999) described a process for extraction of sweet glycosides:

1. Extraction of plant materials in boiling water or ethanol solution for 1–3 h.
2. The liquid extract is mixed with a saturated solution of calcium or aluminium hydroxide and thoroughly mixed for 1–3 h, resulting in precipitation of undesired materials.
3. The liquid is passed through a neutral adsorption column that adsorbs the glycosides.
4. The column is charged with alcohol solution to elute the glycosides in several cycles (2–12).
5. Alcohol solution enriched with glycosides is passed through a second alkaline column where undesired materials are adsorbed – the effluent contains alcohol solution with purified glycosides.
6. The solution is then either spray dried or vacuum dried at 50 °C and the solid powder, of about 80% purity, is obtained.

Abelyan et al. (2010) invented a method to extract high-purity stevioside and rebaudioside A from the plant:

1. Water extraction of the plant material was carried out at 50–60 °C for about 1–6 h.
2. Extraction was enhanced by adding pectinase enzyme (2 g/L).
3. The filtrate was adjusted with calcium hydroxide at about 50 °C for about 1 h up to a pH about 10.0 and cooled to ambient temperature
4. Clarified solution was mixed with bentonite (2–3 g/L).
5. The filtrate was mixed with ethanol at about 50 °C for about 30 min); the precipitate was separated and the powder contained about 84% rebaudioside A.
6. The left-over clear solution was passed through an ion exchange resin bed after evaporation of ethanol and concentrated and dried. The resultant powder contained 93% pure stevioside.

A host of Japanese patents are available for use of various chelating agents for purification of Stevia extract. Some of these include use of stannous chloride, stannous sulfate, stannic acid, etc. (Shinichi et al. 1980), various Ca and Fe salts (Masahiro et al. 1980), and use of $CaCl_2$ and $Ca(OH)_2$ (Kotaro and Tokuo 1987; Taku and Yukio 1983; Yukio et al. 1983).

4.4 Adsorption and chromatographic separation

Selective separation of a species from a liquid stream can generally be attained by adsorption. Highly specific components can be selectively separated by chromatographic separation processes. Chromatography is an extremely powerful analytical tool for separating and analysing complex mixtures. A typical analytical chromatograph is shown in Figure 4.1. It contains the following features: (a) for a liquid system, a pump is used to push the fluid through the column; (b) a pulse of feed is injected into the system; (c) the column is often enclosed in an oven to control temperature; (d) a detector analyses the stream for properties such as refractive index and ultraviolet absorbance which can be related to concentration. The purpose of the column is to separate the feed mixture into peaks that contain only one component in addition to solvent, as shown in Figure 4.2.

The salient features of liquid–liquid chromatography are:

1. a stationary liquid phase is coated over an inert, porous solid;
2. separation is essentially an extraction process;
3. useful for separating non-volatile solutes.

The differences between LLC and modern high-performance liquid chromatography (HPLC) are described below.

- The inert solid is silica. The stationary liquid phase is chemically attached to the solid so there is no loss of stationary phase by bleeding. The most common stationary phase is C8 or C18 compounds attached to the silica gel. Water is the common solvent.
- Short columns have a very small diameter. Packings are operated at high velocity and high pressure drop. The column is 0–25 cm long, 4–8 mm ID, packing is 3–9 μm and ΔP ~1000 psi.

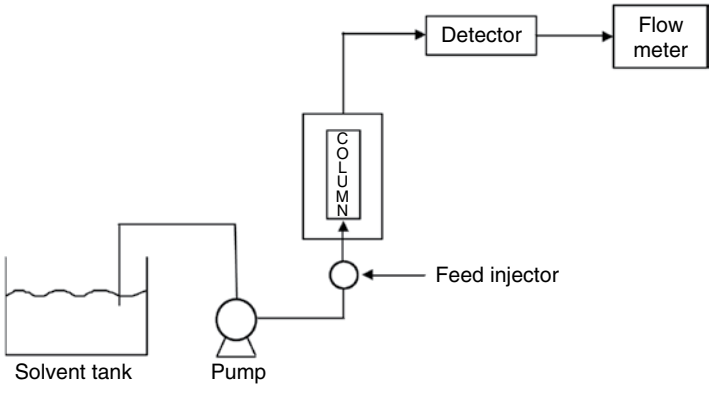

Figure 4.1 Analytical high-pressure liquid chromatogram.

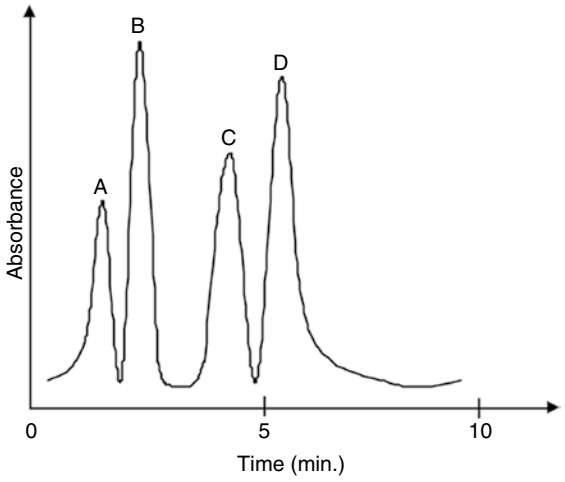

Figure 4.2 Peak separation in a typical chromatographic column for a mixture of various components present in the feed.

The advantage is that changing solvent has a major effect on the distribution coefficient and hence on separation.

Morita et al. (1978) were granted a patent for a process in which alkanol-extracted plant material was fed into a silica gel chromatographic column, producing an effluent rich in various sweeteners which were collected, concentrated and recrystallised to obtain the powder.

Matsushita and Ikushigo (1979) developed a process for separation of glycosides from non-glycosides using column chromatography. The molecular weight of these glycosides and non-glycosides was between 20 and 1000 Daltons. The column could be packed with non-polar gel (cross-linked styrene) or polar gel (starch). When a non-polar gel was used, a non-aqueous solvent was used as the elute and chloroform, water, etc. cannot be used as the eluent. In the case of polar gel, a mixture of organic solvents could be used as eluant. The organic solvents could be C1–C4 alcohols, tetrahydrofuran, etc. Stevioside and other non-glycosidic compounds were dissolved in water in equal proportion. For a styrene gel of a particular pore size (less than 250 A°), all the components were separated very well in a short period.

Hideaki et al. (1979) proposed a method involving treatment of aqueous Stevia extract with non-polar synthetic adsorbent, followed by desorption and further treatment by ion exchange resins. However, in this method, non-polar adsorbent could not adsorb polar glycosides and had affinity for less polar non-sweet components. Thus, a significant amount of stevioside was lost in the effluent.

There are various patents available on clarification of Stevia extract using synthetic polymeric adsorbents and organic solvents, followed by crystallisation (Koji and Takeshi 1979; Masashi and Tadashi 1982; Ryoichi and Isamu 1979; Susumu 1982).

Dobberstein and Ahmed (1982) developed a process for extraction of glycosides from Stevia plants in which chloroform was used as a non-polar solvent to dissolve and remove non-glycosidic compounds or impurities to defat the plant materials. Next, the polar solvent, such as methanol, was used to dissolve the glycosidic materials. The mixture of glycosides was then fed into the chromatographic column that loosely adsorbed the glycosides. 1-Propanol solution was then used to elute and the glycosides were solubilised in it by the column gel materials . An oxygen coated organic stationary phase in the column caused good separation between the glycosidic compounds. The concentration was detected by the UV detector at 210 nm wavelength. Three distinct peaks were obtained for stevioside, rebaudioside C and A at three different retention times.

Chiang et al. (2011) proposed a chromatographic separation for rebaudioside A in which glycosides containing stevioside (38%), rebaudioside A (42%) and other glycosides (20%) were dissolved in a water-ethanol mixture. The solution was passed through the resin bed at a specific rate (one bed volume per hour). The glycosides were attached to the bed material. Next, 3.5 times bed volume of 10 wt% ethanol solution was passed through the column at one bed volume per hour. The eluant contained 69% rebaudioside A, 31% stevioside and other glycosides; 93% of total rebaudioside A fed to the column was thus recovered. Using the developed column, a stream containing stevioside and rebaudioside A could also be fractionated.

A US patent (Yang et al. 2011) divulged a process in which rebaudioside A was recovered from Stevia plant by use of a polar resin in silica gel column chromatography using a suitable solvent. Thereafter, crystalline rebaudioside A was obtained.

Liu et al. (2012) proposed a chromatographic separation method between two glycosides, stevioside and rebaudioside A. The advantages of this method were that it was simple, fast and cost-effective. Extraction and separation of both glycosides were carried out in a single column and single step. A mixture of 41% stevioside and 35.8% rebaudioside A dissolved in ethanol solution was loaded on the special chromatographic column consisting of a particular composition of functionalised polymethacrylate/DVB co-polymer resin under high pressure up to about 1500 psi. The column was eluted under medium pressure (less than 300 psi) with a methanol-acetone solvent mixture at a rate of 4–5 mL/min. Fractions of stevioside and eebaudioside were collected together and then crystallised. The crystals were filtered out and 98% purity of each of two glycosides obtained.

Selective adsorption on zeolite X and A was studied with Stevia and reported by Moraes and Machado (2001). This study concluded that CaX zeolite is more effective in clarification of hot water-assisted Stevia extraction. Both powdered and granular zeolites were almost equally efficient. The optimum treatment conditions were 40% (w/w) zeolite, 60 min contact time at 30 °C. About 70% clarification was obtained. Reused zeolite also showed equivalent performance. The authors also undertook a continuous column experiment showing that using a 30 L/day flow rate, it was possible to clarify the Stevia extract by using zeolite bed up to about 60% for 11 h.

Rajab et al. (2009) developed a two-step process for clarification and purification of Stevia extract. Hot air (70–80 °C for 8 h) dried leaves were boiled with water (leaf to water ratio 1 kg:5 L) for 3 h and the extract was cloth filtered. Next, the crude extract was treated with 10% activated charcoal for 20 min. The extract was filtered and residual charcoal was mixed with boiling water for 10 min and filtered for recovery of stevioside. This was repeated in three cycles. In this process, some amounts of chlorophyll, phenols and carotenoids were removed. In the next step, the yellow extract was treated with 5% celite and stirred for 20 min. The colourless extract was centrifuged at 12,000 rpm for 15 min and clear aqueous solution was collected and stored. The resultant solution was spray dried (inlet temperature 180 °C, outlet temperature 95 °C, pump pressure 500 psi) to obtain white powder. The final concentration of stevioside was 11.6%.

4.5 Ultrasonic extraction

The first ultrasonic-assisted extraction of stevioside was reported by Jaitak et al. (2009). They carried out extraction of Stevia leaf powder using different solvents (water, methanol, ethanol, binary mixture of methanol-water and ethanol-water) in an ultrasonicator bath at 35 °C for 30 min. Extracts were filtered and dried to powder (at 50 °C). The yield reported was 4.2% for stevioside and 2.0% for rebaudioside A for methanol-water (80:20 v/v) mixture which was almost comparable to results obtained with the conventional method (using methanol-water as solvent with duration of 12 h), i.e. 6.54% stevioside and 1.2% rebaudioside A.

A Chinese patent (Ruihua et al. 2010) also described ultrasonic assistance during extraction of Stevia leaves. Stevioside powder 85–98% was produced by adopting various unit operations (flocculation, filtration, absorption, decolouration, concentrating and spray drying) after ultrasonic-assisted extraction.

4.6 Microwave-assisted extraction

Several advantages associated with microwave-assisted extraction (MAE) make it competitive with other conventional processes. These are faster extraction, reduced solvent use and higher recovery. MAE of stevioside and rebaudioside A was first reported by Jaitak et al. (2009). In this study, extraction of Stevia leaves with water, methanol, ethanol and binary mixture methanol-water and ethanol-water was carried out in the presence of microwaves at different power levels in a range from 20 to 160 W with extraction time 30 s to 5 min at a temperature range 10–90 °C. It was concluded that yields of stevioside (8.64%) and rebaudioside A (2.34%) were higher than for the conventional method (6.54% and 1.20%). Microwave power of 80 W, 50 °C and 1 min duration gave the optimum results. Methanol-water (80:20 v/v) was the best medium that responded to microwave assistance to the highest level.

4.7 Supercritical fluid extraction

At a certain temperature and pressure condition (critical condition), liquid and vapour phases of a substance become indistinguishable. A substance whose temperature and pressure are higher than its critical point is known as supercritical fluid (SCF). Figure 4.3 shows a typical pressure and temperature history of a substance.

Physical and thermal properties of SCFs are in between pure liquid and gas. Changes in properties for a SCF are:

1. liquid-like densities;
2. reduction in surface tension;
3. gas-like viscosity;
4. gas-like compressibility properties;
5. diffusivities higher than liquids.

Some commonly used supercritical solvents are carbon dioxide, nitrous oxide, ethylene, propylene, propane, n-heptane, ethanol and ammonia. Among these, CO_2 is widely used as a supercritical solvent. Table 4.1 summarises the properties of some supercritical fluids.

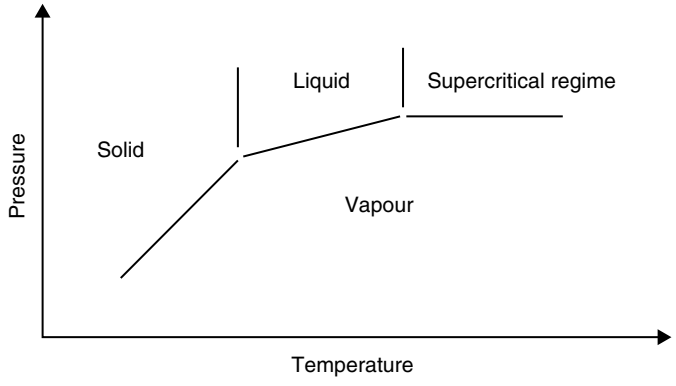

Figure 4.3 Typical pressure–temperature history of a substance.

Table 4.1 Properties of some supercritical fluids

Substance	T_c (K)	P_c (atm)	Density (g/cc)
CO_2	304.2	73	0.47
Ethane	305.5	48.2	0.20
Ethanol	516.6	63.0	0.28
Propane	370.3	42.0	0.22

The following properties of CO_2 make it a suitable SCF:

1. low critical pressure (74 atm) and low critical temperature (32 °C);
2. relatively non-toxic;
3. non-flammable;
4. available as high purity;
5. low cost;
6. easily removable from extract;
7. it has polarity like liquid pentane at supercritical conditions and thus is best suited for lipophilic compounds. The major drawback is that it cannot extract polar solutes.

Application of SCF for extraction of stevioside was first obtained in a Japanese patent (Shoji et al. 1988; Yasunori et al. 1987). Carbon dioxide was used as the supercritical fluid. It was reported that CO_2 was effective only in the presence of water and methanol or ethanol. Also, the stevioside obtained was mixed with many impurities which were deleterious to its taste. Kienle (1992) evaluated various SCFs for extraction of stevioside, including ethane, nitrous oxide, propane, propene, hydrogen fluoride, etc. Removal of bitter and astringent components from Stevia leaves was better achieved by these SCFs. But organic extractants have common drawbacks and as nitrous oxide is explosive, CO_2 is generally used. It was proposed that when 8–50 kg CO_2/kg dry leaves or powder were used at 50–70 °C and 100–400 bar pressure, bitter and taste-repelling compounds were removed from Stevia leaves to a great extent. The rest of the materials devoid of desired components can be extracted using water or any standard organic solvent.

Extraction of non-glycoside fractions from stevioside by supercritical fluid extraction (SCFE) was studied by Pasquel et al. (1999). They identified about 56% of the substances present in the extract. Pasquel et al. (2000) proposed a two-step process: pretreatment of Stevia leaves by SCFE with CO_2; and extraction of Stevia glycosides by CO_2 + water, CO_2 + ethanol and CO_2 + water + ethanol. The pretreatment conditions were 200 bar and 30 °C. Extraction of glycosides was carried out at 120 and 200 bar at 16º, 30º and 45 °C. The best result was obtained at 16 °C and 120 bar with water as co-solvent. Large amounts of ebaudioside A were obtained. The quality of the final powder was as good as with any conventional method but in terms of yield of rebaudioside A, SCFE fared better.

References

Abelyan, V.H., Ghochikyan, V.T., Markosyan, A.A., Adamyan, M.O., Abelyan, L.A. (2010) Extraction, separation and modification of sweet glycosides from the Stevia Rebaudiana plant. US Patent 7,838,044 B2.

Adduci, J., Buddhasukh, D., Ternai, B. (1987) Improved isolation and purification of stevioside. J Sci Soc Thai 13, 179–183.
Chhaya, C., Majumdar, G.C., De, S. (2012) Optimization of process parameters for water extraction of stevioside using response surface methodology. Sep Sci Technol 47, 1–9.
Chiang, C., Evans, J.C., Hahn, J.J., et al. (2011) Separation of rebaudioside A from Stevia glycosides using chromatography. US Patent 2011/0087011 A1.
Deji, W. (2009) High-efficiency method for continuously extracting stevioside from Stevia leaf. Chinese Patent 200810216065.
Dobberstein, R.H., Ahmed, M.S. (1982) Extraction, separation and recovery of diterpene glycosides from Stevia Rebaudiana plants. US Patent 4,361,697.
Fumio, M. (1980) Stevioside extracted from Stevia containing sweetener. Japanese Patent 55-0007039.
Giovanetto, R.H. (1990) Method for the recovery of steviosides from plant raw material. US Patent 4,892,938.
Hideaki, U., Ryoichi, I., Teruo, K. (1979) Purification of Stevia sweetening agent. Japanese Patent 54-030199.
Jackson, M.C., Francis, G.J., Chase, R.G. (2006) High yield method of producing pure rebaudioside A. US Patent 0083838.
Jaitak, V., Bandna, Singh, B., Kaul, V.K. (2009) An efficient microwave-assisted extraction process of stevioside and rebaudioside A from Stevia Rebaudiana (Bertoni). Phytochem Anal 20, 240–245.
Kienle, U. (1992) Method of making a natural sweetener based on Stevia Rebaudiana and use thereof. US Patent 5,112,610.
Koji, I., Takeshi, I. (1979) Purification of stevioside. Japanese Patent 54-041898.
Kotaro, K., Tokuo, O. (1987) Extraction and purification of sweetener component from dry leaf of Stevia. Japanese Patent 62-166861.
Kumar, J.K., Babu, G.K., Kaul, V.K., Ahuja, P.S. (2006) Process for production of stevioside from Stevia Rebaudiana Bertoni. International Patent WO 2006/038221 A1.
Kumar, S. (1986) Method for recovery of stevioside. US Patent 4,599,403.
Liu, J., Zhang, K., Guo, S. (2012) Separation and purification of stevioside and rebaudioside A. US Patent 2012/0083593A1.
Magomet, M., Tomov, T., Somann, T., Abelyan, V.H. (2011) Process for manufacturing of a sweetener and use thereof. US Patent 7,862,845B2.
Masahiro, F., Masaaki, T., Shinichi, K. (1980) Purification of stevioside solution. Japanese Patent 55-138372.
Masashi, O., Tadashi, Y. (1982) Purification of stevioside. Japanese Patent 57-075992.
Matsushita, S., Ikushigo, T. (1979) Separation of sweet component from natural sweet extracts. US Patent 4,171,430.
Moraes, E.P., Machado, N.R.C.F. (2001) Clarification of Stevia Rebaudiana (Bert.) Bertoni extract by adsorption in modified zeolites. Acta Scientiar 23, 1375–1380.
Morita, T., Isamu, F., Iwamura, J. (1978) Sweetening compound, method of recovery, and use thereof. US Patent 4,082,858.
Morita, T., Morita, K., Kanzaki, S. (2011) Novel Stevia variety and method of producing sweeteners. Japanese Patent Application 20110023192.

Pasquel, A., Meireless, M.A.A., Marques, M.O.M. (1999) Stevia (Stevia Rebaudiana Bertoni) leaves pretreatment with pressurized CO_2: an evaluation of the extract composition. Proceedings of the 6th Meeting on Supercritical Fluids: Chemistry and Materials, p.501.

Pasquel, A., Meireless, M.A.A., Marques, M.O.M., Petenate, A.J. (2000) Extraction of Stevia glycosides with CO_2 + water, CO_2 + ethanol and CO_2 + water + ethanol. Braz J Chem Eng 17, 271–282.

Payzant, J.D., Laidler, J.K., Ippolito, R.M. (1999) Method of extracting selected sweet glycosides from Stevia Rebaudiana plant. US Patent 5,962,678.

Persinos, G.J. (1973) Method of producing stevioside. US Patent 3,723,410.

Pol, J., Ostra, E.V., Karasek, P., Roth, M., Karolinka, B., Kaslavsky, J. (2007) Comparison of two different solvents employed for pressurized fluid extraction of stevioside from Stevia Rebaudiana: methanol versus water. Anal Bioanal Chem 388, 1847–1857.

Purakayastha, S., Markosyan, A., Malsagov, M. (2010) Process for manufacturing a sweetener and use thereof. US Patent Application 2010/0227,034.

Rajab, R., Mohankumar, C., Murugan, K., Harish, M., Mohanam, P.V. (2009) Purification and toxicity studied of stevioside from Stevia Rebaudiana Bertoni. Toxicol Int 16, 49–54.

Ruihua, G., Jingwen, S., Xinwei, Y. (2010) Method for ultrasonic extraction of stevioside. Chinese Patent 101798329A.

Ryoichi, I., Isamu, H. (1979) Separation and purification of stevioside sweetening. Japanese Patent 54-132599.

Shigeji, S. (1980) Preparation of stevioside. Japanese Patent 55-162953.

Shinichi, K., Masaaki, T., Masahiro, F. (1980) Purification of stevioside solution. Japanese Patent 55-120770.

Shoji, T., Yasunori, S., Osamu, T. (1988) Separation and production of sweet substance. Japanese Patent 63-177764.

Susumu, O. (1980) Decolorization and purification of stevia sweet component. Japanese Patent 55-111768.

Susumu, O. (1982) Isolation of principal sweetening component of Stevia. Japanese Patent 57-086264.

Tadaaki, H., Ryoichi, I., Teruo, K. (1976) A method for purifying stevioside. Japanese Patent 51-131900.

Tadashi, K., Masato, K. (1995) Production of Stevia sweetener. Japanese Patent 07-143860.

Taku, T., Yukio, O. (1983) Preparation of stevioside. Japanese Patent 58-028246.

Toyoshige, M. (1984) Novel natural sweetener. Japanese Patent 59-045848.

Toyoshige, M., Usei, B. (2002) Sweetener obtained from plant body of variety of Stevia Rebaudiana cultivatable from seed. Japanese Patent 2002-262822.

Wankat, P.C. (2007) *Separation Process Engineering*. New York: Prentice-Hall.

Weiping, H., Zhou, J.H. (1999) Process for extracting sweet diterpene glycosides. US Patent 6,228,996.

Won, S.H., Jin, C.K., Ho, P.C., Hwaseodong, S., Yong, H., Gu, D. (1990a) Process for extracting and separating of sweetening materials from Stevia. Korean Patent 1019900007421.

Won, S.H., Jin, C.K., Hoon, C.H. (1990b) Purification process of stevioside. Korean Patent 1019900005468 B1.

Yang, M., Hua, J., Qin, L. (2011) High purity rebaudioside A and method of extracting same. US Patent 7,923,541B2.
Yasunori, S., Yoshihiko, K., Osamu, T., Hisashi, I. (1987) Method of extracting glycoside. Japanese Patent 62-000496.
Yukio, O., Hajime, I., Taku, T. (1983) Purifying method of stevioside solution. Japanese Patent 58-028247.

5

Brief introduction to pressure-driven membrane-based processes

Pressure-driven membrane-based processes are becoming attractive unit operations in many spheres of today's life. They have wide applications in various fields, including treatment of industrial effluent, juice and beverage processing, production of potable water, pharmaceutical processing, biotechnological applications, recovery of expensive and medicinally important phytochemicals and many more. In most cases, these processes are cheaper, greener and less capital equipment intensive compared to conventional processes. In some cases, one membrane-based process can replace a number of conventional processes.

Two types of separation processes are generally encountered: equilibrium and rate-governed processes (Wankat 2007). The product phases are in equilibrium with the inlet phases in equilibrium-governed separation processes. Some industrially relevant equilibrium separation processes are distillation, absorption, adsorption, drying, etc. Since the product streams are in equilibrium with feed, the process is quite slow and its performance is governed by the equilibrium of the streams at the operating temperature. On the other hand, difference of rate of physical transport of species leading to the separation is critically important in rate-governed processes. Gradient of chemical potential is the driving force in any separation process. It has essentially four contributions: concentration, pressure, temperature and electrochemical potential gradient (Smith et al. 2005). Presence of one or more of such gradients results in the separation of species. Thus, suitable control of the driving forces in the system results in appropriate modification of separation and throughput of the system as well. Most pressure-driven membrane processes belong to the rate-governed separation category.

Stevioside: Technology, Applications and Health, First Edition.
Sirshendu De, Sourav Mondal and Suvrajit Banerjee.

5.1 Advantages of the membrane-based process

The advantages of the membrane-based systems are listed below (Bungay et al. 1986; Cheryan 1998; Rautenbach and Albrecht 1986):

1. Operation at room temperature is advantageous when processing temperature-sensitive materials that are susceptible to being denatured, such as protein solution, fruit juice, etc.
2. Capital and energy-intensive equipment, such as evaporators, is not required as there is no phase change during separation.
3. No chemicals are added and the separation is purely physical in nature, rendering the process less polluting and cheaper.
4. Such systems are modular in nature and hence can easily be scaled up.
5. The operation and maintenance are easy and less labour intensive.

5.2 Classification of the processes

Pressure-driven membrane-based separation processes can be divided into four classes: reverse osmosis, nanofiltration, ultrafiltration and microfiltration. There are no clear-cut definitions of these classes but they are based on the average pore size of the membranes, molecular weight of the solutes to be separated, operating transmembrane pressure drop, filtration mechanism, etc. The important features of each of these processes are described below.

5.2.1 Reverse osmosis

Reverse osmosis (RO) is a process where the membrane has the smallest average pore size, in the range of 2–10 A^0. The pore size is so small that sometimes it is called an almost impervious membrane. The molecular weight of solutes to be separated by this membrane is less than 100. A good RO membrane causes separation of monovalent salt (sodium chloride) to the extent of more than 95%. Since the pore size is very small, the transmembrane pressure drop required for this process is between 25 and 40 atm and even more in some cases. The transport mechanism in RO is called permeation. It has three distinct steps: dissolution of solute molecules from the feed stream into the polymeric membrane matrix, diffusion of solutes through the membrane matrix by diffusion, and desorption from the membrane to the permeate stream. Desalination of sea water to produce potable water is an example of RO.

5.2.2 Nanofiltration

Nanofiltration (NF) is a process in between RO and ultrafiltration. NF membrane is said to be a 'loose' RO membrane. Partial retention (65–80%) of monovalent salt (NaCl) occurs via a good NF membrane. The average pore size of NF membrane is in the range of 5–20 A^0. Since the pore size is slightly larger than that of RO, the transmembrane pressure requirement for this kind of membrane is less, typically between 15 and 25 atm. The molecular weight of solutes to be retained by this membrane is between 200 and 1000 Da. The solute transport mechanism through this membrane is mainly permeation. Processes carried out by NF include filtration of dyes and separation of smaller molecular weight organics like polyphenols.

5.2.3 Ultrafiltration

In ultrafiltration (UF), membrane pore size is slightly larger, the average being between 20 and 1000 A^0. Since pore size is much bigger, the pressure requirement is lower. The typical transmembrane pressure drop is between 6 and 8 atm. The major solute transport mechanism is convection, as well as diffusion. The typical molecular weight of solutes to be separated by UF is in the range of 1000–100,000 Da. Some typical applications of UF include filtration of protein, polymer and polysaccharides such as pectin, etc.

5.2.4 Microfiltration

In microfiltration (MF), the average pore size is more than 1000 A^0 and up to several microns. The transmembrane pressure requirement is the least, at about 2–4 atm. The molecular weight of solutes to be separated by MF is more than 10^5 Da. Convection is the main transport mechanism. Filtration of blood cells, clay, paint, bacteria, etc. can be carried out by microfiltration.

5.3 Characterisation of membranes

Several parameters are used to characterise a membrane: membrane permeability, retention and molecular weight cut-off (MWCO).

5.3.1 Membrane permeability (L_p)

This parameter is an indicator of membrane porosity. For a porous membrane, L_p is more. Mathematically, L_p is defined as:

$$L_p = \frac{J^0}{\Delta P}$$

where J^0 is the pure water flux and ΔP is transmembrane pressure drop. This concept is elaborated in detail in subsequent sections. Membrane permeability is measured by pure distilled water runs as pure water does not have any osmotic pressure. Water flux values are measured by conducting experiments with distilled water at various transmembrane pressure drops. A plot of permeate flux versus operating pressure is typically linear through the origin and the permeability (L_p) of the membrane is measured by the slope of this curve. Permeability of a membrane is its pressure history only – it is independent of flow configuration or flow regime. The unit of permeability is $\frac{m}{Pa.s}$.

5.3.2 Retention

Retention is an indicator of membrane selectivity. This indicates the extent of separation of a solute that can be affected by the membrane with respect to the feed concentration. Two types of retention are defined in the membrane literature: observed and real retention.

Observed retention

This defines the extent of separation of solute by the membrane compared to solute concentration in the feed. Thus, observed retention is defined as:

$$R_o = 1 - \frac{C_p}{C_o} \tag{5.1}$$

where C_p is solute concentration in permeate and C_o is that in feed. R_0 is 1.0 if the solute is completely retained by the membrane and its value is 0 if the solute is completely permeable through the membrane. This is an easily measurable quantity, as the solute concentration in the feed and the permeate can easily be determined by analytical tools.

Real retention

Because of retention of solute over the membrane surface, there exists a concentration gradient over the membrane surface. Typically, solute concentration is higher at the membrane surface than that at the bulk. Hence, in the definition of observed retention, the actual solute concentration over the membrane surface is not accounted for. To overcome this, real retention is defined, which is a measure of extent of separation of solute by the membrane in the permeate stream compared to the solute

concentration at the membrane–solution interface. Since this definition is not masked by any physical phenomenon such as deposition of solutes on the surface, etc., this definition indicates the real separation efficiency of the solute by the membrane.

$$R_r = 1 - \frac{C_p}{C_m} \tag{5.2}$$

Here, C_m is the solute concentration at the membrane–feed solution interface. It may be noted that observed retention underestimates the true retention capacity of the membrane. On the other hand, membrane surface concentration of solute is always greater than the bulk concentration and hence, real retention is always greater than observed retention. For complete solute retention, $R_r = 1.0$.

The determination of real retention is not easy as estimation of solute concentration at the membrane surface concentration is quite difficult experimentally. It can be predicted by theoretical calculations. It can be experimentally measured by conducting experiments with solutes at lower concentration, lower pressure and very high agitation in a small test cell. Since agitation is high, it can be assumed that there exists no concentration profile in the feed chamber and the concentration is uniform in the feed. Under these conditions, observed retention is equivalent to real retention (Opong and Zydney 1991). There also exists a technique called the velocity variation method by which real retention can be estimated (van den Berg et al. 1989). However, this method needs appropriate caution during conduction of the experiments. Since real retention gives the true solute separation efficiency across the membrane, for most of the solute-solvent and membrane system, it is invariant.

5.3.3 Molecular weight cut-off

Estimation of average pore size of the membrane is quite difficult and involves inaccuracy in measurement as there exists a distribution of pore size in the membrane matrix. Since application of the membrane is basically retention of a solute of particular size, a rating of membrane is directly done on its capacity to retain a neutral solute of a particular molecular weight. This is known as molecular weight cut-off (MWCO). A membrane having MWCO 10,000 retains all solutes of molecular weight exceeding 10,000 and allows permeation of solutes of molecular weight less than 10,000. It can be experimentally demonstrated by measuring the retention of neutral solutes (so that charge–charge interaction between solute and membrane can be neglected) of various molecular weights by conducting small test cell experiments. The typical operating conditions of these experiments are low transmembrane pressure drop, high turbulence and low feed concentration. The observed retention values are then plotted against the molecular weight of the solutes in a semi-log plot. The typical solutes are glucose (molecular weight 180), sucrose (molecular weight 342), various fractions of polyethylene glycol (molecular weights 200, 400,

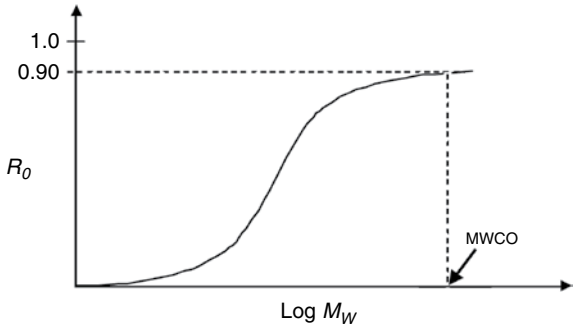

Figure 5.1 Typical molecular weight cut-off (MWCO) curve of a membrane.

600, 1000, 1500, 2000, 4000, 60000, 10,000, 30,000), dextran (molecular weight 40,000, 70,000, 150,000), etc. The molecular weight at 90% solute retention indicates the MWCO of the membrane. This is an easy method to quantify the rating of the membrane. A typical MWCO curve is shown in Figure 5.1.

If the span or width of this 'S'-shaped curve is small, it is called a sharp cut-off and if the width is broad, it is known as diffused cut-off membrane. Needless to say, a sharp cut-off membrane is desired in most cases, but it is quite difficult to tailor-make such membranes.

5.4 Membrane modules (Bungay et al. 1986; Ho and Sirkar 1992; Rautenbach and Albrecht 1986)

The actual membrane is housed in what is known as a module. The purpose of these modules is to provide maximum membrane area in relatively smaller volume. Four types of membrane modules are common: plate and frame modules, hollow-fibre modules, spiral-wound modules, and tubular modules. Each of these modules is described below.

5.4.1 Plate and frame module

In this module, a support plate is sandwiched between two flat sheet membranes. The membranes are sealed to the plate. A flow channel for the permeate collection is provided from the side of the plate. A feed side flow channel is provided by grooves on the plate. The feed channel has a clear path with channel height typically in the range of 0.3–0.75 mm. Higher channel height leads to reduction of friction due to flow and power consumption. Commercial plate and frame units are generally arranged with the plates mounted vertically, so that less module space is required. Several such stacks can be provided to obtain a larger surface area for filtration. Figure 5.2 shows a typical plate and frame module.

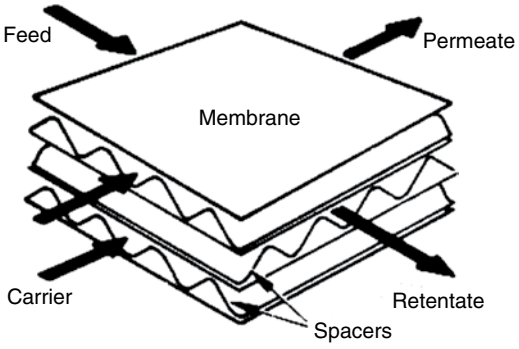

Figure 5.2 A plate and frame module.

5.4.2 Tubular module

In tubular modules, the membrane is cast on the inside surface of a porous tube. Tubular membranes operate under cross-flow mode, where feed is pumped through the module and the permeate comes out at 90º with retentate flow direction to the permeate side. High cross-flow velocity is achieved, which enhances the productivity of the process and helps to enhance membrane life. Some typical advantages of tubular configuration are robust construction, streams with high solid load can be processed and there is no need for significant prefiltration. Tubular membranes are ideally suited to treatment of metal working oily waste, waste water minimisation and recovery from industrial processes, juice clarification, treatment of pulp and paper industry waste, etc. Typical shelf-life of tubular membranes is 2–10 years. Figure 5.3 shows some tubular membranes.

5.4.3 Hollow-fibre module

In this module, a large number of hollow fibres are aligned in a large pipe providing a large surface area in a small volume and a compact design. Potable water treatment, juice clarification, wine filtration and dairy processing are some hollow-fibre applications. The advantages are:

1. reduction in space requirement;
2. lower labour cost;
3. back-washing facility;
4. high throughput;
5. modular in nature for better design.

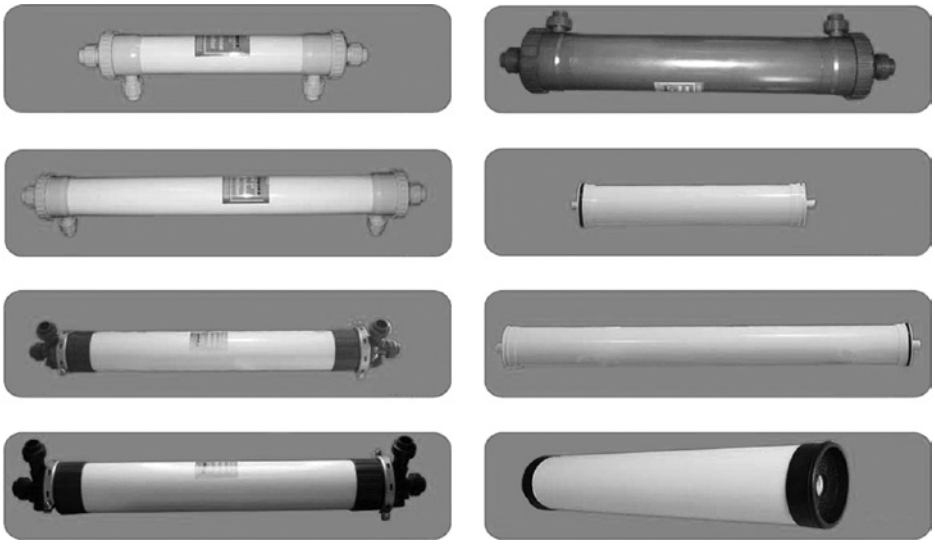

Figure 5.3 Tubular modules.

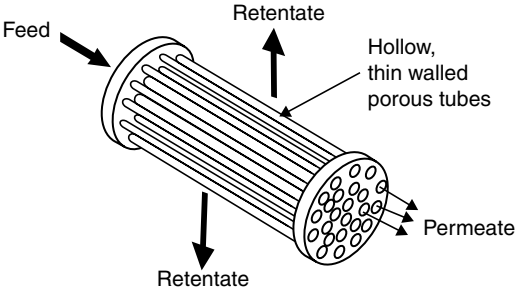

Figure 5.4 Flow pattern in a hollow-fibre module.

The inside diameter of fibres ranges from 0.5 mm up to 2.7 mm. Polysulfone, polyethersulfone and polyacrylonitrile are some typical materials used for hollow-fibre membranes. The flow pattern in a typical hollow-fibre module is shown in Figure 5.4.

5.4.4 Spiral-wound module

In this module, membrane is cast as a film onto a flat sheet like polyester fabric and is sandwiched together with feed spacers and permeate carrier. It is sealed at each edge and wound up around a perforated central tube. The module diameter ranges from 63 to 457 mm and length varies from 760 to 1520 mm. The typical flow pattern of a spiral-wound module is shown in Figure 5.5.

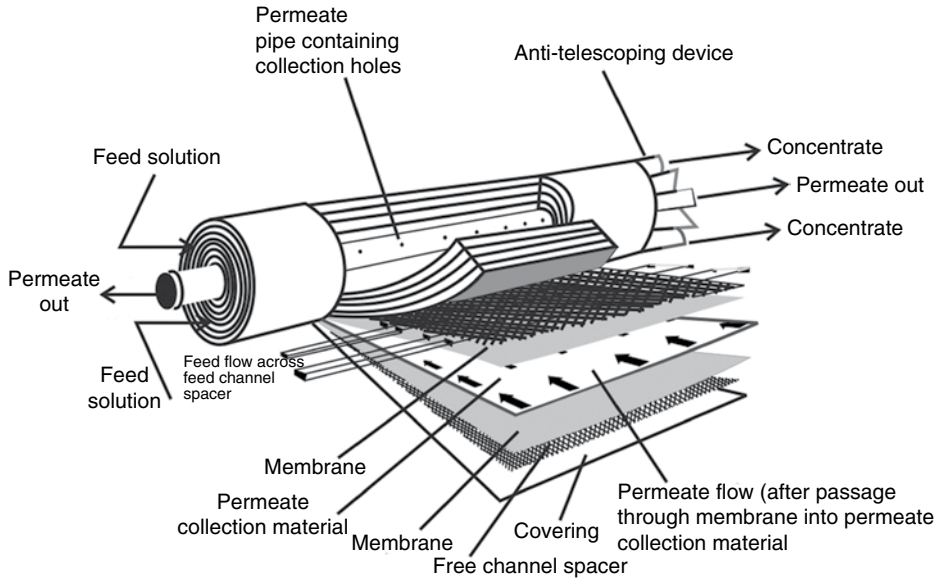

Figure 5.5 Flow pattern in a spiral wound module.

Seawater desalination, brackish water treatment, potable water treatment, dairy processing, electrocoat paint recovery, protein separation and whey protein concentration are some of the applications of this module. Its advantages include:

1. high surface area in a small volume to give high throughput;
2. compact design;
3. module can operate under high transmembrane pressure drop.

5.5 Limitations

5.5.1 Concentration polarisation

During membrane filtration, solute particles (retained by the membrane) are deposited over the membrane surface, making the solute concentration at the membrane surface more than that at the bulk. This establishes a gradient of concentration over a thin boundary layer near the membrane surface. This is known as concentration polarisation (Blatt et al. 1970; De and Bhattacharyya 1997). This phenomenon leads to several manifestations that are deleterious to the membrane performance:

1. reduction in driving force as the osmotic pressure near the membrane surface increases with concentration;
2. formation of a highly viscous gel-type layer over the membrane surface, thereby increasing resistance to the solvent flux;
3. adsorption of solutes on the membrane surface and within the membrane pores, thereby decreasing membrane permeability;
4. increase in solution viscosity near the surface, offering more resistance against the solvent flux.

All these effects lead to a decline in permeate flux or throughput of the system and at the same time, the quality of the permeate stream deteriorates.

5.5.2 Membrane fouling and cleaning

The cause of the flux decline is known as membrane fouling. Two types of fouling generally occur: reversible and irreversible fouling. In reversible fouling, membrane permeability is completely regained after appropriate cleaning. Thus, deposition of solute particles over the membrane surface (concentration polarisation) is an example of reversible fouling. Reversible fouling exists only during the filtration process and it is temporary in nature.

Conversely, irreversible fouling is permanent. It is caused by the adsorption of solute particles on the pore mouth, inside the pore wall, partially or completely clogging the pores, even after a proper cleaning process. This leads to permanent loss of membrane permeability. Irreversible fouling is one of the most harmful occurrences during membrane separation process, reducing its efficiency.

Cleaning of the membrane is an active area of research. The first step in cleaning is flushing the system with tap water, followed by distilled water, in either forward-washing mode or back-washing mode. Back-washing mode is quite effective in tubular and hollow-fibre modules. Cleaning is also carried out with slightly acidic or alkaline solution or one followed by the other (Al-Obeidani et al. 2008; Blanpain-Avet et al. 2009; Liikanen et al. 2002). Specific cleaning solutions exist (Ultrasil) for cleaning the membranes. Cleaning cycles are an integral part of any membrane operation.

5.6 Quantification of concentration polarisation

Concentration polarisation cannot be avoided, it can only be minimised. Before taking any corrective measures, concentration polarisation should be quantified. This quantification has three distinct steps: determining the solute balance equation within the mass transfer boundary layer in the feed side; determining the transport equation of solvent within the porous membrane; determining the solute transport equation within the porous membrane. System performance can be predicted by

simultaneous solution of all these three equations. The simplified one-dimensional model for such purposes is presented below. Based on the type of concentration polarisation, there are two classes of models: an osmotic pressure-controlled model and a gel layer controlling model.

5.6.1 Osmotic pressure-controlled model

In this case, solute particles form a viscous boundary layer over the membrane surface. Solute concentration increases from the bulk to membrane surface concentration across the mass transfer boundary layer. It is assumed that the thickness of the mass transfer boundary layer is constant. At any cross-section of the boundary layer, at steady state, the solute mass balance leads to (Bungay et al.1986; Cheryan 1998; Porter 2005):

$$v_w c - v_w c_p + D\frac{dc}{dy} = 0 \tag{5.3}$$

Integrating the above equation across the thickness of the mass transfer boundary layer, the governing equation of the flux is obtained as:

$$v_w = \left(\frac{D}{\delta}\right)\ln\left(\frac{c_m - c_p}{c_0 - c_p}\right) = k\ln\left(\frac{c_m - c_p}{c_0 - c_p}\right) \tag{5.4}$$

This equation is well known as the film theory equation. In the above equation, v_w is the permeate flux, k is the mass transfer coefficient, c_m, c_p and c_0 are solute concentrations at the membrane surface, in the permeate and in the bulk, respectively. The mass transfer coefficient is estimated from the following equations depending on the channel geometry and flow regimes.

In the rectangular channel, the mass transfer coefficient is estimated using the following Sherwood number relations (Gekas and Hallstrom 1987).

For laminar flow (Leveque's equation):

$$Sh = \frac{kd_e}{D} = 1.85\left(\mathrm{Re}\,Sc\frac{d_e}{L}\right)^{\frac{1}{3}} \tag{5.5a}$$

For turbulent flow (Dittus–Boelter equation):

$$Sh = 0.023(\mathrm{Re})^{0.8}(Sc)^{0.33} \tag{5.5b}$$

In case of flow through the tube, the mass transfer coefficient is estimated for laminar flow (Leveque's equation) (Gekas and Hallstrom 1987):

$$Sh = \frac{kd}{D} = 1.62\left(\mathrm{Re}\,Sc\frac{d_e}{L}\right)^{\frac{1}{3}} \tag{5.5c}$$

and for the turbulent flow, it is calculated from Equation (5.5b). Now, the transport equation in the flow channel, Equation (5.4), must be coupled with the transport law through the porous membrane. It is expressed as Darcy's law (Bungay et al.1986; Cheryan 1998; Porter 2005):

$$v_w = L_P(\Delta P - \Delta\pi) \tag{5.6}$$

where $\Delta\pi$ is the osmotic pressure difference across the membrane. The osmotic pressure being a colligative property, it is a strong function (in fact, an ever increasing function) with concentration. Osmotic pressure is also inversely proportional to the molecular weight of solute. Therefore, it is quite significant for the solutes of lower molecular weights, such as salts, dyes, etc. For salts and lower molecular weight solutes, it is a linear function of concentration and for polymers, proteins and higher molecular weight solutes, it is a non-linear function of concentration.

It can be seen that in Equation (5.4), there are three unknowns, namely, v_w, c_m and c_p. Osmotic pressure difference can be written in terms of concentration at the membrane surface as:

$$\Delta\pi = \pi_m - \pi_p = a_1\left(c_m - c_p\right) + a_2\left(c_m^2 - c_p^2\right) + a_3\left(c_m^3 - c_p^3\right) \tag{5.7}$$

The relationship between c_m and c_p is defined by the partition coefficient across the membrane phase, between upstream and downstream sides of the membrane, known as real retention. This is a constant property as defined in Equation (5.2).

Therefore, Equation (5.7) can be written in terms of the single parameter c_m using Equation (5.2). Now the system variables are reduced to two, namely, c_m and v_w, instead of three. These two can be obtained by solving Equations (5.4) and (5.6) using an iterative algorithm like the Newton–Raphson technique. The above model is known as classic film theory or the osmotic pressure-controlling model.

Solution diffusion model for RO/NF

The concept of real retention is nothing but a partition coefficient between the solute concentration in the permeate and that at the membrane surface. Hence, for a more realistic situation, the solute flux through the membrane is considered using the solution diffusion model described earlier. The osmotic pressure is considered here as linear with concentration in case of salt solution, $\pi = aC$. The starting equations are the osmotic pressure equation, Equation (5.6), and the film theory equation, Equation (5.4). The osmotic pressure model can be written by inserting the expression of the osmotic pressure difference:

$$v_w = v_w^0 \left[1 - \alpha(C_m - C_p)\right] \tag{5.8}$$

where $\alpha = \dfrac{a}{\Delta P}$, $v_w^0 = L_p \Delta P$ is the pure water flux. The above equation can be equated with the film theory equation and the following equation results.

$$v_w^0 \left[1 - \alpha(C_m - C_p)\right] = k \ln \frac{C_m - C_p}{C_0 - C_p} \tag{5.9}$$

From the solution diffusion model, the solute flux is written as:

$$v_w C_p = B(C_m - C_p) \tag{5.10}$$

where B is a constant. Combining Equations (5.8) and (5.10), the following equation is obtained.

$$v_w^0 \left[1 - \alpha(C_m - C_p)\right] = B\left(\frac{C_m - C_p}{C_p}\right) \tag{5.11}$$

The above equation can be simplified as:

$$1 - \alpha C_m + \alpha C_p = \beta \frac{C_m - C_p}{C_p} \tag{5.12}$$

where $\beta = \dfrac{B}{v_w^0}$. From the above equation, the membrane surface concentration is obtained as:

$$C_m = C_p \left[1 + \frac{1}{\beta + \alpha C_p}\right] \tag{5.13}$$

Putting C_m from the above equation into Equation (5.9), we get:

$$\frac{\beta v_w^0}{\alpha C_p + \beta} - k \ln \left[\frac{C_p}{(\alpha C_p + \beta)(C_0 - C_p)}\right] = 0 \tag{5.14}$$

Again, a trial and error solution for C_p is sought using a standard iterative technique.

Kedem–Katchalsky equation for RO/NF/UF

Another variant of the osmotic pressure model is the Kedem–Katchalsky equation. In this case, the imperfect retention of the solutes by the membrane is incorporated by a reflection coefficient in the expression of permeate flux.

$$v_w = L_p(\Delta P - \sigma\Delta\pi) \tag{5.15}$$

where σ = Reflection coefficient. Incorporating the expression of osmotic pressure in the above equation leads to the following expression of flux.

$$v_w = L_p\left[\Delta P - a\sigma(C_m - C_p)\right] \tag{5.16}$$

From the film theory equation, the membrane surface concentration can be expressed as:

$$C_m = C_p + (C_0 - C_p)e^{\frac{v_w}{k}} \tag{5.17}$$

Combining Equations (5.15) and (5.17), the following equation is obtained:

$$v_w = L_p\left[\Delta P - a\sigma\left\{(C_0 - C_p)e^{\frac{v_w}{k}}\right\}\right] \tag{5.18}$$

The permeate concentration, C_p, can be expressed in terms of C_m by using either the definition of real retention or the solution diffusion model, Equation (5.10). After that, Equation (5.18) has to be solved by adopting an iterative scheme.

Modified solution diffusion model for RO/NF/UF

In this case, the solute transport through the membrane is modified by incorporating the convective transport of the solutes through the pores, in addition to the diffusive transport. Thus, this model is more applicable for more porous membranes. The solute flux is written as:

$$v_w C_p = B(C_m - C_p) + (1-\sigma)v_w C_{avg} \tag{5.19}$$

where $C_{avg} = \dfrac{C_m - C_p}{\ln\left(\dfrac{C_m}{C_p}\right)}$

By combining Equations (4) and (19), we get:

$$C_p = \frac{\beta}{v_w}\left[(C_0 - C_p)e^{\frac{v_w}{k}}\right] + \frac{(1-\sigma)(C_0 - C_p)e^{\frac{v_w}{k}}}{\ln\left[1 + \dfrac{C_0 - C_p}{C_p}e^{\frac{v_w}{k}}\right]} \tag{5.20}$$

We have three equations, (5.16), (5.19) and (5.20), and three unknowns in C_m, v_w and C_p. The above problem can be solved iteratively, to obtain a system prediction.

The osmotic pressure model based on film theory has several shortcomings:

1. the mass transfer boundary layer is assumed to be fully developed, whereas the entrance length required for the mass transfer boundary layer to be fully developed is substantial;
2. variation of physical properties with concentration, such as diffusivity, viscosity, etc., is not considered;
3. mass transfer coefficients are used as obtained from heat–mass transfer analogies applicable for impervious conduits.

However, the film theory-based osmotic pressure model presents a simple and quick method for quantifying system performance. In order to overcome these shortcomings, the two-dimensional mass transfer boundary layer equation can be solved and/or detailed pore flow models can be incorporated. Many studies are available including these intricacies of the model (Banerjee and De 2010; Bowen and Welfoot 2002; Chen et al. 2011; Déon et al. 2011; Idris et al. 2002).

5.6.2 Gel layer controlling model

In the gel layer controlling model, it is assumed that a gel of concentrated solutes has been deposited over the membrane surface with constant thickness. It is assumed that the solute concentration within the gel is uniform. Outside the gel layer, there exists a mass transfer boundary layer where the solute concentration ranges from feed concentration and gel concentration. Therefore, in this case, the solute undergoes drastic variation in viscosity, diffusivity and density as these properties are functions of concentration. Under steady-state conditions, one can apply film theory (constant thickness boundary layer outside the gel layer) and can obtain the equation of permeate flux as:

$$v_w = k \ln\left(\frac{c_g}{c_0}\right) \tag{5.21}$$

5.7 Applications of membrane-based processes

5.7.1 Reverse osmosis

Desalination of sea water to make it potable is the most important application of reverse osmosis (Ho and Sirkar 1992; Porter 2005; Rautenbach and Albrecht 1986; Wankat 2007). The relative comparison of the different types of modules available for RO separation is presented in Table 5.1.

Table 5.1 Reverse osmosis membrane module comparison

Characteristic	Module type			
	Spiral-wound	Hollow-fiber	Tubular	Plate and frame
Typical packing density (m^2/m^3)	800	6000	70	500
Operating pressure (psi)	200–800	200–400	400–800	500–1000
Range of pH tolerance	4–7	4–10	4–7	4–7
Resistance to fouling	High	High	Low	Moderate
Ease of cleaning	Poor to good	Poor	Excellent	Good
Production per unit space	Good	Excellent	Fair	Poor
Relative expense	Low	Low	High	High

Sources: Bungay et al. 1986; Ho and Sirkar 1992.

Pretreatment of feed water

Feed water pretreatment prior to RO is necessary to prevent membrane degradation and fouling by brackish and sea water components or oxidising agents. The degree of pretreatment that is needed is determined by both the quality of the intake feed water and the type of membrane used in the plant. The raw feed water can contain materials such as silt and other suspended solids, colloidal material, microbiological organisms and dissolved solids. The suspended solids and colloidal materials must be removed to reduce fouling of the membrane, thereby subsequently reducing the chances of flux reduction. Different pretreatment methods suitable for particular situations are explicitly discussed in Table 5.2.

A typical flowsheet of a reverse osmosis plant is presented in Figure 5.6.

Some desalination plant installations

Israel

In Israel three major plants have been installed. The first is located at Ashkelon, on the Mediterranean coast, with a capacity of 330,000 m^3/day. The price of treated water is around 0.5 US$/$m^3$. It provides about 13% of the country's fresh water requirement. The second plant is located at Palmachin and the third is at Hadera. This plant will be able to desalinate 33 million gallons of fresh drinking water per year. Israel plans to set up five such plants, expecting to supply about two-thirds of the country's drinking water.

Pakistan

The government has set up 382 RO plants in the province of Sindh. Out of these, 207 are installed in remote areas, including arid districts. The rest are on the verge of completion. Asia's biggest RO plant is under construction in Nawabshah, which will give 8 million gallons of water per day.

Table 5.2 Pretreatment methods used in sea water and brackish water desalination

Species	Problem	Pretreatment method
Suspended solids	Fouling of membrane by particles caused reduced flux	Sand filtration Coagulation filtration Cartridge filtration Microfiltration
Precipitation/scale formation by $CaCO_3$, $MgCO_3$, $CaSO_4$, SiO_2, $BaSO_4$, etc.	Fouling of membrane by precipitate or scale causes reduced flux	Operate at low water recovery (so solubility not exceeded) Acid or chelating agent addition to prevent precipitation Chemical precipitation Addition of antiscalants
Colloids (clays, iron colloids, $Al(OH)_3$)	Fouling of membrane by colloids causes reduced flux	Coagulation followed by filtration Ultrafiltration
Micro-organisms	Slime layers on membranes cause reduced flux; some membranes are degraded by micro-organisms	Chlorination Sodium bisulphate addition UV light treatment Ozonisation Chloramine addition
Chlorine	Chlorine added for disinfection will damage most membranes	Sodium bisulphate addition Activated carbon filters
Organics	Adsorption on membrane can cause loss of water flux over time; some high molecular weight organics can coagulate to form colloids	Activated carbon Replace use of cationic polymers (coagulant), which cause formation of organic colloids
pH	Should be in the acceptable operating range of membrane	Adjust with acid (HCl, H_2SO_4) or base (lime, NaOH)

From Bungay et al. 1986.
UV, ultraviolet.

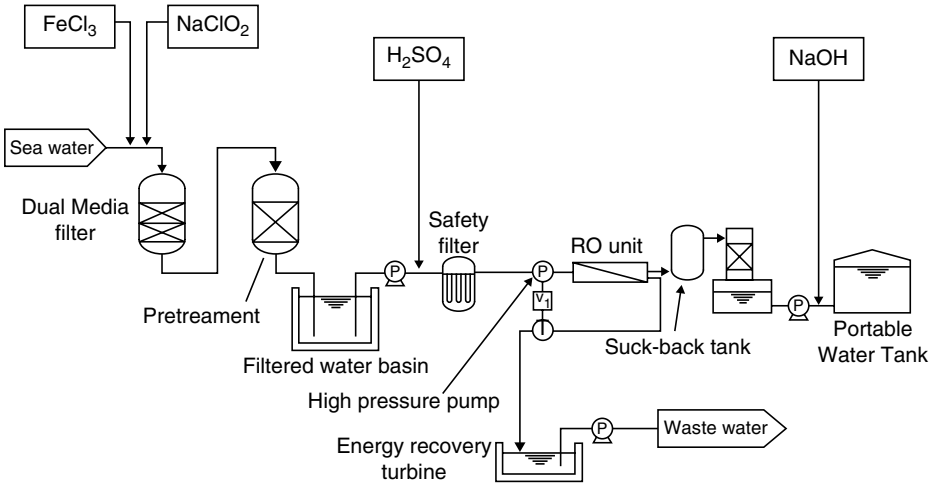

Figure 5.6 Typical flowsheet of a reverse osmosis plant set-up.

Middle East

The Spanish company Cadagua has installed over 200 water plants using RO technology in 15 countries, including Saudi Arabia, Jordan and Kuwait. In 2006, the first RO desalination plant was commissioned in Madinat Yanbu in Saudi Arabia, with a capacity of 13.3 million gallons per day.

Africa

General Electric installed a 200,000 m^3/day capacity plant in the city of Algiers, Algeria, in 2008. The plant cost was US$250 million. It provides 25% of the city's daily needs. In 2011, a 15 million megalitre per day capacity plant was installed in the Western Cape province of South Africa. The other desalination plants in South Africa are at nearby Knysna (1.5 megalitres a day), Bitou Municipality, Sedgefield on the Garden Route and Boknes in the Eastern Cape. In 2010, a 20 million m^3 per annum desalination plant was set up in Namibia, located 30 km north of Swakopmund on the Atlantic coast.

India

Three desalination plants have been set up near Chennai in Tamil Nadu. The first is located in Kattupalli village in Minjur, with a capacity of 100 million litres per day. The second one is at Pattipulam, with a capacity of 200 million litres per day. The third is at Nimelli, having a capacity of 100 million litres per day.

Other applications

Reverse osmosis is used in a series of pretreatment procedures to treat the municipal waste water and the water requirement of a petroleum refinery in Riyadh, Saudi Arabia (Porter 2005). For recovery of various metals from electroplating industries, RO can safely be used (Benito and Ruiz 2002; Chai et al. 1997). Some other applications include production of bottled water, removal of nitrates, fluoride, arsenic, cyanide, etc., production of feed water for power plants, beverage industries, pharmaceuticals, etc. (Ning 2002; Porter 2005; Richards et al. 2010; Sehn 2008). RO has been successfully used for treatment of tannery effluent (Das et al. 2006; Gisi et al. 2009) and dairy plant effluent (Vourch et al. 2005, 2008).

5.7.2 Nanofiltration

Nanofiltration is used for separation of divalent salts and molecules with molecular weight up to 1000. Therefore, NF is widely used for pretreatment of RO feed to reduce the solid load on RO. It is in use for production of bottled water as well because retention of sodium chloride is partial and its presence is required for human health. The most widespread industrial application of NF is in the

removal of dyes. Most dyes have a molecular weight in the range of 200–900 and they are removed by NF membranes (Akbari et al. 2002; Avlonitis et al. 2008; Chakraborty et al. 2003; Jiraratananon et al. 2000). NF also has applications in the treatment of tannery effluent (Ahmed et al. 2004; Cassano et al. 2001; Prabhavathy and De 2010; Religa et al. 2011).
In summary, NF applications are categorised into:

1. desalination and concentration (Wang et al. 2002a);
2. separation and purification (Li et al. 2003; Wang et al. 2002b);
3. waste water treatment (Ahmed et al. 2004; Akbari et al. 2002; Avlonitis et al. 2008; Cassano et al. 2001; Chakraborty et al. 2003; Jiraratananon et al. 2000; Prabhavathy and De 2010; Religa et al. 2011);
4. selective separation of salts (Su et al. 2006; Wang et al. 2005);
5. concentration of neutral solutes (Wang et al. 2009);
6. separation and purification of amphoteric solutions (Gyura et al. 2002; Vellenga and Trgardh 1998).

5.7.3 Ultrafiltration

Ultrafiltration is becoming one of the major industrially important unit operations. It is used for various purposes, including separation, concentration and fractionation. Recovery of high-value products, recycling of permeate and controlling pollution can be achieved using UF. Some important applications are presented below.

Ultrafiltration is used to separate solvent and low molecular weight solutes from paint and filtrate before recycling to the feed paint tank (Bjerke 1980). In the textile industry, UF is used for recovery of sizing chemicals, such as polyvinyl alcohol, carboxymethylcellulose, etc. (El Defrawy and Shaalan 2007; Hao and Zhao 1994). Grease and oil from metal pieces in metal finishing industries are removed before they are painted. UF is used to remove oil from the metal finishing rinse stream and enhances the life of the detergent bath (Hesampour et al. 2008; Qin et al. 2004).

Ultrafiltration in diafiltration mode can be used to concentrate solids in dairy industries. UF is also used to produce protein-rich milk and is useful in soft cheese making (Brans et al. 2010; Tang et al. 2010).

Ultrafiltration is widely used nowadays in juice processing industries and can replace several unit operations, such as enzymatic treatment, centrifugation, addition of fining agents, filtration of fining agents by diatomaceous earth, final polish filtration, sterilisation, etc. The major objective of these processing steps is to impart a high shelf-life to the processed juice (Chhaya et al. 2010; Conidi et al. 2011; de Barros et al. 2003; Onsekizoglu et al. 2010; Rai and De 2009; Rai et al. 2006).

Effluent emerging from pulp and paper industries contains huge amounts of lignin, salts and organic matters and hence high biological and chemical oxygen demand. UF can be used to treat these streams by separating lignin and recovering salts and inorganic materials (Dal-Cin et al. 1996; De and Bhattacharya 1996; Puro et al. 2011).

In tannery effluent, UF can be applied to treat soaking, liming, degreasing and other process streams (Das et al. 2008; Purkait et al. 2005).

Bioactive components with medicinal importance are available in various natural products, including phytochemicals such as polyphenols in green tea leaves, steviosides in Stevia leaves, lycopenes in tomato and water melon juice, etc. They have antioxidant, anticarcinogenic properties and hence have applications in food industries as food supplements and additives, pharmaceutical and cosmetic industries. UF is used for extraction of polyphenols, lycopenes and stevioside from their water extract (Chhaya 2012; Kumar et al. 2012; Todisco et al. 2002).

Ultrafiltration is used in the pharmaceutical sector for separation of various enzymes from fermentation, plasma separation, separation and fractionation of protein solution, separation of antibodies and to produce pyrogen-free solution (Ko et al. 1993; Latulippe et al. 2007; Yoon et al. 2006). UF is used to produce purer water for many applications, e.g. boiler feed water to prevent scaling, rinsing of electronic components, beverage production, etc. (Todisco et al. 2002). It is used as a pretreatment step for RO and ion exchange processes to avoid fouling of equipment.

Some recent applications of UF include polyelectrolyte-enhanced UF (PEUF) (Juang and Chen 1996; Tabatabai et al. 1995), micellar-enhanced UF (MEUF) (Huang et al. 2010; Kim et al. 1998; Zeng et al. 2008) and electric field-enhanced UF (EUF) (Sarkar et al. 2008, 2009), etc. In PEUF, low molecular weight inorganic solutes (typically carcinogenic heavy metal cations, like cadmium, zinc, etc.) are attached to a polyelectrolyte and the moiety is removed by UF. In MEUF, organic solutes are solubilised inside the hydrophobic core and oppositely charged pollutants (cations or anions) are attached to the outer surface of micelles which are removed by UF membranes. In EUF, an electrical field of suitable polarity is applied to remove the charged solutes from the membrane surface. This reduces concentration polarisation and increases throughput significantly.

5.7.4 Microfiltration

Microfiltration is used for separation of micro-sized solutes. Removal of bacteria is one of the important applications of MF. Using membrane with an average pore size of 0.2 micron, bacteria can be removed and it is possible to produce a sterile solution (Allegrezza et al. 2008; Rajniak et al. 2008; Sundaram et al. 1999). Concentration and clarification of cells (Lee 2009; Russotti et al. 1995), separation of products from fermentation broth (Conrad and Lee 1998; Liew et al. 1997), separation of proteins, antibiotics, lactic acid, polysaccharides (Baruah and Belfort 2004;

Davies et al. 2000; Harscoat et al. 1999; Nishikawa and Dunn 1999) and purification of nanoparticles (Charcosset 2012; Limayem et al. 2004) can be carried out using MF. In fact, MF can be utilised as a pretreatment process in various industrial applications.

References

Ahmed, M.T., Taha, S., Chaabane, T., Cabon, J., Maachi, R., Dorange, G. (2004) Treatment of the tannery effluents from a plant near Algiers by nanofiltration (NF): experimental results and modeling. Desalination 165, 155–160.

Akbari, A., Desclaux, S., Remigy, J.C., Aptel, P. (2002) Treatment of textile dye effluents using a new photografted nanofiltration membrane. Desalination 149, 101–107.

Allegrezza, A., Ireland, T., Kools, W., et al. (2008) Membranes in the biopharmaceutical industry. In: Pienemann, K.V., Pereira-Nunes, S. (eds) *Membrane for Life Science*. Germany: Wiley-VCH, pp91–154.

Al-Obeidani, S.K.S., Al-Hinai, H., Goosen, M.F.A., Sablani, S., Taniguchi, Y., Okamura, H. (2008) Chemical cleaning of oil contaminated polyethylene hollow fiber microfiltration membranes. J Membr Sci 307, 299–308.

Avlonitis, S.A., Poulios, I., Sotiriou, D., Pappas, M., Moutesidis, K. (2008) Simulated cotton dye effluents treatment and reuse by nanofiltration. Desalination 221, 259–267.

Banerjee, P., De, S. (2010) Coupled concentration polarisation and pore flow modeling of nanofiltration of an industrial textile effluent. Sep Purif Technol 73, 355–362.

Baruah, G.L., Belfort, G. (2004) Optimized recovery of monoclonal antibodies from transgenic goat milk by microfiltration. Biotechnol Bioeng 87, 274–285.

Benito, Y., Ruíz, M.L. (2002) Reverse osmosis applied to metal finishing wastewater. Desalination 142, 229–234.

Bjerke, B. (1980) Membrane technology and costs; state of the art. Desalination 35, 375–382.

Blanpain-Avet, P., Migdal, J.F., Bénézec, T. (2009) Chemical cleaning of a tubular ceramic microfiltration membrane fouled with a whey protein concentrate suspension – characterization of hydraulic and chemical cleanliness. J Membr Sci 337, 153–174.

Blatt, W.F., Dravid, A., Michaels, A.S., Nelsen, L. (1970) Solute polarisation and cake formation in membrane ultrafiltration: causes, consequences, and control techniques. In: Flinn, J.E. (ed) *Membrane Science and Technology*. New York: Plenum Press, pp47–94.

Bowen, W.R., Welfoot, J.S. (2002) Modelling the performance of membrane nanofiltration – critical assessment and model development. Chem Eng Sci 52, 1121–1137.

Brans, G., Schroën, C.G.P.H., van der Sman, R.G.M., Boom, R.M. (2010) Membrane fractionation of milk: state of the art and challenges. J Membr Sci 352, 71–75.

Bungay, P.M., Lonsdale, H.K.M., de Pinho, N. (1986) *Synthetic Membranes: Science, Engineering and Applications*. NATO Scientific Affairs Division. Dordrecht: Reidel.

Cassano, A., Molinari, R., Romano, M., Drioli, E. (2001) Treatment of aqueous effluents of the leather industry by membrane processes: a review. J Membr Sci 181, 111–126.

Chai, X., Chen, G., Po-Lock, Y., Mitrerfe, Y. (1997) Pilot scale membrane separation of electroplating waste water by reverse osmosis. J Membr Sci 123, 235–242.

Chakraborty, S., Purkait, M.K., DasGupta, S., De, S., Basu, J.K. (2003) Nanofiltration of textile plant effluent for color removal and reduction in COD. Sep Purif Technol 31, 141–151.

Charcosset, C. (2012) *Membrane Processes in Biotechnology and Pharmaceutics*. Amsterdam: Elsevier.

Chen, Y., Hu, X., Kim, H. (2011) Monte Carlo simulation of pore blocking phenomena in cross-flow microfiltration. Water Res 45, 6789–6797.

Cheryan, M. (1998) *Ultrafiltration and Microfiltration Handbook*. Lancaster: Technomic.

Chhaya, C. (2012) Processing of Stevia (*Stevia Rebaudiana*) extract using membrane technology. PhD dissertation. I.I.T. Kharagpur, India.

Chhaya, C., Rai, P., Majumdar, G.C., De, S., DasGupta, S. (2010) Mechanism of permeate flux decline during microfiltration of water melon (Citrullus lanatus) juice. Food Bioproc Technol 3, 545–553.

Conidi, C., Cassano, A., Drioli, E. (2011) A membrane-based study for the recovery of polyphenols from bergamot juice. J Membr Sci 375, 182–190.

Conrad, P.B., Lee, S.S. (1998) Two phase bioconversion product recovery by microfiltration: 1. Steady state studies. Biotechnol Bioeng 57, 631–641.

Dal-Cin, M.M., McLellan, F., Striez, C.N., Tam, C.M., Tweddle, T.A., Kumar, A. (1996) Membrane performance with a pulp mill effluent: relative contributions of fouling mechanisms. J Membr Sci 120, 273–285.

Das, C., Patel, P., De, S., DasGupta, S. (2006) Treatment of tanning effluent using nanofiltration followed by reverse osmosis. Sep Purif Technol 50, 291–299.

Das, C., DasGupta, S., De, S. (2008) Steady state modeling for membrane separation of pretreated soaking effluent under cross flow mode. Environ Prog 27, 346–352.

Davies, J.L., Baganz, F., Isom, A.P., Lye, G.J. (2000) Studies on interaction of fermentation and microfiltration operations: erithromycin recovery from saccharopolyspora erythraea fermentation broths. Biotechnol Bioeng 69, 429–439.

De Barros, S.T.D., Andrade, C.M.G., Mendes, E.S., Peres, L. (2003) Study of fouling mechanism in pineapple juice clarification by ultrafiltration. J Membr Sci 215, 213–224.

De, S., Bhattacharya, P.K. (1996) Recovery of water with inorganic chemicals from kraft black liquor using membrane separation processes. Tappi J 79, 103–111.

De, S., Bhattacharya, P.K. (1997) Modeling of ultrafiltration process for a two component aqueous solution of low and high (gel-forming) molecular weight solutes. J Membr Sci 136, 57–69.

Déon, S., Escoda, A., Fievet, P. (2011) A transport model considering charge adsorption inside pores to describe salts rejection by nanofiltration membranes. Chem Eng Sci 66, 2823–2832.

El Defrawy, N.M.H., Shaalan, H.F. (2007) Integrated membrane solutions for green textile industries. Desalination 204, 241–254.

Gekas, V., Hallstrom, B. (1987) Mass transfer in the membrane concentration polarisation layer under turbulent cross flow. I. Critical literature review and adaptation of existing Sherwood correlations to membrane operations. J Membr Sci 80, 153–170.

Gisi, S.D., Galasso, M., Feo, G.D. (2009) Treatment of tannery wastewater through the combination of a conventional activated sludge process and reverse osmosis with a plane membrane. Desalination 249, 337–342.

Gyura, J., Seres, Z., Vatai, G., Molnar, E.B. (2002) Separation of non-sucrose compounds from the syrup of sugar-beet processing by ultra- and nanofiltration using polymer membrane. Desalination 148, 49–56.

Hao, J., Zhao, Q. (1994) The development of membrane technology for wastewater treatment in the textile industry in China. Desalination 98, 353–360.

Harscoat, C., Jaffrin, M.Y., Paullier, P., Courtois, B., Courtois, J. (1999) Recovery of microbial polysaccharides from fermentation broths by microfiltration on ceramic membranes. J Chem Technol Biotechnol 74, 571–579.

Hesampour, M., Krzyzaniak, A., Nyström, M. (2008) Treatment of waste water from metal working by ultrafiltration, considering the effects of operating conditions. Desalination 222, 212–221.

Ho, W.S.W., Sirkar, K.K. (1992) *Membrane Handbook*. New York: Chapman and Hall.

Huang, J.H., Zhou, C.F., Zeng, G.M., et al. (2010) Micellar-enhanced ultrafiltration of methylene blue from dye wastewater via a polysulfone hollow fiber membrane. J Membr Sci 365, 138–144.

Idris, A., Ismail, A.F., Shilton, S.J., Roslina, R., Musa, M. (2002) The deduction of fine structural details of reverse osmosis hollow fiber membranes using surface force–pore flow model. Sep Purif Technol 29, 217–227.

Jiraratananon, R., Sungpet, A., Luangsowan, P. (2000) Performance evaluation of nanofiltration membranes for treatment of effluents containing reactive dye and salt. Desalination 130, 177–183.

Juang, R.S., Chen, M.N. (1996) Retention of copper(II)-EDTA chelates from dilute aqueous solutions by a polyelectrolyte-enhanced ultrafiltration process. J Membr Sci 119, 25–37.

Kim, C.K., Kim, S.S, Kim, D.W, Lim, J.C, Kim, J.J. (1998) Removal of aromatic compounds in the aqueous solution via micellar enhanced ultrafiltration: Part 1. Behavior of nonionic surfactants. J Membr Sci 147, 13–22.

Ko, M.K., Pellegrino, J.J., Nassimbene, R., Marko, P. (1993). Characterization of the adsorption-fouling layer using globular proteins on ultrafiltration membranes. J Membr Sci 76, 101–120.

Kumar, A., Thakur, B.K., De, S. (2012) Selective extraction of (-) epigallocatechin gallate from green tea leaves using two stage infusion coupled with membrane separation. Food Bioproc Technol 5, 2568–2577.

Latulippe, D.R., Ager, K., Zydney, A.L. (2007) Flux-dependent transmission of supercoiled plasmid DNA through ultrafiltration membranes. J Membr Sci 294, 169–177.

Lee, T.S. (2009) A methodological approach to scaling up fermentation and primary recovery processes to the manufacturing scale for vaccine production. Vaccine 27, 6439–6443.

Li, S.L., Li, C., Liu, Y.S., Wang, X.L., Cao, Z.A. (2003) Separation of L-glutamine from fermentation broth by nanofiltration. J Membr Sci 222, 191–201.

Liew, M.K.H., Fane, A.G., Rogers, P.L. (1997) Fouling of microfiltration membranes by broth-free antifoam agents. Biotechnol Bioeng 56, 89–98.

Liikanen, R., Yli-Kuivila, J., Laukkanen, R. (2002) Efficiency of various chemical cleanings for nanofiltration membrane fouled by conventionally-treated surface water. J Membr Sci 195, 265–276.

Limayem, I., Charcosset, C., Fessi, H. (2004) Purification of nanoparticle suspensions by a concentration/diafiltration process. Sep Purif Technol 38, 1–9.

Ning, R.Y. (2002) Arsenic removal by reverse osmosis. Desalination 143, 237–241.

Nishikawa, A., Dunn, I.L. (1999) Performance of a two-stage fermentor with cell recycle for continuous production of lactic acid. Bioproc Eng 21, 299–305.
Onsekizoglu, P., Bahceci, K.S., Acar, M.J. (2010) Clarification and the concentration of apple juice using membrane processes: a comparative quality assessment. J Membr Sci 352, 160–165.
Opong, W.S., Zydney, A.L. (1991) Diffusive and convective protein transport through asymmetric membranes. AIChE J 37, 1497–1510.
Porter, M.C. (2005) Handbook of Industrial Membrane Technology. New Delhi: Crest Publishing.
Prabhavathy, C., De, S. (2010) Treatment of fatliquoring effluent from a tannery using membrane separation process: experimental and modeling. J Hazard Mater 176, 434–443.
Purkait, M.K., Bhattacharya, P.K., De, S. (2005) Membrane filtration of leather plant effluent: flux decline mechanism. J Membr Sci 258, 85–96.
Puro, L., Kallioinen, M., Mänttäri, M., Nyström, M. (2011) Evaluation of behavior and fouling potential of wood extractives in ultrafiltration of pulp and paper mill process water. J Membr Sci 368, 150–158.
Qin, J., Wai, M.N., Oo, M.H., Lee, H. (2004) A pilot study for reclamation of a combined rinse from a nickel-plating operation using a dual-membrane UF/RO process. Desalination 161, 155–167.
Rai, P., De, S. (2009) Clarification of pectin containing juice using ultrafiltration. Curr Sci 96, 1361–1371.
Rai, P., Majumdar, G.C., Sharma, G., DasGupta, S., De, S. (2006) Effects of various cutoff membranes on permeate flux and quality during filtration of mosambi (Citrus sinensis (L.) Osbeck) juice. Food Bioprod Proc 84, 213–219.
Rajniak, P., Tsinontides, S.C., Pham, D., Hunke, W.A., Reynolds, S.D., Chern, R.T. (2008) Sterilizing filtration – principles and practice for successful scale-up to manufacturing. J Membr Sci 325, 223–237.
Rautenbach, R., Albrecht, R. (1986) *Membrane Processes*. New York: John Wiley & Sons, Inc.
Religa, P., Kowalik, A., Gierycz, P. (2011) Application of nanofiltration for chromium concentration in the tannery wastewater. J Hazard Mater 186, 288–292.
Richards, L.A., Vuachère, M., Schäfer, A.I. (2010) Impact of pH on the removal of fluoride, nitrate and boron by nanofiltration/reverse osmosis. Desalination 261, 331–337.
Russotti, G., Osawa, A.E., Sitrin, R.D., Buckland, B.C., Adams, W.R., Lee, S.S. (1995) Pilot-scale harvest of recombinant yeast employing microfiltration: a case study. J Biotechnol 42, 235–246.
Sarkar, B., DasGupta, S., De, S. (2008) Cross-flow electro-ultrafiltration of mosambi (Citrus Sinensis (L.) Osbeck) juice. J Food Eng 89, 241–245.
Sarkar, B., DasGupta, S., De, S. (2009) Electric field enhanced fractionation of protein mixture using ultrafiltration. J Membr Sci 341, 11–20.
Sehn, P. (2008) Fluoride removal with extra low energy reverse osmosis membranes: three years of large scale field experience in Finland. Desalination 223, 73–84.
Smith, J.M., van Ness, H.C., Abbott, M.M. (2005) *Introduction to Chemical Engineering Thermodynamics*. New York: McGraw-Hill.
Su, M., Wang, D.X., Wang, X.L., Ando, M., Shintani, T. (2006) Rejection of ions by NF membranes for binary electrolyte solutions of NaCl, $NaNO_3$, $CaCl_2$, and $Ca(NO_3)_2$. Desalination 191, 303–308.

Sundaram, S., Auriemma, M., Howard, G., Brandwein, H., Leo, F. (1999) Application of membrane filtration for removal of diminutive bioburden organisms in pharmaceutical products and processes, PDA. J Pharm Sci Technol 53, 186–201.

Tabatabai, A., Scamehorn, J.F., Christian, S.D. (1995) Economic feasibility study of polyelectrolyte-enhanced ultrafiltration (PEUF) for water softening. J Membr Sci 100, 193–207.

Tang, X., Flint, S.H., Bennett, R.J., Brooks, J.D. (2010) The efficacy of different cleaners and sanitizers in cleaning biofilms on UF membranes used in the dairy industry. J Membr Sci 352, 71–75.

Todisco, S., Tallarico, P., Gupta, B.B. (2002) Mass transfer and polyphenols retention in the clarification of black tea with ceramic membranes. Innov Food Sci Emerg Technol 3, 255–262.

Van den Berg, G.B., Racz, I.G., Smolders, C.A. (1989) Mass transfer coefficients in cross flow ultrafiltration. J Membr Sci 47, 25–51.

Vellenga, E., Trgardh, G. (1998) Nanofiltration of combined salt and sugar solutions: coupling between retentions. Desalination 120, 211–220.

Vourch, M., Balannec, B., Chaufer, B., Dorange, G. (2005) Nanofiltration and reverse osmosis of model process waters from the dairy industry to produce water for reuse. Desalination 172, 245–256.

Vourch, M., Balannec, B., Chaufer, B., Dorange, G. (2008) Treatment of dairy industry wastewater by reverse osmosis for water reuse. Desalination 219, 190–202.

Wang, D.X., Su, M., Yu, Z.Y., Wang, X.L., Ando, M., Shintani, T. (2005) Separation performance of a nanofiltration membrane influenced by species and concentration of ions. Desalination 175, 219–225.

Wang, X.L., Ying, A.L., Wang, W.N. (2002b) Nanofiltration of L-phenylalanine and L-aspartic acid aqueous solutions. J Membr Sci 196, 59–67.

Wang, X.L., Zhang C.H., Ouyang, P.K. (2002a) The possibility of separating saccharides from a NaCl solution by using nanofiltration in diafiltration mode. J Membr Sci 204, 271–281.

Wang, X.L., Shang, W.J., Wang, D.X., Wu, L., Tu, C.H. (2009) Characterization and applications of nanofiltration membranes: state of the art. Desalination 236, 316–326.

Wankat, P.C. (2007) *Separation Process Engineering*. New York: Prentice Hall.

Yoon, Y., Westerhoff, P., Snyder, S.A., Wert, E.C. (2006) Nanofiltration and ultrafiltration of endocrine disrupting compounds, pharmaceuticals and personal care products. J Membr Sci 270, 88–100.

Zeng, G.M., Xu, K., Huang, J.H., Li, X., Fang, Y.Y., Qu, Y.H. (2008) Micellar enhanced ultrafiltration of phenol in synthetic wastewater using polysulfone spiral membrane. J Membr Sci 310, 149–160.

6

State of the art of stevioside processing using membrane-based filtration

As outlined in the preceding chapter, membrane-based processes are becoming important unit operations in fruit juice and beverage processing. Typical juice processing involves various unit operations, including enzymatic treatment for removal of pectin, centrifugation for removal of cell debris, treatment by fining agents (bentonite and gelatin) for removal of residual pectin and protein, filtration by diatomaceous earth (i.e. celite) followed by fine filtration. Fine filtration may include adsorption by ion exchange resin, etc. The duration of the whole procedure may be about 24–36 h. For recovery of expensive phytochemicals, such as stevioside and rebaudioside A, the conventional processes include several steps, including extraction (either water based or toxic solvent based, such as methanol), clarification by chelating agents (calcium chloride, calcium hydroxide, ferric chloride, bentonite, pectinase, etc.), filtration by diatomaceous earth, fine filtration using cation and/or anion exchange resin, solvent recovery, etc. These processes are described in detail in Chapter 4.

In membrane-based separation processes, many of these steps can be omitted. Pretreatment of aqueous extract by microfiltration (MF) can replace centrifugation and primary clarification steps using chelating agents. During microfiltration, chlorophylls, cell debris, most of the high molecular weight proteins, organic matter, etc. are removed. Fine filtration can be replaced by appropriately selected ultrafiltration (UF). In this process, the glycosides permeate through the membrane and the remaining high molecular weight undesired substances are removed. The permeate stream can be concentrated using an appropriately selected nanofiltration (NF) membrane. During NF, water from the glycoside-rich solution is extracted, leading to the concentrated solution that can easily be spray dried or vacuum dried to produce powder.

Additionally, being rate governing, membrane-based systems have high throughput and offer commercially viable solutions. Having higher throughput,

Stevioside: Technology, Applications and Health, First Edition.
Sirshendu De, Sourav Mondal and Suvrajit Banerjee.

these systems are less time consuming. Also, complicated operations and expensive equipment like column chromatographs are not required. Moreover, being modular in nature, membrane-based processes are easy to scale up and hence provide a faster, easier and economic solution to processes involving extraction of phytochemicals. Membrane-based processes can provide solutions to clarification and purification, concentration and even fractionation by judicious selection of the appropriate membrane. In the following text, a detailed description of the use of state-of-the-art membrane-based systems for processing Stevia extract is presented.

6.1 Clarification and purification

As we have seen earlier, water extraction of Stevia leaves is the most health-friendly operation. Removal of various unwanted non-glycosidic materials from the extract leads to clarification and purification of the glycoside-containing streams. Fuh and Chiang (1990) investigated the possibility of ultrafiltration followed by diafiltration (DF) as clarification and purification steps. They also compared the efficiency of UF with that of chelating agents (i.e. use of inorganic salts). Three types of chelating agents were used:

1. 3% $AlCl_3$ solution adjusted to pH 7.0–7.5 by $Ca(OH)_2$;
2. saturated $Ca(OH)_2$ solution adjusted to pH to 8–8.5 by bubbling carbon dioxide gas;
3. 3% ferric sulfate solution adjusted to pH 7.0–7.5 with NaOH.

These solutions were mixed with aqueous extract (extraction conditions are 1 kg dry leaves to 16 L water at 55 °C for 1 h) and were filtered through Whatman filter paper.

For ultrafiltration, a tubular module (effective membrane area 0.85 m^2) was used with two UF membranes, namely, 25 kDa and 100 kDa molecular weight cu-off (MWCO) membranes. The operating pressure was 12 bar for 25 kDa and 8 bar for 10 kDa membranes. The extract was first concentrated by UF to an optimum concentration of impurities and the retentate was then processed by constant volume diafiltration (CVDF) to recover maximum glycosides in the permeate. All the membrane processes were carried out with flow rate 25 L/min at 25 °C. It was observed that the 100 kDa MWCO membrane recovered more stevioside and caused more depigmentation compared to the 25 kDa MWCO membrane. Also, the permeate flux of the 100 kDa membrane was greater compared to that of the 25 kDa membrane. Recovery of stevioside increased up to 90% for combined the UF and DF method. The comparative performance of clarification by chelating agents and UF + DF is presented in Table 6.1.

The permeate flux of the 100 kDa MWCO membrane was 60–80 L/m^2.h for a weight concentration ratio from 2 to 9 and that for the 25 kDa MWCO membrane was 20–75 L/m^2.h.

Table 6.1 Comparative performance of clarification by chelating agents and UF + DF

Property	$Ca(OH)_2$	$Fe_2(SO_4)_3$	$AlCl_3$	Membrane, 100 kDa MWCO + DF
Colour removal (%)	71.5	91.2	96.8	93
Stevioside + rebaudioside A recovery (%)	86.0	82.1	70.3	90
Stevioside purity (%)	28.5	11.0	9.4	90

DF, diafiltration; MWCO, molecular weight cut-off.

The first patent reporting a fully fledged membrane-based process for extraction of stevioside was that of Kutowy et al. (1999). The invention involved the following steps:

1. aqueous extraction in a column;
2. pretreatment by MF;
3. purification by a 2–3 kDa UF membrane;
4. concentration by NF at elevated temperature.

In the first step, aqueous extraction was carried out in a column between 0 °C and 25 °C, with a dry plant material to water ratio of 0.02:1 (w/w) to 0.1:1 (w/w), with a solvent flow rate of 24–30 mL/min and dwell time of 10–20 min. It was observed that at acidic pH (about 2), stevioside extraction was maximal (about 8100 ppm). The extract was then microfiltered at 100–200 kPa pressure for primary clarification. The MF membrane was zirconia, with an area of 0.0155 m^2. Permeate was fed to a UF membrane (preferably 2.5 kDa cut-off with effective area 0.0055 m^2) to remove higher molecular weight impurities (proteins, pectin and pigments) and the glycosides were permeated through the membranes. A DF loop was operated to extract the maximum amount of stevioside. The operating temperature was 10–65 °C. The permeate flux was in the range of 35–65 $L/m^2.h$ with the transmembrane pressure drop of 200–700 kPa. Recovery rates of about 78% stevioside and 80% rebaudioside A were obtained during MF. For UF in DF mode, 1.51 g/L concentration of stevioside was obtained at a permeate flux of 35 $L/m^2.h$. With increase in DF volume, recovery of stevioside decreases and at the same time permeate flux increases considerably.

Another study showed that addition of a small amount of flocculating agent (1% w/w) improved the permeate flux almost two times (Zhang et al. 2000).

Silva et al. (2007) demonstrated purification of atevioside using a membrane-based process, pretreated by adsorption with zeolite. Water extraction of stevioside was performed in cold water. It was pretreated by passing the extract through a zeolite column (modified CaX). Next, the resultant solution was passed through a UF ceramic membrane. Three membranes with average pore diameter 0.05, 0.1 and 0.2 µm were used. The membrane area was 0.005 m^2. Experiments were conducted

at 25 °C, for 150 min at three transmembrane pressure drops – 2, 4 and 6 bar. The best results were obtained by using a 0.05 µm membrane at 2 bar. Yields of about 90% stevioside and 95% rebaudioside A were obtained with these condition and almost 100% clarification was achieved. The permeate flux realised was about 25 L/m^2.h. In another study, the authors concluded that complete pore blocking was the main fouling mechanism (Reis et al. 2009).

Vanneste et al. (2011) proposed a tailor-made membrane having high selectivity for clarification of Stevia extract. They conducted experiments with a synthetic solution of stevioside-rebaudioside A (75%:25%) as well as pulverised Stevia leaves. Twenty grams of leaves were mixed with 1 L water and extraction was carried out for 2 h at 5 °C. Eleven percent total glycoside (7% stevioside and 4% rebaudioside A) was extracted. Primary clarification was done using a 0.05 µm commercial MF membrane. The authors investigated in detail the performance of various commercial UF and NF membranes with tailor-made laboratory membranes in terms of selectivity, permeability and flux decline. They concluded that tailor-made 27% polyethersulfone (PES) and 24% PES membranes were better performers than commercial membranes. Although the selectivity of lab-made membranes was slightly lower, their retention (with respect to stevioside and rebaudioside A) was less than other commercial membranes, except PW010 membrane. In fact, less retention of glycoside was preferred for UF applications.

The major drawback of the commercial membranes was that they were highly prone to fouling and huge flux decline was observed. On the other hand, the lab-made membranes had comparatively lower flux decline. Starting with 11% purity, the selected membranes including the DF mode of operation could increase purity up to 37% with an overall yield of 30%. The authors concluded that further purification would be possible by coupling with other purification processes, such as crystallisation.

Chhaya et al. (2012a) carried out a similar study for selection of membrane and effects of operating conditions for clarification of Stevia extract by UF. They extracted the leaves with water in a proportion 1 g to 14 mL at 78 °C for 56 min. The primary clarification was carried out by centrifugation at 5334 g rotational speed for 26 min. Four UF membranes of cut-off 5, 10, 30 and 100 kDa were selected. Unstirred experiments under batch mode were performed with the preclarified extract at 30 °C at 414 kPa pressure and the results were analysed in terms of yield of stevioside and permeate flux. It was observed that a 30 kDa membrane resulted in maximum permeate flux (60 L/m^2.h) with the highest yield of stevioside, about 50%. It was also observed that for a 100 kDa membrane, the permeate flux was low as it was fouled quite fast due to pore blocking, leading to lower recovery of stevioside. For lower cut-off membranes, such as 5 kDa, the permeate flux was up to 40 L/m^2.h but recovery was low. Next, they carried out a detailed analysis for 30 kDa membranes under various operating conditions in a stirred cell. It was observed that purity and concentration of stevioside were higher at lower transmembrane pressure drops. At higher pressure drops, due to membrane fouling, more stevioside was retained by the dynamic membrane formed. It was concluded that

414 kPa transmembrane pressure drop and 1800 rpm were the optimum operating conditions, resulting in a reasonable permeate flux of 36 L/m^2.h and stevioside recovery of about 45%.

The same group conducted UF experiments in continuous cross-flow mode and observed the effects of the operating conditions both in total recycle mode (permeate was recycled to feed tank) and batch concentration mode (permeate was not recycled) using a 30 kDa membrane (Chhaya et al. 2012b). The effective membrane area was 80 cm^2. The transmembrane pressure drop was in the range of 276–552 kPa and the cross-flow rate was 60–120 L/h for the total recycle mode. In batch concentration mode, the pressure range was same but all the experiments were conducted at 100 L/h cross-flow rate. The duration of total recycle mode experiments was 45 min and that for batch concentration mode was 10 h. It was observed that high recovery of stevioside was obtained at a lower transmembrane pressure drop (276 kPa), about 58–70%. Purity and selectivity of stevioside were also higher. However, cross-flow rate did not have a significant effect on these parameters. On the other hand, cross-flow rate had a significant effect on the permeate flux. At 276 kPa, permeate flux increased from 6 to 12 L/m^2.h as the cross-flow rate increased from 60 to 120 L/h. Flux also increased almost twice at pressure 690 kPa but recovery and yield of stevioside decreased in these conditions. Thus, lower operating pressure and higher cross-flow rate were desired operating conditions.

In another recent study, an improved membrane-based process was proposed for obtaining high-purity stevioside and rebaudioside A (Rao et al. 2012a). The air-dried leaves were soaked with hexane to remove unwanted colour pigments and waxy materials. The leaves were dried again and pulverised to 20–30 mesh size. The powdered material was soaked in aqueous solution (leaf:water = 1:10) at 80 °C for 2–3 h. Next, the leaves were subjected to a pressurised hot water extractor (at 100 kPa, 120 rpm, 100–110 °C for 10 min). The crude extract was cloth filtered and subjected to a spiral-wound 30 kDa UF membrane at feed pressure 200–500 kPa to remove cell debris and other impurities; 70–80% leaf carotenoid pigments were retained during UF. More than 90% of plant pigments in the extract were removed by UF. The permeate flux was reduced from 30 to 7.5 L/m^2.h as the time of operation increased from 10 to 100 min. The decrease in flux was attributed to concentration polarisation by chlorophyll, biomass, etc. In the permeate concentration of stevioside increased from 55 to 126 µg/mL. It was concluded that an enrichment of stevioside in the permeate occurred due to preferential affinity and hydrogen bonding and polar interactions.

6.2 Concentration by nanofiltration

The molecular weight of stevioside and rebaudioside A is 804 Da and 967 Da, respectively. Thus, selection of an appropriate NF membrane cut-off in the range of 200–400 kDa would be able to retain the glycosidic compounds and allow water and smaller molecular weight impurities to permeate through the membrane, thereby

Table 6.2 Summary of the flux decline phenomena of different membranes and operating conditions

Operation	Operating conditions	Filtration duration or concentration/volume factor	% Flux decline	Reference
UF 25 kDa	Δ P = 12 bar, FR = 25 L/min	WCR = 9	80	Fuh and Chiang (1990)
UF 100 kDa	Δ P = 8 bar, FR = 25 L/min		25	
UF 2.5 kDa	Δ P = 440 kPa	3 h	8	Zhang et al. (2000)
UF (0.05 µm)	Δ P = 2, 4, 6 bar	150 min	37, 44, 33	Reis et al. (2009)
MF (0.1 µm)			40, 49, 42	
MF (0.2 µm)			50, 47, 43	
UF (27% PES)	Δ P = 3 bar	2 h	40	Vanneste et al. 2011
UF (24% PES)			37	
UF, 5 kDa			50	
UF, 5 kDa			60	
UF, 20 kDa			20	
UF, 30 kDa (total recycle)	Δ P = 276 kPa	50 min		Chhaya et al. (2012a)
stirred cell	600, 1200, 1800 rpm		42, 29, 20	
	Δ P = 690 kPa		46, 37, 30	
	600, 1200, 1800 rpm			
UF, 30 kDa	Δ P = 276 kPa	50 min		Chhaya et al. (2012b)
(total recycle)	Cross-flow rate = 60, 80, 100, 120 L/h		28, 18, 14, 17	
Cross-flow	Δ P = 276 kPa		27, 13, 13, 15	
UF, 30 kDa (batch concentration)	Cross-flow rate = 60, 80, 100, 120 L/h		63, 69, 72	
NF, 400 kDa	Δ P = 276, 414, 552 kPa		32, 30, 26	
(stirred batch)	Cross-flow rate = 100 L/h	1.1 h	35, 33, 28	
	Δ P = 827 kPa			
	500, 1000, 1500 rpm			
	Δ P = 1241 kPa			
	500, 1000, 1500 rpm			
UF, 30 kDa	Δ P = 200–500 kPa	Volume concentration factor = 4.3	75	Rao et al. (2012a, b)
Hollow-fibre module, batch mode	Cross-flow rate = 1020 L/h			
NF, 200–250 kDa	Δ P = 1350–4100 kPa	Volume concentration factor = 2.5	75	
stirred batch mode				

MF, microfiltration; NF, nanofiltration; UF, ultrafiltration; WCR, weight concentration factor (initial weight of feed/final weight of retentate).

concentrating the glycoside-rich stream. This concentration would reduce load on the drying equipment to produce powder. Reverse osmosis (RO) can also be used to concentrate the clarified Stevia extract but at the expense of energy. Fuh and Chiang (1990) used RO for concentration of ultrafiltered clarified extract. They concentrated the extract 10 times and stored it at 5 °C for 12 h. It was observed that crystals of stevioside were precipitated and the crystal purity was about 56%. The supernatant of RO concentrate was passed through two mixed bed ion exchange resins (Amberlite 458 and IRC 50). The purity of stevioside was 66% after the first ion exchange column and increased to 90% at the exit of the second column, and overall recovery was about 80%. The solution was dried and powder was obtained.

Kutowy et al. (1999) carried out UF for clarification of Stevia extract as mentioned earlier. The permeate stream of UF was heated to 80 °C and was treated with a 400 kDa cut-off commercial NF membrane, operated at 517 kPa and 80 °C in DF mode. The impurities were reduced by 55% in the retentate and no trace of glycosides was found in the permeate stream. Thus, retentate glycosides became purer.

Chhaya et al. (2012b) also carried out NF for concentration of their ultrafiltered extract. NF was carried out in a stirred batch cell with a 400 kDa MWCO membrane. The transmembrane operating pressure drop was in the range of 827–1241 kPa and stirrer speed was 800–1500 rpm. The experiments were conducted for 1 h. At the end of 1 h, the permeate flux was in the range of 18–35 $L/m^2.h$ for various operating conditions. The volume concentration ratio was in the range of 1.3–2.0 times. It was reported that retention of stevioside was in the range 93–98%. Overall purity of stevioside using combined UF and NF was found to be about 60%.

Rao et al. (2012b) also used NF to concentrate their clarified extract by UF. They used a NF membrane of MWCO 200–250 kDa operated at 1500 kPa transmembrane pressure. This process removed 80–90% of water as permeate, thus concentrating the product in the retentate. Retentate was extracted thrice with butanol. The organic layer was separated and washed with basic/neutral solution to remove smaller impurities. The solvent was further filtered through activated charcoal and celite to obtain a golden yellow-coloured solution rich in stevioside which on further concentration and crystallisation produced colourless powder. NF resulted in concentration of stevioside from 2 to 46 μg/mL. Increase in pressure from 1350 to 4100 kPa resulted in an increase in permeate flux from 25 to 39 $L/m^2.h$ at water recovery of 60% with rejection of stevioside by 100%. After a final purification step through organic washing, the purity of stevioside was 98% with a total yield of 9 g out of 100 g of Stevia leaves.

6.3 Limitations

Flux decline or reduction in throughput is the most important limitation of any membrane-based separation process. Table 6.2 presents a summary of flux decline occurring during operation of various membranes. From this table, it is clear that significant flux decline, i.e. reduction of throughput, occurs during any membrane-based filtration process with a real-life feed solution, such as Stevia extract.

References

Chhaya, C., Sharma, C., Mondal, S., Majumdar, G.C., De, S. (2012a) Clarification of Stevia extract by ultrafiltration: selection criteria of the membrane and effects of operating conditions. Food Bioprod Proc 90, 525–532.

Chhaya, C., Mondal, S., Majumdar, G.C., De, S. (2012b) Clarifications of Stevia extract using cross flow ultrafiltration and concentration by nanofiltration. Sep Purif Technol 89, 125–134.

Fuh, W.S., Chiang, B.H. (1990) Purification of steviosides by membrane and ion exchange process. J Food Sci 55, 1454–1457.

Kutowy, O., Zhang, S.Q., Kumar, A. (1999) Extraction of sweet compounds from Stevia Rebaudiana Bertoni. US Patent 5,972,120.

Rao, A.B., Reddy, G.R., Ernala, P., Sridhar, S., Ravikumar, Y.V.L. (2012a) An improvised process of isolation, purification of steviosides from Stevia Rebaudiana Bertoni leaves and its biological activity. Int J Food Sci Technol 47, 2554–2560.

Rao, A.B., Prasad, E., Roopa, G., Sridhar, S., Ravikumar, Y.V.L. (2012b) Simple extraction and membrane purification process in isolation of steviosides with improved organoleptic activity. Adv Biosci Biotechnol 3, 327–335.

Reis, M.H.M., Silva, F.V., Andrade, C.M.G., Rezende, S.L., Wolfmaciel, M.R., Bergamasco, R. (2009) Clarification and purification of aqueous Stevia extract using membrane separation process. J Food Proc Eng 32, 338–354.

Silva, F.V., Bergamasco, R., Andrade, C.M.G., et al. (2007) Purification process of stevioside using zeolites and membranes. Int J Chem React Eng 5, A40.

Vanneste, J., Sotto, A., Coutin, C.M. (2011) Application of tailor-made membranes in a multi-stage process for the purification of sweeteners from Stevia Rebaudiana. J Food Eng 103, 285–293.

Zhang, S.Q., Kumar, A., Kutowy, O. (2000) Membrane-based separation scheme for processing sweeteners from Stevia leaves. Food Res Int 33, 617–620.

7

Detailed membrane-based technologies for extraction of stevioside

Extraction and separation of stevioside from Stevia leaves using membrane processing has huge potential for commercialisation of stevioside-based products, in terms of economics, feasibility and purity.

7.1 Outline of processing

Powder of dry Stevia leaves, obtained from RAS Agro Associates, Maharashtra, India, was used as raw material for preparing Stevia extract. The different stages of clarification of Stevia leaf extract are outlined in Figure 7.1.

7.2 Optimisation of water extraction process

Stevioside extraction from *S. rebaudiana* leaves by a hot water extraction process is safer from a health point of view as no chemicals are involved. Some analyses have reported that more than 93% extraction efficiency was achieved by hot water extraction (Midmore and Rank 2006; Nishiyama 1991). After extraction, the aqueous extract is subjected to other unit operations such as clarification, purification, crystallisation, etc., for further processing leading to the final product. Many researchers have undertaken a hot water extraction process (Abou-Arab et al. 2010; Dacome et al. 2005) and some have tried other methods such as methanol extraction, water and methanol extraction, ultrasonically assisted water extraction, ethanol extraction using water and carbon dioxide, supercritical fluid extraction using carbon dioxide, etc. (Erkucuk et al. 2009; Liu et al. 2010; Pasquel et al. 2000; Pól et al. 2007). But most of these studies did not use an appropriate optimisation method to establish the optimum process conditions. Optimisation of the process parameters is necessary to maximise the productivity to effort ratio.

Stevioside: Technology, Applications and Health, First Edition.
Sirshendu De, Sourav Mondal and Suvrajit Banerjee.

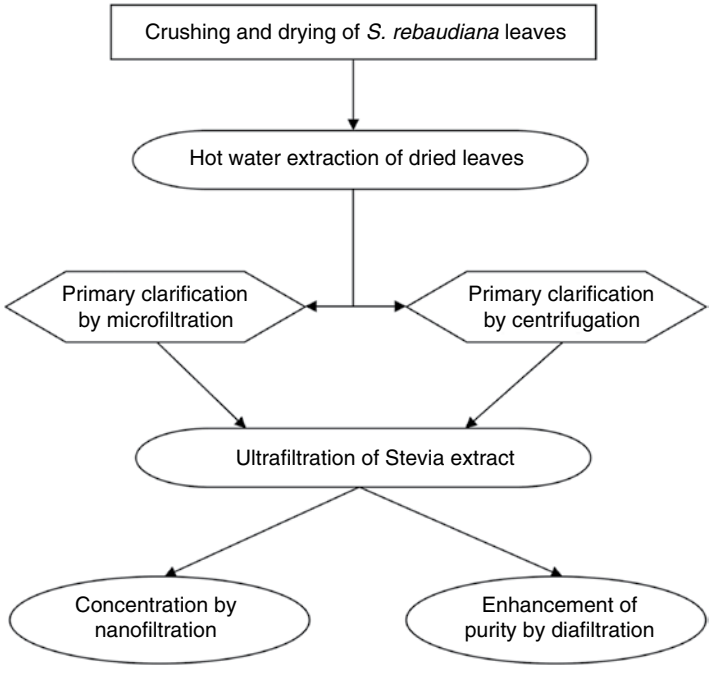

Figure 7.1 Extraction, clarification and purification of Stevia extract using membrane technology.

The hot water extraction method was used for preparing aqueous Stevia extract. A specific ratio of leaf to water (weight to volume) was measured and the dry Stevia leaves were mixed with hot water. This sample was exposed to a particular temperature for a fixed duration. After termination of the heating process, the Stevia extract was allowed to cool and then filtered using Whatman filter papers. This extract was analysed for its stevioside concentration and colour. A thermostatic water bath was used to control the temperature (±1°C) of the process.

Response surface methodology (RSM) was used in this process to obtain the optimum conditions for maximum stevioside extraction from *S. rebaudiana* leaves. Three independent variables selected for this optimisation process were heating temperature, time and leaf to water ratio. These variables were represented as T, t and R, respectively, in terms of their actual values. The experimental ranges selected for independent variables were: heating temperature (30–90°C), time (10–120 min) and leaf to water ratio in g:mL (1:5 to 1:20).

After selection of independent variables and their ranges, experimental design was applied to generate combinations for conducting the experiments using the commercial statistical software package Stat-Ease Design Expert 7.0.0. A three-variable (five levels of each variable), second-order rotatable central composite experimental design (Khuri and Cornell 1989; Myers 1971) and response surface methodology (RSM) were employed to understand the linear, quadratic and

interaction effects of temperature of water, time of heating and leaf to water ratio on two responses: stevioside concentration and colour of the extract. Twenty experimental runs were conducted, out of which eight were factorials, six were axial and six were at centre point. Five extra experimental runs, at the same combination of centre points, were conducted in order to allow estimation of pure error. All the experiments were conducted in a randomised order to minimise the effect of unexplained variability in the observed responses due to extraneous factors (Montgomery 2001).

The dependent parameter (response, Y) was related to the independent variables (coded values, X_i : i = 1, 2 and 3) by using the following second-order polynomial model:

$$Y = b_0 + b_1X_1 + b_2X_2 + b_3X_3 + b_{12}X_1X_2 + b_{13}X_1X_3 + b_{23}X_2X_3 + b_1^2X_1^2 + b_2^2X_2^2 + b_3^2X_3^2 \quad (7.1)$$

where the coefficients of the model were represented as: b_0 (constant term), b_1, b_2 and b_3 (linear coefficients); b_1^2, b_2^2 and b_3^2 (quadratic coefficients); b_{12}, b_{13} and b_{23} (interaction coefficients). X_1, X_2 and X_3 in the model represent the coded values of the independent variables heating temperature, time and leaf to water ratio, respectively. The regression coefficients of all the terms (linear, quadratic and interaction) involved in the model and their effects were analysed by generating analysis of variance (ANOVA) tables. All the terms of the model were judged stastistically by computing the F-values at probability levels (p) of 0.001, 0.01 or 0.05. The adequacy of the developed models was tested by performing lack of fit test, model analysis and coefficient of determination (R^2) analysis. R^2 is the measure of the degree of fit and it ranges between 0 and 1, with larger values being more desirable. It is used for describing the proportion of the variability in the data explained by the ANOVA model (Montgomery 2001). Significant lack of fit (low probability value) indicates that the model may not adequately fit the data. After fitting the models, the generated data were employed for plotting response surfaces and contour plots.The coded values of any experimental parameter used in the regression model can be related to their respective actual values and can be expressed as:

$$X = (x - x_m) / x_d \quad (7.2)$$

Here, X is the coded value of any independent variable, x is the uncoded (actual) value of the corresponding independent variable in the original unit, x_m is the mean of two extreme values (actual) of independent variable and x_d is the step change value (Das 2005).

A numerical optimisation technique was followed for optimising the various responses simultaneously involved in the extraction process. All the independent variables were kept within range while the responses were either maximised or minimised according to the requirement of the process. The desirability function

method was applied for generating optimum conditions having some specific desirability value. First, each of the responses is converted into an individual desirability function (d_i) that varies over the range 0–1 depending on whether the response is out of range or is approaching the target, respectively. The desired criterion (target) was fixed for each of the variables and responses involved in order to maximise the overall desirability. The overall desirability (D) can be expressed as:

$$D = (d_1.d_2 \ldots\ldots\ldots\ldots d_m)^{1/m} \tag{7.3}$$

where $d_{i\,(i = 1, 2 \ldots..m)}$ represents the individual desirability function for each response and m represents the total number of responses taken into consideration.

Table 7.1 represents the independent variables in terms of their actual and coded values. The various combinations of design parameters with their respective responses are given in Table 7.2. After fitting the second-order polynomial model for both the responses, regression analysis was carried out and an ANOVA table was generated. The F-values, regression coefficients, R^2, lack of fit and coefficient of variation of the second-order polynomial model are represented in Table 7.3. The significance of each term was judged by comparing them with respect to their probability (p) values. The analysis of variance concluded that for both the responses (stevioside concentration and colour), the models were highly significant at probability level $p < 0.001$. The values of coefficient of determination for both the responses were more than 0.90, indicating that a high proportion of variability was explained by the data and the models were adequate. The fitness of model is measured statistically by verifying the lack of fit of the model. Lack of fit was insignificant in both the cases, indicating that the developed models can be used effectively for predicting the responses. Coefficient of variation (CV) measures the unexplained or residual variability in the data as a percentage of the mean of the response variable. Lower values of CV for stevioside concentration (CV=3.56) and colour (CV=3.48) indicated the precision and reliability by which the experiments were conducted.

Table 7.1 Experimental range and levels of the independent variables. Reproduced from Rai et al. (2012) with permission from Taylor & Francis.

Coded values	Actual values		
	Temperature(°C)	Time (min)	Ratio (g:mL)
−1.682	29.73	9.5	4.93
−1	42	32	8
0	60	65	12.5
+1	78	98	17
+1.682	90.27	120.50	20.07

Table 7.2 Experimental conditions and responses for three variables (in coded level) for stevioside extraction process. Reproduced from Rai et al. (2012) with permission from Taylor & Francis.

Experiment no.	Temperature (°C) $T(X_1)$	Time (min) $t(X_2)$	Ratio (leaf:water) g:mL $R(X_3)$	Responses	
				Stevioside %	Colour (A_{420})
1	42.00(–1)	32.00(–1)	8.00(–1)	6.64	11.97
2	78.00(+1)	32.00(–1)	8.00(–1)	9.50	13.94
3	42.00(–1)	98.00(+1)	8.00(–1)	7.76	17.03
4	78.00(+1)	98.00(+1)	8.00(–1)	10.03	19.49
5	42.00(–1)	32.00(–1)	17.00(+1)	7.04	10.60
6	78.00(+1)	32.00(–1)	17.00(+1)	9.70	11.23
7	42.00(–1)	98.00(+1)	17.00(+1)	9.90	11.50
8	78.00(+1)	98.00(+1)	17.00(+1)	10.75	12.80
9	29.73(–1.68)	65.00(0)	12.50(0)	6.72	9.70
10	90.27(+1.68)	65.00(0)	12.50(0)	11.01	13.50
11	60.00(0)	9.50(–1.68)	12.50(0)	7.63	9.90
12	60.00(0)	120.50(+1.68)	12.50(0)	10.40	15.50
13	60.00(0)	65.00(0)	4.93(–1.68)	7.45	20.50
14	60.00(0)	65.00(0)	20.07(+1.68)	9.80	11.60
15	60.00(0)	65.00(0)	12.50(0)	9.90	12.60
16	60.00(0)	65.00(0)	12.50(0)	9.64	12.80
17	60.00(0)	65.00(0)	12.50(0)	9.23	12.01
18	60.00(0)	65.00(0)	12.50(0)	9.60	12.85
19	60.00(0)	65.00(0)	12.50(0)	9.95	12.32
20	60.00(0)	65.00(0)	12.50(0)	9.38	12.60

Table 7.3 The regression coefficients of the second-order polynomial model for the response functions (stevioside and colour) in coded level. Reproduced from Rai et al. (2012) with permission from Taylor & Francis.

Coefficients of the regression model	F-values		Coefficients values (coded)	
	Stevioside (%)	Colour (A_{420})	Stevioside (%)	Colour (A_{420})
b_0 (intercept)	36.09***	81.53***	9.61	12.53
b_1 (temperature)	175.02***	56.21***	1.16	0.93
b_2 (time)	72.70***	174.99***	0.75	1.65
b_3 (ratio)	38.25***	338.0***	0.54	–2.29
b_1^2	7.82*	6.76*	–0.24	–0.32
b_2^2	4.73	0.37	–0.19	0.074
b_3^2	14.36**	107.69***	–0.32	1.26
b_{12}	6.85*	0.79	–0.30	0.14
b_{13}	3.12	3.69	–0.20	–0.31
b_{23}	6.07*	39.10***	0.28	–1.02
Lack of fit	1.64	3.24		
R^2	–	–	0.97	0.98
Adjusted R^2	–	–	0.94	0.97
CV (%)			3.56	3.48

*Significant at $p < 0.05$;
**significant at $p < 0.01$;
***significant at $p < 0.001$.

7.2.1 Stevioside

Stevioside extraction was highly significant at probability level $p < 0.001$ for first-order terms of heating temperature, heating time and leaf to water ratio. Among the quadratic terms, only two of them, heating temperature and ratio, had a significant effect on stevioside extraction at probability levels of $p < 0.05$ and $p < 0.01$, respectively. The contribution of heating temperature and leaf to water ratio interaction term was not significant ($p > 0.05$) but the other two interaction terms were significant, with a probability level of $p < 0.05$ for stevioside extraction (see Table 7.3). The regression equation of the model showing the net effect of independent parameters on stevioside extraction, in coded level of the parameters, is given as:

$$\text{Stevioside}\,(\%) = 9.61 + 1.16 \times X_1 + 0.75 \times X_2 + 0.54 \times X_3 - 0.24 \times X_1^{\,2} - 0.19 \times X_2^{\,2} - 0.32 \times X_3^{\,2} - 0.30 \times X_1 \times X_2 - 0.20 \times X_1 \times X_3 + 0.28 \times X_2 \times X_3 \quad (7.4)$$

The coefficient of determination value of the above equation is 0.97. It indicates that the model explained 97% of the variability of the stevioside extracted in the liquid. The F-value for lack of fit of this model was 1.64 with a probability level of $p > 0.05$. The model coefficient of the regression equation explained that the model was highly significant ($p < 0.001$). Positive linear terms of independent parameters indicated that when increasing these paremeters, stevioside extraction also increases. The quadratic coefficients of both the significant terms of heating temperature and ratio showed a negative response. Among interaction terms, the temperature–time combination term had a negative effect and the time–ratio combination term had a positive effect on the stevioside extraction process.

Figures 7.2, 7.3 and 7.4 represent a three-dimensional plot demonstrating the variation of stevioside concentration with respect to any two parameters when the other parameter is kept constant at the centre point. From Figure 7.2, it is clear that stevioside extraction increases significantly with an increase in heating time or temperature while keeping the leaf to water ratio constant at the centre point. Figure 7.3 explains that when time is kept constant at the centre point, stevioside extraction efficiency increases with increase in leaf to water ratio or temperature with respect to a particular temperature or ratio respectively. The same trend can be observed in Figure 7.4, where the operating temperature is fixed at the centre point. Stevioside extraction increases with increase in leaf to water ratio at a particular time. Similarly, concentration of extracted stevioside increases significantly with increase in time at a particular ratio. At low leaf to water ratio, the percentage of stevioside extracted is less and as the ratio increases, i.e. the volume of water increases, the percentage of stevioside extraction also increases. The reason is that when water is at low volume it cannot extract all the stevioside from the leaves but when the volume of water is increased, the extraction efficiency increases but again after a certain limit of leaf to water ratio, the further increase in volume of water does not add any significant

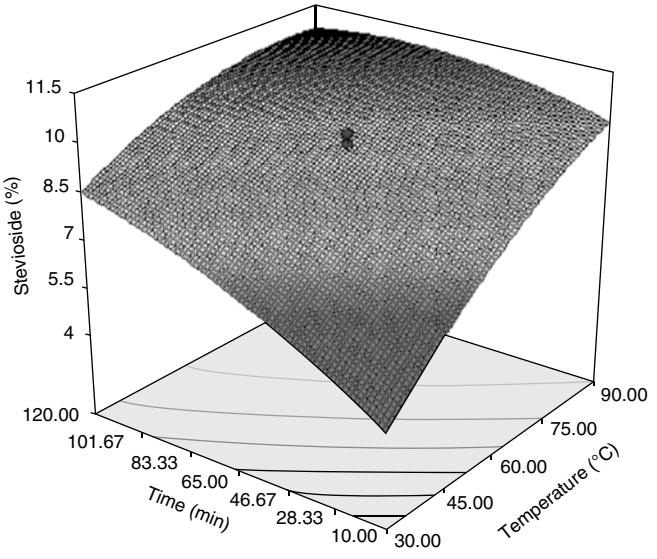

Figure 7.2 Response surface plot for stevioside as a function of time and temperature (leaf to water ratio kept constant at centre point). Reproduced from Rai et al. (2012) with permission from Taylor & Francis.

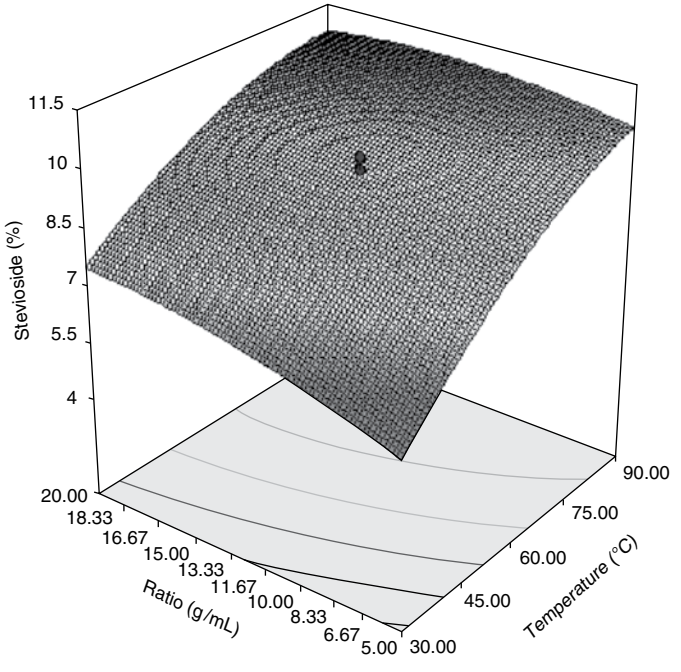

Figure 7.3 Response surface plot for stevioside as a function of ratio and temperature (time kept constant at centre point). Reproduced from Rai et al. (2012) with permission from Taylor & Francis.

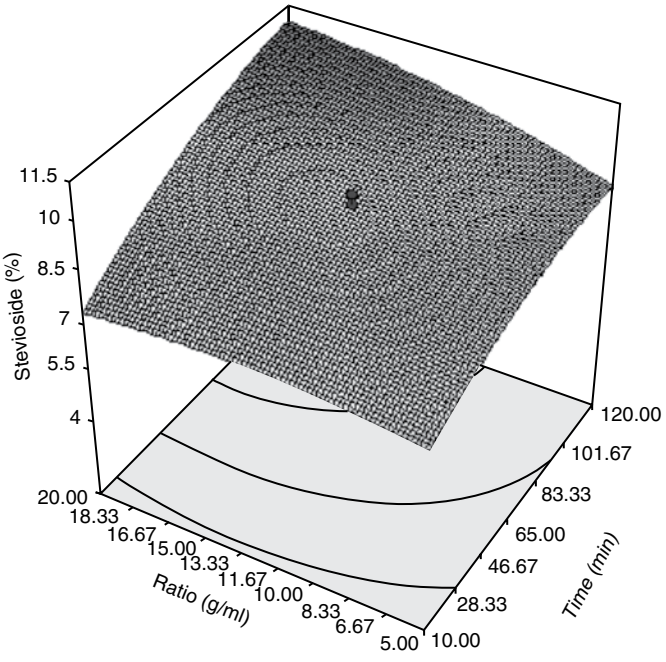

Figure 7.4 Response surface plot for stevioside as a function of ratio and time (temperature kept constant at centre point). Reproduced from Rai et al. (2012) with permission from Taylor & Francis.

extraction efficiency. The percentage of stevioside extracted ranged from 6.64% to 10.75% of the dried *S. rebaudiana* leaves throughout the experiment.

The colour developed in the extract was significantly affected ($p < 0.001$) by first-order terms of heating temperature, heating time and leaf to water ratio. The first-order terms of heating temperature and time had a significant positive effect whereas leaf to water ratio had a significant negative effect on the colour developed. The second-order term of heating temperature and leaf to water ratio showed a significant effect whereas the second-order term of time was not significant at the probability level of $p > 0.05$. Among both significant second-order terms, temperature had a negative effect and ratio had a positive effect on the colour developed. The second-order term of leaf to water ratio of the colour regression model was highly significant ($p < 0.001$). The contribution of the interaction terms of heating time and leaf to water ratio together was highly significant ($p < 0.001$) and indicated a negative effect on the colour developed while the other interaction terms had no significant effect on this response.

The regression equation of the model showing the net effect of independent parameters on the colour developed, in coded level of the parameters, is given as:

$$\text{Colour}\,(A_{420}) = 12.53 + 0.93 \times X_1 + 1.65 \times X_2 - 2.29 \times X_3 - 0.32 \times X_1^{\,2} + 0.074 \times X_2^{\,2} + 1.26 \times X_3^{\,2} + 0.14 \times X_1 \times X_2 - 0.31 \times X_1 \times X_3 - 1.02 \times X_2 \times X_3 \quad (7.5)$$

The coefficient of determination is 0.98 for the above equation. The model was highly significant ($p < 0.001$) and it explained 98% of the variability of the colour developed during the hot water extraction process. The lack of fit for this model was not significant ($p > 0.05$) with an F-value of 3.24, indicating that the model fits well. The first-order positive coefficients of extraction temperature and time in the model indicated that with the increase in heating temperature and time, the extract becomes darker in colour. The linear negative coefficient of leaf to water ratio indicated that with an increase in the ratio (i.e. with the increase in volume of water), there is a decrease in the colour of the extract (liquor). This suggests that if the ratio is less, i.e. the volume of water is less, the colour developed is in high concentration and vice versa. The high volume of water dilutes the liquor and hence the colour decreases. The value of colour of the liquor ranged from 9.7 to 20.5 throughout the experiment.

Figure 7.5 represents the three-dimensional plot for expressing the variation of developed colour with respect to time and temperature when leaf to water ratio is set constant at the centre point. From this figure, it is obvious that at a fixed heating time, the colour of the extract becomes more concentrated with an increase in heating temperature. Also, at a fixed temperature the colour increases with the increase in heating time. Figure 7.6 represents the response surface plot of colour with

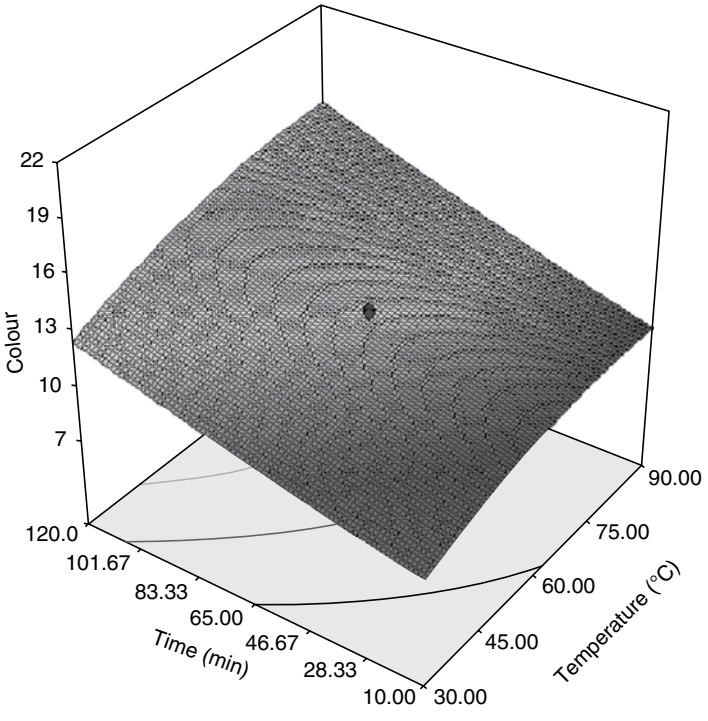

Figure 7.5 Response surface plot for colour (A_{420}) as a function of time and temperature (leaf to water ratio kept constant at centre point). Reproduced from Rai et al. (2012) with permission from Taylor & Francis.

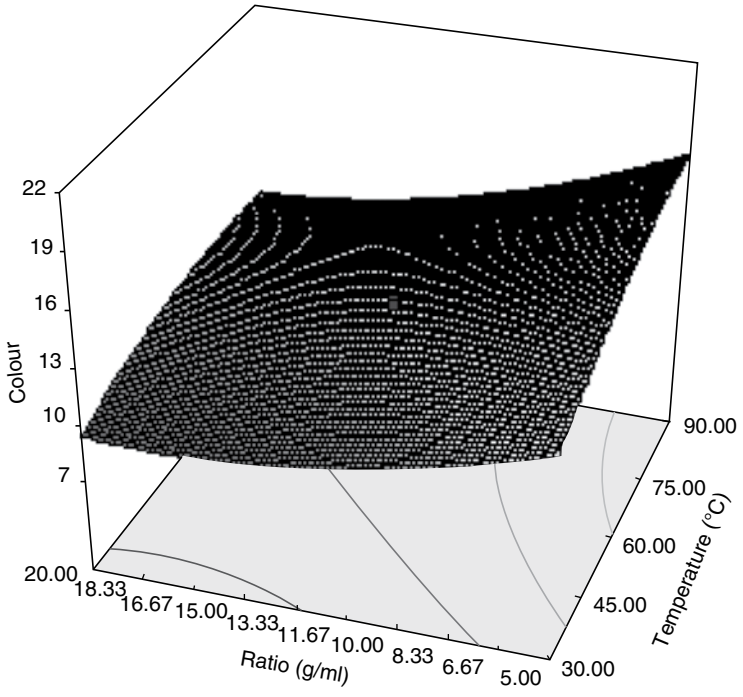

Figure 7.6 Response surface plot for colour (A_{420}) as a function of ratio and temperature (time kept constant at centre point). Reproduced from Rai et al. (2012) with permission from Taylor & Francis.

respect to heating temperature and leaf to water ratio when heating time is kept constant at the centre point. From this figure, it can be concluded that when temperature is fixed at a particular point, the concentration of colour decreases as the value of leaf to water ratio increases. Similarly, from Figure 7.7, it is obvious that for a specific heating time, the colour decreases with increase in leaf to water ratio when heating temperature is kept constant at the centre point. Hence, with increase in heating time and temperature, the colour increases. With an increase in leaf to water ratio, the colour of the extract decreases when other independent variables are kept constant.

The optimisation of process parameters was carried out using Stat-Ease Design Expert 7.0.0 software. Simultaneous optimisations of the multiple responses were carried out using the numerical optimisation technique of the Design Expert software. The numerical optimisation evaluates a point that maximises the desirability function. In this case, stevioside concentration was maximised and colour was minimised. Solution having the maximum desirability value (0.828) was selected as the optimum condition for extraction of maximum stevioside from dried Stevia leaves. Optimised results according to Design Expert are given as: temperature of water 78 °C, time of heating 56 min and leaf to water ratio 1:14 (g:mL). The predicted values for stevioside concentration and colour (A_{420}) were 10.45% and 12.

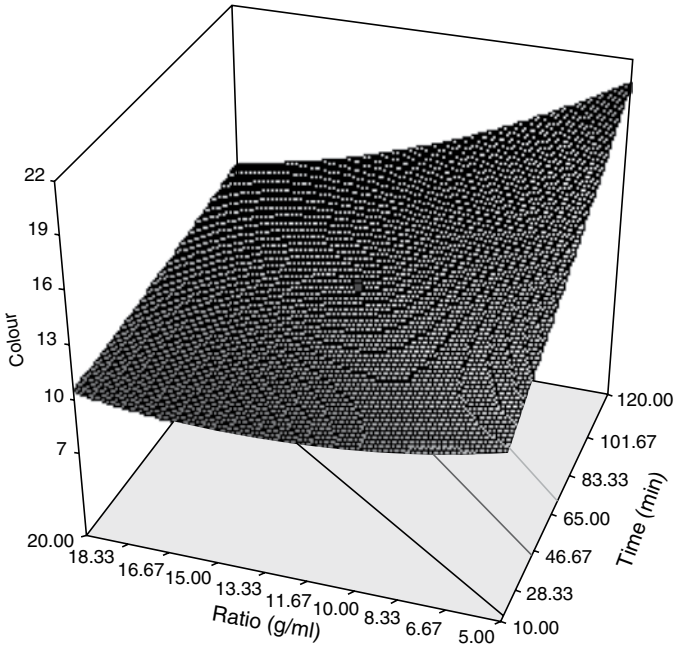

Figure 7.7 Response surface plot for colour (A_{420}) as a function of ratio and time (temperature kept constant at centre point). Reproduced from Rai et al. (2012) with permission from Taylor & Francis.

Thus, the following recommendations for practical applications arise from this work:

1. Water should be used as the extracting medium for stevioside for human consumption.
2. The optimum operating conditions for maximum extraction of stevioside from *S. rebaudiana* leaves (Indian variety) are temperature 78°C, time of heating 56 min and leaf to water ratio 1:14 (g:mL); under these conditions, the amount of stevioside extracted is 10.45 g per 100 g of dry *S. rebaudiana* leaves.
3. Response surface methodology coupled with numerical optimisation can be useful for maximum extraction of stevioside from any variety of *S. rebaudiana* leaves using an aqueous medium.

7.3 Optimisation of primary clarification (centrifugation or microfiltration)

The liquor of Stevia extract is rich in natural sweeteners and dark brown in colour. This extract also contains impurities in the form of suspended particles and plant materials (colour pigments, protein, carbohydrates, lipids, etc.). Therefore, after

extraction, clarification is a vital unit operation for removal of these suspended particles from the Stevia extract. The presence of the suspended particles reduces the efficiency of the downstream unit operations for processing of Stevia extract and also adds impurity to the product.

Centrifugation and microfiltration are two popular methods used for clarification of liquid extracts or fruit juices. One advantage of using these methods is that they are chemical free and thus can be used safely for clarification processes in food industries. Microfiltration was generally used as the pretreatment method prior to ultrafiltration in diafiltration mode. Comparison of the effectiveness of centrifugation and microfiltration as a primary clarification step of Stevia extract and the effects of transmembrane pressure drop as well as the stirring speed in the filtration cell on the permeate flux and permeate concentration of the Stevia extract during microfiltration are reported by Chhaya et al. (2012a). The operating conditions of centrifugation are optimised using response surface methodology. The performance of the two processes is compared in terms of properties of extract and the cost of energy involved.

Dry Stevia leaf powder was mixed with hot distilled water at a ratio of 1:14 (g:mL). The heating temperature was fixed at 78 ± 1°C and the extraction process was continued for 56 min. These operating conditions were selected based on the optimisation experiments described in the previous section. A constant-temperature water bath was used for the heating process. Next, the aqueous Stevia extract was cooled and cloth filtered. The filtered extract was used as the feed material for all the clarification experiments. The original Stevia extract and filtered Stevia extract were analysed for their colour, clarity, stevioside concentration and total solid content.

The centrifugation of Stevia extract, after hot water extraction, was performed using a laboratory-scale batch mode of operation. The operating parameters taken into account were rotation speed (g) and time (min) of operation. Microfiltration membranes of average pore size 0.2 micron were procured from Sartorius Mechatronics, Kolkata, India. The water permeability of this membrane was 5.14×10^{-9} m/Pa.s.

The clarification process was optimised using response surface methodology for removing the maximum amount of suspended particles from the Stevia extract. The independent parameters were speed (g) and time (min) of rotation and the dependent parameters (responses) were colour, clarity, total solid and Stevioside content of the clarified extract. The experimental ranges selected for independent parameters were: speed (550–10,450 g) and time (8–51 min). In the present study, a second-order central composite rotatable design of two variables (five levels of each variable) was employed for generating experimental conditions. Response surface methodology was applied to study the combined effects of individual, quadratic and interaction terms of independent parameters on the responses (Khuri and Cornell 1989). Thirteen experiments were carried out and among these, four experiments at the centre point were conducted in order to improve the precision of the experiment.

The relation between independent parameters and response (Y) was represented by a second-order polynomial model given by the equation:

$$Y = c_0 + c_{10}Z_1 + c_{20}Z_2 + c_{11}Z_1^{\ 2} + c_{22}Z_2^{\ 2} + c_{12}Z_1Z_2 \tag{7.6}$$

where b_0 represents the constant term of the model, b_{10} and b_{20} represent the coefficients of the linear terms, c_{11} and b_{22} represent the coefficients of the quadratic terms and b_{12} represents the coefficient of the interaction term. In the model, Z_1 and Z_2 represent the coded values of the independent variables, rotation speed and time, respectively. The combined effect of all the terms (linear, quadratic and interaction) involved in the model and significance of regression coefficients were analysed by generating ANOVA tables. All the terms of the model were judged statistically by computing the F-values at probability levels (p) of 0.001, 0.01 or 0.05. An F-value is a statistical measure of a parameter. It is a random variable that has a distribution, known as F-distribution, with degrees of freedom (n_1–1) and (n_2–1), where n_1 is size of a random sample from a normal population having a standard deviation equal to σ_1, and n_2 is size of a random sample from a normal population having a standard deviation equal to σ_2. The adequacy of the developed models was tested by performing lack of fit test and coefficient of determination (R^2) analysis. Insignificant lack of fit indicates that the model fits the data adequately. R^2 is the measure of the degree of fit and is defined as the ratio of the explained variation to the total variation (Haber and Runyon 1977).

The data generated from the regression models were used for plotting 3-D response surfaces and contour plots. For optimising the various process parameters involved in the clarification process, the numerical optimisation technique was followed. All the independent parameters were kept within range and the responses were either maximised or minimised in order to achieve the maximum desirability for the clarification process achieved by centrifugation.

The actual and coded values of independent parameters are given in Table 7.4. The various combinations of experimental conditions and values of all the responses are given in Table 7.5. After conducting the experiments, RSM was used for model analysis and the results were generated in the form of an ANOVA table. The values of R^2 and regression coefficients related to all the responses are presented in Table 7.6. It is evident from Table 7.6 that the models for colour,

Table 7.4 Experimental range and levels of the independent variables for centrifugation of stevioside extract. Reproduced from Chhaya et al. (2012a) with permission from Taylor & Francis.

Coded values	Actual values	
	Speed (g)	Time (min)
–1.682	550.25	8.79
–1	2000	15
0	5500	30
+1	9000	45
+1.682	10449.75	51.21

Table 7.5 Experimental conditions and responses for two variables (in coded level) for centrifugation of stevioside extract. Reproduced from Chhaya et al. (2012a) with permission from Taylor & Francis.

Serial no.	Speed (g) R (Z_1)	Time (min) T (Z_2)	Responses			
			Colour A	Clarity %T	Total solid g/100 mL	Stevioside %
1	2000 (–1)	15 (–1)	7.5	3.3	3.1	95.8
2	9000 (+1)	15 (–1)	7.5	5.0	2.8	90.0
3	2000 (–1)	45 (+1)	7.5	4.0	2.8	88.5
4	9000 (+1)	45 (+1)	7.3	7.0	2.6	87.5
5	550.25 (–1.682)	30 (0)	7.5	2.7	3.0	93.6
6	10449.75 (+1.682)	30 (0)	7.3	6.9	2.6	87.1
7	5500 (0)	8.79 (–1.682)	7.6	3.7	3.0	94.7
8	5500 (0)	51.21 (+1.682)	7.4	6.6	2.6	87.1
9	5500 (0)	30 (0)	7.3	6.5	2.6	88.7
10	5500 (0)	30 (0)	7.3	6.4	2.7	89.2
11	5500 (0)	30 (0)	7.3	6.0	2.7	88.3
12	5500 (0)	30 (0)	7.3	6.4	2.6	89.4
13	5500 (0)	30 (0)	7.3	6.6	2.6	87.1

R and T represent the actual values of the independent parameters centrifugation speed and time respectively.

Table 7.6 The regression coefficients of the second-order polynomial model for the response functions (colour, clarity, total solids and stevioside) in coded level. Reproduced from Chhaya et al. (2012a) with permission from Taylor & Francis.

Coefficients of the regression equation	Colour (A)	Clarity (%T)	Total solids (g/100 mL)	Stevioside (%)
F-values				
c_0 (intercept)	85.79***	54.08***	60.86***	36.12***
c_{10}	106.57***	140.63***	94.50***	56.19***
c_{20}	152.98***	56.02***	129.42***	91.67***
c_{11}	32.25***	47***	45.43***	9.54*
c_{22}	144.24***	31.02***	37.52***	15.68**
c_{12}	7.97*	4.51	6.97*	10.36*
Coefficient values				
c_0 (intercept)	+7.32***	+6.37***	+2.65***	+88.54***
c_{10}	–0.065***	+1.32***	-0.11***	–2.01***
c_{20}	–0.077***	+0.84***	-0.13***	–2.56***
c_{11}	+0.038***	–0.82***	+0.082***	+0.89*
c_{22}	+0.081***	–0.67***	+0.075***	+1.14**
c_{12}	–0.025*	+0.34	+0.043*	+1.22*
R^2	0.98	0.97	0.97	0.96
Adjusted R^2	0.97	0.95	0.96	0.93

*Significant at $p < 0.05$;
**significant at $p < 0.01$;
***significant at $p < 0.001$.

clarity, total solids and stevioside recovery are highly significant at the probability level of $p < 0.001$. For all the responses, R^2 values are greater than 0.9, indicating that the models are adequate and are able to explain a high proportion of variation. The values of adjusted R^2 for colour, clarity, total solids and stevioside recovery are 0.97, 0.95, 0.96 and 0.93, respectively. These values are also high, indicating the goodness of fit for the model. Insignificant lack of fit was obtained for all the models ($p < 0.05$), suggesting that the models can be used effectively for predicting the responses.

7.3.1 Colour

From Table 7.6, it is obvious that the linear terms of centrifugation speed and time are highly significant in relation to the colour of the clarified extract. The quadratic terms of both independent parameters are also highly significant ($p < 0.001$) whereas the interaction term is significant at $p < 0.05$. The effects of linear and quadratic terms are greater compared to the interaction term. The regression model describing the effect of centrifugation speed and time on the colour of the clarified Stevia extract, in terms of their coded level, is given as:

$$\text{Colour} = 7.32 - 0.065Z_1 - 0.077Z_2 + 0.038Z_1^2 + 0.081Z_2^2 - 0.025\,Z_1Z_2 \quad (7.7)$$

The R^2 value for the above equation is 0.98. Thus, the regression model explains 98% of the total variability ($p < 0.001$) for colour of the clarified extract. The negative coefficients for both the linear terms indicate that with increase in the centrifugation speed and time, the colour of the clarified extract decreases. The interaction term again shows a negative effect whereas the quadratic terms have a positive effect on the clarification process in relation to the colour of the clarified extract. Figure 7.8 represents the variation of colour during the clarification process as a function of centrifugation speed and time. It is clear from this figure that with increase in both of the independent parameters, the colour of the clarified extract decreases.

7.3.2 Clarity

The independent parameters centrifugation speed and time are highly significant ($p < 0.001$) at linear and quadratic levels, while the interaction term is insignificant ($p > 0.05$). The nature of both linear terms is positive in relation to clarity of the extract, suggesting that clarity increases with centrifugation speed and time (see Table 7.5). Negative effect is noticed for the terms at quadratic level. The regression model representing the effect of centrifugation speed and time on the clarity of the Stevia extract, in terms of their coded level, is given as:

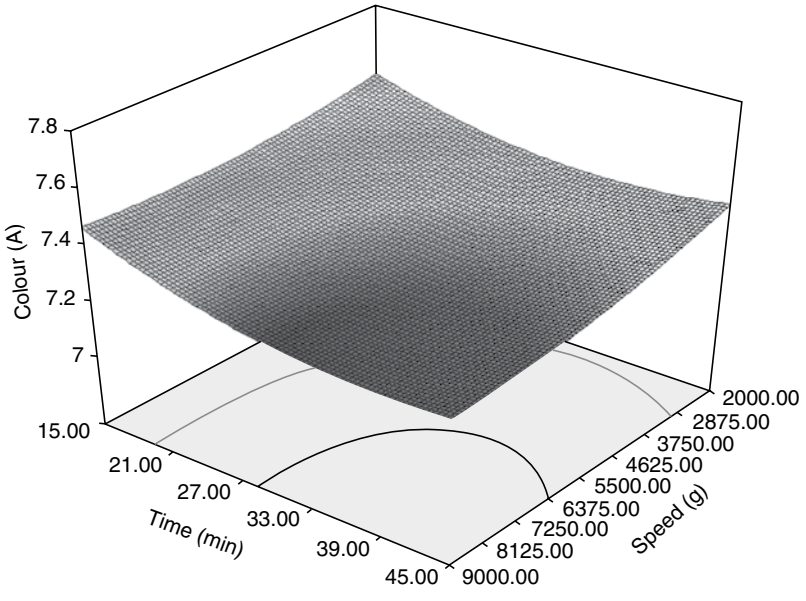

Figure 7.8 Variation of colour as a function of speed and time. Reproduced from Chhaya et al. (2012a) with permission from Taylor & Francis.

$$\text{Clarity} = 6.37 + 1.32Z_1 + 0.84Z_2 - 0.82Z_1^2 - 0.67Z_2^2 + 0.34Z_1Z_2 \qquad (7.8)$$

The R^2 value for the above equation is 0.97. The R^2 value indicates that the regression model is able to explain 97% of the variability of data in relation to clarity. Figure 7.9 explains the dependence of clarity on the centrifugation speed and time. The value of clarity (%T) ranges from 2.7 to 7.0 throughout the experiment. Figure 7.9 also shows that the clarity of the extract increases with centrifugation speed and time.

7.3.3 Total solids

In relation to total solids, the linear and quadratic terms of centrifugation speed and time are highly significant ($p < 0.001$). The interaction effect of both independent parameters is less significant ($p < 0.05$) in nature compared to other effects (see Table 7.5). The linear effects of both independent parameters represent a negative variation whereas quadratic and interaction effects represent a positive variation on the total solids of the Stevia extract during the clarification process. The regression model representing the effect of centrifugation speed and time on the total solids, in terms of their coded level, is given as:

$$\text{Total solid} = 2.65 - 0.11Z_1 - 0.13Z_2 + 0.082Z_1^2 + 0.075Z_2^2 + 0.043Z_1Z_2 \quad (7.9)$$

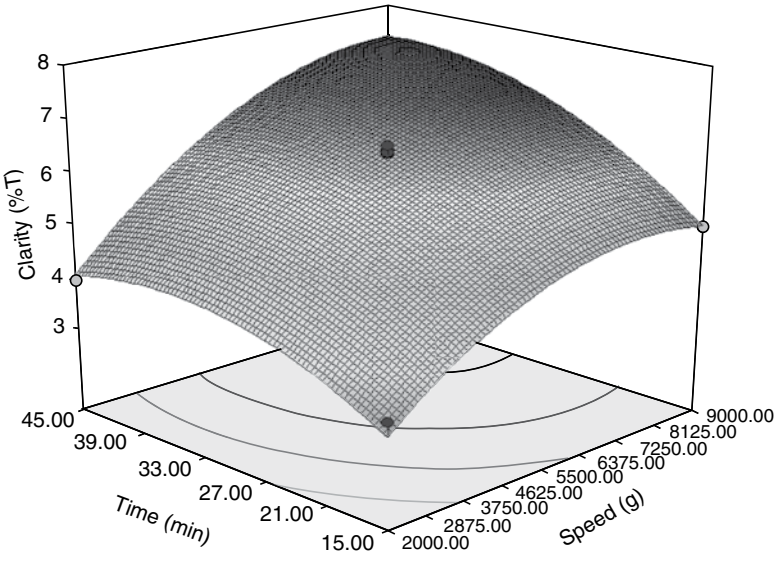

Figure 7.9 Variation of clarity as a function of speed and time. Reproduced from Chhaya et al. (2012a) with permission from Taylor & Francis.

The R^2 value of the above equation is 0.97, indicating that only 3% of variation is not explained by the regression model. Figure 7.10 presents the variation of total solids as a function of centrifugation speed and time. It shows that total solids decrease significantly with increase in centrifugation speed and time. As the speed of rotation and time increase, the suspended particles get separated from the Stevia extract, leading to the decrease in total solids of the clarified Stevia extract. The values of maximum and minimum total solids of the clarified Stevia extract during the experiments are 3.1 and 2.6, respectively.

7.3.4 Stevioside

From Table 7.5, it is obvious that the linear terms of centrifugation speed and time are highly significant ($p < 0.001$) and both of them showed a negative response on the concentration of stevioside in the clarified extract. Among quadratic terms, the centrifugation speed is significant at a probability level of $p < 0.05$ and centrifugation time is significant at a probability level of $p < 0.01$. Both of them have a positive effect on stevioside concentration during the clarification process. The interaction term is less significant ($p < 0.05$) compared to terms at linear level and has a positive effect. The regression model representing the effect of centrifugation speed and time on the stevioside concentration, in terms of their coded level, is given as:

$$\text{Stevioside} = 88.54 - 2.01Z_1 - 2.56Z_2 + 0.89Z_1^2 + 1.14Z_2^2 + 1.22Z_1Z_2 \quad (7.10)$$

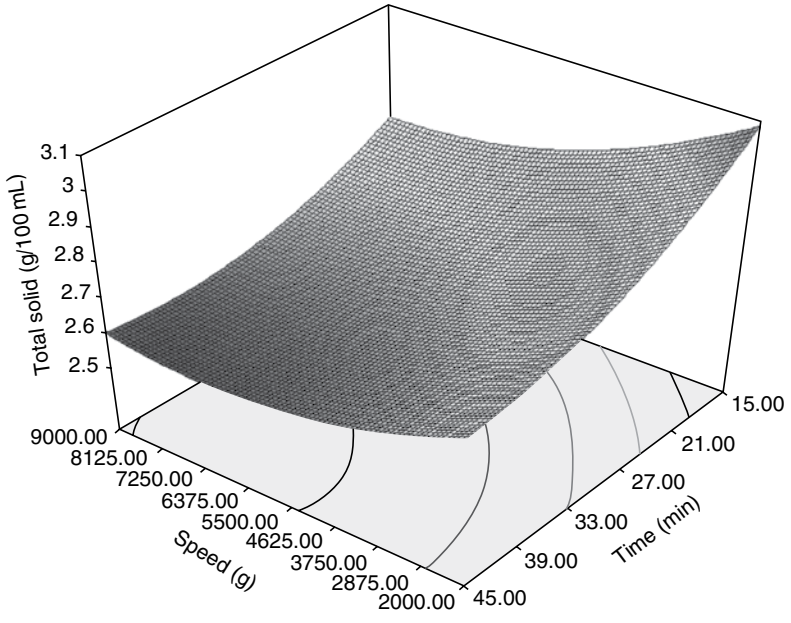

Figure 7.10 Variation of total solids as a function of speed and time. Reproduced from Chhaya et al. (2012a) with permission from Taylor & Francis.

The R^2 value is 0.96 for the above equation. The stevioside retained in the clarified extract (as compared to feed) varies between 87.1% and 95.8% of that present in crude extract throughout the experiments. Figure 7.11 represents the percentage variation of stevioside retained in the clarified Stevia extract as a function of centrifugation speed and time. The graph indicates that the stevioside content decreases with the increase in centrifugation speed and time.

7.3.5 Optimisation

The optimisation of process parameters involved in centrifugation process is carried out using Stat-Ease Design Expert 7.0.0 software. Numerical optimisation is used for this purpose. Stevioside should be retained at the maximum amount in the final clarified extract. Total solids contain suspended and dissolved particles. Removal of suspended particles during centrifugation results in increased clarity of the Stevia extract. Decrease in total solids and colour pigments also increases the purity of the clarified extract. Taking the above facts into consideration for optimisation, both the independent parameters are kept in range and two of the responses, colour and total solids, are minimised whereas clarity and stevioside are maximised. Solution having the maximum overall desirability (0.83) for the clarification process is selected as the optimum condition. Numerical optimisation generated optimum conditions as: centrifugation speed (g) 5334 and time (min) 25.62, for which the corresponding values

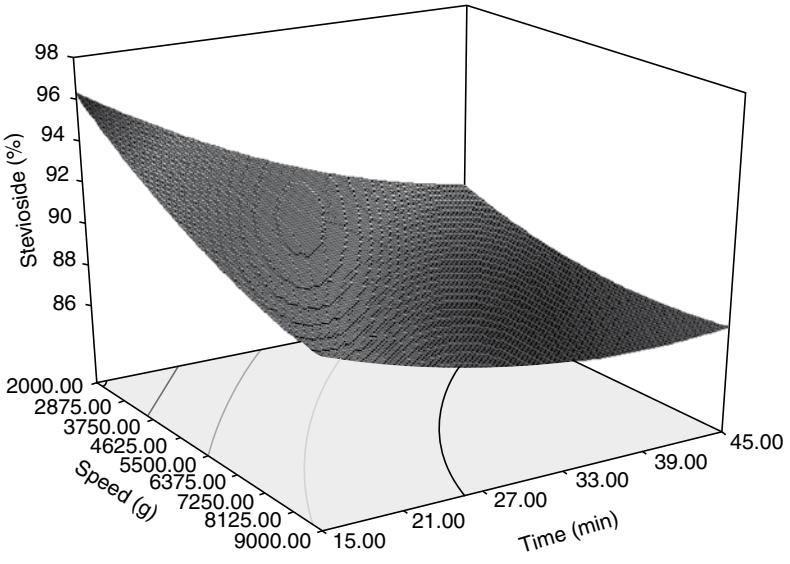

Figure 7.11 Variation of stevioside as a function of speed and time. Reproduced from Chhaya et al. (2012a) with permission from Taylor & Francis.

of all the responses are: colour (A) 7.4, clarity (%T) 6.0, total solids (g/100 mL) 2.7 and stevioside (% of that in crude extract) 89.5.

7.3.6 Microfiltration

A stirred batch cell (dead-end filtration unit) made of stainless steel was used for the clarification of Stevia extract by microfiltration. The effective filtration area of the circular membrane module was 33.16 cm^2. The feed chamber of 500 mL capacity was connected to a nitrogen cylinder to generate pressure in the test cell. A stirrer was connected at the top of the feed chamber and was externally attached to a motor through a belt. A voltage control device was used to control the speed of the stirrer and it was measured by a hand-held digital tachometer. First, the membrane was compacted for 2 h at 550 kPa pressure using distilled water. Water flux was measured at five different transmembrane pressure drop values. From the slope of the permeate flux and pressure drop curve, the membrane permeability was determined. Next, the cell was filled with crude Stevia extract and the operating pressure was set using the nitrogen cylinder. Nine experiments were conducted at operating pressures of 138, 207 and 276 kPa and stirring speeds of 500, 1500 and 2500 rpm. Each experiment was conducted for 30 min at a room temperature of 30 ± 2 °C and the clarified Stevia extract (permeate) was collected in a measuring cylinder. After the experiment, the membrane was carefully rinsed with distilled water and kept in 2% surfactant, sodium dodecyl sulfate solution overnight. The cleaned membrane was

Figure 7.12 Stirred batch cell set-up. For a colour version of this figure, see Plate 7.1.

then rinsed carefully so that traces of surfactant were removed and again its permeability was measured using distilled water. The set-up is shown in Figure 7.12.

Clarification of Stevia extract using microfiltration membrane is performed in a stirred batch cell. In any membrane separation process, permeate flux decline is a major limitation. This is due to accumulation of solutes over the membrane surface (known as concentration polarisation), leading to membrane fouling. This phenomenon cannot be avoided but can be minimised. Severity of concentration polarisation depends upon the operating conditions, such as transmembrane pressure drop and degree of agitation (stirring speed in this case). Therefore, the effects of operating conditions are of paramount importance.

Figure 7.13 represents the variation of permeate flux with time at fixed transmembrane pressure drops and different stirring speeds. Three general trends are observed. First, the permeate flux declines rapidly within 5 min from the start of the operation and gradually thereafter. Second, at a fixed pressure, permeate flux increases with stirrer speed. Third, at a fixed stirrer speed, the permeate flux enhances with transmembrane pressure drop. For example, at 138 kPa pressure and 500 rpm stirrer speed, permeate flux declines from 78 L/m^2.h to 9.8 L/m^2.h within 5 min (Figure 7.13a). Degree of decline is more at higher operating pressure. At 276 kPa pressure and 500 stirrer rpm (Figure 7.13c), the permeate flux declines to about 17 L/m^2.h from 165 L/m^2.h within 5 min. This rapid decline of permeate flux is attributed to membrane fouling. As the pore size of the microfiltration membrane is larger, the solute particles can move inside the pores and block them partially or completely. There are four mechanisms of pore blocking: complete, intermediate, standard and partial. Any one or more of these mechanisms can occur at a time (Hermia 1982; Jonsson et al. 1996).

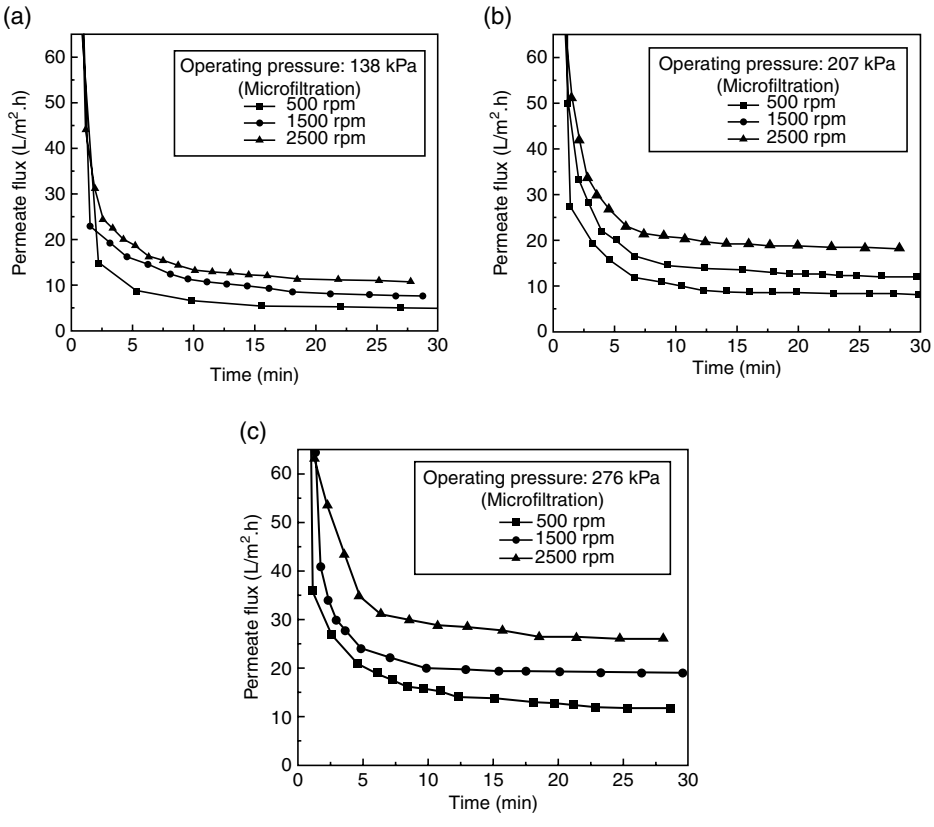

Figure 7.13 Variation of permeate flux as a function of time at varying stirring speeds and fixed operating pressure. (a) 138 kPa. (b) 207 kPa. (c) 276 kPa. Reproduced from Chhaya et al. (2012a) with permission from Taylor & Francis.

Once the pores are blocked, the solute particles deposit over the membrane surface, forming a gel type of layer that develops gradually with time of operation. Thus, the initial rapid decline of permeate flux is due to membrane fouling via pore blocking and the subsequent gradual decline is due to development of a gel layer once the pore blocking is completed (Mondal and De 2009, 2010).

Pore blocking in microfiltration is a common observation, as reported by several researchers (Chamchong and Noomhorm 1991; Fukumoto et al. 1998). It is noted from Figure 7.13 that after about 20 min of operation, the rate of decrease in permeate flux is extremely small. After 20 min, the flux values increase with stirrer speeds at a fixed transmembrane pressure drop. For example, at 138 kPa pressure, the permeate flux increases from 5 to 12 L/m^2.h (2.4 times) as the stirrer speed increases from 500 to 2500 rpm (Figure 7.13a). At 207 kPa pressure, the increase in flux is from 10 to 20 L/m^2.h, i.e. 2 times (Figure 7.13b) and at 276 kPa, permeate flux increases from 12 to about 30 L/m^2.h i.e. 2.5 times (Figure 7.13c). As the stirrer speed increases, turbulence in the flow channel also increases, leading to restriction

of the growth of the gel layer over the membrane surface. Therefore, the permeate flux increases with stirrer speed at a fixed transmembrane pressure drop. At a fixed stirrer speed, the permeate flux values increase with the transmembrane pressure drop. For example, at 2500 rpm, the permeate flux (at the end of 20 min) increases from 10 to about 30 L/m^2.h as the transmembrane pressure drop increases from 138 to 276 kPa (comparing Figures 7.13a and 7.13c). As the operating pressure increases, the driving force of the solvent flux through the membrane also increases.

Silva et al. (2007) and Reis et al. (2009) conducted experiments with Stevia extract using 0.05, 0.1 and 0.2 μm pore size silica-alumina ceramic microfiltration membranes. They observed that maximum permeate flux of 80 L/m^2.h was obtained at 6 bar with 0.2 μm membrane and the best clarification was obtained with 0.1 μm membrane at 4 bar. Thus, a trade-off between permeate quantity and quality must exist. The permeate flux value in the present study using polymeric 0.2 μm membrane at 276 kPa (2.74 bar) and 2500 rpm stirring speed is obtained as 30 L/m^2.h (see Figure 7.13a), which is comparable (at 6 bar this flux is extrapolated as 65 L/m^2.h) to the observation of Reis et al. (2009). Zhang et al. (2000) used microfiltration (0.35 μm ceramic membrane) as a pretreatment of ultrafiltration in diafiltration mode. However, they did not report on the permeate flux during microfiltration.

Table 7.7 represents various properties of clarified Stevia extract. The values of absorbance for colour of clarified Stevia extract range between 7.2 and 7.8. The maximum and minimum values of clarity are reported to be 6.8 and 5.5 respectively in terms of percentage transmittance (%T). Maximum clarity is obtained with higher operating pressure (276 kPa). Total solids of clarified extracts have almost the same values but some variation in stevioside concentration is found. Recovery of stevioside retained in the clarified extract is maximal (87.4–89.0%) at 138 kPa operating pressure. The minimum value (81.3–84.8%) of stevioside concentration is found at 276 kPa operating pressure.

The variation of different properties needs some discussion. From this table, it is observed that as the operating pressure increases, the colour of the extract decreases and the clarity increases. But at the same time, recovery of stevioside decreases. For

Table 7.7 Properties of stevia extract clarified by microfiltration process. Reproduced from Chhaya et al. (2012a) with permission from Taylor & Francis.

Transmembrane pressure (kPa)	Stirring speed (rpm)	Colour (A)	Clarity (%T)	Total solids (g/100 mL)	Stevioside (%)
138	500	7.5 ± 1.2	5.6 ± 1.2	2.7 ± 0.2	87.4 ± 2.2
	1500	7.3 ± 1.5	5.9 ± 1.4	2.7 ± 0.5	89.1 ± 2.5
	2500	7.8 ± 1.3	5.5 ± 1.6	2.7 ± 0.4	88.5 ± 2.7
207	500	7.4 ± 1.4	6.2 ± 1.5	2.7 ± 0.3	86.7 ± 2.4
	1500	7.5 ± 1.2	6.0 ± 1.3	2.7 ± 0.5	85.1 ± 2.3
	2500	7.2 ± 1.5	6.5 ± 1.5	2.7 ± 0.3	87.7 ± 2.5
276	500	7.2 ± 1.2	6.8 ± 1.3	2.7 ± 0.2	84.8 ± 2.2
	1500	7.2 ± 1.4	6.5 ± 1.2	2.7 ± 0.4	84.4 ± 2.6
	2500	7.5 ± 1.5	6.6 ± 1.4	2.7 ± 0.2	81.3 ± 2.23

example, at 138 kPa pressure and 1500 rpm, the extract colour is 7.3, clarity 5.9 and stevioside recovery 89.1%. As we increase pressure to 276 kPa, these values are 7.2, 6.8 and 84.8% at 500 rpm. Thus, at higher operating pressure, although the colour decreases by 0.8% and clarity increases by 15%, recovery of stevioside decreases by 5%. This occurs because, at higher transmembrane pressure drops, more solutes are deposited on the membrane surface, forming a gel layer. This layer of solutes acts as a dynamic membrane to retain more stevioside, thereby reducing the recovery of stevioside in the permeate at higher operating pressure. Since it is required to maximise the recovery of stevioside, a lower operating pressure, for example 138 kPa, may be preferred. Regarding selection of the stirrer speed, Table 7.7 indicates that the recovery of stevioside is almost the same at 138 kPa and both 1500 and 2500 rpm. But, as shown in Figure 7.13(a), the permeate flux at 2500 rpm is about 50% more than that at 1500 rpm. Thus, 138 kPa pressure and 2500 rpm can be selected as the optimum operating conditions for microfiltration of Stevia extract.

Silva et al. (2007) and Reis et al. (2009) reported maximum sweetener recovery of about 90%. Zhang et al. (2000) reported 80% recovery of sweeteners after microfiltration at 104 kPa transmembrane pressure drop. However, using a polymeric membrane, around 88–89% recovery of stevioside is obtained.

7.3.7 Comparison

Two methods, centrifugation and microfiltration, are used for the clarification of Stevia extract. After clarification, both the clarified extracts along with the feed are compared on the basis of their properties. The most suitable operating conditions and the product quality of the clarified extract using both of these methods are presented in Table 7.8. It can be seen from the values of colour, clarity, total solids and stevioside content that the properties of clarified extract in both the cases were similar but the results from centrifugation are marginally better.

Centrifugation and microfiltration were carried out for primary clarification of Stevia extract. The operating conditions of the centrifugation were optimised using response surface methodology and were: centrifugation speed 5334 g and operating time 25.6 min with recovery of 89.5% stevioside. In relation to microfiltration, the effects of operating pressure and stirrer speed on the permeate flux and

Table 7.8 Comparison of the properties of the extract clarified by two different clarification methods (centrifugation and microfiltration). Reproduced from Chhaya et al. (2012a) with permission from Taylor & Francis.

Clarified extract	Colour (A)	Clarity (%T)	Total solids (g/100 mL)	Stevioside (%)
Centrifugation	7.4	6.0	2.7	89.5
Microfiltration	7.8	5.5	2.7	88.5
Crude extract	11.0	0.12	3.2	13.5 g/L

properties of clarified extract were investigated. It was found that 138 kPa pressure and 2500 rpm were the best operating conditions for 0.2 μm membrane with a recovery of 88.5% stevioside.

7.4 Selection of membrane

The choice of a suitable membrane for ultrafiltration of primary clarified Stevia extract is the key to the entire process. For identification of a suitable membrane, four polymeric ultrafiltration membranes of molecular cut-off, 5, 10, 30 and 100 kDa were used. These membranes were supplied by Permionics Membranes, Gorwa, Vadodara, India. Permeability values of these membranes were measured using distilled water and are presented in Table 7.9.

The stirred batch cell as described earlier was used for the different ultrafiltration (UF) membranes. Selection of a suitable UF membrane depends on the permeate flux, i.e. throughput of the process, and the permeate quality as well. Hot water extraction followed by centrifugation of Stevia extract was used as feed for the ultrafiltration experiments.

Values of permeate flux at the end of about 120 min for various membranes were:

- 5 kDa membrane: 1.2–3 L/m^2.h (transmembrane pressure drop 276–690 kPa);
- 10 kDa membrane: 1.5–3.2 L/m^2.h (transmembrane pressure drop 276–690 kPa);
- 30 kDa membrane: 2–4.1 L/m^2.h (transmembrane pressure drop 276–690 kPa);
- 100 kDa membrane: 1.25–3.1 L/m^2.h (transmembrane pressure drop 276 to 690 kPa).

The index of flux decline was defined as the ratio of permeate flux at 120 min to pure water flux at 276 kPa. This index is 0.05 for 5 kDa, 0.048 for 10 kDa, 0.04 for 30 kDa and 0.01 for 100 kDa membrane at 276 kPa. Similar trends were observed for other pressure drop values. From this calculation, it is clear that the membrane

Table 7.9 Characteristics of the membranes used (temperature 30 ± 2°C and transmembrane pressure range 276–690 kPa). Reproduced from Chhaya et al. (2012b) with permission from Elsevier.

Molecular weight cut-off	Permeability × 10^{11} (m/Pa.s) (before the experiment)	Permeability × 10^{11} (m/Pa.s) (after the experiment)	Membrane material
5 kDa	2.4 ± 0.1	2.1 ± 0.1	Thin film composite (TFC)
10 kDa	3.16 ± 0.1	1.7 ± 0.1	Polyethersulfone (PES)
30 kDa	5.4 ± 0.3	1.7 ± 0.3	PES
100 kDa	9.0 ± 0.4	4.5 ± 0.4	PES

fouling and subsequent flux decline are highest for 100 kDa but almost the same for 5, 10 and 30 kDa membranes. In terms of absolute value of the permeate flux, it is highest for the 30 kDa membrane. Permeate flux values at the end of 120 min and stevioside yield in the permeate for different membranes at 414 kPa pressure are shown in Figure 7.14. As the pore size of the membrane increases (as the molecular weight cut-off increases), pores get blocked first. This leads to an initial sharp decline in permeate flux. Once pores get blocked, the solute particles start depositing over the membrane surface, leading to a gradual flux decline. Therefore, pore blocking is severe for 100 kDa membrane (having the highest pore size) and lower for lower cut-off membranes. Thus, higher cut-off membranes do not necessarily produce higher permeate flux. This phenomenon has been observed by other researchers (Chamchong and Noomhorm 1991; Fukumoto et al. 1998). The occurrence of pore blocking can be verified by observing membrane permeability after the experiment, as shown in Table 7.9.

The recovery of stevioside in the permeate was lowest for the 100 kDa membrane, followed by 10, 5 and 30 kDa membranes. For the 100 kDa membrane, due to larger pore size, most of the pores were blocked faster and gel formation was severe. Due to the blockage of pores, even smaller sized particles were rejected by the membrane and the rejection of stevioside was more in this case. However, for 5 and 10 kDa membranes, this effect resulted in almost similar stevioside rejection by the gel layer that behaves like another dynamic membrane. For example, at 414 kPa pressure, the yield of stevioside in the permeate was 37% and 20% for 5 and 10 kDa membranes, respectively. On the other hand, for the 30 kDa membrane, the stevioside yield in the permeate was about 50%. For lower cut-off membranes,

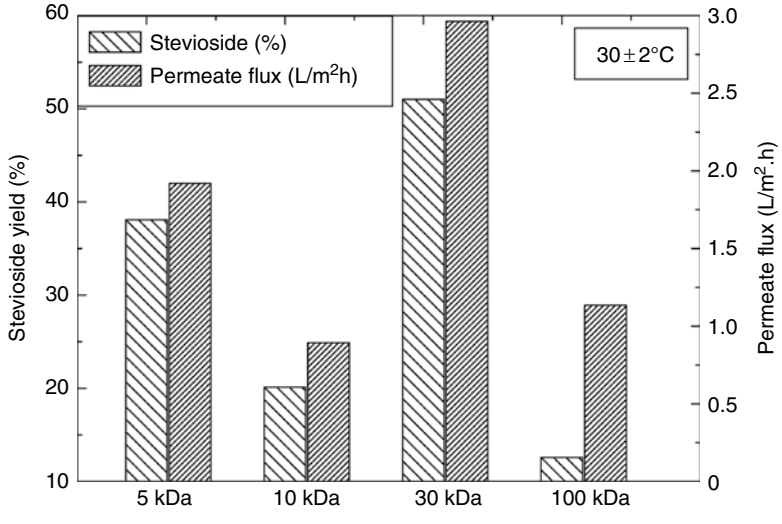

Figure 7.14 Yield of stevioside and steady-state permeate flux at 414 kPa; comparison of the different membranes. Reproduced from Chhaya et al. (2012b) with permission from Elsevier.

pore blocking effects are less and most of the higher molecular weight solutes are rejected due to the smaller pore size of the membrane and the dynamic gel layer formed over it, resulting in low recovery of stevioside in the permeate. Pore blocking and consequent gel layer (dynamic membrane) formation have optimal occurrence in the 30 kDa membrane, resulting in higher stevioside recovery and high throughput in the studied range of membranes. Thus, permeate flux and stevioside recovery are maximal for the 30 kDa membrane. Hence, this membrane was selected for clarification of centrifuged Stevia extract.

7.5 Optimisation of operating conditions

The composition of permeate is the significant factor for determining the selection criteria as well as optimum operating conditions because the permeate is the desired end-product. For efficient design of an industrial-scale processing unit, choice of appropriate membrane and optimum operating conditions is an important factor. The selection of the membrane has already beendescribed in the previous section. Here, the effects of operating conditions on the permeate flux and quality in relation to the selected membrane are analysed.

Using a 30 kDa molecular weight cut-off (MWCO) polyethersulfone (PES) membrane, a well-planned set of experiments were designed using centrifuged extract in order to observe the effects of operating conditions (transmembrane pressure drop and stirring speed) on the permeate flux and permeate quality. First, the feed tank was filled with distilled water and a fresh membrane was compacted at 800 kPa pressure for 3 h to attain steady flux. Membrane permeability was determined by measuring the flux values at various operating pressures. In the actual experiments, the feed tank was filled with the centrifuged Stevia extract. By adjusting the flow rate through the bypass and retentate valves, the pressure in the filtration cell and the flow rate were maintained constant. Cumulative volumes of permeate were collected during the experiment. Permeate samples were recycled back to the feed chamber so that the concentration of the feed remained constant. The duration of each experiment was 45 min. Permeate samples were collected at the end of experiments for analysis. Transmembrane operating pressures of 276, 414, 552 and 690 kPa and three stirring speeds, 600, 1200 and 1800 rpm, were used.

Once an experimental run was over, the membrane was thoroughly washed, *in situ*, with distilled water for 20 min, applying a maximum pressure of 200 kPa. The cell was dismantled and the membrane was rinsed with distilled water and dipped in 2% sodium dodecyl sulfate solution overnight. Next, the membrane was washed carefully with distilled water to remove traces of surfactant. The cell was reassembled and the membrane permeability was again measured using distilled water before the next experiment.

Based on the results of unstirred ultrafiltration experiments, the steady-state stirred ultrafiltration experiments were carried out using a 30 kDa membrane. Profiles of permeate flux for four transmembrane pressure drop values and various stirring speeds are presented in Figure 7.15. The remarkable feature of these figures

is that the flux decline was not sharp compared to the flux decline in the unstirred experiments, and the permeate flux reached a steady state which was much higher than the flux after 2 h in the unstirred experiments. External stirring creates turbulence in the flow channel which leads to backward diffusive transport of solutes from the gel layer to the bulk. After some time, this flux and the convective flux of solutes towards the membrane due to pressure gradient become equal and a steady state is attained. External stirring also controls the growth of the gel layer on the membrane surface by inducing forced convection. The effect of forced convection was greater at higher stirring speeds, resulting in lower gel thickness and higher permeate flux at steady state. The stirring also had a significant effect on the onset of the steady state, as seen in Figure 7.15.

The scanning electron microscope (SEM) photographs of 30 kDa membrane before and after the experiments are shown in Figure 7.16. It is clear from Figure 7.16(b) that there is indeed a deposition on the membrane surface during ultrafiltration.

In view of flux decline patterns with the various operating conditions (Figure 7.16), a simple resistance-in-series analysis is carried out. It is assumed that the solvent flows through the membrane overcoming two resistances kept in series. The first

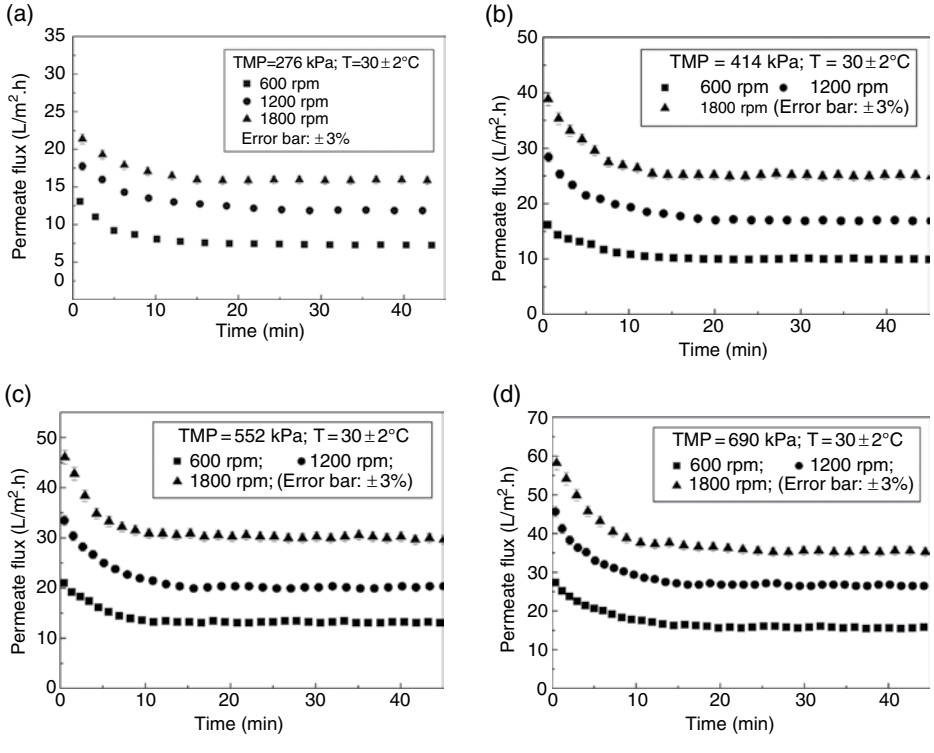

Figure 7.15 (a–d) Profiles of permeate flux for 30 kDa membranes at various operating pressure drops and stirring speeds. Reproduced from Chhaya et al. (2012b) with permission from Elsevier.

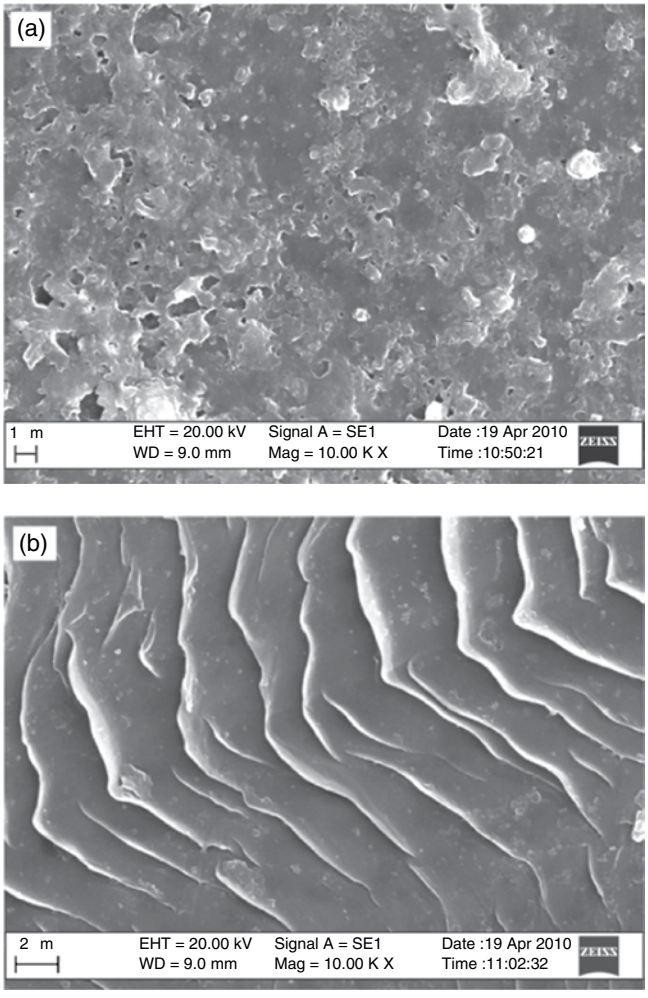

Figure 7.16 Top view of SEM image of ultrafiltration (30 kDa) membrane. (a) Nascent membrane; (b) after the experiment. Reproduced from Chhaya et al. (2012b) with permission from Elsevier.

one is the hydraulic resistance of the membrane (R_m) followed by the fouling resistance (R_f). The fouling resistance includes both the pore blocking resistance and the gel resistance due to concentration polarisation. The fouling resistance can be quantified by the following equation:

$$J = \frac{\Delta P}{\mu(R_m + R_f)} \tag{7.11}$$

In the above equation, J is the permeate flux at any point of time, ΔP is the trans-membrane operating pressure. The value of R_m was calculated from pure water

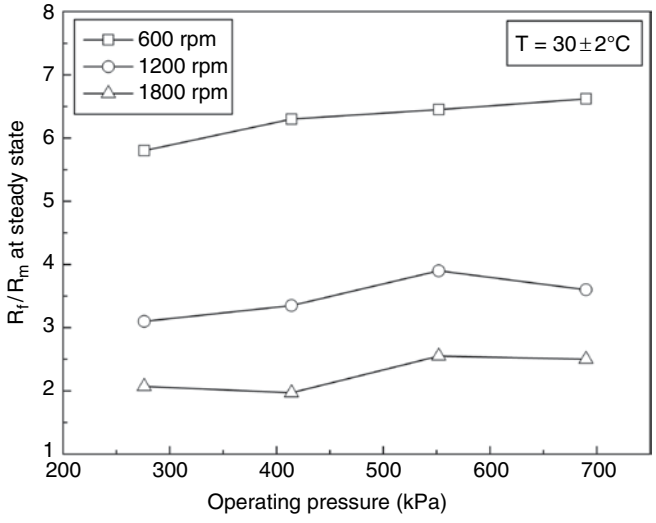

Figure 7.17 Variations of fouling resistance with respect to the membrane hydraulic resistance, with operating pressure at different stirrer speeds. Reproduced from Chhaya et al. (2012b) with permission from Elsevier.

flux (R_f=0) as 2.04×10^{13} m^{-1}. The values of R_f were calculated over time for each experiment. The variation of the ratio of the resistances of R_f to R_m at steady state is plotted as a function of operating pressure and stirrer speed in Figure 7.17. It is observed from this figure that the fouling resistance was more than twice the membrane resistance for all the operating conditions. Thus, the fouling resistance was about six times the membrane resistance at the lower stirring speed (600 rpm) and it was twice the membrane resistance at the higher stirring speed (1200 rpm). Hence, the filtration of stevioside was gel layer controlled. Another important observation is made from Figure 7.17: the ratio R_f/R_m at steady state is almost independent of transmembrane pressure drop. Thus, the gel layer deposited over the membrane surface is incompressible in nature.

Variation of the steady-state flux with the operating pressure at different stirrer speeds is presented in Figure 7.18. It is observed from this figure that the steady-state permeate flux increased with transmembrane pressure drop as well as stirrer speed. Hence, in order to get higher permeate flux, one has to select a higher operating pressure and stirring speed. However, selection of the operating conditions also depends on the permeate quality. The permeate quality for all the operating conditions at steady state is presented in Table 7.10. Some general trends are observed from this table. At lower operating pressures (276 kPa and 414 kPa), recovery of stevioside in the permeate varies between 46% and 50%. The values of colour were in the range 0.74–0.87 at this level of operating pressure. There is a marked decrease in recovery of stevioside in permeate accompanied by lower values of colour at

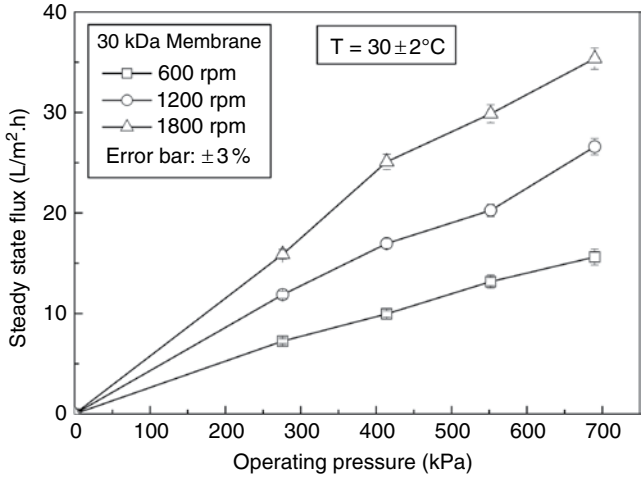

Figure 7.18 Variation of steady-state permeate flux with transmembrane pressure drop and stirrer speed under continuous stirred ultrafiltration. Reproduced from Chhaya et al. (2012b) with permission from Elsevier.

higher operating pressures (552 and 690 kPa). Stirring does not have a significant effect on the properties of the permeate.

The ultrafiltration feed essentially contains various components, of which only stevioside is desirable. The mixture of components can be clubbed together as high molecular weight (HMW) components, stevioside and low molecular weight (LMW) components. It is considered that the HMW is completely rejected and LMW is freely permeable and that LMW components have a lower molecular weight than stevioside. Following this categorisation, one can essentially obtain an approximate estimate of the amount of HMW and LMW present in the feed. Thus: $TS^{feed} = LMW^{feed} + HMW^{feed} + Stev^{feed}$ and $TS^{per} = LMW^{per} + Stev^{per}$. Since LMW^{feed} is freely permeable, it is equal to LMW^{per}, therefore HMW in feed can be estimated as $HMW^{feed} = (TS^{feed} - TS^{per}) - (Stev^{feed} - Stev^{per})$. LMW in permeate can be estimated by $TS^{per} - Stev^{per}$. On the basis of this, the average concentration of HMW and LMW in feed is 8.8 ± 0.8 and 4.5 ± 0.8 g/L, respectively. With these definitions, one can estimate the purity and selectivity of stevioside in permeate by:

$$Purity = \frac{Stevioside\ Concentration\ in\ permeate}{Concentration\ of\ total\ solids\ in\ permeate} \text{ and,}$$

$$Selectivity = \frac{Stevioside\ Concentration\ in\ permeate}{Concentration\ of\ LMW\ in\ permeate}$$

Table 7.10 Properties of the permeate with the operating conditions under stirred continuous mode of ultrafiltration using 30 kDa membrane. Reproduced from Chhaya et al. (2012b) with permission from Elsevier.

Operating pressure (kPa)	Stirring speed (rpm)	Colour (A)	Clarity (%T)	Purity of stevioside $\left(\frac{Stev^{per}}{TS^{per}}\right)$	Selectivity of stevioside $\left(\frac{Stev^{per}}{LMW^{per}}\right)$	Stevioside concentration (g/L)	Total solids (g/L)	Stevioside yield (%)
276	600	0.87 ± 0.03	86.9 ± 2.6	0.61	1.77	7.95	13 ± 0.4	47.6 ± 1.4
	1200	0.77 ± 0.02	86.9 ± 2.6	0.67	1.77	7.98	12 ± 0.4	47.8 ± 1.4
	1800	0.79 ± 0.02	84.5 ± 2.5	0.61	1.75	7.86	13 ± 0.4	47.1 ± 1.4
414	600	0.76 ± 0.02	85.0 ± 2.6	0.61	1.77	7.98	13 ± 0.4	47.8 ± 1.4
	1200	0.74 ± 0.02	86.3 ± 2.6	0.65	1.87	8.43	13 ± 0.4	50.5 ± 1.8
	1800	0.77 ± 0.02	86.6 ± 2.6	0.60	1.71	7.68	13 ± 0.4	46.0 ± 1.4
552	600	0.48 ± 0.01	91.8 ± 2.8	0.64	1.42	6.40	10 ± 0.3	38.3 ± 1.2
	1200	0.44 ± 0.01	91.8 ± 2.8	0.50	1.11	5.01	10 ± 0.3	30.0 ± 0.9
	1800	0.43 ± 0.01	92.6 ± 2.8	0.52	1.04	4.67	9 ± 0.3	28.5 ± 8.0
690	600	0.41 ± 0.01	89.5 ± 2.7	0.64	1.42	6.38	10 ± 0.3	38.2 ± 1.2
	1200	0.37 ± 0.01	88.7 ± 2.7	0.56	1.12	5.06	9 ± 0.3	30.3 ± 0.9
	1800	0.40 ± 0.01	95.0 ± 2.8	0.65	1.30	5.85	9 ± 0.3	35.0 ± 1.0
Centrifuged extract (feed)		10.4 ± 0.3	1.62 ± 0.05			16.7 ± 0.5	30 ± 1.0	
Actual stevia extract		12.3 ± 0.4	0.02 ± 0.006			18.7 ± 0.6	31 ± 1.0	

These values are presented in Table 7.11 for different operating conditions. It is observed from this table that both purity and selectivity of stevioside in the permeate are higher at lower operating pressures.

At lower operating pressures (276 and 414 kPa), the yield of stevioside (averaged over all the stirring speeds) in permeate is about 47.8%. On the other hand, at 552 kPa pressure, the average yield of stevioside in the permeate is 34.9% and this value at 690 kPa is 34.5%. Hence, the operating conditions should be selected such that maximum stevioside in the permeate with a reasonable flux would be obtained. At lower pressure, the stevioside yield is more but the permeate flux is less. On the other hand, at higher pressure, the flux is more but the stevioside yield is less. In the lower pressure range, at both 276 and 414 kPa, the stevioside recovered in the permeate (average over three stirrer speeds) is maximal among the pressure values studied herein, i.e. about 44.5%. Fuh and Chiang (1990) reported 45% recovery of stevioside using a 25 kDa membrane. Between 276 and 414 kPa, the permeate flux is higher at higher pressure and stirring speed. Therefore, 414 kPa pressure at 1800 rpm (with a flux of 36 $L/m^2.h$ and about 44.5% recovery of stevioside) can be selected as a suitable operating condition for continuous stirred ultrafiltration experiments under total recycle mode for clarification of Stevia extract.

7.6 Mechanism of flux decline

Membrane fouling, classified as reversible or irreversible, is one of the major problems in the application of the membrane process. Reversible fouling is due to deposition of solid particles over the membrane surface, also known as concentration polarisation, and it can be removed by following a suitable cleaning protocol for the membrane. Irreversible fouling mainly occurs from blockage of the pores by solutes and this cannot be removed completely even after efficient cleaning of the membrane. Therefore, it is imperative to identify the fouling mechanism during the membrane process, so that the process can be efficiently designed and scaled up. This section provides information to:

- identify the flux decline mechanism during ultrafiltration of pretreated Stevia extract using four molecular weight cut-off membranes;
- quantify the development of gel resistance with operating time for various membranes;
- evaluate the nature of the prevalent mechanism.

The stevioside extract has been ultrafiltered using different molecular weight cut-off membranes in an unstirred batch cell. The flux decline profiles show a significant trend in the behaviour of the solute, affecting the filtration characteristics and permeate quality. Since the feed contains a number of different components with a wide range of molecular weights, the concentration polarisation layer developed over the membrane surface is dominant in controlling the permeate flux mecha-

nism. For all practical purposes, the contribution of osmotic pressure to the decline of flux has been ignored. The existence of various pore blocking and gel development mechanisms is investigated in the current work.

7.6.1 Characteristic flux decline profile

The mode of flux decline during filtration can be identified by analysis of the characteristics curves (Hermia 1982; Ho and Zydney 2000).

$$\frac{d^2t}{dV^2} = k\left(\frac{dt}{dV}\right)^n \tag{7.12}$$

where t is the cumulative time of the instant measuring the cumulative volume (V), k and n are the parameter constants. For different modes of ultrafiltration one assumes different values: 2.0 for complete pore blocking (CPB), 1.5 for standard pore blocking, 1.0 for intermediate pore blocking and 0 for gel filtration.

Complete pore blocking

In this mode of filtration, the solute particles are expected to block the membrane pores completely without any superposition. It is likely that molecules having molecular weight greater than the MWCO of the membrane are involved. The pore blocking occurs during the initial few moments of the filtration regime (Bowen et al. 1995; Purkait et al. 2005). The permeate flux profile becomes:

$$J(t) = J_0 \exp(-k_1 t) \tag{7.13a}$$

where $J(t)$ is permeate flux at any instant t, J_0 is the initial flux (pure water flux) and k_1 is the parameter constant related to solute property. The above equation can be modified as:

$$\ln J = \ln J_0 - k_1 t \tag{7.13b}$$

Thus, a plot of ln (J) with t is a straight line if CPB is the prevalent blocking mechanism.

Intermediate pore blocking

In intermediate pore blocking (IPB), the membrane pores are partially accessible to the permeable solutes. On arriving at the membrane surface, the solute sits on another particle present already. The particles sometimes also adsorb on the cylindrical wall surfaces and thereby reduce the effective path of solute transport.

The variation of permeate flux with time of the experiment is represented as (Bowen et al. 1995; Purkait et al. 2005):

$$J(t) = \beta \frac{1}{1 + k_2 t} \tag{7.14a}$$

Similar to the previous instance, the above equation can be modified as:

$$\frac{1}{J} = \frac{1}{\beta} + \frac{k_C}{\beta} t \tag{7.14b}$$

Thus, a plot of $\frac{1}{J}$ with t is a straight line if IPB is the prevalent blocking mechanism.

Standard pore blocking (SPB)

It is assumed that the pore volume decreases proportional to filtrate volume and the decrease is due to particle deposition inside the pore walls which may lead to blocking of pores. The time variation of the permeate flux is expressed as (Bowen et al. 1995; Purkait et al. 2005):

$$J(t) = \frac{J_0}{(1 + \alpha t)^2} \tag{7.15a}$$

where α is the parameter constant. Equation (7.15a) can be modified as:

$$\frac{1}{\sqrt{J(t)}} = f + gt \tag{7.15b}$$

where f is $\frac{1}{\sqrt{J_0}}$ and g is $\frac{\alpha}{\sqrt{J_0}}$. Thus, a plot of $\frac{1}{\sqrt{J}}$ with t is a straight line if SPB is the prevalent blocking mechanism.

Gel filtration

Once the membrane pores are blocked, the particles arriving now deposit on the other particles already present on the surface, and a gel layer is built up that grows with time and therefore causes further flux decline. The time history of flux decline is expressed as (Bowen et al. 1995; Purkait et al. 2005):

$$\frac{1}{J(t)^2} = \frac{1}{J_0^2} + k_c t \tag{7.16}$$

where k_c is the gel resistance constant related to the solute property of the solution. Thus, a plot of $\frac{1}{J^2}$ with t is a straight line if gel formation is the prevalent blocking mechanism. However, it must be realised that once the gel layer starts to form, there is hardly any possibility of pore blocking occurring.

7.6.2 Response surface model

It has been observed that the ratio of gel resistance (R_c) to membrane hydraulic resistance (R_m) does not vary considerably on changing the transmembrane pressure (variation is less than ± 10%). This also verifies that the gel is incompressible in nature. A two-variable functional relationship has been developed for estimating R_c/R_m as a function of the experimental time and MWCO of the membrane used for filtration using response surface methodology (Draper and Smith 1998; Huber 1981; Marquardt 1963).

$$\begin{aligned}\frac{R_c}{R_m} &= p_{00} + p_{10}t + p_{01}(MWCO) + p_{20}t^2 + p_{11}(MWCO)t \\ &\quad + p_{30}t^3 + p_{21}(MWCO)t^2 + p_{12}(MWCO)^2 t \\ &\quad + p_{40}t^4 + p_{31}(MWCO)t^3 + p_{22}(MWCO)^2 t^2\end{aligned} \tag{7.17}$$

The experiments were conducted using clarified Stevia extract, produced by hot water extraction followed by centrifugation at optimum conditions. An unstirred batch cell was used for clarification. All membrane filtration experiments were carried out in triplicate. The permeate flux data were within ± 5% variation. The permeability values had ± 5% variation. Statistical parameters for the fitting of each blocking mechanism are presented in detail in Table 7.11.

The experimental flux profiles with time for all the different membranes at four different operating conditions are presented in Figure 7.19. In case of complete pore blocking, ln*(J)* versus time plot should be a straight line corresponding to Equation (12b). The results of linear regression analysis are presented in Table 7.11(a) for all the operating pressure values and membranes. It is observed that the average R^2 values (averaged over all the operating conditions) are 0.76, 0.8, 0.72 and 0.88 for 5, 10, 30 and 100 kDa membranes. The poor fitting of the experimental data with the complete pore blocking model indicates that complete pore blocking can never be a possible mechanism.

The regression analysis for the characteristic equation for intermediate pore blocking and comparison of the corresponding experimental data are presented in Table 7.11(b). Corresponding R^2 values are also calculated. The average values of R^2 (over the different pressure range) are 0.9, 0.88, 0.90 and 0.98 for 5, 10, 30 and 100 kDa membranes. Similar values of R^2 corresponding to standard pore blocking and gel formation mechanism for various membranes are presented in Table 7.11(c) and 7.11(d) respectively. R^2 values for the SPB model are 0.85, 0.82, 0.8 and 0.93

Table 7.11(a) Statistical parameters for the fitting of the characteristic complete pore blocking equation with the experimental data. Reproduced from Mondal et al. (2011) with permission from Springer Science and Business Media.

Membrane MWCO (kDa)	TMP (kPa)	SSE	df	RMSE	Adj. R^2
5	276	0.29	9	0.18	0.74
	414	0.34	11	0.18	0.79
	552	0.74	15	0.22	0.77
	690	1.00	19	0.23	0.77
10	276	0.22	6	0.19	0.70
	414	0.10	6	0.13	0.84
	552	0.19	8	0.15	0.79
	690	0.28	9	0.18	0.77
30	276	0.99	6	0.41	0.68
	414	1.76	22	0.28	0.69
	552	1.21	18	0.26	0.74
	690	1.32	18	0.27	0.75
100	276	0.17	4	0.21	0.89
	414	0.09	7	0.12	0.93
	552	0.25	9	0.17	0.86
	690	0.38	9	0.21	0.83

Table 7.11(b) Statistical parameters for the fitting of the characteristic intermediate pore blocking equation with the experimental data. Reproduced from Mondal et al. (2011) with permission from Springer Science and Business Media.

Membrane MWCO (kDa)	TMP (kPa)	SSE	df	RMSE	Adj. R^2
5	276	0.05	9	0.08	0.86
	414	0.02	11	0.05	0.90
	552	0.02	15	0.04	0.92
	690	0.01	19	0.02	0.94
10	276	0.03	6	0.08	0.85
	414	0.005	6	0.03	0.92
	552	0.006	8	0.03	0.88
	690	0.006	9	0.02	0.87
30	276	0.02	6	0.06	0.93
	414	0.03	22	0.04	0.85
	552	0.008	18	0.02	0.93
	690	0.005	18	0.02	0.93
100	276	0.002	4	0.02	0.99
	414	0.0007	7	0.01	0.99
	552	0.0024	9	0.02	0.97
	690	0.002	9	0.02	0.96

Table 7.11(c) Statistical parameters for the fitting of the characteristic standard pore blocking equation with the experimental data. Reproduced from Mondal et al. (2011) with permission from Springer Science and Business Media.

Membrane MWCO (kDa)	TMP (kPa)	SSE	df	RMSE	Adj. R^2
5	276	0.03	9	0.06	0.80
	414	0.02	11	0.05	0.85
	552	0.03	15	0.05	0.86
	690	0.03	19	0.04	0.87
10	276	0.02	6	0.06	0.78
	414	0.006	6	0.03	0.88
	552	0.009	8	0.03	0.84
	690	0.01	9	0.03	0.82
30	276	0.03	6	0.08	0.83
	414	0.06	22	0.05	0.78
	552	0.02	18	0.04	0.85
	690	0.02	18	0.03	0.85
100	276	0.007	4	0.04	0.96
	414	0.003	7	0.02	0.97
	552	0.007	9	0.03	0.92
	690	0.008	9	0.03	0.90

Table 7.11(d) Statistical parameters for the fitting of the characteristic gel layer equation with the experimental data. Reproduced from Mondal et al. (2011) with permission from Springer Science and Business Media.

Membrane MWCO (kDa)	TMP (kPa)	SSE	df	RMSE	Adj. R^2	$k_c \times 10^8$ ($s.m^{-2}$)
5	276	0.04	9	0.07	0.93	13.1
	414	0.006	11	0.02	0.97	7.51
	552	0.002	15	0.01	0.99	5.18
	690	0.0002	19	0.004	1.00	3.13
10	276	0.008	3	0.05	0.92	9.20
	414	0.001	6	0.01	0.97	3.69
	552	0.0008	8	0.01	0.95	2.42
	690	0.0005	9	0.007	0.94	1.72
30	276	0.003	6	0.02	0.98	7.97
	414	0.003	22	0.01	0.94	3.03
	552	0.0002	18	0.003	0.99	1.73
	690	0.00003	18	0.001	0.99	1.03
100	276	0.003	3	0.03	0.98	11.0
	414	0.0004	7	0.007	0.99	3.75
	552	0.00003	9	0.002	1.00	2.11
	690	0.00002	9	0.002	1.00	1.56

df, degrees of freedom; MWCO, molecular weight cut-off, RMSE, root mean square error; SSE, sum of square error; TMP, transmembrane pressure.

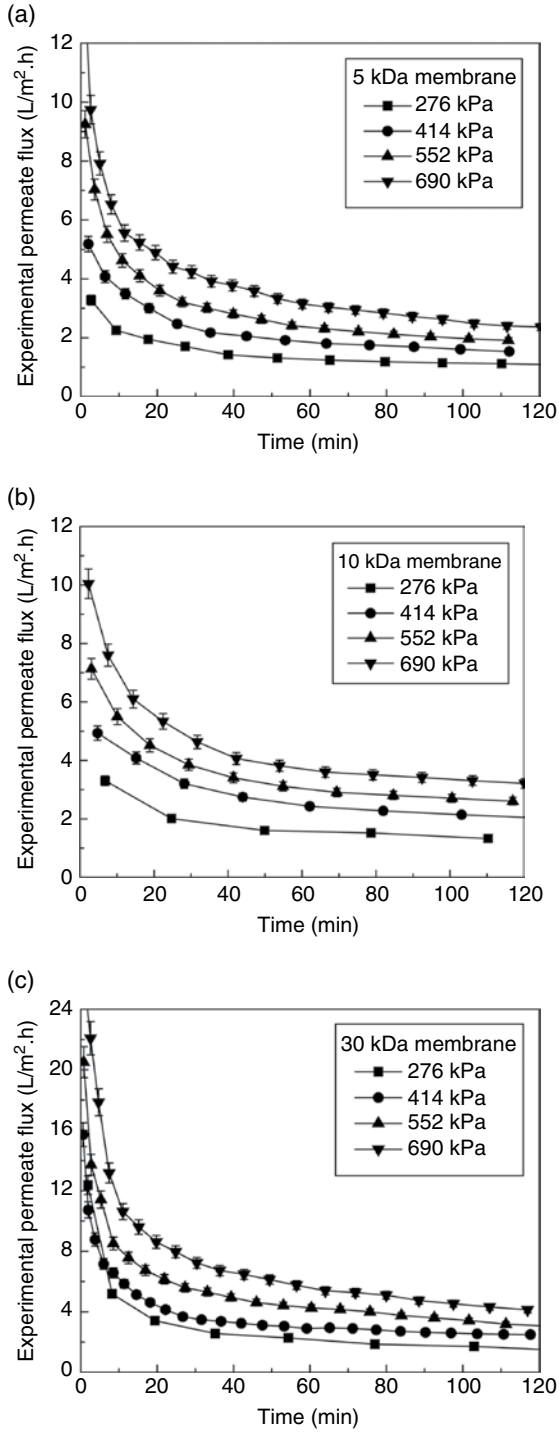

Figure 7.19 Variation of experimental flux with time at different operating transmembrane pressures using (a) 5 kDa, (b) 10 kDa, (c) 30 kDa and (d) 100 kDa membranes. Error bar ± 5%. Reproduced from Mondal et al. (2011) with kind permission from Springer Science and Business Media

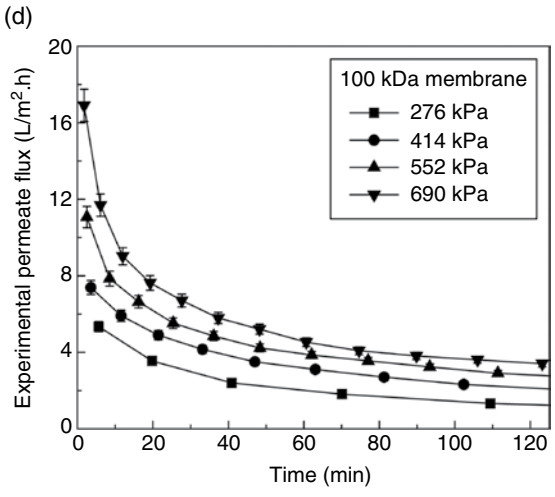

Figure 7.19 (*Continued*)

for 5, 10, 30 and 100 kDa membranes (Table 7.11(c)). These values are 0.96, 0.95, 0.97 and 0.99 for 5, 10, 30 and 100 kDa membranes respectively for gel formation (Table 7.11(d)). Comparing these values, it is clearly evident that gel formation is the dominant mechanism in all four ultrafiltration membranes.

Figure 7.20 shows that the characteristic gel equation is in good agreement with experimental values which strengthens the suggestion that stevioside clarification is dominated by gel formation during ultrafiltration. One interesting observation is noted for the 100 kDa membrane: the fitting of IPB and gel formation models is extremely good. As the MWCO of the membrane increases, the pore size of the membrane also increases. Higher pore size membranes are more prone to fouling by pore blocking. As the pore size increases, more solutes can move inside the pores and block them. This observation is also reported in the literature (Cheryan 1998; Rai et al. 2006). Once the pores are blocked by any one of the four mechanisms, the solutes deposit over the membrane surface and form a gel. In this case, for the 100 kDa membrane, both intermediate pore blocking and gel filtration mechanisms are equally important. On the other hand, for other UF membranes, gel formation is the dominant mechanism.

Reis et al. (2009) studied the fouling of a ceramic microfiltration membrane during treatment of Stevia extract. They identified complete pore blocking is the prevalent fouling mechanism. Although their conclusion was not based on strong statistical analysis, their study indicates that pore blocking was the more prevalent mechanism for more open membranes (such as higher MWCO ultrafiltration and microfiltration membranes). On the other hand, the present study confirms that gel filtration is the dominant flux decline mechanism for lower cut-off ultrafiltration membranes. It is reported in the literature that pore blocking is not desired as it causes severe flux decline (Cheryan 1998). However, in most cases, pore

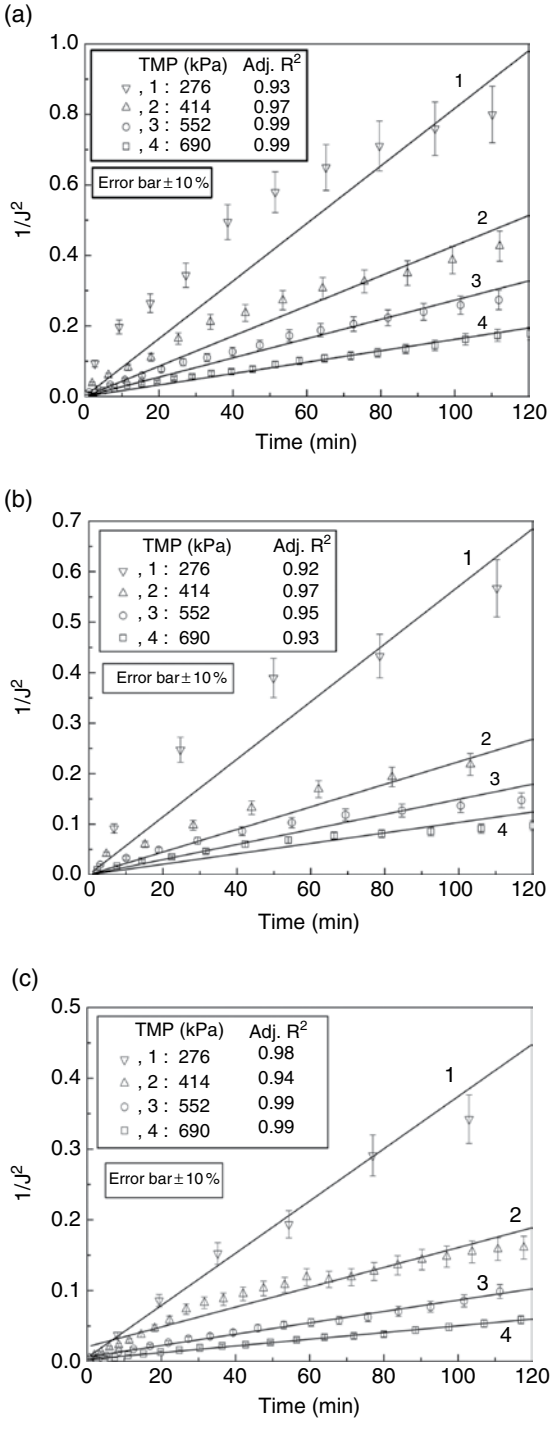

Figure 7.20 Characteristic curves for gel layer. (a) 5 kDa. (b) 10 kDa. (c) 30 kDa.

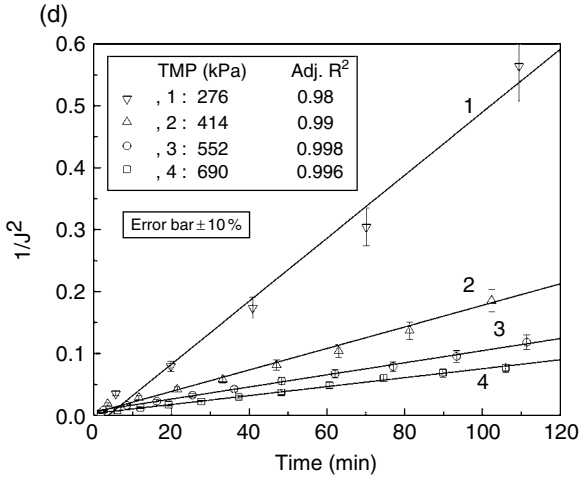

Figure 7.20 (*Continued*) (d) 100 kDa. Reproduced from Mondal et al. (2011) with kind permission from Springer Science and Business Media.

blocking and gel formation occur in sequence. Once the mechanism of membrane fouling is identified, the operating conditions can be controlled suitably in order to achieve a higher permeate flux (productivity) of the process (Mondal and De 2009, 2010).

Using a simple resistance-in-series analysis, one can express the permeate flux as:

$$J = \frac{\Delta P}{\mu\left(R_m + R_C\right)} \tag{7.18}$$

where ΔP is the transmembrane pressure drop, μ is the filtrate viscosity, R_m is the membrane resistance and R_C is the gel resistance. At a particular operating pressure, at any time t, gel resistance can be calculated from the experimental flux data as:

$$\frac{R_C}{R_m} = \frac{\Delta P}{\mu R_m J} - 1 \tag{7.19}$$

A response surface-based model (as outlined in the theory section) has been developed using the experimental data presented in Figure 7.19 to correlate the R_C/R_m values with operating time and MWCO of the membrane. The statistical parameters of the correlation developed for the resistance ratio with MWCO and time of operation for various membranes (using Equation 7.7) are presented in Table 7.12 in terms of 95% confidence level for the coefficients in the correlation. R^2 values, root mean square error and sum of square errors for the correlation are also presented in Table 7.12.

Table 7.12 Various statistical parameters of the cubic-square polynomial surface fit of the ratio of R_c/R_m varying MWCO and time. Reproduced from Mondal et al. (2011) with permission from Springer Science and Business Media.

Coefficients	Values with 95% confidence limits	Goodness of fit properties
p00	22.44 ± 1.12	SSE (sum of square error): 384.3
p10	2.02 ± 0.100	R^2: 0.99
p01	−0.64 ± 0.032	Degrees of freedom: 95
p20	−0.03 ± 0.0014	R^2, adjusted: 0.99
p11	−0.03 ± 0.00126	Root mean square error: 2.0
p02	0.005 ± 0.00027	
p30	0.00018 ± 0.0000089	
p21	0.00022 ± 0.00001079	
p12	0.00015 ± 0.0000075	
p40	$(-4.33 \pm 0.22) \times 10^{-07}$	
p31	$(-5.322 \pm 0.27) \times 10^{-07}$	
p22	$(-7.879 \pm 0.39) \times 10^{-07}$	

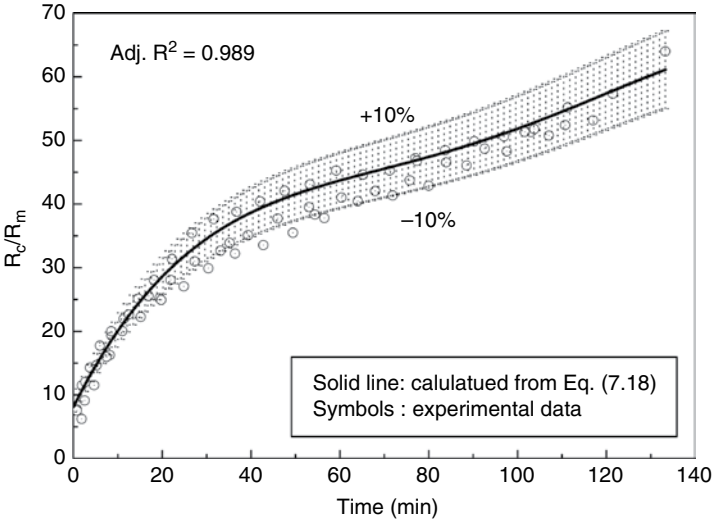

Figure 7.21 Ratio of gel layer to membrane resistance (30 kDa) for all operating TMP. Reproduced from Mondal et al. (2011) with kind permission from Springer Science and Business Media.

The values of R_C/R_m for all the pressure values and for a typical membrane (30 kDa) are shown in Figure 7.21. Three trends are observed from these figures. First, R_C/R_m values can go up to 60–90 for various membranes. This simply indicates that the gel resistance is almost two orders of magnitude higher than the membrane hydraulic resistance and is the dominant one. Second, gel resistance increases with time. As time of filtration progresses, more solutes deposit on the membrane surface and gel thickness increases, leading to an increase in gel resistance. Third, the gel

resistance values over the pressure range of 276–690 kPa vary in a narrow range. This indicates the incompressible (pressure-independent) nature of the gel. Pressure independence of permeate flux values also indicates the gel controlling mechanism (Trettin and Doshi 1981).

The characteristic curve during ultrafiltration of pretreated Stevia extract in an unstirred batch cell indicates that the dominant fouling mechanism is gel formation over the membrane surface for 5, 10 and 30 kDa membranes. For a 100 kDa membrane, both pore blocking and gel formation are equally important. It must be emphasised that even though the molecular weight of stevioside is much less than the MWCO of the membrane, the combined relative effects of pore blocking and gel formation due to the presence of a wide range of components actually determine the recovery of stevioside in the process. Also, analysis of the resistance has shown that gel resistance is dominant compared to membrane hydraulic resistance. The independence of the gel resistance with respect to the transmembrane pressure drop also signifies the incompressible nature of the gel deposited over the membrane surface.

7.7 Ultrafiltration of primary clarified Stevia extract

7.7.1 Unstirred batch cell studies

The effects of the molecular weight cut-off of the membrane and operating pressure on the physical properties of permeate are presented in Table 7.13. Clarity of the solution shows that transmittance is maximal for the larger pore size membrane (100 kDa) and lowers for the 30 kDa membrane. This is particularly due to the fact that using the 30 kDa membrane, the stevioside concentration in the permeate is maximal, as expressed in Figure 7.22(c). The clarity is, however, independent of the operating pressure used. The total solids concentration shows a similar trend to that of the clarity of the solution, which is obvious, since the presence of dissolved and suspended solids in the solution is responsible for optical absorption. But, comparing the values of clarity and total solids (TS) for 10 kDa and 100 kDa membranes, it is observed that there is a marked difference in the clarity, although both permeate solutions have almost equal amounts of total solids present in them. This is due to the difference in the amount of stevioside present in the permeate. Presence of stevioside decreases the clarity of the solution, even though the total solids content in the solution is the same. So permeate analysis of the membrane ultrafiltration which reveals minimum clarity having the same amount of total solids content is to be preferred.

The stevioside recovery in permeate and the average flux after 2 h for different membranes and various pressures are shown in Figure 7.22. These figures show that permeation of stevioside is greater at lower operating pressures. At higher pressures, gel formation is severe and the dynamic gel layer screens stevioside more effectively. Stevioside recovery is minimal for 100 kDa and higher for other membranes,

Table 7.13 Properties of the stevioside permeate. Reproduced from Mondal et al. (2011) with permission from Springer Science and Business Media.

Membranes (MWCO)	Operating pressure (kPa)	Clarity (%T)	Total solids concentration (g/100 mL)
5 kDa	276	75.9 ± 2.3	2.3 ± 0.1
	414	75.9 ± 2.3	1.8 ± 0.1
	552	74.1 ± 2.2	1.7 ± 0.1
	690	74.1 ± 2.2	1.8 ± 0.1
10 kDa	276	80.3 ± 2.4	1.0 ± 0.0
	414	79.1 ± 2.4	0.9 ± 0.0
	552	79.6 ± 2.4	0.9 ± 0.0
	690	81.2 ± 2.4	0.9 ± 0.0
30 kDa	276	62.4 ± 1.9	2.4 ± 0.1
	414	63.1 ± 1.9	2.2 ± 0.1
	552	61.7 ± 1.9	2.2 ± 0.1
	690	59.6 ± 1.8	2.3 ± 0.1
100 kDa	276	94.0 ± 2.8	1.0 ± 0.0
	414	93.5 ± 2.8	1.0 ± 0.0
	552	94.5 ± 2.8	0.9 ± 0.0
	690	95.2 ± 2.8	1.0 ± 0.0
Centrifuged feed		1.047	3.52
Actual stevia extract		0.0109	3.62

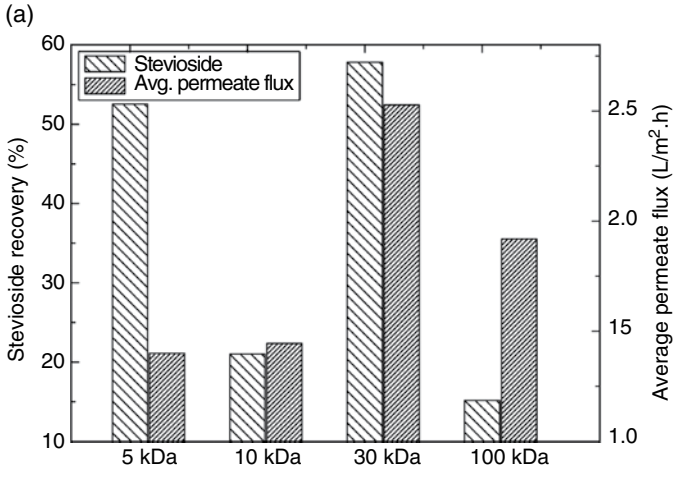

Figure 7.22 Stevioside recovery and permeate flux at different operating pressures. (a) 276 kPa.

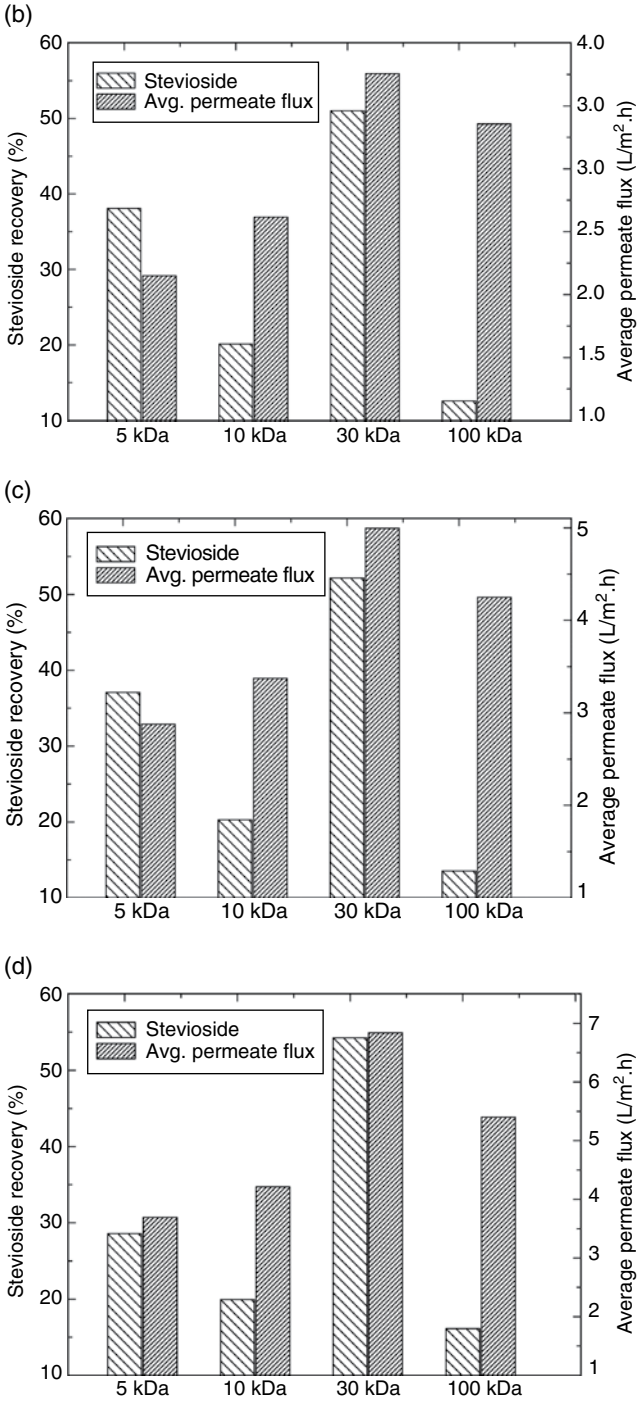

Figure 7.22 (*Continued*) (b) 414 kPa. (c) 552 kPa. (d) 690 kPa. Reproduced from Mondal et al. (2011) with kind permission from Springer Science and Business Media.

maximal for the 30 kDa membrane. For the 100 kDa membrane, both pore blocking and gel formation occur so retention of stevioside is maximal for 100 kDa but the recovery is lowest. On the other hand, for lower cut-off ultrafiltration membranes, only the gel layer is formed. This layer screens stevioside and so retention of stevioside is lower or recovery in permeate is higher. Among the four ultrafiltration membranes, gel formation is severe for 5 and 10 kDa membranes so recovery of stevioside and permeate flux both are less for these membranes. On the other hand, for the 30 kDa membrane, formation of gel is optimal, so maximal flux and stevioside recovery are realised. For the 30 kDa membrane at all pressures, stevioside recovery varies in the range of 51–58%, the maximum being at 276 kPa. Hence, the 30 kDa membrane, operated at 276 kPa pressure, allows maximum recovery of stevioside during UF.

7.7.2 Stirred batch cell studies

The experimental analysis for this has already been presented in section 7.5.

7.7.3 Cross-flow ultrafiltration

During ultrafiltration, a thin layer of solute particles accumulates on the membrane surface, providing a resistance against the solvent flux. In an unstirred operation, the thickness of this deposited layer keeps on increasing, leading to a decrease in system productivity. To minimise this effect, a separate operating configuration is adopted, in which feed is allowed to flow over the membrane surface. The convection of feed arrests the growth of this layer and thus prevents the decrease in productivity. This mode of operation is known as cross-flow.

Cross-flow ultrafiltration experiments under total recycle mode were performed using operating pressures of 276, 414, 552 and 690 kPa. The cross-flow rates were 60, 80, 100 and 120 L/h. The same experiments under batch concentration mode were undertaken at 276, 414 and 552 kPa pressure and 100 L/h cross-flow rate. A fresh membrane was compacted at a pressure higher than the maximum operating pressure for 3 h using distilled water and then its permeability was measured. The extract was placed in a stainless steel feed tank of 3 L capacity. A high-pressure reciprocating pump was used to feed the effluent into the cross-flow membrane cell. Cumulative volumes of permeate were collected during the experiment.

Permeate samples were collected at different time intervals for analysis. A bypass line was provided from the pump delivery to the feed tank. Retentate and bypass control valves were used to vary the pressure and flow rate accordingly. Values of permeate flux were determined from the slopes of cumulative volume versus time plot. The precision of flux measurement was in the order of ± 5%. After collecting the required amount of sample, the permeate stream was recycled to the feed tank to maintain a constant concentration in the feed tank under total recycle mode. The

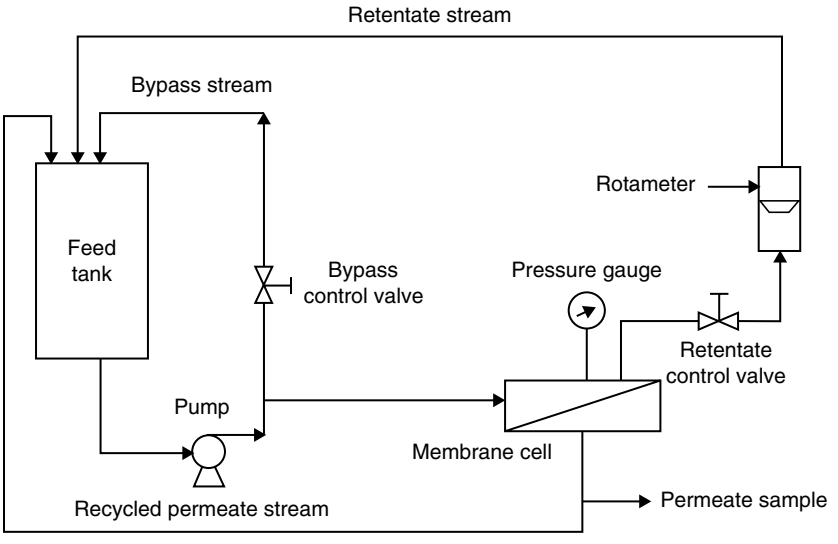

Figure 7.23 Schematic diagram of cross-flow set-up.

permeate was not recycled under the batch concentration mode of operation. Duration of the cross-flow experiments was 45 min for the total recycle mode of operation and 10 h for the batch concentration mode. The feed volume was 2 L for the total recycle mode and the initial feed volume was 1.8 L for the batch concentration mode. The cross-flow experimental set-up is shown in Figure 7.23.

Once an experimental run was over, the membrane was thoroughly washed, *in situ*, with distilled water for 30 min, applying a maximum pressure of 200 kPa. The cell was dismantled and the membrane was rinsed with distilled water and then dipped in 2% sodium dodecyl sulfate solution overnight. Next, the membrane was washed carefully with distilled water to remove traces of surfactant. The cell was reassembled and the membrane permeability was again measured using distilled water. After that, the set-up was ready for the next experiment with centrifuged Stevia extract. All the experiments were conducted at a room temperature of 32 ± 2°C.

Two modes were used for conducting thesecross-flow ultrafiltration experiments. In total recycle mode, the permeate was recycled back and the feed concentration was maintained constant. In batch concentration mode, the feed concentration was not recycled and the volume of the feed tank continued to reduce and the feed concentration increased.

Total recycle mode

In this mode of operation, variations of permeate flux as a function of time for various transmembrane pressure drops and cross-flow rates are shown in Figure 7.24. Three general trends are observed from these figures. First, the permeate flux

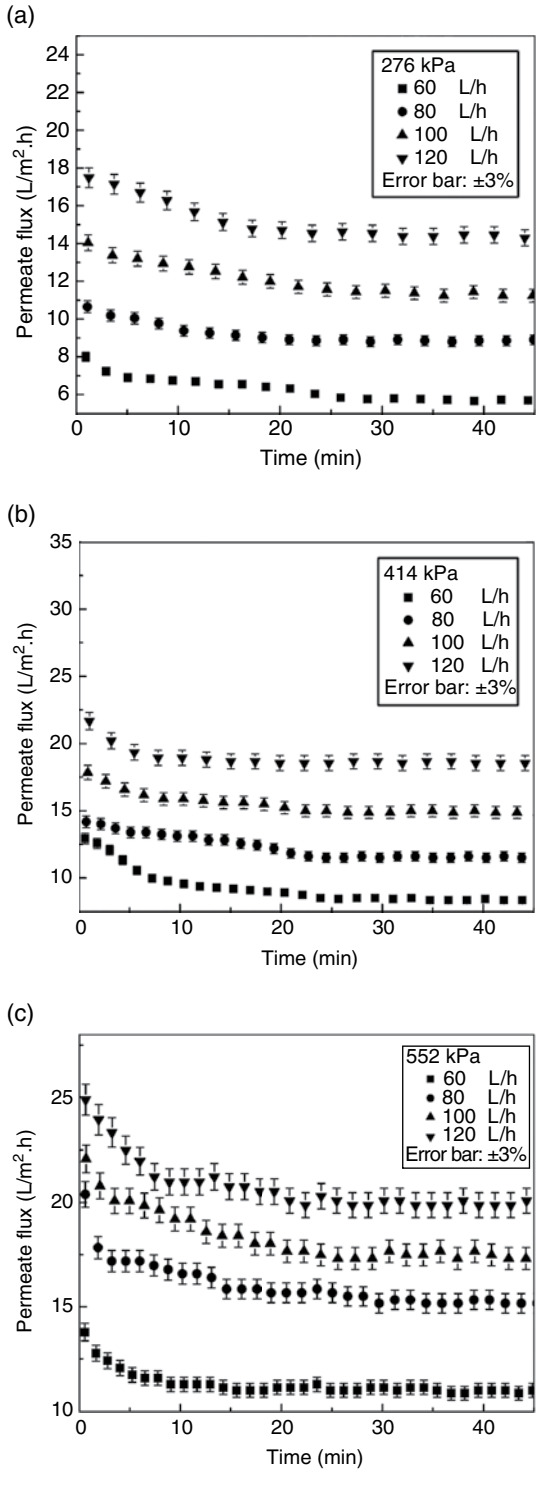

Figure 7.24 Flux decline profiles during ultrafiltration in total recycle mode. (a) 276 kPa. (b) 414 kPa. (c) 552 kPa.

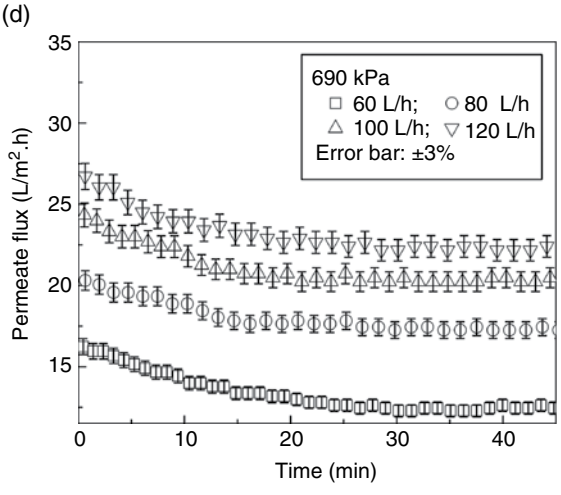

Figure 7.24 (*Continued*) (d) 690 kPa. Reproduced from Chhaya et al. (2012c) with permission from Elsevier.

declines over time of operation and finally, a steady state is reached. Second, at any point of time, the permeate flux increases with cross-flow rates at a fixed transmembrane pressure drop. Third, at any point of time, the permeate flux increases with transmembrane pressure drop at a fixed cross-flow rate.

The first observation is due to concentration polarisation. As time of filtration progresses, more solutes are convected towards the membrane and a gel layer starts growing over the membrane surface. The thickness of this layer increases with the time of filtration; it offers a resistance against the solvent flux and thus permeate flux declines. For example, at 276 kPa operating pressure and 120 L/h cross-flow rate, the permeate flux decreases from about 18 to 14 L/m^2.h (a decrease of 22%) after 45 min (Figure 7.24a). At the same transmembrane pressure drop and 80 L/h cross-flow rate, the decrease in flux is about 35% over 45 min (Figure 7.24a). Similarly, decline in flux over the filtration duration for 414 kPa at 120 and 80 L/h of cross-flow rates is 20% and 38% (Figure 7.24b). The values of flux decline for 552 kPa are 20% and 22% at these flow rates (Figure 7.24c). At 690 kPa, these values are 17% and 16% (Figure 7.24d). Therefore, the permeate flux declines over the filtration time between 16% to 38% for different transmembrane pressure drops and cross-flow rates.

Thus, at higher cross-flow rates, the flux decline is less. This is due to the fact that at higher cross-flow rates, the thickness of the gel layer decreases due to increased forced convection. It is also observed from these figures that a steady state is attained in all cases. Initially, the convective flux of solutes towards the membrane due to pressure gradient is greater and more solutes are deposited over the membrane surface, forming a gel layer. This layer keeps on growing as more solutes are convected towards the membrane. After some time, the growth of this layer is arrested by the forced convection imposed by the cross-flow rate in the flow channel and a steady state is attained. As observed from Figure 7.24(a), at 276 kPa pressure,

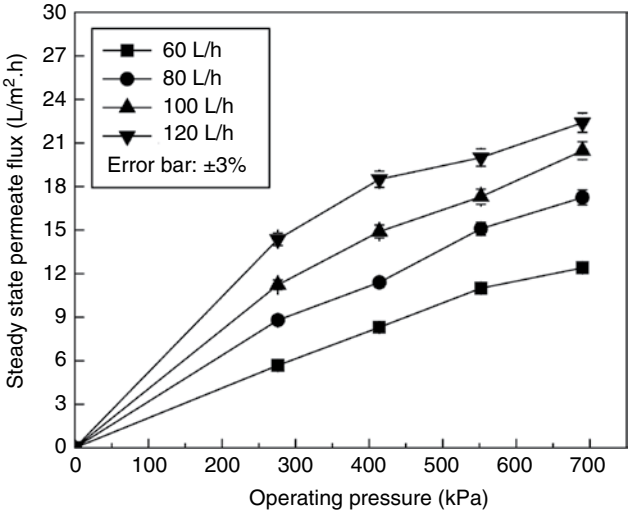

Figure 7.25 Variation of steady-state permeate flux with transmembrane pressure drop and cross-flow rate. Reproduced from Chhaya et al. (2012c) with permission from Elsevier.

steady state is attained after about 22 min. This time is reduced to 10–20 min at higher operating pressure drops.

At a fixed transmembrane pressure drop, the permeate flux increases with the cross-flow rates. At higher cross-flow rates, the shearing action of the convective flow on the gel layer is greater and its growth is restricted. Therefore, the resistance against the solvent flow offered by the gel layer is less, leading to an increase in permeate flux. For example, at 276 kPa pressure drop, the steady-state flux increases from 5 to 15 L/m^2.h as the cross-flow rate increases from 60 to 120 L/h, affecting an increase of 200%. This increase is 125% at 414 kPa, 100% at 551 kPa and 83% at 690 kPa.

At a fixed cross-flow rate, the permeate flux also increases with the transmembrane pressure drop. Increase in pressure drop has two opposing effects. First, it increases the driving force leading to flux enhancement. Second, more solutes are convected towards the membrane surface, thereby increasing the thickness of the gel layer, resulting in an increase in resistance against the solvent flow and consequently a decline in permeate flux. However, by observing the trends of flux decline profiles in Figure 7.24, it is clear that the first effect dominates the second and the flux increases with pressure. For example, at 60 L/h cross-flow rate, the steady-state permeate flux increases from 5 to 12 L/m^2.h (140% flux enhancement) as the pressure increases from 276 to 690 kPa. This enhancement over this pressure range is about 100% for 80 L/h, 81% for 100 L/h and 57% for 120 L/h cross-flow rates.

The steady-state flux values at different operating pressure drops and cross-flow rates are presented in Figure 7.25. The trends are as expected and the reasons have been discussed earlier. The properties of the permeate at the steady state with

different operating conditions are presented in Table 7.14. Some general trends are observed from this table. As the operating pressure drop increases, stevioside recovery in the permeate decreases. The selectivity and purity of stevioside in the permeate are almost independent of flow rate. Both selectivity and purity decrease with transmembrane pressure drop. At higher pressure drops, the gel layer becomes compact (associated with increasing porosity) and acts as a dynamic membrane. Therefore, this layer retains some of the stevioside and recovery of stevioside in the permeate becomes less. For example, average (over various cross-flow rates) recovery of stevioside at 276 kPa is 56%, 44% at 414 kPa, 40% at 552 kPa and 31% at 690 kPa. This dynamic gel layer retains other solids at higher pressure drops, thereby increasing the clarity of the permeate remarkably at higher operating pressures. Clarity is about 87% at 690 kPa and 120 L/h cross-flow rate whereas that in the feed of ultrafiltration is only 1.26%. Thus, the total solids in the permeate also decrease at higher operating pressures.

It is also noted from Table 7.14 that stevioside recovery decreases marginally with cross-flow rates. Except the first two experiments, at 276 kPa, 60 and 80 L/h, the variation of permeate recovery for different cross-flow rates at a fixed pressure value is insignificant. This is due to the fact that the membrane for the first experiment is fresh and after one experiment, some irreversible fouling occurs that reduces stevioside recovery drastically. This fouling is present for subsequent experiments, but it is marginal and stevioside recovery shows a declining trend (although extremely small) with the cross-flow rates at a fixed transmembrane pressure drop.

Batch concentration mode

As mentioned earlier, in this mode of operation, the permeate is not recycled back. In fact, for clarification of the Stevia extract, the permeate is the product and this is the most favourable mode of operation. Three experiments were conducted in this case; at 100 L/h cross-flow rate, the operating pressure differences were varied at 276, 414 and 552 kPa. The permeate flux profile along with the volume concentration ratio are presented in Figure 7.26, as a function of time.

Two general trends are observed from this figure. First, the permeate flux decline is greater in this case compared to the total recycle mode (see Figure 7.24) and second, there exists no steady state. Flux decline is more at higher operating pressures. In this mode of operation, the permeate is not recycled to the feed tank and as a result, the volume of the feed tank reduces, leading to an increase in feed concentration. As the feed concentration increases, the concentration polarisation becomes more severe. More solutes are convected towards the membrane surface, resulting in a thicker gel layer. This increases the resistance against the solvent flux and the permeate flux declines. At higher operating pressures, solute deposition on the membrane surface is augmented by forced convection, leading to a further decline in permeate flux. As the above phenomenon increases as time of filtration increases, a steady state is never attained. Over a period of 10 h of operation, the flux decline is 6–2 L/m^2.h at 276 kPa, 8.2–2.2 L/m^2.h at 414 kPa and 11.5–3 L/m^2.h at 552 kPa.

Table 7.14 Various properties of the ultrafiltered liqour at different operating conditions under total recycle mode of operation. Reproduced from Chhaya et al. (2012c) with permission from Elsevier.

Operating pressure (kPa)	Flow rate (L/h)	Permeate colour (A)	Permeate clarity (%T)	Permeate total solids (g/L)	Permeate stevioside (%)	Purity of stevioside $\left(\frac{Stev^{per}}{TS^{per}}\right)$	Selectivity of stevioside $\left(\frac{Stev^{per}}{LMW^{per}}\right)$
276	60	1.5 ± 0.13	53.1 ± 1.1	17	71.8 ± 3.1	0.67	2.0
	80	1.4 ± 0.12	62.5 ± 1.3	15	58.0 ± 2.1	0.61	1.6
	100	1.1 ± 0.13	69.2 ± 2.3	12	49.0 ± 2.4	0.64	1.8
	120	1.1 ± 0.15	69.5 ± 1.3	11	49.0 ± 3.2	0.70	2.4
414	60	0.9 ± 0.14	80.9 ± 1.5	14	49.0 ± 3.5	0.55	1.2
	80	0.9 ± 0.13	81.3 ± 2.1	14	45.0 ± 2.8	0.51	1.0
	100	0.9 ± 0.12	81.8 ± 2.3	13	43.3 ± 2.6	0.52	1.1
	120	0.8 ± 0.14	81.5 ± 2.4	11	40.4 ± 2.9	0.58	1.4
552	60	0.8 ± 0.15	83.4 ± 1.5	13	45.0 ± 2.4	0.55	1.2
	80	0.7 ± 0.16	84.9 ± 2.6	11	40.5 ± 3.2	0.58	1.4
	100	0.7 ± 0.12	85.5 ± 2.4	10	39.7 ± 2.6	0.63	1.7
	120	0.6 ± 0.13	87.3 ± 1.8	10	37.3 ± 3.5	0.59	1.4
690	60	0.6 ± 0.14	85.3 ± 1.7	11	37.2 ± 2.6	0.53	1.1
	80	0.6 ± 0.12	86.1 ± 1.6	11	29.7 ± 2.8	0.43	0.7
	100	0.6 ± 0.15	86.9 ± 2.2	10	31.1 ± 2.5	0.49	1.0
	120	0.4 ± 0.12	87.5 ± 2.3	10	27.5 ± 2.2	0.43	0.8
Centrifuged extract (feed)	_	10.31 ± 1.13	1.3 ± 0.5	27 ± 1.3	15753 ± 5.2 (mg/L)		
Crude extract	_	_	_	_	17167 ± 8.4 (mg/L)		

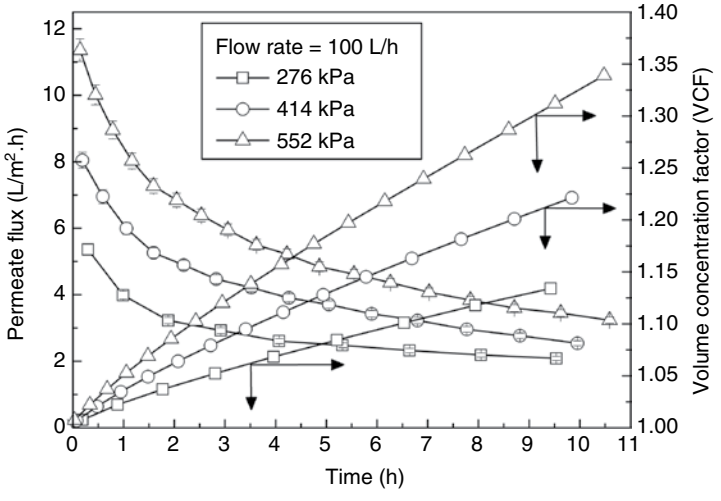

Figure 7.26 Flux decline profile and variation of volume concentration factor with transmembrane pressure drop in batch concentration mode of cross-flow ultrafiltration. Reproduced from Chhaya et al. (2012c) with permission from Elsevier.

Volume concentration factor (VCF) is defined as V_0/V, where V_0 is the initial volume of feed and V is the volume at any time. Variation of VCF with time is presented in Figure 7.26. It is observed from this figure that VCF is greater at higher pressures as more volume of permeate is filtered. After 10 h of operation, VCF reaches a value of 1.35 at 552 kPa pressure and 100 L/h cross-flow rate.

The properties of the permeate were also monitored over the filtration period. Profiles of colour, clarity, total solids, stevioside recovery and purity in permeate are presented in Figure 7.27. It is observed from this that colour, total solids and stevioside recovery in permeate decrease with time and clarity increases with time. As discussed earlier, with progress in filtration time, the gel layer acts as a dynamic membrane and retains the solutes. Thus, total solids and stevioside recovery decrease. Although colour decreases with time, its variation is marginal.

An interesting observation is made from Figure 7.27(d). Stevioside recovery at the end of 10 h for all three operating pressures is between 30% (at higher pressure, i.e. 552 kPa) and 38% (at lower pressure, i.e. 276 kPa). This is due to enhanced retention of the dynamic membrane at higher pressure by making it more compact. From Figure 7.26, it is also observed that the permeate flux after 10 h is 2 $L/m^2.h$ at 276 kPa which is marginally less than that at 552 kPa (3 $L/m^2.h$). Since stevioside recovery is our main concern, a lower transmembrane pressure drop must be selected with a reasonable permeate flux. On the other hand, the cross-flow rate should be maximal to obtain a higher permeate flux (see Figure 7.24). Thus, among the operating conditions studied, 276 kPa pressure and 120 L/h cross-flow rate are suitable for ultrafiltration of Stevia extract with a 30 kDa membrane.

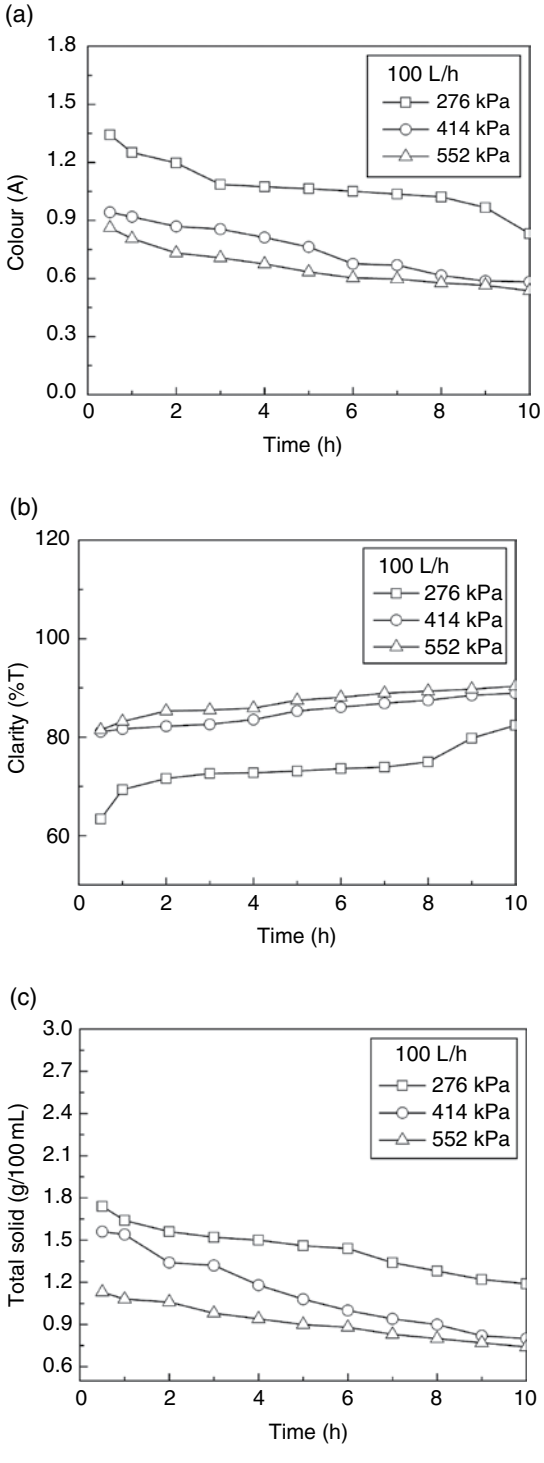

Figure 7.27 Profiles of permeate properties for various operating conditions in batch concentration mode of ultrafiltration. (a) Colour; (b) clarity; (c) total solids;

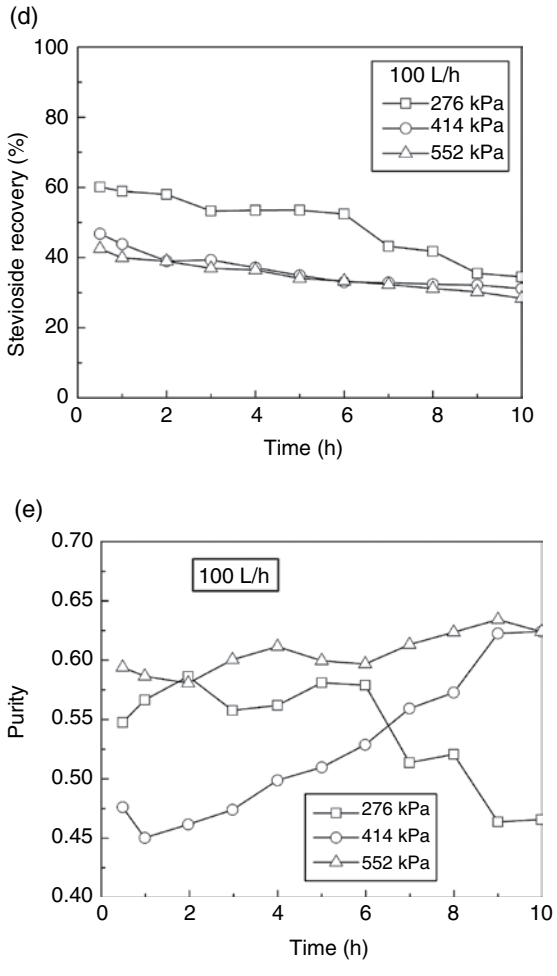

Figure 7.27 (*Continued*) (d) recovery of stevioside; (e) purity of stevioside. Reproduced from Chhaya et al. (2012c) with permission from Elsevier.

Another interesting feature that can be observed from Figure 7.27(e) is that the purity in case of lower pressure decreases with increasing time of operation, which is not the case for higher pressure. The compactness of the dynamic gel layer over the membrane is not significant enough to screen other solids at lower pressure. This results in an increase in total solids in the permeate (see Figure 7.27(c)), thereby decreasing purity. It must be noted here that purity does not exclusively depend on the amount of stevioside present in the permeate, but also the relative ratio of the amount of stevioside to total solids. So, even for the same amount of stevioside content, purity can be increased if the total solids content is decreased. So, ideally, batch operation at lower pressure and high flow rate should be limited to 5 h (as observed from the present study) in order to maintain high purity of stevioside in the permeate.

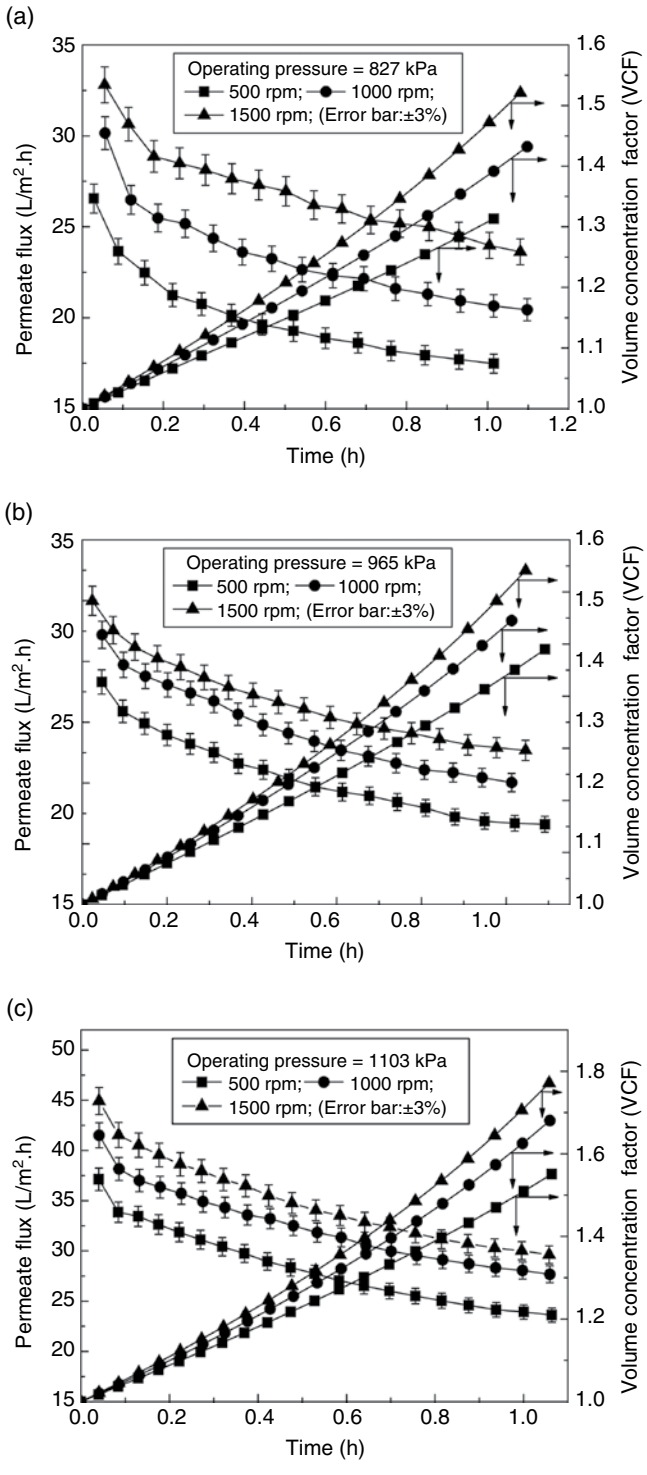

Figure 7.28 Flux decline profiles and variation of volume concentration factor with operating conditions during stirred batch nanofiltration. (a) 827 kPa. (b) 965 kPa. (c) 1103 kPa.

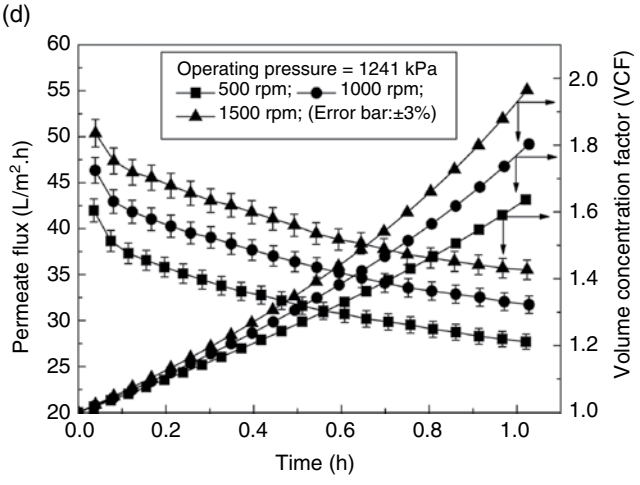

Figure 7.28 (*Continued*) (d) 1241 kPa. Reproduced from Chhaya et al. (2012c) with permission from Elsevier.

7.8 Concentration by nanofiltration

The nanofiltration experiments were conducted in batch cell form. Nanofiltration was conducted using a 400 MWCO membrane consisting of a polyamide skin over a polysulfone support, supplied by Genesis Membrane Sepratech, Mumbai, India. First, the membrane was compacted for 2 h at 800 kPa pressure using distilled water. Water flux was measured at five different transmembrane pressure drop values. From the slope of the permeate flux and pressure drop curve, the membrane permeability was found to be 1.44×10^{-11} m/Pa.s. Next, the cell was filled with 300 mL of ultrafiltered Stevia extract (collected at 550 kPa and 100 L/h) and the operating pressure was set using the nitrogen cylinder through a regulator. The stirring speed in the cell was set at an appropriate rpm by using a Variac. Each experiment was conducted for 1 h at a room temperature of 30 ± 2°C. Clarified Stevia extract (permeate) was collected in a measuring cylinder. Cumulative volume of permeate as a function of time was measured. From the slope of the cumulative volume–time plot, the permeate flux as a function of time was obtained. At the end of the experiment, the permeate samples were collected and analysed for total solids, colour, clarity and stevioside concentration. After the experiment, the set-up was dismantled and the membrane was rinsed with distilled water carefully and then kept in 2% surfactant, sodium dodecyl sulfate solution overnight. The cleaned membrane was rinsed carefully so that the traces of surfactant were removed and again its permeability was measured using distilled water.

Profiles of permeate flux and volume concentration factor with transmembrane pressure drop are shown in Figure 7.28 at various stirring speeds. It is observed from this figure that the permeate flux declines with time and the flux is higher at

Table 7.15 Various properties of permeate of nanofiltration at the end of the experiment (feed is ultrafiltration permeate at 552 kPa and 100 L/h). Reproduced from Chhaya et al. (2012c) with permission from Elsevier.

Operating pressure (kPa)	Stirring speed (rpm)	Permeate colour (A)	Permeate clarity (%T)	Permeate total solid (g/100 mL)	Permeate stevioside (mg/L)	Product (retentate) total solid (g/100 mL)	Product (retentate) stevioside (mg/L)	Overall recovery (%) [UF + NF]	Overall purity (%) [UF + NF]
827	500	0.02 ± 0.003	99.5 ± 0.4	0.2 ± 0.05	127.9 ± 1.4	1.1 ± 0.05	6486 ± 5	41.3	59.0
	1000	0.02 ± 0.002	99.9 ± 0.3	0.2 ± 0.04	143.1 ± 1.4	1.2 ± 0.04	7250 ± 3	46.2	60.4
	1500	0.02 ± 0.003	99.1 ± 0.4	0.2 ± 0.02	196.8 ± 2.4	1.3 ± 0.02	7462 ± 6	47.5	57.4
965	500	0.02 ± 0.003	99.0 ± 0.5	0.2 ± 0.06	173.0 ± 3.4	1.2 ± 0.06	7283 ± 4	46.4	60.7
	1000	0.02 ± 0.002	99.5 ± 0.4	0.2 ± 0.05	107.7 ± 2.4	1.3 ± 0.05	7606 ± 8	48.4	58.5
	1500	0.02 ± 0.004	99.6 ± 0.3	0.2 ± 0.04	208.5 ± 1.4	1.3 ± 0.04	7976 ± 3	50.8	61.4
1103	500	0.01 ± 0.005	99.3 ± 0.2	0.2 ± 0.05	348.0 ± 3.4	1.3 ± 0.05	7565 ± 5	48.2	58.2
	1000	0.02 ± 0.003	98.6 ± 0.3	0.2 ± 0.04	179.2 ± 2.4	1.4 ± 0.04	8233 ± 2	52.4	58.8
	1500	0.02 ± 0.002	98.1 ± 0.2	0.2 ± 0.03	349.5 ± 3.4	1.4 ± 0.03	8529 ± 7	54.3	60.9
1241	500	0.02 ± 0.004	99.3 ± 0.4	0.1 ± 0.04	246.5 ± 2.4	1.4 ± 0.04	7952 ± 6	50.6	56.8
	1000	0.02 ± 0.002	99.3 ± 0.4	0.1 ± 0.03	276.7 ± 1.4	1.5 ± 0.03	8726 ± 8	55.6	58.2
	1500	0.02 ± 0.005	99.1 ± 0.3	0.2 ± 0.04	201.3 ± 2.4	1.6 ± 0.04	9594 ± 10	61.1	60.0
UF extract (feed for NF)	552 kPa, 100 L/h	0.62 ± 0.003	92.8 ± 0.3	0.9 ± 0.05	4945 ± 5.4				
Centrifuge extract	Optimum operating condition	10.6 ± 1.4	_	_	14129 ± 6.2				
Crude extract	Optimum operating condition	12.3 ± 1.6	0.006 ± 0.003	2.9 ± 0.4	15699 ± 4.4				

NF, nanofiltration; UF, ultrafiltration.

higher operating pressure, as expected. At 1241 kPa pressure and 1500 rpm, flux is the highest and hence volume concentration factor is the maximum to about 2 in the test cell. Various properties of the permeate are reported in Table 7.15. It is observed from this table that the clarity of permeate is more than 99% in most of the cases. Colour and total solids in the permeate are quite low. Retention of colour is between 96% and 98% for different operating conditions studied herein. Retention of stevioside is in the range of 93–98%. The concentration factor (ratio of feed concentration of stevioside to its initial concentration in feed) of stevioside is also presented. It is observed that at 1241 kPa pressure and 1500 rpm, the feed is concentrated about two times in 1 h of operation.

It can be concluded that the purity of the overall process (UF + NF) is constant around 60%. However, the overall recovery of stevioside increases with stirring and transmembrane pressure drop. Maximum recovery is obtained at 1241 kPa and 1500 rpm.

References

Abou-Arab, A.E., Abou-Arab, A.A., Abu-Salem, M.F. (2010) Physico-chemical assessment of natural sweeteners Steviosides produced from Stevia Rebaudiana bertoni plant. Africa J Food Sci 4, 269–281.

Bowen, W.R., Calvo, J.I., Hernández, A. (1995) Steps of membrane blocking in flux decline during protein microfiltration. J Membr Sci 101, 153–16.

Chamchong, M., Noomhorm, A. (1991) Effect of pH and enzymatic treatment on microfiltration and ultrafiltration of tangerine juice. J Food Proc Eng 14, 21–34.

Cheryan, M. (1998) *Ultrafiltration and Microfiltration Handbook*. Lancaster: Technomic, pp83–85.

Chhaya, Majumdar, G.C., De, S. (2012a) Primary clarification of Stevia extract: a comparison between centrifugation and microfiltration. Sep Sci Technol 48, 113–121.

Chhaya, Sharma, C., Mondal, S., Majumdar, G.C., De, S. (2012b) Clarification of Stevia extract by ultrafiltration: selection criteria of the membrane and effects of operating conditions. Food Bioprod Proc 90, 525–532.

Chhaya, Mondal, S., Majumdar, G.C., De, S. (2012c) Clarification of Stevia extract using cross flow ultrafiltration and concentration by nanofiltration, Sep and Purif Tech 89, 125–134.

Dacome, A.S., Silva, C.C., Costa, C.E.M. (2005) Sweet diterpenic glycosides balance of a new cultivar of Stevia Rebaudiana (Bert.) Bertoni: isolation and quantitative distribution by chromatographic, spectroscopic, and electrophoretic methods. Proc Biochem 40, 3587–3594.

Das, H. (2005) *Food Processing Operations Analysis*. New Delhi: Asian Books.

Draper, N.R., Smith, H. (1998) *Applied Regression Analysis*, 3rd edn. New Jersey: John Wiley & Sons, Inc.

Erkucuk, A., Akgun, I.H., Yesil-Celiktas, O. (2009) Supercritical CO_2 extraction of glycosides from Stevia Rebaudiana leaves: identification and optimisation. J Supercrit Fluids 51, 29–35.

Fuh, W.S., Chiang, B.H. (1990) Purification of Stevioside by membrane and ion exchange processes. J Food Sci 55, 1454–1457.

Fukumoto, L.R., Delaquis, P., Girard, B. (1998) Microfiltration and ultrafiltration ceramic membranes for apple juice clarification. J Food Sci 63, 845–850.

Haber, A., Runyon, R. (1977) *General Statistics*, 3rd edn. Reading, MA: Addison-Wesley.

Hermia, J. (1982) Constant pressure blocking filtration laws: applications to power-law non-Newtonian fluids. Trans Inst Chem Eng 60, 183–187.

Ho, C., Zydney, A.L. (2000) A combined pore blocking and cake filtration model for protein fouling during microfiltration. J Coll Interf Sci 232, 389–399.

Huber, P.J. (1981) *Robust Statistics*. New Jersey: John Wiley & Sons, Inc.

Jonsson, G., Pradanos, P., Hernandez, A. (1996) Fouling phenomena in microporous membranes: flux decline kinetics and structural modifications. J Membr Sci 112, 171–183.

Khuri, A.I., Cornell, J.A. (1989) *Response Surfaces: Designs and Analyses*. New York: Marcel Dekker.

Liu, J., Li, J.W., Tang, J. (2010) Ultrasonically assisted extraction of total carbo-hydrates from Stevia Rebaudiana Bertoni and identification of extracts. Food Bioprod Proc 88, 215–221.

Marquardt, D. (1963) An algorithm for least-squares estimation of nonlinear parameters. SIAM J Appl Math 11, 431–441.

Midmore, J.D., Rank, A.H. (2006) *An Intense Natural Sweetener – Laying the Ground Work for a New Rural Industry*. RIRDC Publication No 06/020. Australia: RIRDC.

Mondal, S., De, S. (2009) Generalized criteria for identification of fouling mechanism under steady state membrane filtration. J Membr Sci 344, 6–13.

Mondal, S., De, S. (2010) A fouling model for steady state cross flow membrane filtration considering sequential intermediate pore blocking and cake formation. Sep Purif Technol 75, 222–228.

Mondal, S., Rai, C., De, S. (2011) Identification of fouling mechanism during ultrafiltration of stevia extract. Food Bioproc Technol 6(4), 931–940.

Montgomery, D.C. (2001) *Design and Analysis of Experiments*, 5th edn. Singapore: John Wiley.

Myers, R.H. (1971) *Response Surface Methodology*. Boston, MA: Allyn and Bacon.

Nishiyama, P. (1991) Correlation between total carbohydrate content and stevioside content in Stevia Rebaudiana leaves. Arch Bio Technol 34, 3–4.

Pasquel, A., Meireles, M.A.A., Marques, M.O., Petenate, A.J. (2000) Extraction of Stevia glycosides with CO_2+water, CO_2+ethanol, and CO_2+water+ethanol. Braz J Chem Eng 17, 271–282.

Pól, J., Varadová, O.E., Karásek, P., et al. (2007) Comparison of two different solvents employed for pressurized fluid extraction of stevioside from Stevia Rebaudiana: methanol versus water. Anal Bioanal Chem 388, 1847–1857.

Purkait, M.K., Bhattacharya, P.K., De, S. (2005) Membrane filtration of the leather effluent: flux decline mechanism. J Membr Sci 258, 85–96.

Rai, P., Majumdar, G.C., Sharma, G., DasGupta, S., De, S. (2006) Effect of various cutoff membranes on permeate flux and quality during filtration of mosambi (Citrus sinensis (L.) Osbeck) juice. Food Byprod Proc 84, 213–219.

Rai, C., Majumdar, G.C., De, S. (2012) Optimization of process parameters for water extraction of stevioside using response surface methodology. Sep Sci Technol 47, 1014–1022.

Reis, M.H.M., Silva, F.V., Andrade, C.M.G., Rezende, S.L., Wolfmaciel, M.R., Bergamasco, R. (2009) Clarification and purification of aqueous Stevia extract using membrane separation process. J Food Proc Eng 32, 338–354.

Silva, F.V., Bergamasco, R., Andrade, C.M.G., et al. (2007) Purification process of stevioside using zeolites and membranes. Int J Chem React Eng 5, A40.

Trettin, D.R., Doshi, M.R. (1981) Pressure independent ultrafiltration – is it gel limited or osmotic pressure limited? In: Turbak, A.E. (ed) *Synthetic Membranes, Vol II: Hyper and Ultrafiltration Uses*. Washington, DC: American Chemical Society.

Zhang, S.Q., Kumar, A., Kutowy, O. (2000) Membrane based separation scheme for processing sweeteners from Stevia leaves. Food Res Int 33, 617–620.

8

Performance modelling of stevioside separation using membrane processing

The major drawback of membrane filtration is concentration polarisation, i.e. accumulation of solute particles over the membrane surface. This causes membrane fouling, by increasing the osmotic pressure difference across the membrane or formation of gel over the membrane surface, and/or blocking of membrane pores by the solutes (Bungay et al. 1986). This phenomenon leads to decline in permeate flux, i.e. reduction in throughput, as well as the quality of permeate. Therefore, a comprehensive modelling of the process is warranted to achieve an efficient design and subsequent scaling up.

The models for transport through membranes can be classified into three types. The first-generation models are based on a film theory equation which is one-dimensional in nature (Rautenbach and Albrecht 1986). This leads to an algebraic equation in cases of gel controlling filtration (Porter 2005) and two simultaneous coupled non-linear algebraic equations for osmotic pressure controlling filtration to characterise the system performance. The main feature of this model is constant thickness of the mass transfer boundary layer. This is an oversimplification as in most cases, the mass transfer boundary layer grows slowly over a substantial distance in a module before attaining steady state. Therefore, the permeate flux is underpredicted by film theory (Gekas and Hallstrom 1987; van den Berg et al. 1989).

To overcome this, second-generation models are invoked which involve a two-dimensional analysis to account for the developing boundary layer (De and Bhattacharya 1997a; Minnikanti et al. 1999). The governing partial differential equations are solved either numerically (Bouchard et al. 1994; Fimbres-Weihs and Wiley 2007; Kleinstreuer and Paller 1983) or semi-analytically (De and Bhattacharya 1997a; Minnikanti et al. 1999).

In both the first- and second-generation models, transport in the flow channel is considered. Transport through the membrane becomes a boundary condition. The solute concentration profile in the membrane pores is approximated by a single

Stevioside: Technology, Applications and Health, First Edition.
Sirshendu De, Sourav Mondal and Suvrajit Banerjee.

parameter, namely, real retention (a distribution coefficient of solute upstream and downstream of a membrane), or a simple equation like the Kedem–Katchalsky equation (Bungay et al. 1986; Ho and Sirkar 1992).

Thus, to improve understanding of pore transport, third-generation models have been evolved. In this case, solute transport through membrane pores is considered, either one-dimensional (Bhattacharjee et al. 2001; Bungay et al. 1986; Ho and Sirkar 1992) or two-dimensional (Bungay et al. 1986), and coupled with the transport equation in the mass transfer boundary layer in the flow channel. This presents a quite detailed and computationally intensive system of equations. It may be noted that these models are validated using synthetic solutions where the properties of solutes are known. In actual processes (e.g. industrial effluent, plant extract, etc.), streams are complex mixtures of various solutes with unknown properties. Very few studies are reported to model such real-life streams (Das and De 2009; Prabhavathy and De 2001; Rai et al. 2007). Limited reports on clarification of Stevia extract by microfiltration (MF) and ultrafiltration (UF) are available (Fuh and Chiang, 1990; Silva et al. 2007; Vanneste et al. 2011; Zhang et al. 2000).

8.1 Modelling of stirred ultrafiltration

Stevia extract contains a mixture of solutes, of which some are high molecular weight (HMW) components, like proteins and polysaccharides, and others are low molecular weight (LMW), like stevioside. It is assumed that HMW solutes are completely retained by the membrane and form a gel type layer over the membrane surface. Among LMW solutes, stevioside is selectively rejected by the membrane as well as partially retained by the gel layer of HMW solutes that acts like a dynamic membrane. Solutes having molecular weight less than stevioside (molecular weight 804.87 g/mol) are considered to be freely permeable through UF membrane and their hindered transport through gel layer is ignored.

Therefore, permeate flux decline and stevioside retention during ultrafiltration (UF) are a consequence of complex phenomena arising out of the growing gel layer thickness and selective transport of stevioside through it, along with the osmotic pressure difference of stevioside across the membrane. Subscripts 1 and 2 in the text refer to the gel-forming solutes (HMW) and stevioside, respectively.

The growth of the gel layer and transport of stevioside through it and across the membrane along with the co-ordinate system for consequent transport of species are shown in Figure 8.1. In this figure, $y=0$ signifies the bulk of solution. HMW solutes form a gel layer of thickness 'L' over the membrane surface at any time. Before that, there exists a concentration profile of HMW solutes between bulk and gel concentration within the mass transfer boundary layer thickness δ. As shown in this figure, the gel layer acts as a dynamic membrane that retains stevioside to some extent. The permeate contains mainly stevioside and lower molecular weight solutes.

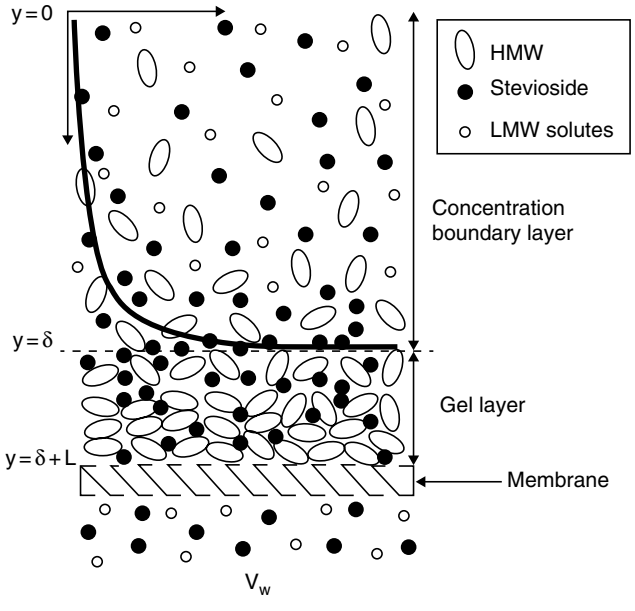

Figure 8.1 Transport of molecules during ultrafiltration of the mixture.

8.1.1 Steady-state model

The experiments are performed in a stirred continuous set-up in which both retentate and permeate streams are recycled to the feed tank. Thus, the concentration in the feed tank is maintained constant and a steady state is attained for every set of operating conditions. Since HMW solutes are assumed to form a gel layer over the membrane surface, the steady-state permeate flux is expressed by classic film theory (Blatt et al. 1970).

$$v_w = k_1 \ln\left(\frac{C_{1g}}{C_{1b}}\right) \tag{8.1}$$

Mass transfer coefficients for the stirred cell can be estimated from the following expression of Sherwood number (Blatt et al. 1970):

$$\begin{aligned} Sh = \frac{k_1 r}{D_1} &= 0.285(Re)^{0.55}(Sc)^{0.33} \qquad \text{for } Re < 32{,}000 \\ &= 0.0443(Re)^{0.8}(Sc)^{0.33} \qquad \text{for } Re > 32{,}000 \end{aligned} \tag{8.2}$$

where Sc is Schmidt number of solute 1 ($Sc=\mu/\rho D_1$) and Reynolds number, Re, is defined as $\mathrm{Re}=\dfrac{\rho(\omega r)r}{\mu}$. It is assumed that solution ρ and μ are the same as those of aqueous solution.

In an ideal gel-controlling filtration model, the mass transfer coefficient is independent of the transmembrane pressure drop (Trettin and Doshi 1980). However, several studies reveal that the mass transfer coefficient exhibits a weak dependence on transmembrane pressure drop (Johnston and Deen 1999; Mondal et al. 2011; Rai et al. 2007). It is assumed that the mass transfer coefficient is a linear function of the transmembrane pressure drop within the range of operating pressure studied. Thus, the following expression of permeate flux is proposed.

$$v_w = k_0 \ln\left(\frac{C_{1g}}{C_{1b}}\right) \tag{8.3}$$

where $k_0=k_1(b\Delta P)$. Since, the HMW solutes are a complex mixture of various components, effective diffusivity (D_1) and gel concentration C_{1g} are difficult to estimate. Thus, b, D_1 and C_{1g} are three parameters of Equation (8.3), which are determined using the optimisation routine of interior point algorithm following a trust region method (Byrd et al. 2000), by minimising the sum of square of errors of the steady-state permeate flux of all the experiments. Sum of square error is defined as:

$$S_0 = \sum_{i=1}^{N_{\exp}} \left[\frac{v_{w,\exp}^{i} - v_{w,cal}^{i}}{v_{w,\exp}^{i}}\right]^2 \tag{8.4}$$

where $N_{\exp}$ is the number of experiments conducted. The flowchart of the calculation algorithm is shown in Figure 8.2. The diffusivity (D_1) and gel concentration (C_{1g}) are completely solute characteristic properties and independent of the operating conditions such as stirring, pressure drop, type of membrane used, bulk concentration of the solute, etc. Hence, these are fixed for a particular solute system.

8.1.2 Transient model

Referring to Figure 8.1, the mass balance of HMW solutes in the mass transfer boundary layer ($0<y<\delta$) results in De and Bhattacharya (1997b).

$$\rho_g \frac{dH}{dt} = v_w C_1 - D_1 \frac{dC_1}{dy} \tag{8.5}$$

Integrating the above equation within the mass transfer boundary layer with the conditions $y=0$, $C_1=C_{1b}$ and at $y=\delta$, $C_1=C_{1g}$, the following equation is obtained:

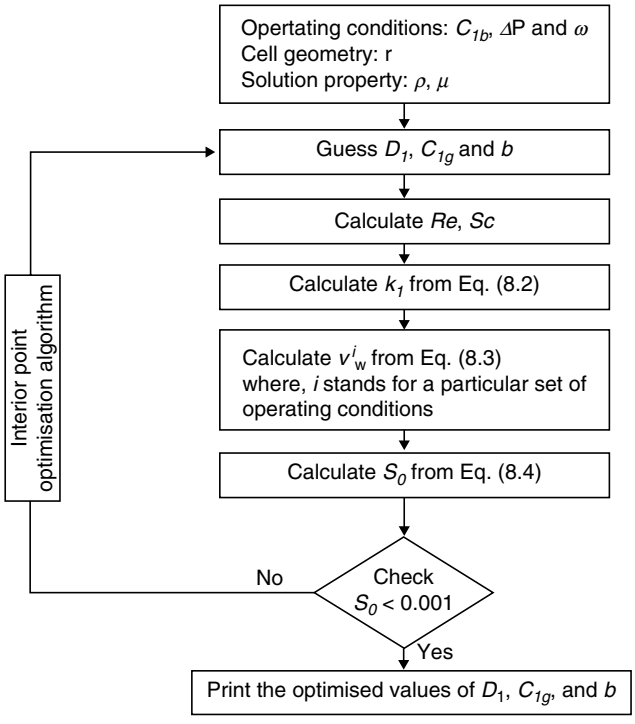

Figure 8.2 Sequence of calculations (algorithm) for optimisation of steady-state experimental data.

$$\rho_g \frac{dH}{dt} = v_w \frac{C_{1g} - C_{1b}\exp(v_w / k_1)}{1 - \exp(v_w / k_1)} \tag{8.6}$$

The initial condition of the above equation is $t=0$, H=0. It may be noted that at a limiting case (steady sate), Equation (8.6) is reduced to Equation (8.1).

Next, a mass balance of stevioside in the mass transfer boundary layer and gel layer is carried out. Following the derivation of De and Bhattacharyya (1997b), the final expression of stevioside at the membrane surface is given as:

$$C_{2m} = \frac{C_{2b}\exp\left[v_w\left(\frac{1}{k_2} + \frac{H}{\varepsilon_g D_2}\right)\right]}{\gamma_g R_{r2} + (1 - R_{r2})(\gamma_g - 1)\exp\left(\frac{v_w H}{\varepsilon_g D_2}\right) + (1 - R_{r2})\exp\left[v_w\left(\frac{1}{k_2} + \frac{H}{\varepsilon_g D_2}\right)\right]} \tag{8.7}$$

where γ_g is defined as $C_2(\delta^-) = \gamma_g C_2(\delta^+)$. Real retention ($R_{r2}$) of stevioside can be quantified as:

$$R_{r2} = 1 - \frac{C_{2p}}{C_{2m}} \tag{8.8}$$

The osmotic pressure difference of solution due to variation in concentration of stevioside across the membrane is given as:

$$\Delta\pi = \pi_m - \pi_p \tag{8.9}$$

The osmotic pressure of solutes due to stevioside is expressed according to van Hoff's relation:

$$\pi = \frac{RT}{M_2} C_2 \tag{8.10}$$

Thus, the osmotic pressure difference across the membrane is obtained by:

$$\Delta\pi = \frac{RT}{M_2} C_{2m} R_{r2} \tag{8.11}$$

Permeate flux at any point of time can be written as:

$$v_w(t) = \frac{\Delta P - \Delta\pi}{\mu(R_m + R_g)} \tag{8.12}$$

where R_g is expressed as:

$$R_g = \beta H \tag{8.13}$$

where $\beta = \alpha(1 - \varepsilon_g)\rho_g$ is constant as a characteristic of thegel layer.

Equations (8.6, 8.7, 8.11, 8.12 and 8.13) constitute a set of differential algebraic equations (DAE). In this set, the parameters are D_2, ρ_g, β, γ_g and ε_g. Real retention of stevioside (R_{r2}) is independently estimated, as described in the experimental section. Five parameters, D_2, ρ_g, β, γ_g and ε_g, are estimated by comparing the sum of square errors between the calculated and experimental data. Two separate sums of square errors are defined in the solution algorithm corresponding to minimisation of permeate flux and permeate stevioside concentration. These are:

$$S_1 = \sum_{j=1}^{N_2} \sum_{i=1}^{N_j} \left[\frac{v_{w,cal}^{ij} - v_{w,\exp}^{ij}}{v_{w,\exp}^{ij}} \right]^2 \tag{8.14}$$

where j represents the number of experiments, i represents the number of experimentally measured data points, N_j is number of data points at various time points in the j^{th} experiment.

As described in the experimental section, stevioside concentration was measured at the end of the experiment, containing the cumulative permeate. Thus, the stevioside concentration in the permeate is calculated as:

$$\overline{C_{2p}} = \frac{1}{t} R_{r2} \int_0^t (1 - C_{2m})\, dt \tag{8.15}$$

Based on the above definition, the sum of squares S_2 is defined as:

$$S_2 = \sum_{k=1}^{N_p} \left[\frac{C_{2p,cal}^k - C_{2p,\exp}^k}{C_{2p,\exp}^k} \right]^2 \tag{8.16}$$

where N_p is the number of experiments at a particular transmembrane pressure drop. The detailed constrained optimisation is presented in Figure 8.3.

Using this procedure, five parameters (as mentioned earlier) are estimated using the optimisation routine of interior point algorithm following a trust region method (Byrd et al. 2000), minimising S_1 and S_2 simultaneously. Utilising these values, the profiles of gel layer thickness, permeate flux, stevioside concentration in permeate and gel layer resistance are calculated, using Equations (8.6, 8.7, 8.11, 8.12 and 8.13).

The experimental details concerning the process of extraction and primary clarification have been described in the previous chapter. The stirred experiments were conducted in a 650 mL capacity filtration cell in a continuous mode using a 30 kDa polyethersulfone (PES) membrane. The 30 kDa membrane was found to result in the highest permeate flux and maximum recovery of stevioside in the permeate (Mondal et al. 2012a). Permeability value of the 30 kDa membrane was measured using distilled water and was $(5.4 \pm 0.3) \times 10^{-11}$ m/Pa.s.

A solution of 1 kg/m^3 concentration of stevioside (obtained from Sigma-Aldrich, USA) was prepared and a stirred experiment was conducted at high stirring speed, 2000 rpm, and low transmembrane pressure drop, 128 kPa. These conditions maintain a low polarised situation. The permeate concentration of stevioside was measured. The observed retention under this situation is a reasonably good estimate of real retention (De and Bhattacharya 1997b). The value of real retention of stevioside (*Rr2*) was 0.1. This parameter is generally constant for a particular membrane–solute–solvent system (Opong and Zydney 1991). Many studies involving modelling of the membrane process in the literature have been performed

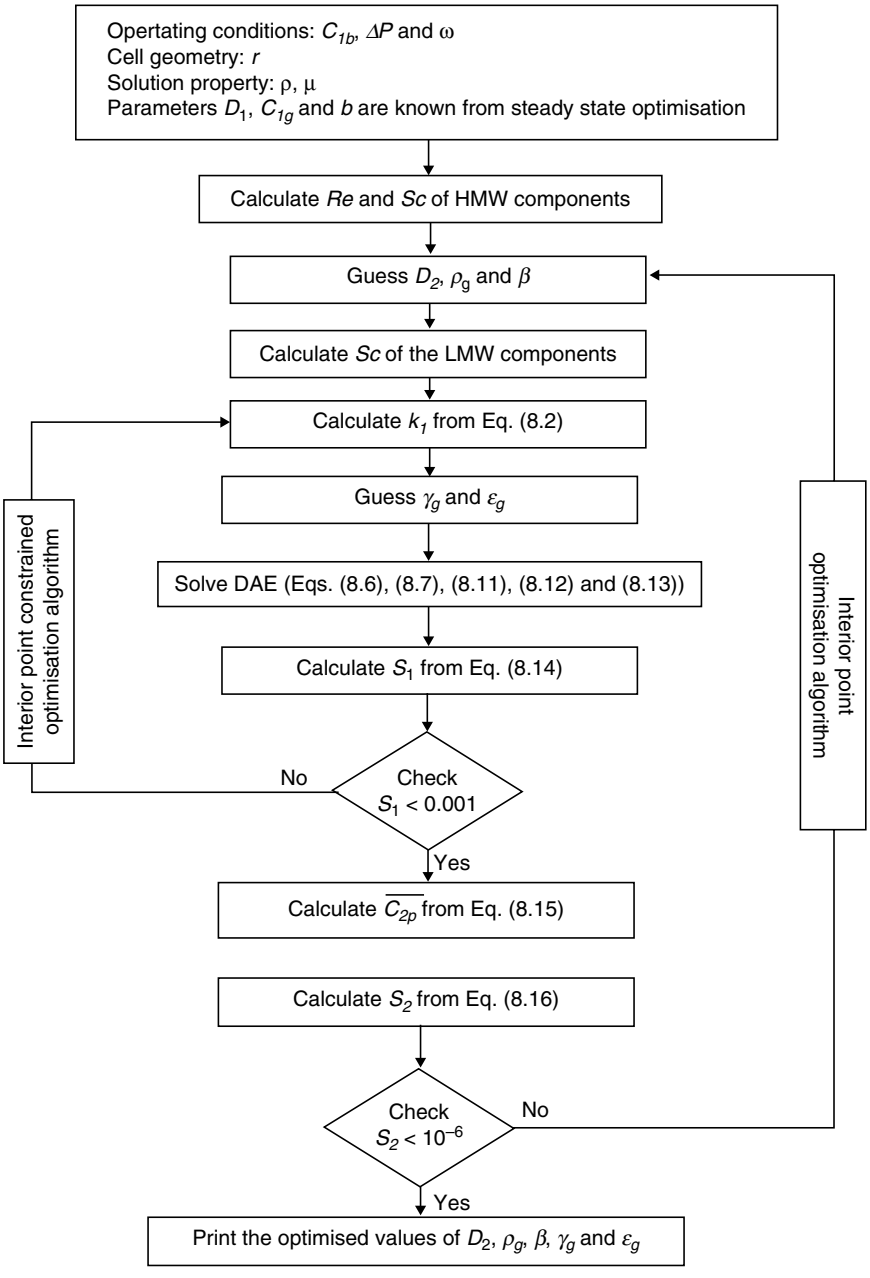

Figure 8.3 Sequence of calculations (algorithm) for optimisation of transient state modelling.

considering real retention as an inherent membrane–solute–solvent property (Bouchard et al. 1994; De et al. 1997; Trettin and Doshi 1981).

The original centrifuged and ultrafiltered Stevia extract was analysed for total solids content and stevioside concentration. Total solids in the sample were measured gravimetrically by heating the extract in a hot air oven at $104 \pm 2\,^{\circ}C$ until the difference in the weight of the extract became constant at successive intervals (Ranganna 1986).

The ultrafiltration feed contains various components, of which only stevioside is desirable. The mixture of components can be clubbed together as HMW components. Components with lower molecular weight than stevioside are grouped as LMW solutes. It is considered that HMW components are completely rejected, LMW components are freely permeable, and stevioside is partially retained by the gel layer and membrane. Following this categorisation, one can achieve an approximate estimate of the amount of HMW and LMW present in the feed. Thus, $TS^{feed} = LMW^{feed} + HMW^{feed} + Stev^{feed}$ and $TS^{per} = LMW^{per} + Stev^{per}$. Since LMW^{feed} is freely permeable, it is equal to LMW^{per}, therefore HMW in feed can be estimated as $HMW^{feed} = (TS^{feed} - TS^{per}) - (Stev^{feed} - Stev^{per})$. LMW in permeate can be estimated by $TS^{per} - Stev^{per}$. On the basis of this, the average concentration of HMW in feed (C_{1b}) is 8.8 ± 0.8 g/L. With these definitions, one can estimate the purity and selectivity of stevioside in permeate by:

$$Purity = \frac{Stevioside\ concentration\ in\ permeate}{Concentration\ \ of\ \ total\ solids\ in\ permeate} \text{ and,}$$

$$Selectivity = \frac{Stevioside\ concentration\ in\ permeate}{Concentration\ of\ LMW\ in\ permeate}$$

These values were presented in Table 7.11 (Chapter 7) for different operating conditions.

The steady-state permeate flux of pre-treated Stevia extract can be calculated using the modified film theory equation. This calculation involves estimation of three parameters: effective diffusivity of gel-forming material, gel concentration and the parameter '*b*' in Equation (8.3). Since Stevia extract is a complex mixture of various polysaccharides, proteins, steviosides and other glycosides, these three parameters are estimated by the optimisation technique as outlined earlier. The estimated values of these parameters are: $D_1 = (3.7 \pm 0.8) \times 10^{-11}\,m^2/s$; $C_{1g} = (51.5 \pm 1.5)\,kg/m^3$; $b = (3.3 \pm 0.5) \times 10^{-7}\,Pa^{-1}$. It may be noted that the values of effective diffusivity and gel concentration are similar to those of UF mosambi juice, as reported in literature (Sarkar et al. 2008). For mosambi juice, these values were effective diffusivity $6.5 \times 10^{-11}\,m^2/s$ and gel concentration $48.5\,kg/m^3$. The comparison between the calculated steady-state permeate flux values and the experimental data is within ± 10% (Mondal et al. 2012a).

Table 8.1 Values of distribution coefficient with transmembrane pressure drop. Reproduced from Mondal et al. (2012a) with permission from Elsevier.

TMP, kPa	Distribution coefficient (γ_g)
276	2.0 ± 0.01
414	2.05 ± 0.02
552	3.00 ± 0.05
690	3.00 ± 0.07

TMP, transmembrane pressure.

8.1.3 Transient state

The profiles of transient flux decline and concentration of stevioside in the permeate have been calculated by adopting an algorithm as presented in Figure 8.3. The estimated values of these parameters are: $D_2 = (1.85 \pm 0.4) \times 10^{-10}\ m^2/s$; $\rho_g = (1545 \pm 20)\ kg/m^3$; $\beta = (7 \pm 2) \times 10^{18}\ m^{-2}$; $\varepsilon_g = (0.5 \pm 0.005)$. The distribution coefficient γ_g is observed to be varying with transmembrane drop and is presented in Table 8.1.

As described earlier, γ_g represents the partition coefficient of stevioside concentration in the bulk–gel layer interface and the gel layer. So, at higher transmembrane pressure drops, the gel layer retains more stevioside, as is evident from Table 8.1. Thus, it is expected that permeation of stevioside is lower at higher transmembrane pressure drops.

With the estimated parameter values, as outlined earlier, Equations (8.6, 8.7, 8.11, 8.12 and 8.13) are solved to obtain the profiles of permeate flux, stevioside concentration, gel layer thickness and gel layer resistances.

Figure 8.4 represents the profiles of permeate flux at four transmembrane pressure drops and various stirrer speeds. These figures show reasonable agreement with calculated profiles and the experimental data. It is observed that the matching is not good for the initial time points. There are two reasons for this: first, the experimental error margin involved in the initial permeate flux data is high; second, the simplistic approach of the two-component model represents filtration of a complex mixture. However, in all the cases, long-term flux decline (which is more important from a practical point of view) is predicted at high accuracy. The effects of operating conditions are evident from these figures. At a fixed operating pressure, the permeate flux increases with the stirrer speed. At higher stirrer speed, the turbulence in the flow channel is greater, leading to enhancement of the mass transfer coefficient and reduction in gel layer thickness which is responsible for increased permeate flow. For example, at 276 kPa, permeate flux at steady state increases from 2×10^{-6} to $4.5 \times 10^{-6}\ m^3/m^2/s$, as the stirrer speed increases from 600 to 1800 rpm. At fixed stirrer speed, permeate flux is greater at higher transmembrane drops. At higher pressure, two opposite phenomena occur. First, the driving force increases, leading to flux enhancement. Second, the gel layer thickness increases as more solutes are convected towards the membrane, leading to decrease in flux. At lower pressures, the first

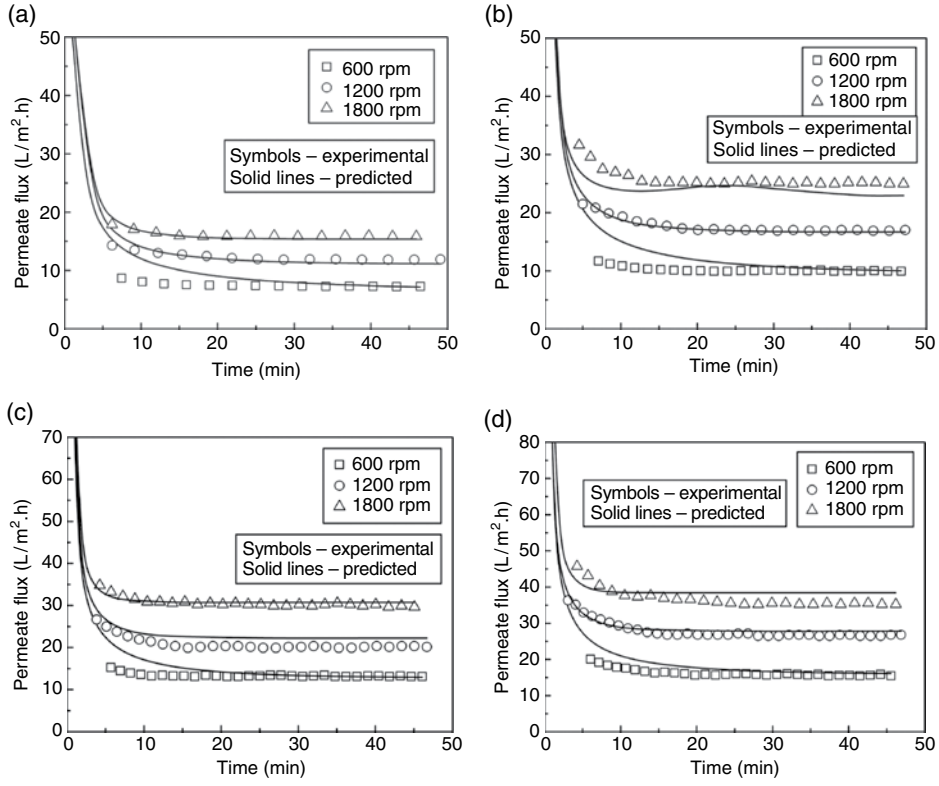

Figure 8.4 Comparison of the experimental and predicted fluxes at different operating conditions. (a) ΔP = 276 kPa; (b) ΔP = 414 kPa; (c) ΔP = 552 kPa; (d) ΔP = 690 kPa. Reproduced from Mondal et al. (2012a) with permission from Elsevier.

phenomenon dominates and a significant flux enhancement is observed. For example, at 1800 rpm, steady-state permeate flux is increased from 4.2×10^{-6} to 7×10^{-6} $m^3/m^2/s$ (67% increase) as pressure drop increases from 276 to 414 kPa. At this stirrer speed, the corresponding values of permeate flux are 9.0×10^{-6} $m^3/m^2/s$ at 552 kPa and 10.5×10^{-6} $m^3/m^2/s$ at 690 kPa. Thus, flux enhancement is reduced at higher pressure because the second phenomenon becomes dominant and the filtration domain approaches the pressure-independent region which is an ideal gel polarised case.

The simulated profiles of stevioside concentration in permeate for various operating conditions are presented in Figure 8.5 which shows a general trend that the stevioside concentration decreases with time. This confirms that the gel layer of HMW solutes acts as a dynamic membrane and retains some amount of stevioside. At higher stirrer speed and fixed transmembrane pressure drop, stevioside concentration is greater. As stirrer speed increases, the gel layer thickness decreases and hence the retention of stevioside by the gel layer is less, leading to increased permeation of stevioside in the permeate. Thus, at higher stirrer speed, it takes

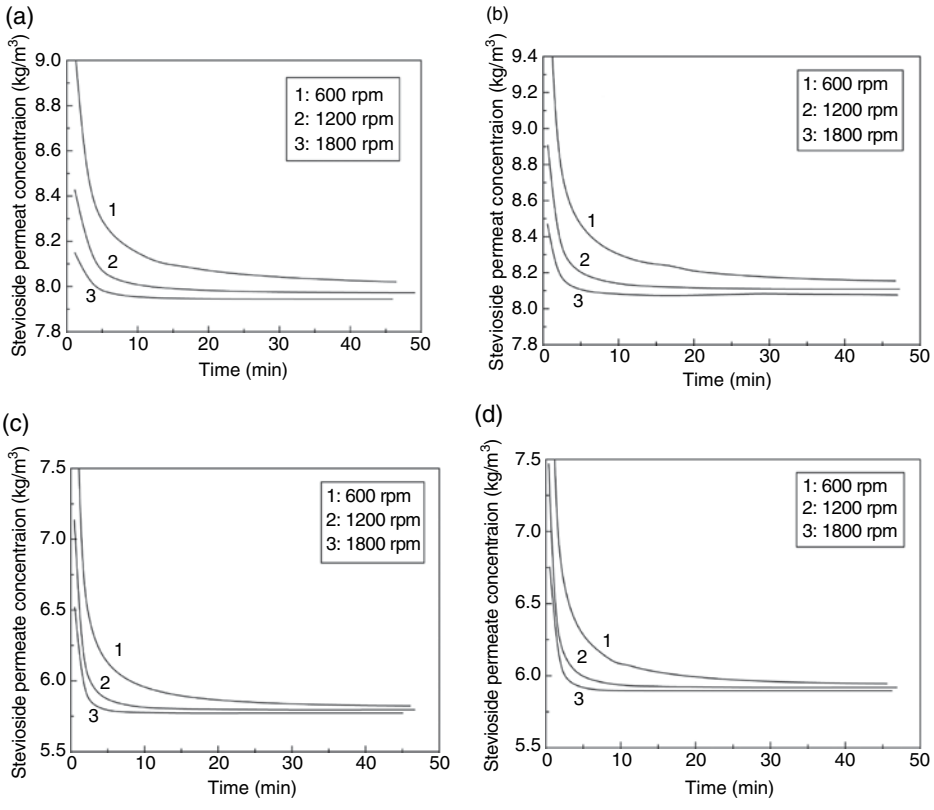

Figure 8.5 Predicted permeate stevioside concentration profiles at different operating conditions. (a) ΔP=276 kPa; (b) ΔP=414 kPa; (c) ΔP=552 kPa; (d) ΔP=690 kPa. Reproduced from Mondal et al. (2012a) with permission from Elsevier.

longer (~25 min) for stevioside concentration to reach the steady state. At lower stirrer speed, stevioside concentration reaches steady state at about 10 min. At higher transmembrane pressure drop, stevioside concentration in permeate decreases. For example, at 1800 rpm, the steady-state stevioside concentration in permeate decreases from 8.1 to 5.8 kg/m^3 as transmembrane pressure drop increases from 276 to 690 kPa. As pressure drop increases, gel layer thickness increases and this layer retains more stevioside (as is evident from γ_g values in Table 8.1). Thus, the permeation of stevioside decreases with pressure drop.

Figure 8.6 represents the growth of gel layer thickness for various operating conditions. It is observed that gel layer thickness decreases with stirrer speed significantly at a fixed transmembrane pressure drop, due to forced convection on increased stirring effect. For example, at 276 kPa, gel layer thickness decreases from 30 μm to 10 μm as stirrer speed is increased from 600 to 1800 rpm. At fixed stirrer speed, gel layer thickness increases with transmembrane pressure drop as more solutes are convected towards the membrane. For example, at 600 rpm, the

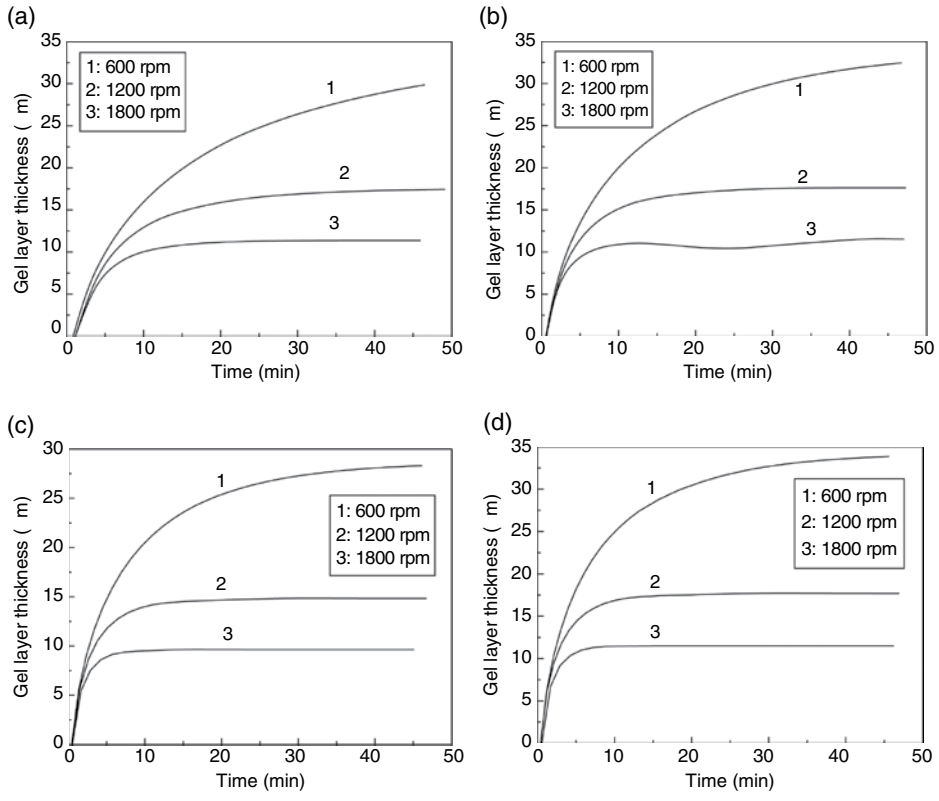

Figure 8.6 Predicted gel layer thickness profiles at different operating conditions. (a) ΔP=276 kPa; (b) ΔP=414 kPa; (c) ΔP=552 kPa; (d) ΔP=690 kPa. Reproduced from Mondal et al. (2012a) with permission from Elsevier.

gel layer thickness increases from 30 μm to about 35 μm as pressure drop increases from 276 to 690 kPa.

Variation of gel layer resistance with operating conditions is shown in Figure 8.7. It is observed from this figure that filtration is gel layer dominated almost from the very beginning. Gel layer resistance grows and becomes steady with time. At higher stirrer speed (comparing curves 3 and 1), gel layer resistance becomes steady earlier. For example, at 690 kPa and 1800 rpm, steady state is reached in 10 min whereas at 1200 rpm, it takes about 30 min to reach the steady state. This is due to quick attainment of steady state at higher turbulence. Comparing curves 1 and 2, it is observed that gel layer resistance becomes almost identical at steady state, indicating the incompressible nature of the gel.

Comparison of percentage recovery of stevioside in the permeate between calculated and experimental data is presented in Figure 8.8. It is observed from this figure that the agreement between these two is within ± 10%. The other relevant properties of the permeate and feed are presented in Table 7.11 (Chapter 7).

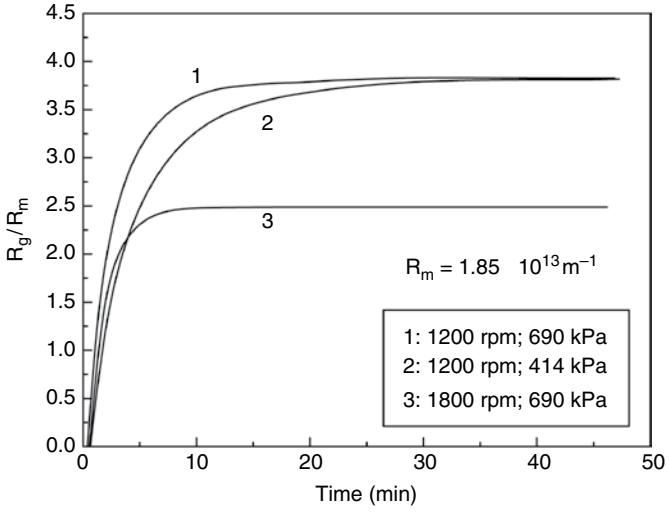

Figure 8.7 Variation of ratio of the gel layer resistance to membrane hydraulic resistance with time. Reproduced from Mondal et al. (2012a) with permission from Elsevier.

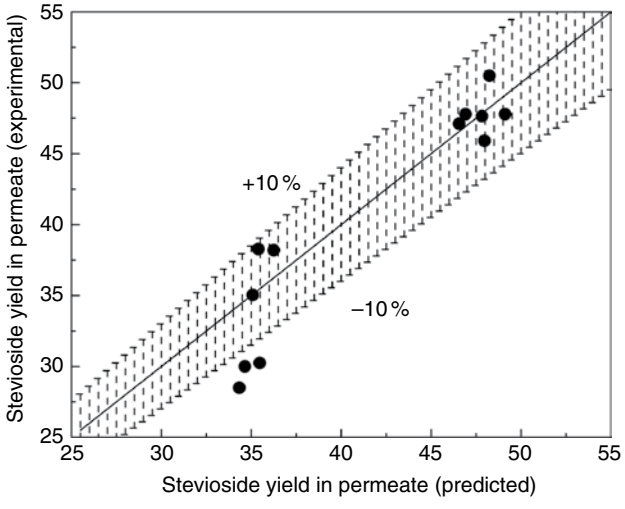

Figure 8.8 Comparison of the predicted and experimental values of stevioside yield at the end of the experiment. Reproduced from Mondal et al. (2012a) with permission from Elsevier.

8.2 Modelling of cross-flow ultrafiltration

Continuous cross-flow configuration is commercially more feasible and economical. An actual fruit juice or plant extract is a complex mixture of gel-forming materials (several HMWsolutes) and other permeable (HMW) solutes. Thus, independent

determination of system and model parameters is extremely difficult. The model is based on the work of De and Bhattacharya (1997). Modelling of both total recycle and batch concentration modes of operation is attempted. The model can be useful for appropriate scaling up of this system.

Similar to the modelling approach of stirred ultrafiltration, the components having molecular weight greater than stevioside (or rebaudioside A) are considered as HMW. It is assumed that HMW solutes are completely retained by the membrane and form a gel layer over the membrane surface. Likewise, the LMW components are freely permeable through the membrane. Stevioside is selectively rejected by the membrane as well as partially retained by the gel layer of HMW solutes that acts like a dynamic membrane. The schematic of the transport phenomena is shown in Figure 8.1.

8.2.1 Steady-state model (total recycle mode)

The experiments were performed in continuous cross-flow mode with total recycle. Thus, the concentration in the feed tank is maintained constant and a steady state is attained for every set of operating conditions. Since HMW solutes are assumed to form a gel layer over the membrane surface, the steady-state permeate flux is expressed by classic film theory (Blatt et al. 1970).

$$v_w = k_0^R \ln\left(\frac{C_{1g}}{C_{1b}}\right) \tag{8.17}$$

where k_0^R is the mass transfer coefficient for HMW solutes in total recycle mode; C_{1b} and C_{1g} are bulk and gel concentration of these solutes, respectively. Mass transfer coefficient for cross-flow set-up can be estimated from the following expression of Sherwood number (Wijmans 1984):

$$Sh = \frac{k_0^R d_e}{D_1} = 1.86\left(Re.Sc.\frac{d_e}{L}\right)^{\frac{1}{3}} \tag{8.18}$$

where d_e is the equivalent diameter of the channel cross-section, equal to $4h$; h is the channel half height, D_1 is diffusivity of gel-forming solutes, Sc is Schmidt number for HMW components ($Sc = \mu/\rho D_1$) and Reynolds number, Re, is defined as $Re = \frac{\rho u d_e}{\mu}$, where u is the cross-flow velocity, ρ and μ are effective solution density and viscosity, respectively. It is assumed that solution density and viscosity are the same as those of an aqueous solution.

In an ideal gel-controlling filtration model, the mass transfer coefficient is independent of transmembrane pressure drop (Trettin and Doshi 1980). However, several earlier literature studies reported that mass transfer coefficient exhibits a

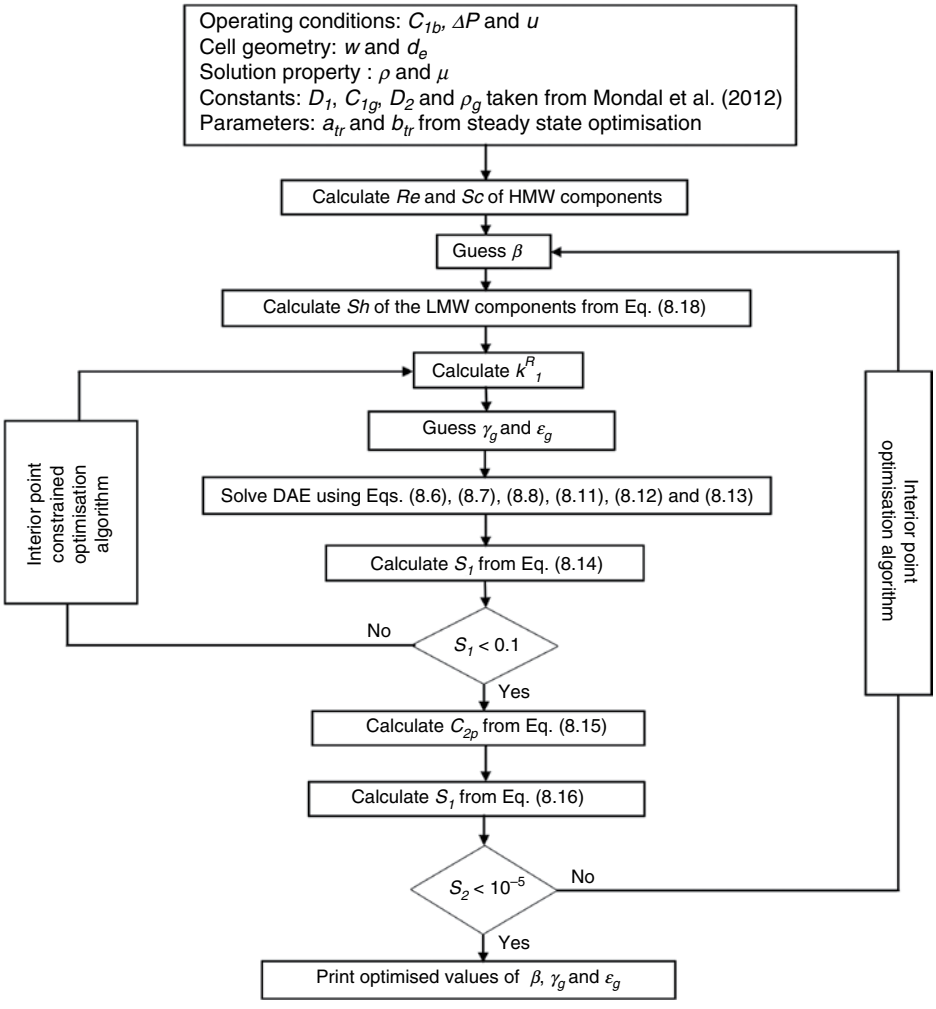

Figure 8.9 Sequence of calculations (algorithm) for optimisation of transient state modelling.

weak dependence on transmembrane pressure drop (Banerjee and De 2012; Johnston and Deen 1999; Mondal et al. 2011; Rai et al. 2007). Following an assumption of linear dependence of mass transfer coefficient with transmembrane pressure drop, $k_1^R = k_0^R(a_{tr} + b_{tr}\Delta P)$, within the range of operating pressure studied (Johnston and Deen 1999), the subsequent analysis for modelling of permeate flux and retention, using the two-component model developed by De and Bhattacharyya (1997), the derivation is performed similar to the case of stirred batch ultrafiltration (see Equations 3–16). The sequence of calculation of for prediction of flux and retention, together with optimisation of the partition coefficient and gel porosity, is illustrated in Figure 8.9. The optimisation routine of interior point algorithm is

invoked following a trust region method (Byrd et al. 2000), by minimising the sum of the squares of the experimental flux and retention separately.

8.2.2 Batch concentration mode (theory)

In this mode of operation, the permeate is not recycled back to the feed tank. As a result, the feed concentration of the stevioside and HMW components increases. The thickness of the gel layer depends on the feed concentration of the gel-forming solutes and transmembrane pressure drop across the membrane. Therefore, with time of operation, the gel layer grows and is responsible for significant decline of the permeate flux compared to the total recycle mode, as the gel layer resistance increases considerably. It can be noted that the total resistance to driving force, in the entire process of ultrafiltration, can be constituted as membrane hydraulic resistance (R_m), gel layer resistance (R_g) and resistance due to boundary layer (R_{bl}):

$$R_T = R_m + R_g + R_{bl} \tag{8.19}$$

Thus, the permeate flux is expressed as:

$$v_w = \frac{\Delta P}{\mu R_T} \tag{8.20}$$

The average permeate flux in total recycle mode is greater than in batch mode at identical operating conditions. Thus, it can be interpreted that:

$$R_T^R < R_T^b \tag{8.21}$$

where R_T^R and R_T^b are total resistance in total recycle and batch mode, respectively. Since R_g in total recycle mode is less than that of batch mode, it can be concluded that:

$$R_{bl}^R < R_{bl}^b \tag{8.22}$$

where R_{bl}^R and R_{bl}^b are boundary layer resistance in total recycle and batch mode, respectively. As mass transfer coefficient is inversely proportional to boundary layer resistance, it assumes a higher value in the batch concentration mode.

$$k_1^b < k_1^R \tag{8.23}$$

The expression of mass transfer coefficient for the total recycle mode has already been described in Equation (8.18). However, it must be observed that the effective channel thickness ($2h$) decreases, due to deposition of gel layer over the membrane

surface. Since the cross-sectional area to flow is reduced, the cross-flow velocity through the channel (u) increases. Rearranging the expression in Equation (8.18), the mass transfer coefficient (k_0^b) in batch mode can be represented as:

$$k_0^b = \left(\frac{uD_1^2}{d_e L} \right)^{\frac{1}{3}} \tag{8.24}$$

As already shown, in batch mode, the ratio $\frac{u}{d_e}$ increases compared to total recycle mode. Hence, the following inequality holds:

$$k_0^b > k_0^R \tag{8.25}$$

Thus, the mass transfer coefficient in batch mode has a different numerical value compared to total recycle mode. Now, similar to total recycle mode, a pressure correlation factor has to be incorporated to account for variation in permeate flux with transmembrane pressure drop:

$$k_1^b = k_0^b (a_b + b_b \Delta P) \tag{8.26}$$

Considering Equations (8.25) and (8.26), it can be concluded that the constant parameters a_b and b_b will be less than a_{tr} and b_{tr} respectively.

Considering an overall material balance, the following equation is obtained:

$$\frac{d}{dt}(\rho_f V) = -v_w A_m \rho_p \tag{8.27}$$

where ρ_f and ρ_p are densities in feed and permeate streams, V is the feed volume and A_m is the effective membrane area. Assuming $\rho_f \simeq \rho_p$, the above equation is modified as:

$$\frac{dV}{dt} = -v_w A_m \tag{8.28}$$

Using overall species balance of gel-forming components, the following equation is obtained:

$$\frac{d}{dt}(C_{1b} V) = -v_w A_m C_{p1} \tag{8.29}$$

Since concentration of the gel-forming material in the permeate is zero ($C_{p1}=0$) (Cheryan 1998), the above equation reduces to a simple algebraic equation:

$$C_{1b}V = C_{01}V_0 \tag{8.30}$$

using initial boundary condition as $C=C_{01}$ and $V=V_0$ at $t=0$. Rearranging Equation (8.30), we get:

$$C_{1b} = \frac{C_{01}V_0}{V} \tag{8.31}$$

Using overall species balance of stevioside, the following equation is obtained:

$$C_{2b}\frac{dV}{dt} + V\frac{dC_{2b}}{dt} = -v_w A_m C_{p2} \tag{8.32}$$

with the initial conditions as $C=C_{02}$ and $V=V_0$ at $t=0$.

It may be noted that as time of operation proceeds, the effective channel thickness decreases by deposition of gel layer and is quantified as:

$$d_e^t = d_e - 2H(t) \tag{8.33}$$

Consequently, the cross-flow velocity u^t inside the channel changes as:

$$u^t = \frac{Q}{w \times (d_e^t / 2)} \tag{8.34}$$

where w is the width of the channel.

The above expressions of equivalent diameter and cross-flow velocity within the channel have been utilised to evaluate the mass transfer coefficient k_0^b. Using Equations (8.6, 8.7, 8.8, 8.11, 8.12 and 8.13) and combining Equations (8.28, 8.31, 8.32, 8.33 and 8.34), a system of DAE has been set up involving five state variables: H, C_{1b}, C_{2b}, V and C_{2m}. The system of stiff-coupled DAE involves a state-dependent mass matrix. The solution is based on the numerical differentiation formulae with Gears method, through a MATLAB function *ode15s* (Shampine and Reichelt 1997; Shampine et al. 1999).

Similar to the total recycle mode, two separate non-linear constrained multi-objective optimisation functions have been implemented to minimise the square of error of the permeate flux and stevioside permeate concentration. The parameters a_b and b_b are determined by the flux optimisation routine, while the parameter γ_g is determined by the permeate concentration optimisation routine.

A cross-flow ultrafiltration set-up was used for clarification of Stevia extract. The details of the set-up were described in Chapter 7. Cross-flow ultrafiltration experiments under total recycle mode were performed using the operating pressure difference as 276, 414, 552 and 690 kPa. The cross-flow rates were 60, 80, 100 and

120 L/h. Experiments under batch concentration mode were undertaken at 276, 414 and 552 kPa pressure and 100 L/h cross-flow rate.

In this study, there are altogether 10 parameters (R_{r2}, D_1, C_{1g}, $D_{2,}$ ρ_g, a_{tr}, b_{tr}, γ_g, ε_g and β). The first is independently determined as described in the previous section. The values of D_1, C_{1g}, ρ_g and D_2 are already obtained (described in the previous section). These are 3.7×10^{-11} m^2/s, 51.5 kg/m^3, 1550 kg/m^3 and 2.0×10^{-10} m^2/s, respectively. Both D_1 and C_{1g} are obtained by minimising the sum of square of error of the experimental and predicted steady-state flux values, while D_2 and ρ_g are determined by minimising the sum of square of error of the experimental and predicted transient flux values. Both these algorithms employ non-linear constrained optimisation. The parameters a_{tr} and b_{tr} are estimated from the steady-state analysis and the other three parameters, γ_g, ε_g and β, are estimated from the transient analysis. The value of C_{1b} and C_{2b} are 6.3 and 15.75 g/L, respectively. The complete list of parameters involved in this study is presented in Table 8.2.

8.3 Steady state

As described earlier, the steady-state permeate flux of pretreated Stevia extract can be calculated using the modified film theory. The comparison between the calculated steady-state permeate flux values and the experimental data is within ± 15% (Mondal et al. 2012b).

8.4 Transient state

As discussed earlier, the profiles of transient flux decline and concentration of stevioside in the permeate have been calculated for the procedure described earlier. It may be mentioned that this optimisation procedure was adopted for different transmembrane pressure drops, separately. It is observed that the parameters β and ε_g vary in a narrow range over ΔP and the average values are reported. These are $(4.55 \pm 0.47)\times10^{19}$ m^{-2} and 0.56 ± 0.03, respectively. The distribution coefficient γ_g is observed to vary with transmembrane drop and is presented in Table 8.3. As discussed earlier, γ_g represents the partition coefficient of stevioside concentration in the bulk–gel layer interface and the gel layer. So, at higher transmembrane pressure drops, the gel layer retains more stevioside. Thus, it is expected that permeation of stevioside is lower at higher transmembrane pressure drops.

With the estimated parameter values as outlined in Figure 8.10, Equations (8.22, 8.23, 8.27, 8.28 and 8.29) are solved to obtain the profiles of permeate flux, stevioside concentration, gel layer thickness and gel layer resistances.

Figure 8.10 represents the permeate flux decline for various operating conditions. As time of filtration progresses, the gel layer thickness increases, leading to an increase in gel layer resistance and hence the permeate flux decreases. Finally, due to forced convection imposed by the cross-flow of the feed, the growth

Table 8.2 Details of the parameters estimated. Reproduced from Mondal et al. (2012b) with permission from Elsevier.

Parameter	Type	Value	Method of determination
D_1	Physical property of the solution mixture	3.7×10^{-11} m^2/s	Minimising the sum of square of error of the experimental and predicted steady-state flux values
D_2		2.0×10^{-11} m^2/s	Constrained non-linear optimisation by minimising the sum of square of error of the experimental and predicted transient flux values
C_{1g}	Gel layer characteristics	51.5 kg/m^3	Minimising the sum of square of error of the experimental and predicted steady state flux values
ε_g		0.56	Simultaneous optimisation of the experimental flux and stevioside permeate concentration values with the predicted ones
ρ_g		1550 kg/m^3	Constrained non-linear optimisation by minimisingthe sum of square of error of the experimental and predicted transient flux values
β	Gel layer resistance model parameter	4.55×10^{19} m^{-2} (average value in total recycle mode)	Simultaneous optimisation of the experimental flux and stevioside permeate concentration values with the predicted ones
γ_g	Partition coefficient specific to operating conditions, solute-solution system	Reported in Table 8.3	
R_{r2}	Membrane feature	0.1	Measured experimentally
a_{tr}	Adjustable parameter to relate the effect of pressure in gel layer controlling ultrafiltration	0.35	Optimisation of the experimental flux profile with change in pressure drop
a_b		0.22	
b_{tr}		1.22×10^{-6} Pa^{-1}	
b_b		2.22×10^{-7} Pa^{-1}	

of gel layer thickness is arrested and a steady state is attained. For example, it is observed from Figure 8.10 that the steady state is attained after 10 min. At higher cross-flow rate, the thickness of the gel layer at the steady state is less due to enhanced forced convection, resulting in higher steady-state permeate flux. For

Table 8.3 Values of the partition coefficient with pressure in total recycle as well as batch mode. Reproduced from Mondal et al. (2012b) with permission from Elsevier.

TMP (kPa)	γ_g	
	Total recycle mode	Batch concentration mode
276	2.25 ± 0.11	3.51 ± 0.17
414	3.14 ± 0.16	4.53 ± 0.27
552	3.88 ± 0.20	5.53 ± 0.28
690	6.13 ± 0.35	–

TMP, transmembrane pressure.

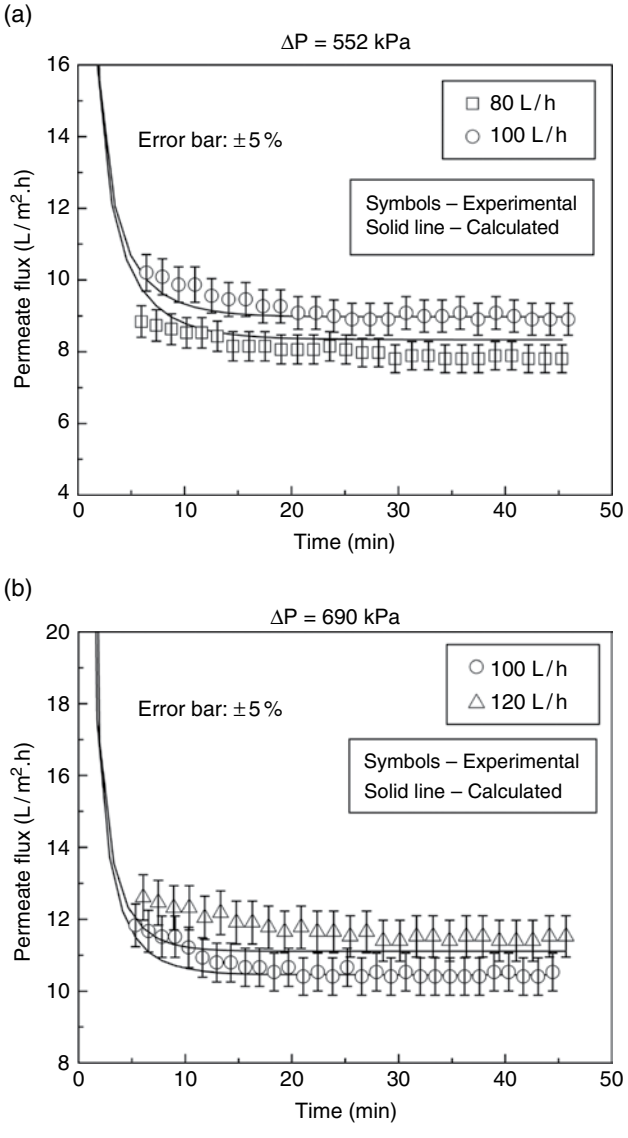

Figure 8.10 Transient flux profile of the experimental as well as the predicted fluxes at different transmembrane pressure drop and cross-flow rates. (a) ΔP = 552 kPa; (b) ΔP = 690 kPa. Reproduced from Mondal et al. (2012b) with permission from Elsevier.

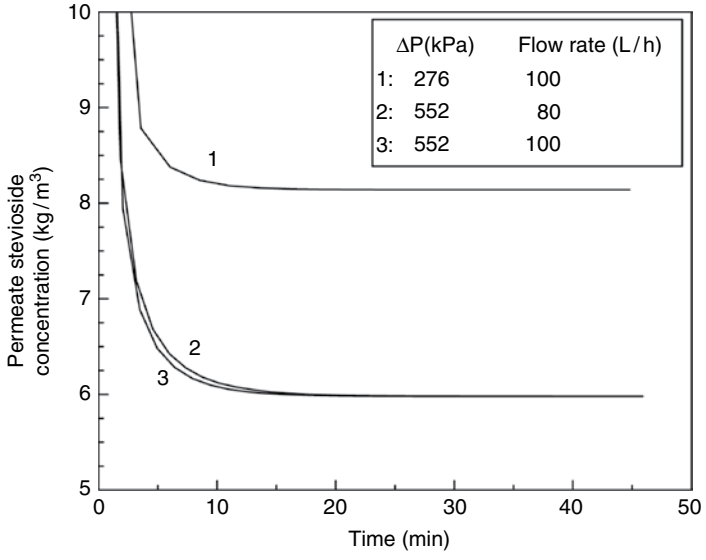

Figure 8.11 Transient profiles of stevioside at different operating conditions. Reproduced from Mondal et al. (2012b) with permission from Elsevier.

Table 8.4 Comparison of the stevioside recovery (in percentage) values. Reproduced from Mondal et al. (2012b) with permission from Elsevier.

TMP (kPa)	80 L/h		100 L/h		120 L/h	
	Predicted	Experiment	Predicted	Experiment	Predicted	Experiment
276	51.6	58.0	51.4	49.0	51.3	49.0
414	43.0	45.0	42.7	43.3	42.5	40.4
552	39.3	40.5	39.0	39.7	38.9	37.3
690	29.5	29.7	29.3	31.1	29.1	27.5

TMP, transmembrane pressure.

example, at 552 kPa, the permeate flux increases from 8 to 9 L/m^2.h (12.5 % increase) as the cross-flow rate increases from 80 to 100 L/h. At 690 kPa, the permeate flux increases from 10 to 11.5 L/m^2.h (15% increase) with increase in cross-flow rate from 100 to 120 L/h.

The profiles of stevioside concentration in the permeate are shown in Figure 8.11 for different operating conditions. As represented in Table 8.4, the predicted and experimental steady-state recovery values are in close agreement. A general trend is observed from the curves of Figure 8.11 that the stevioside concentration in the permeate decreases with time and finally reaches a steady state after about 10 min. This time coincides with that required to attain the steady-state permeate flux. The

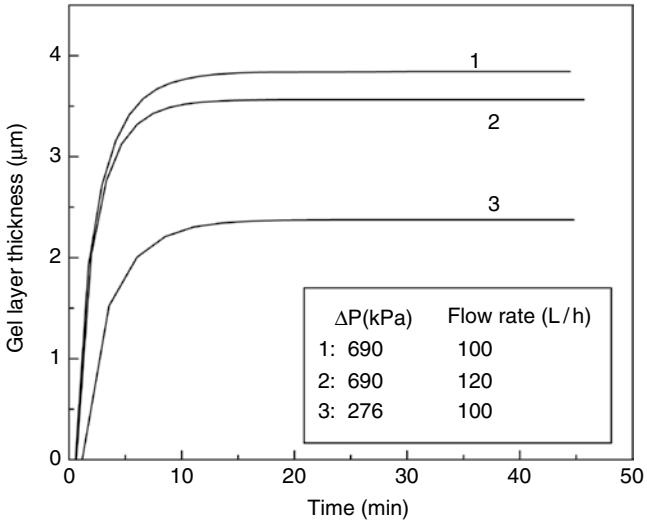

Figure 8.12 Predicted profiles of gel layer thickness. Reproduced from Mondal et al. (2012b) with permission from Elsevier.

effect of transmembrane pressure drop is also observed from curves 1 and 2. The steady-state concentration of stevioside in permeate is greater at lower operating pressure (see Table 8.4).

As discussed earlier, the limiting step of transport of stevioside in the permeate is its transport through the gel layer which is dictated by the partition coefficient γ_g. The value of this parameter increases with transmembrane pressure drop. A higher value of this parameter indicates that the gel layer arrests more stevioside, leading to lower concentrations of it in the permeate. The value of this parameter is 2.3 and 3.7 at 276 and 552 kPa. Thus, stevioside concentration is greater in permeate at lower transmembrane pressure drops. Since the partition coefficient is a function of transmembrane pressure drop only, at 552 kPa pressure γ_g is constant and the amount of stevioside in the gel layer remains the same. Therefore, its concentration profile in the permeate does not change significantly with cross-flow rate (from curves 2 and 3) at 552 kPa pressure drop.

Figure 8.12 shows the profile of gel layer thickness with different operating conditions. The effects of transmembrane pressure drop should be clear from curves 2 and 3. At higher transmembrane pressure drop, the gel layer thickness is greater due to enhanced convection of gel-forming solutes towards the membrane surface. Thus, at the steady state and 100 L/h cross-flow rate, the gel layer thickness increases from 2.4 to 3.9 μm as the transmembrane pressure drop increases from 276 to 690 kPa. The effect of cross-flow rate is observed by comparing curves 1 and 2. At higher cross-flow rate, due to forced convection of the retentate stream, the growth of the gel layer is arrested and its thickness is less. As the cross-flow rate increases from 100 to 120 L/h, the gel layer thickness is reduced from 3.9 to 3.5 μm.

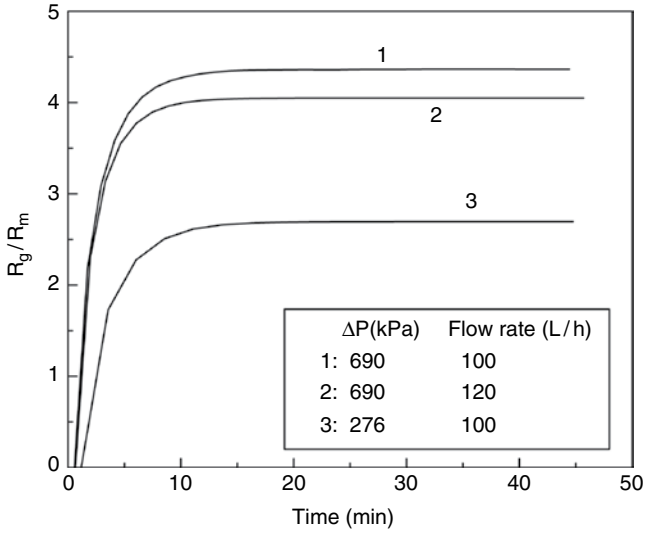

Figure 8.13 Profiles of gel layer to membrane resistance for different operating conditions. Reproduced from Mondal et al. (2012b) with permission from Elsevier.

The profile of gel layer resistance with operating conditions is shown in Figure 8.13. Since gel layer resistance is directly proportional to gel thickness, it shows a similar trend to gel layer thickness. Gel layer resistance is greater at higher transmembrane pressure drops and less at higher cross-flow rates. It is observed from this figure that the gel layer resistance at steady state is about four times the membrane resistance.

8.4.1 Batch concentration mode

As explained earlier, Equations (8.28, 8.29, 8.30, 8.31 and 8.32) are solved simultaneously to obtain the profiles of permeate flux, stevioside concentration in permeate, volume concentration factor, bulk concentration of stevioside and HMW solute, gel layer thickness and gel layer resistance. Three parameters, a_b, b_b and γ_g, are evaluated during this calculation, as these parameters depend on the mode of operation. The values of other parameters are considered as used in the analysis of total recycle mode. As observed in the case of total recycle mode, γ_g values are mainly a function of transmembrane pressure drop and are independent of cross-flow rate. Variation of γ_g with transmembrane pressure drop in this case is shown in Table 8.3.

Profiles of permeate flux at various transmembrane pressure drops are presented in Figure 8.14. This figure shows that the permeate flux declines sharply within 100 min of operation and slowly thereafter. The permeate flux is greater at higher

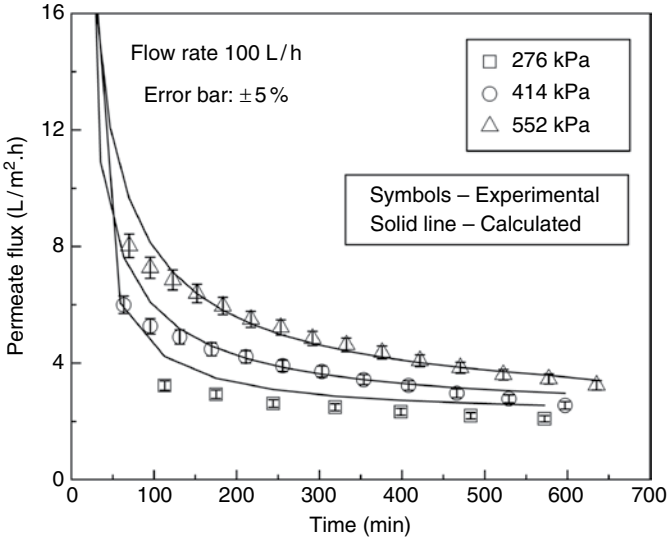

Figure 8.14 Profile of permeate flux at different transmembrane pressure drops. Reproduced from Mondal et al. (2012b) with permission from Elsevier.

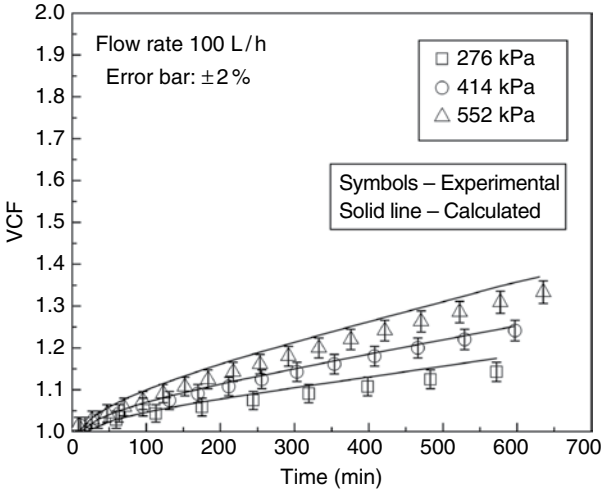

Figure 8.15 Variation of VCF with time. Reproduced from Mondal et al. (2012b) with permission from Elsevier.

transmembrane pressure drops. The model calculations show excellent matching with the experimental data. In the batch concentration mode, since the filtrate is withdrawn, the feed volume is reduced. Profiles of volume concentration factor are shown in Figure 8.15. At higher transmembrane pressure drops, as more filtrate is

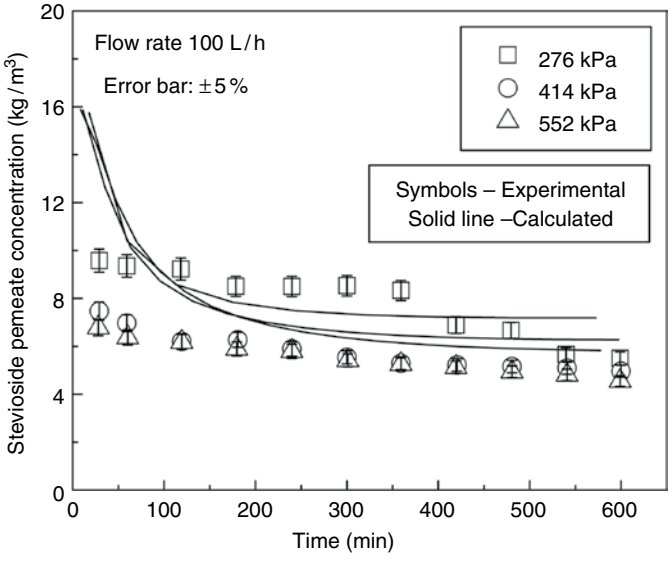

Figure 8.16 Variation of stevioside permeate concentration with time. Reproduced from Mondal et al. (2012b) with permission from Elsevier.

taken out, this leads to higher values of VCF. At 552 kPa pressure, VCF attains a value of 1.4 after 10 h of operation. It is observed from this figure that the calculated profiles agree closely with the experimental data.

Recovery of stevioside in the permeate was calculated for various operating conditions and the comparison of experimental and calculated values is presented in Table 8.3. It is observed from this table that the calculated values agree well with the experimental results. The concentration profile of stevioside in the permeate for different pressures is presented in Figure 8.16. As observed for the total recycle mode, the stevioside concentration in the permeate is greater at lower transmembrane pressure drops. Profiles of bulk concentration of HMW solute and stevioside are shown in Figure 8.17. As more solvent is drawn out, bulk concentration of HMW solutes increases due to reduction of volume. Bulk concentration is greater at higher operating pressures due to filtering out of more solvent. Variation of gel layer thickness with transmembrane pressure drop is shown in Figure 8.18. The curves show the usual trends, i.e. gel layer thickness increases with transmembrane pressure drop. Comparing this to the corresponding figure in total recycle mode (Figure 8.12), it can be observed that gel layer thickness does not attain a steady state in this case, but rather grows with time.

Since this mode is a batch operation, the steady state is never attained and the gel layer thickness grows slowly. However, gel layer thickness increases with transmembrane pressure drop as expected. Gel thickness in this case is quite large, about 200 μm after 10 h of operation at 552 kPa and 100 L/h, whereas that in Figure 8.13

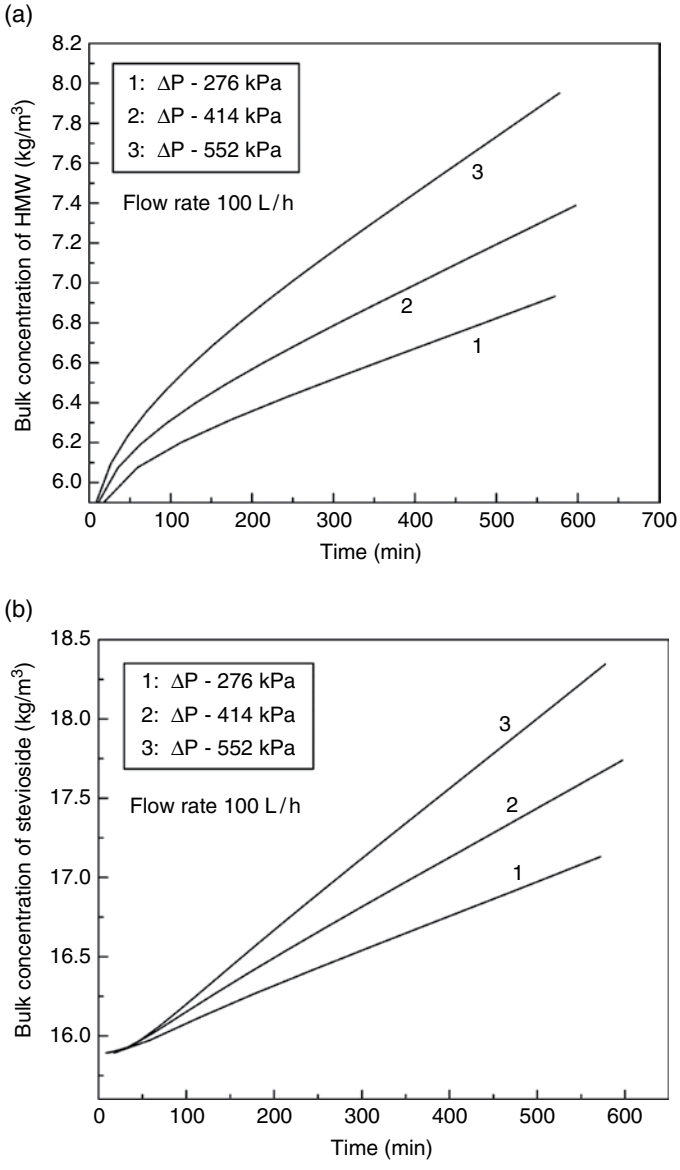

Figure 8.17 Variation of bulk concentration with time. (a) HMW components. (b) Stevioside.

is only 4.4 μm. This is because in total recycle mode, steady state is attained within 10 min. Gel layer resistance increases with time continuously as it is a batch operation. Gel layer resistance is greater at higher transmembrane pressure drops as the gel thickness increases with pressure. It is also noted that gel layer resistance can be as high as 100 times the membrane resistance after 10 h of operation.

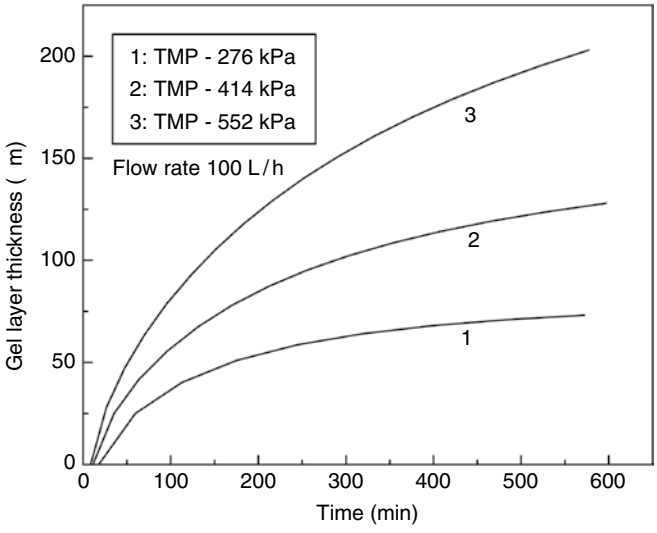

Figure 8.18 Variation of the gel layer thickness with time. Reproduced from Mondal et al. (2012b) with permission from Elsevier.

The gel layer controlling model for UF of Stevia extract for both total recycle and batch concentration modes was successfully applied in a rectangular filtration cell. Prediction of permeate flux and permeate concentration in operating mode, steady and transient conditions agreed well with the experimental data. In the total recycle mode, the effect of cross-flow is prominent due to less concentration polarisation as the feed concentration remains constant and gel layer thickness was between 2.5 to 4 μm for various operating conditions. In batch mode, gel layer thickness was between 75 to 200 μm after 10 h as the bulk concentration increases simultaneously. The parameter γ_g dictated the concentration of stevioside in the permeate, which increases with pressure drop. At higher transmembrane pressure drops, the gel holds more stevioside. Thus, stevioside recovery is higher at lower transmembrane pressure drops. The proposed model can be used to scale up the efficient filtration of Stevia extract and recovery of stevioside.

Nomenclature

a_b	Pressure-dependent coefficient in mass transfer coefficient relation for batch mode in cross-flow filtration
A_m	Membrane area, m^2
a_{tr}	Pressure-dependent coefficient in mass transfer coefficient relation for total recycle mode in cross-flow filtration, similar to Equation (8.3)
b	Optimisation parameter in the mass transfer coefficient k_0, kPa^{-1}
b_b	Pressure-dependent coefficient in mass transfer coefficient relation for total recycle mode in cross-flow filtration, in Equation (8.24), Pa^{-1}

b_{tr}	Pressure-dependent coefficient in mass transfer coefficient relation for total recycle mode in cross-flow filtration, similar to Equation (8.3), Pa^{-1}
C	Concentration, kg/m^3
C_{01}	Initial concentration of component 1 (HMW), kg/m^3
C_1	Local concentration of gel-forming solutes in the boundary layer, kg/m^3
C_{1b}	Bulk concentration of component 1 (HMW), kg/m^3
C_{1g}	Gel layer concentration of component 1 (HMW), kg/m^3
C_2	Concentration of component 2 (stevioside), kg/m^3
C_{2b}	Bulk concentration of component 2 (stevioside), kg/m^3
C_{2m}	Membrane surface concentration of component 2 (stevioside), kg/m^3
C_{2p}	Permeate concentration of component 2 (stevioside), kg/m^3
$\overline{C_{2p}}$	Average concentration of component 2 (stevioside) in permeate, kg/m^3
$C_{2p,cal}$	Predicted permeate concentration of component 2 (stevioside), kg/m^3
$C_{2p,exp}$	Experimental permeate concentration of component 2 (stevioside), kg/m^3
D_1	Diffusivity of the component 1 (HMW) in water, m^2/s
D_2	Diffusivity of component 2 (stevioside), m/s^2
d_e	Equivalent channel diameter, m
H	Gel layer thickness, m
k_0	Modified mass transfer coefficient given by $k_0 = k_1(b\Delta P)$, m/s
k_0^b	Mass transfer coefficient without pressure correction in batch mode (of HMW components), m/s
k_0^R	Mass transfer coefficient without pressure correction in total recycle mode (of HMW weight components), m/s
k_1	Mass transfer coefficient of component 1 (HMW), m/s
k_1^b	Mass transfer coefficient in batch mode, m/s
k_1^R	Mass transfer coefficient in total recycle mode, m/s
k_2	Mass transfer coefficient of component 2 (stevioside), m/s
L	Length of the channel, m
M_2	Molecular weight of component 2 (stevioside), g/mol
N_{exp}	Number of experiments
N_j	Number of experimentally measured data points at j^{th} experiment
N_p	Number of experiments at a particular transmembrane pressure drop
r	Radius of the stirred cell, m
R	Universal gas constant, J/mol/K
R_{bl}	Boundary layer resistance, m^{-1}
R_{bl}^b	Boundary layer resistance in batch mode, m^{-1}
R_{bl}^R	Boundary layer resistance in total recycle mode, m^{-1}
Re	Reynolds number
R_g	Gel layer resistance, m^{-1}
R_m	Membrane resistance, m^{-1}
R_{r2}	Real retention of component 2 (stevioside) by the membrane
R_T	Total resistance, m^{-1}
R_T^b	Total resistance in batch mode, m^{-1}
R_T^R	Total resistance in total recycle mode, m^{-1}
S_0	Relative sum of squares of error in Equation (8.4)

S_1 Relative sum of squares of error in Equation (8.14)
S_2 Relative sum of squares of error in Equation (8.16)
Sc Schmidt number
Sh Sherwood number
T Temperature, K
t Time of experiment, s
u Cross-flow velocity, m/s
V Volume, m^3
V_0 Initial volume in batch mode, m^3
v_w Permeate flux, $m^3/m^2/s$
$v_{w,cal}$ Predicted permeate flux, $m^3/m^2/s$
$v^i_{w,cal}$ Calculated permeate flux of the i^{th} experiment, $m^3/m^2/s$
$v_{w,exp}$ Experimental permeate flux, $m^3/m^2/s$
$v^i_{w,exp}$ Experimental permeate flux of the i^{th} experiment, $m^3/m^2/s$
w Width of the channel, m
y Co-ordinate normal to membrane surface, m

Greek symbols

α Parameter in the definition of β, m/kg
β Optimisation parameter in gel layer resistance, m^{-2}
γ_g Distribution coefficient
δ Thickness of mass transfer boundary layer as shown in Figure 8.1, m
ΔP Transmembrane pressure drop, kPa
$\Delta\pi$ Osmotic pressure difference, kPa
ε_g Gel layer porosity
π_m Osmotic pressure at the membrane surface, kPa
π_p Osmotic pressure at the permeate side, kPa
ρ Density, kg/m^3
ρ_g Gel layer density, kg/m^3
ω Stirrer speed, rad/s
μ Viscosity of the bulk solution, Pa.s

References

Banerjee, S., De, S. (2012) An analytical solution of Sherwood number in a stirred continuous cell during steady state ultrafiltration. J Membr Sci 389, 188–196.

Bhattacharjee, S., Chen, J.C., Elimelech, M. (2001) Coupled model of concentration polarization and pore transport in crossflow nanofiltration. AIChE J 47, 2733–2745.

Blatt, W.F., Dravid, A., Michaels, A.S., Nelsen, L. (1970) Solute polarization and cake formation in membrane ultrafiltration: causes, consequences, and control techniques. In: Flinn, J.E. (ed) *Membrane Science and Technology*. New York: Plenum Press, pp47–94.

Bouchard, C.R., Carreau, P.J., Matsuura, T., Sourirajan, S. (1994) Modeling of ultrafiltration: predictions of concentration polarization effects. J Membr Sci 97, 215–229.
Bungay, P.M., Lonsdale, H.K., de Pinho, M.N. (1986) *Synthetic Membranes: Science, Engineering and Applications*. NATO Scientific Affairs Division. Dordrecht: Reidel.
Byrd, R.H., Gilbert, J.C., Nocedal, J. (2000) A trust region method based on interior point techniques for nonlinear programming. Mathem Progr 89, 149–185.
Cheryan, M. (1998) *Ultrafiltration and Microfiltration Handbook*. Lancaster: Technomic.
Das, C., De, S. (2009) Steady state modeling for membrane separation of pretreated liming effluent under cross flow mode. J Membr Sci 338, 175–181.
De, S., Bhattacharya, P.K. (1997a) Prediction of mass transfer coefficient with suction in the application of reverse osmosis and ultrafiltration. J Membr Sci 128, 119–131.
De, S., Bhattacharya, P.K. (1997b) Modeling of ultrafiltration process for a two component aqueous solution of low and high (gel-forming) molecular weight solutes. J Membr Sci 136, 57–69.
De, S., Bhattacharjee, S., Sharma, A., Bhattacharya, P.K. (1997) Generalized integral and similarity solutions of the concentration profiles for osmotic pressure controlled ultrafiltration. J Membr Sci 130, 99–121.
Fimbres-Weihs, G.A., Wiley, D.E. (2007) Numerical study of mass transfer in three-dimensional spacer-filled narrow channels with steady flow. J Membr Sci 306, 228–243.
Fuh, W.S., Chiang, B.H. (1990) Purification of Stevioside by membrane and ion exchange processes. J Food Sci 55, 1454–1457.
Gekas, V., Hallstrom, B. (1987) Mass transfer in the membrane concentration polarization layer under turbulent cross flow. I. Critical literature review and adaptation of existing Sherwood correlations to membrane operations. J Membr Sci 80, 153–170.
Ho, W.S.W., Sirkar, K.K. (1992) Membrane Handbook. New York: Chapman and Hall.
Johnston, S.T., Deen, W.M. (1999) Hindered convection of proteins in agarose gels. J Membr Sci 153, 271–279.
Kleinstreuer, C., Paller, M.S. (1983) Laminar dilute suspension flows in plate-and-frame ultrafiltration units. AIChE J 29, 529–533.
Minnikanti, V.S., DasGupta, S., De, S. (1999) Prediction of mass transfer coefficient with suction for turbulent flow in cross flow ultrafiltration. J Membr Sci 157, 227–239.
Mondal, S., Cassano, S., Tasselli, F., De, S. (2011) A generalized model for clarification of fruit juice during ultrafiltration under total recycle and batch mode. J Membr Sci 366, 295–303.
Mondal, S., Chhaya, C., De, S. (2012a) Prediction of ultrafiltration performance during clarification of Stevia extract. J Membr Sci 396, 138–148.
Mondal, S., Chhaya, C., De, S. (2012b) Modeling of cross flow ultrafiltration of Stevia extract in a rectangular cell. J Food Eng 112, 326–337.
Opong, W.S., Zydney, A.L. (1991) Diffusive and convective protein transport through asymmetric membranes. AIChE J 37, 1497–1510.
Porter, M.C. (2005) *Handbook of Industrial Membrane Technology*. New Delhi: Crest Publishing.
Prabhavathy, C., De, S. (2001) Modeling and transport parameters during nanofiltration of degreasing effluent from a tannery. Asia Pac J Chem Eng 6, 101–109.
Rai, P., Majumdar, G.C., DasGupta, S., De, S. (2007) Modeling of permeate flux decline of synthetic fruit juice and mosambi juice (Citrus sinensis (L.) Osbeck) in stirred continuous ultrafiltration. LWT Food Sci Technol 40, 1765–1773.

Ranganna, S. (1986) *Hand Book of Analysis and Quality Control for Fruit and Vegetable Products*. New Delhi: Tata McGraw-Hill.

Rautenbach, R., Albrecht, R. (1986) *Membrane Processes*. New York: John Wiley & Sons, Inc.

Sarkar, B., Dasgupta, S., De, S. (2008) Pulsed electric field enhanced ultrafiltration of synthetic and fruit juice. Sep Purif Technol 63, 582–591.

Shampine, L.F., Reichelt, M.W. (1997) The MATLAB ODE Suite. SIAM J Sci Comp 18, 1–22.

Shampine, L.F., Reichelt, M.W., Kierzenka, J.A. (1999) Solving Index-1 DAE's in MATLAB and Simulink. SIAM Rev 41, 538–552.

Silva, F.V., Bergamasco, R., Andrade, C.M.G., et al. (2007) Purification process of stevioside using zeolites and membranes. Int J Chem React Eng 5, A40.

Trettin, D.R., Doshi, M.R. (1980) Ultrafiltration in an unstirred batch cell. Ind Eng Chem Fundam 19, 189–194.

Van den Berg, G.B., Racz, I.G., Smolders, C.A. (1989) Mass transfer coefficients in cross flow ultrafiltration. J Membr Sci 47, 25–51.

Vanneste, J., Sotto, A., Courtin, C.M., et al. (2011) Application of tailor-made membranes in a multi-stage process for the purification of sweeteners from Stevia Rebaudiana. J Food Eng 103, 285–293.

Wijmans, J.G. (1984) The mass transfer coefficient in ultrafiltration. PhD thesis. Twente University of Technology, Enschede, Netherlands.

Zhang, S.Q., Kumar, A., Kutowy, O. (2000) Membrane based separation scheme for processing sweeteners from Stevia leaves. Food Res Int 33, 617–620.

9

Enhancement of stevioside recovery by diafiltration

The aim of ultrafiltration of natural Stevia extract is removal of cell debris, proteins and other haze-forming materials in order to achieve maximum permeation of stevioside and rebaudioside (Leung and Foster 1996; Reis et al. 2009). Achieving the desired recovery and purity of a particular component during membrane filtration is essential. Often, due to concentration polarisation and membrane fouling, the permeate quality decreases. Multiple filtration of the retentate is often useful to extract the maximum amount of stevioside (or any other product) (Zhang et al. 2000).

As discussed earlier, a single stage of ultrafiltration is capable of recovering about 50% steviosides (Chhaya 2012) for a particular set of operating conditions. For effective removal of solute from feed, fresh solvent may be added to the feed to replace the permeate volume and such a diluted solution may be subjected to further ultrafiltration. This process of dilution and reconcentration is referred to as diafiltration. This might be done in several batches of ultrafiltration processes (multiple stage diafiltration), ensuring that the volume of the feed is constant for all stages by diluting with distilled water (constant volume diafiltration) (Fuh and Chiang 1990). This is analogous to the washing of filter gel to remove soluble components. This process can effectively extract more steviol glycosides from the feed solution, thus enhancing the recovery of these compounds from feed. Diafiltration is of interest to researchers in the realm of membrane separations and various models have been developed to predict the performance of diafiltration processes (Sen et al. 2011; Takaci et al. 2009). Various important applications of diafiltration are presented below:

- Improving solvent extraction of benzylpencillin, erythromycin and madmycin (Li et al. 2004).

Stevioside: Technology, Applications and Health, First Edition.
Sirshendu De, Sourav Mondal and Suvrajit Banerjee.

- Increasing galacturonic acid content of pectin and removal of flavonoids, polyphenols and carotenoids, which are impurities in pectin products (Cho et al. 2003).
- Separation of two dyes, solvent yellow 7 and brilliant blue R, and also separation of the intermediate of a new drug candidate (API-INT) and its oligomeric impurities (Sereewatthanawut et al. 2010).
- Extraction of *Agaricus bisporus* tyrosinase in the presence of ascorbate (Rescigno et al. 1997).
- Concentration desalting of chondroitin sulfate obtained by enzymatic extraction from skate cartilage (Lignot et al. 2003).
- Removal of PEG molecules during purification of a recombinant protein from *Escherichia coli* (Strandberg et al. 1991).
- Removal of impurities and low molecular weight protease-related fragments during the purification of HIV-1 protease from *E. coli* inclusion bodies (Gustafson et al. 1995).
- Enhancing purity of zein during extraction of oil from corn (Cheryan 2010).
- Production of standardised bioactive products of desired concentration and activity during preparation of enzymes from crustaceans (Olsen et al. 1991).
- Purification and recovery of waste gelatin (Schmidt 1999).
- Concentration of zeamatin to remove ACN using a tangential flow filter (Wilson et al. 2000).
- Preparation of rapeseed protein isolate (Tzeng et al. 1988).
- Purification of recombinant α-glucuronidase from transgenic corn (Evangelista et al. 1998).
- Purification of capsular polysaccharide from *Streptococcus pneumoniae* (Gonçalves et al. 2003).
- Purification of gelatin by ultrafiltration with a forced solvent stream (Dutre and Tragardh 1995).
- Increasing methemoglobin level and oxygen affinity of purified bovine hemoglobin (Elmer et al. 2009).
- Purification of soluble fulvic acids carried out on Antarctic water and snow samples, characterised by low humic compound content (Calace et al. 1998).
- Purification of the blue-green pigment ‘marennine’ from *Haslea ostrearia*, a marine diatom (Pouvreau et al. 2006).
- Purification and size separation of gold nanoparticles (Sweeney et al. 2006).

9.1 Multiple stage diafiltration

In this method, diafiltration is applied in multiple stages for the extraction of steviol glycosides from Stevia extract. Centrifuged Stevia extract (using optimum conditions of extraction and centrifugation) was subjected to a 30 kDa ultrafiltration membrane in a cross-flow set-up of effective dimension 14.5 cm in length, 5.5 cm in width and 0.3 cm channel height. Permeate samples were collected from the bottom of the cell and analysed for colour, clarity, total solids and concentration of stevioside and rebaudioside A.

A fresh membrane was compacted at a pressure higher than the maximum operating pressure for 3 h using distilled water and then its permeability was measured. The extract was placed in a stainless steel feed tank of 3 L capacity. A high-pressure reciprocating pump was used to feed the effluent into the cross-flow membrane cell. Cumulative volumes of permeate were collected during the experiment. Permeate samples were collected at different time intervals for quantitative analysis. A bypass line was provided from the pump delivery to the feed tank, and retentate and bypass control valves were used to vary the pressure and flow rate accordingly. Values of permeate flux were determined from the slopes of cumulative volume versus time plots. The precision of flux measurement was in the order of ±5%. The permeate was not recycled back. The feed volume was 1.5 L and a maximum of four stages of ultrafiltration were performed. A volume reduction factor (VRF) was maintained at 1.5. The retentate was diluted with distilled water (to bring back the feed volume to 1.5 L) after each experiment, which formed the feed for the next stage. The experiments were conducted at flow rates of 50 and 100 L/h and at different transmembrane pressures (690 kPa and 414 kPa). All the runs were conducted at room temperature of 32 ± 2 °C.

Once an experimental run was over, the membrane was thoroughly washed, *in situ*, with distilled water for 30 min, applying a maximum pressure of 200 kPa. The cell was dismantled and the membrane was rinsed with distilled water and then dipped in 2% sodium dodecyl sulfate solution overnight. Next, the membrane was washed carefully with distilled water to remove traces of surfactant. The cell was reassembled and the membrane permeability was again measured using distilled water. After that, the set-up was ready for the next experiment with centrifuged Stevia extract.

The initial total solids concentration after hot water extraction was 3.2% w/w and after centrifugation it was 1.6 % w/w. The feed concentration of stevioside and rebaudioside to cross-flow ultrafiltration was 12,150 mg/L and 2680 mg/L, respectively. Three-stage diafiltration was performed at 690 kPa and 50 L/h. Figure 9.1(a) represents the variation of stevioside and rebaudioside concentration during ultrafiltration. It can be observed from this figure that the rebaudioside concentration in stage 1 reached a maximum in 3–5 h and decreased thereafter. In the subsequent stages, rebaudioside was present in trace amounts. Since the level of rebaudioside in the Stevia extract was small compared to stevioside, most of it was permeated in the first stage. Stevioside concentration decreased sharply after 2 h in the second stage without any appreciable change in permeate flux (see Figure 9.1(b)). In the third

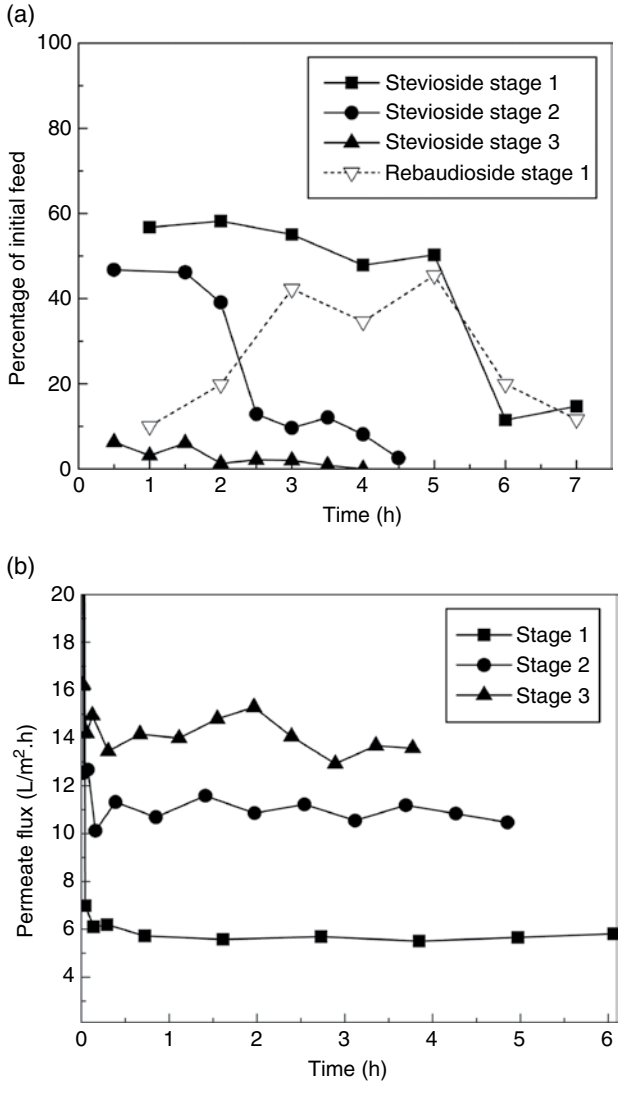

Figure 9.1 (a) Stevioside and rebaudioside profile. (b) Permeate flux variation with time of operation at 690 kPa and 50 L/h cross-flow rate.

stage, stevioside concentration was considerably less and insignificant after 2 h. The flux decline profile is presented in Figure 9.1(b).

As the filtration stage increased, the feed was diluted to maintain a constant feed volume, resulting in enhanced permeate flux. Since the feed was diluted after the first stage, the time required for the second and third stages was much less to obtain an equivalent quantity of permeate volume. It can be inferred from the figure that the permeate flux almost doubled from the first to the second stage of filtration. The average permeate flux was 2.5 times that of the first stage. Properties of the permeate at these conditions for various stages are presented in Table 9.1.

Table 9.1 Properties of permeate (colour, clarity and total solids) for the experimental conditions: TMP 690 kPa and cross-flow rate 50 L/h

Stage 1				Stage 2				Stage 3			
Time (h)	Colour (A)	Clarity (%T)	Total solids (% w/w)	Time (h)	Colour (A)	Clarity (%T)	Total solids (% w/w)	Time (h)	Colour (A)	Clarity (%T)	Total solids (% w/w)
1.0	0.44	89.1	0.75	0.5	0.62	74.8	0.36	0.5	0.33	87.0	0.03
2.0	0.44	90.2	0.76	1.5	0.21	93.3	0.28	1.0	0.35	87.0	0.03
3.0	0.50	86.5	0.77	2.0	0.24	85.5	0.40	1.5	0.29	90.0	0.01
4.0	0.34	92.5	0.77	2.5	0.76	56.9	0.22	2.0	0.36	87.5	0.03
5.0	0.66	66.4	0.82	3.0	0.54	82.0	0.15	2.5	0.36	86.5	0.04
6.0	0.46	72.4	0.65	3.5	0.63	71.1	0.09	3.0	0.26	92.3	0.03
7.0	0.39	71.6	0.73	4.0	0.88	60.2	0.10	3.5	0.32	87.9	0.01
				4.5	0.77	62.8	0.13	4.0	0.33	87.3	0.01
Centrifuged product (feed to 1st stage)									3.55	1.5	1.60

TMP, transmembrane pressure.

The total solids content in the permeate decreased sharply on increasing the stages of diafiltration. For example, the total solids content reduced to half of the feed in the first stage and it was marginal in the third stage. The colour and clarity data are presented in Table 9.1, indicating that as time progressed, the clarity decreased for the first and second stages, while colour was almost invariant at any particular stage. For the third stage, both colour and clarity were constant at 0.32 A and 88.0%, respectively. This is because the total solids in the permeate were also constant. Since the permeate was not recycled back to the feed, the feed became concentrated and hence the colour values increased and clarity decreased. Stevioside and rebaudioside A (and other glycosides) present in the solution are completely soluble and do not impart any change in colour or clarity. However, the presence of other insoluble (undesired) solids comprising cell debris, lignin, cellulose, starch, chlorophyll, etc., is responsible for colour and clarity. So the presence of stevioside and rebaudioside in a clear solution is ideally favoured. The cumulative recovery of stevioside was greater than 80% after stage 3, as shown in Figure 9.1(a).

Stevioside and rebaudioside concentration in the permeate during ultrafiltration at a lower transmembrane pressure (414 kPa) is illustrated in Figure 9.2(a). Comparing this figure with Figure 9.1(a), it can be seen that the total stevioside and rebaudioside recovery was more at lower pressure at a particular flow rate. However, rebaudioside recovery was maximal in first stage and was negligible in subsequent stages, similar to Figure 9.1(a). The cumulative stevioside recovery after three stages was around 92%. The permeate flux in the first stage was lower in the case of lower pressure (414 kPa) compared to 690 kPa (Figure 9.1(b)). However, in the second and third stages, the flux for both the operating pressures was comparable. This suggests that diafiltration should be carried out at lower transmembrane pressure drops, leading to less energy consumption.

Table 9.2 presents the property values of the permeate. It can be inferred from this table that the colour and clarity varied in a narrow range with time of filtration. On the other hand, colour decreased and clarity increased with stage of filtration. The total solids content also decreased with stage of filtration but remained almost constant with time of filtration, unlike the case of higher transmembrane pressure (690 kPa). In stage 3, the total solids content was lower at higher pressure. However, the colour and clarity were almost similar in this stage. This suggests the presence of more soluble components in the permeate at lower pressures, enriching the permeate with stevioside. This fact is supported by comparing the third stage curves in Figures 9.1(a) and 9.2(a). So it can be summarised that in diafiltration, cumulative stevioside recovery is effective at lower operating pressure and higher number of stages.

Two more experiments were performed at an operating flow rate of 100 L/h at 690 kPa and 414 kPa, respectively. The results from these experiments are shown in Tables 9.3 and 9.4 and in Figures 9.3 and 9.4. As seen before, the recovery of stevioside was greater for the lower transmembrane pressure drop of 414 kPa. However, there was no observable trend seen in increasing the flow rate with respect to stevioside recovery. The permeate flux at 100 L/h became almost twice

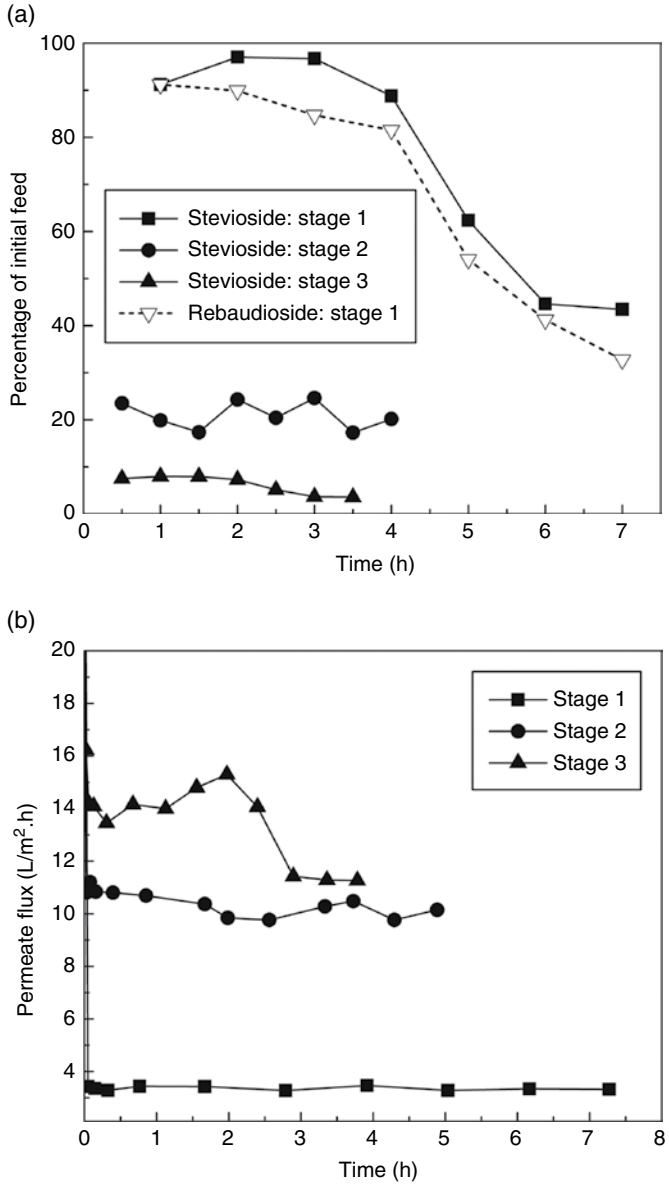

Figure 9.2 (a) Stevioside and rebaudioside profile. (b) Permeate flux variation with time of operation at 414 kPa and 50 L/h cross-flow rate.

as much as that obtained for a flow rate of 50 L/h. This is mainly due to the reduced effect of concentration polarisation as the gel deposition is lowered by enhanced forced convection at higher velocities of the circulating feed.

Analysing Tables 9.1 and 9.3, it can be observed that colour of the permeate was almost double in the first stage, operated at a higher flow rate. However, the total

Table 9.2 Properties of permeate (colour, clarity and total solids) for the experimental conditions: TMP 414 kPa and cross-flow rate 50 L/h

Stage 1				Stage 2				Stage 3			
Time (h)	Colour (a)	Clarity (%t)	Total solids (% w/w)	Time (h)	Colour (a)	Clarity (%t)	Total solids (% w/w)	Time (h)	Colour (a)	Clarity (%t)	Total solids (% w/w)
1.0	1.37	74.8	0.93	0.5	0.75	72.4	0.24	0.5	0.3	79.2	0.12
2.0	1.08	75.9	1.01	1.0	0.79	59.2	0.23	1.0	0.34	80.4	0.23
3.0	1.09	79.4	1.16	1.5	0.82	71.9	0.26	1.5	0.31	83.6	0.11
4.0	0.93	87.3	0.98	2.0	0.74	82.4	0.27	2.0	0.28	87.7	0.23
5.0	0.84	84.9	0.89	2.5	0.81	78.7	0.26	2.5	0.32	86.3	0.14
6.0	1.35	74.3	0.48	3.0	0.83	76.2	0.25	3.0	0.35	91.2	0.20
7.0	1.25	78.5	0.63	3.5	0.78	73.1	0.26	3.5	0.3	88.5	0.22
				4.0	0.72	77.6	0.28	4.0	0.38	90.8	0.11

TMP, transmembrane pressure.

Table 9.3 Properties of permeate (colour, clarity and total solids) for the experimental conditions: TMP 690 kPa and cross-flow rate 100 L/h

Stage 1				Stage 2				Stage 3			
Time (h)	Colour (a)	Clarity (%t)	Total solids (% w/w)	Time (h)	Colour (a)	Clarity (%t)	Total solids (% w/w)	Time (h)	Colour (a)	Clarity (%t)	Total solids (% w/w)
1.0	0.89	84.7	0.73	0.5	1.37	72.7	0.24	0.5	0.33	89.9	0.02
2.0	1.26	79.2	0.80	1.0	1.41	68.3	0.30	1.0	0.41	88.3	0.05
3.0	0.87	85.0	0.73	1.5	0.47	85.5	0.16	1.5	0.29	92.2	0.02
4.0	1.17	80.2	0.76	2.0	0.49	85.4	0.19	2.0	0.33	91.8	0.02
				2.5	0.51	82.0	0.24	2.5	0.32	91.4	0.03
				3.0	0.49	84.9	0.16				

TMP, transmembrane pressure.

Table 9.4 Properties of permeate (colour, clarity and total solids) for the experimental conditions: TMP 414 kPa and cross-flow rate 100 L/h

Stage 1				Stage 2				Stage 3			
Time (h)	Colour (a)	Clarity (%t)	Total solids (% w/w)	Time (h)	Colour (a)	Clarity (%t)	Total solids (% w/w)	Time (h)	Colour (a)	Clarity (%t)	Total solids (% w/w)
1.0	1.34	63.5	0.94	0.5	0.62	81.2	0.27	0.5	0.19	93.3	0.10
2.0	1.35	67.4	0.95	1.0	0.68	85.6	0.22	1.0	0.28	90.9	0.17
3.0	1.31	69.6	0.89	1.5	0.71	83.9	0.26	1.5	0.31	90.3	0.17
4.0	1.23	70.0	0.85	2.0	0.74	83.9	0.27	2.0	0.11	98.4	0.04
				2.5	0.57	88.1	0.21				
				3.0	0.49	87.6	0.20				

TMP, transmembrane pressure.

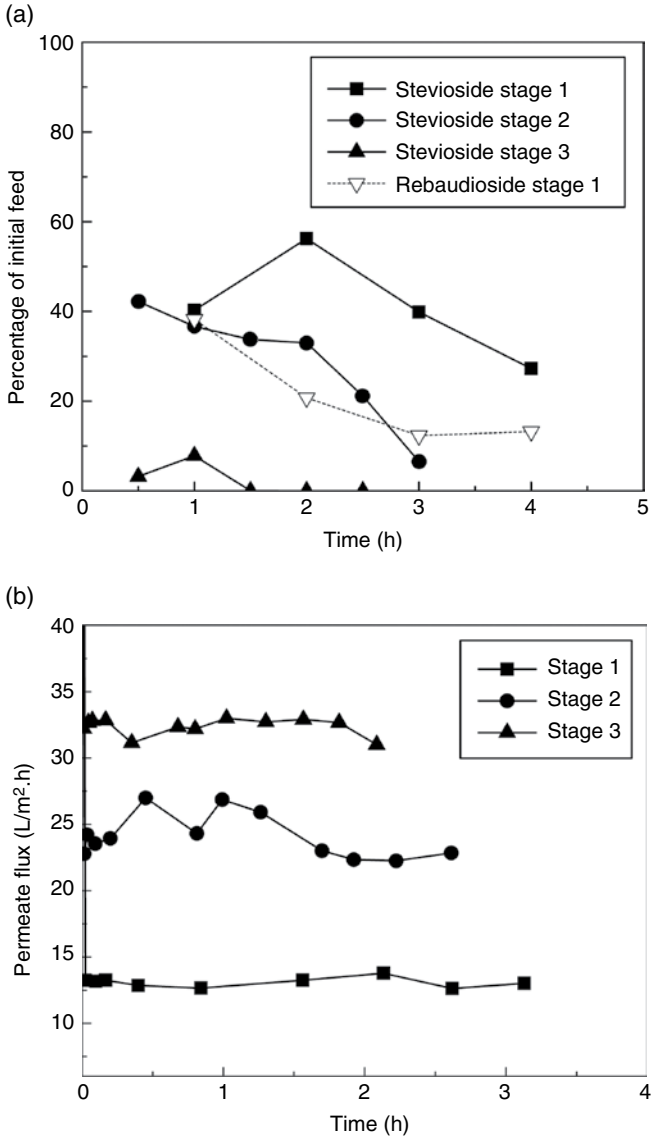

Figure 9.3 (a) Stevioside and rebaudioside profile. (b) Permeate flux variation with time of operation at 690 kPa and 100 L/h cross-flow rate.

solids content in all three stages for both set of experiments remained constant. The average colour and clarity in the second and third stages were similar with variation in cross-flow rate. Comparing Tables 9.2 and 9.4, the permeate clarity in stage 1 was higher for lower cross-flow rate but lower in the second stage. Permeate quality in stage 3 showed higher clarity and lower colour, corresponding to a 100 L/h cross-flow rate. Thus, the optimum permeate quality and overall process efficiency are

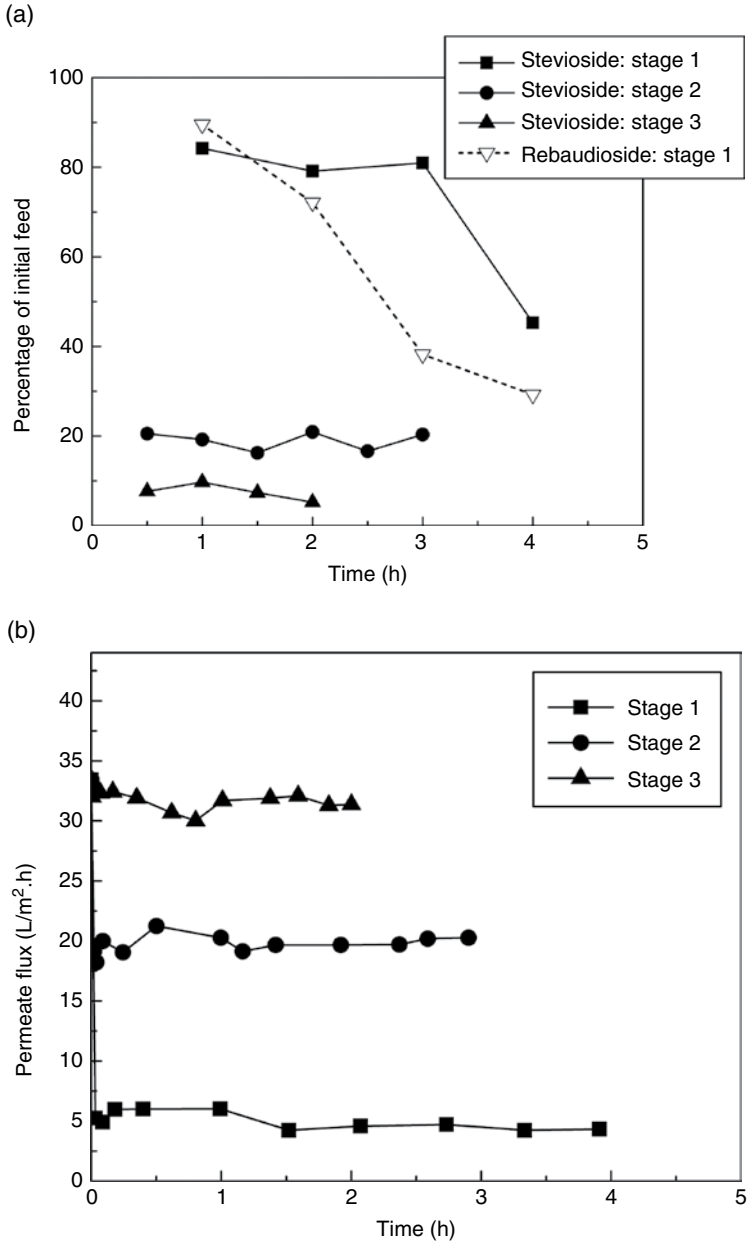

Figure 9.4 (a) Stevioside and rebaudioside profile. (b) Permeate flux variation with time of operation at 414 kPa and 100 L/h cross-flow rate.

obtained at lower transmembrane pressure drops and higher cross-flow rates. As far as purity of stevioside is concerned (purity is defined as the ratio of steviol glycosides to total solids content), maximum purity was attained in the second stage of diafiltration for all the operating conditions in the range of 90–98%.

References

Calace, N., de Paolis, F., Minniti, F., Petronio, B.M. (1998) Purification of soluble fulvic acid low concentrations by a diafiltration technique. Talanta 47, 803–809.

Cheryan, M. (2010) Method and system for extraction of oil from corn. US Patent 7767836.

Chhaya, C., Sharma, S., Mondal, S., Majumdar, G.C., De, S. (2012) Clarification of Stevia extract by ultrafiltration: selection criteria of the membrane and effects of operating conditions. Food Bioprod Proc 90, 525–532.

Cho, C.W., Lee, D.Y., Kim, C.W. (2003) Concentration and purification of soluble pectin from mandarin peels using crossflow microfiltration system. Carbohydr Polym 54, 21–26.

Dutre, B., Tragardh, G. (1995) Purification of gelatin by ultrafiltration with a forced solvent stream along the membrane permeate side: an experimental approach. J Food Eng 25, 233–244.

Elmer, J., Harris, D.R., Sun, G., Palmer, A.F. (2009) Purification of hemoglobin by tangential flow filtration with diafiltration. Biotechnol Progr 25, 1402–1410.

Evangelista, R.L., Kusnadi, A.R., Howard, J.A., Nikolov, Z.L. (1998) Process and economic evaluation of the extraction and purification of recombinant a-glucuronidase from transgenic corn. Biotechnol Progr 14, 607–614.

Fuh, W.S., Chiang, B.H. (1990) Purification of steviosides by membrane and ion exchange processes. J Food Sci 55, 1454–1457.

Gonçalves, V.M.M., Takagi, M., Lima, R.B., Massaldi, H., Giordano, R.C., Tanizaki, M.M. (2003) Purification of capsular polysaccharide from Streptococcus pneumoniae serotype 23F by a procedure suitable for scale-up. Biotechnol Appl Biochem 37, 283–287.

Gustafson, M.E., Junger, K.D., Foy, B.A., et al. (1995) Large-scale production of HIV-1 protease from Escherichia coli using selective extraction and membrane fractionation. Protein Expression Purif 6, 512–518.

Leung, A.Y., Foster, S. (1996) *Encyclopedia of Common Natural Ingredients Used in Food, Drugs and Cosmetics*. New York: John Wiley & Sons, Inc.

Li, S.Z., Li, X.Y., Cui, Z.F., Wang, D.Z. (2004) Application of ultrafiltration to improve the extraction of antibiotics. Sep Purif Technol 34, 115–123.

Lignot, B., Lahogue, V., Bourseau, P. (2003) Enzymatic extraction of chondroitin sulfate from skate cartilage and concentration-desalting by ultrafiltration. J. Biotechnol 103, 281–284.

Olsen, R.L., Stenberg, E., Sandsdalen, E., Almas, K.A. (1991) Method for preparing enzymes from crustaceans. US Patent 5061627.

Pouvreau, J.B., Morancais, M., Masse, G., et al. (2006) Purification of the blue-green pigment 'marennine' from the marine tychopelagic diatom Haslea ostrearia (Gaillon/Bory) Simonsen. J Appl Phycol 18, 769–781.

Reis, M.H.M., da Silva, F.V., Andrade, C.M.G., Rezende, S.L., Wolf Maciel, M.R., Bergamasco, R. (2009) Clarification and purification of aqueous Stevia extract using membrane separation process. J Food Process Eng 32, 338–354.

Rescigno, A., Sollai, F., Sanjust, E., Rinaldi, A.C., Curreli, N., Rinaldi, A. (1997) Diafiltration in the presence of ascorbate in the purification of mushroom tyrosinase. Phytochemistry 46, 21–22.

Schmidt, W. (1999) Method for the purification and recovery of waste gelatin using diafilters. US Patent 5945001.

Sen, D., Roy, A., Bhattacharya, A., Banerjee, D., Bhattacharjee, C. (2011) Development of a knowledge based hybrid neural network (KBHNN) for studying the effect of diafiltration during ultrafiltration of whey. Desalination 273, 168–178.

Sereewatthanawut, I., Lim, F.W., Bhole, Y.S., et al. (2010) Demonstration of molecular purification in polar aprotic solvents by organic solvent nanofiltration. Org Process Res Dev 14, 600–611.

Strandberg, L., Kiihler, K., Enfors, S.O. (1991) Large-scale fermentation and purification of a recombinant protein from Escherichia coli. Proc Biochem 26, 225–234.

Sweeney, S.F., Woehrle, G.H., Hutchison, J.E. (2006) Rapid purification and size separation of gold nanoparticles via diafiltration. J Am Chem Soc 128, 3190–3197.

Takaci, A., Žikic-Došenovic, T., Zavargó, Z. (2009) Mathematical model of variable volume diafiltration with time dependent water adding. Eng Comp 26, 857–867.

Tzeng, Y.M., Diosady, L.L., Rubin, L.J. (1988) Preparation of rapeseed protein isolate by sodium hexametaphosphate extraction, ultrafiltration, diafiltration, and ion-exchange. J Food Sci 53, 1537–1541.

Wilson, S., Mahiou, B., Reiger, R., et al. (2000) Pilot-scale purification of zeamatin, an antifungal protein from maize. Biotechnol Progr 16, 38–43.

Zhang, S.Q., Ashwani, K., Kutowy, O. (2000) Membrane-based separation scheme for processing sweeteners from Stevia leaves. Food Res Int 33, 617–620.

10
Economics of the process

The processing of stevioside (or steviol glycosides) has been limited so far due to the economy of the overall process. It must be realised that to gain significant popularity in application, the price of stevioside in terms of relative sweetening effect must be equivalent to or less than that of sucrose. The energy requirement at various stages of the extraction, clarification and purification is different and has an impact on the cumulative cost of production, starting from dried leaves and ending with pure Stevia powder or granules. As described in preceding chapters, the steps involved are hot water extraction, centrifugation, cross-flow ultrafiltration and diafiltration followed by evaporation and drying to obtain the final powdered product. For commercial scale-up, initial investment and operating costs must be taken into consideration, so that the final product is competitive and attractive to consumers.

The energy associated with hot water extraction depends on the energy required by the water bath to maintain a constant temperature. The energy lost from the open water surface to the atmosphere, together with loss from the insulation, both radiative and convective, for the period of heating (56 min) accounts for the heat input to the extraction process. The heat required to raise the temperature of the bath from the ambient to the specified temperature (78 °C) can be considered as negligible compared to that required to maintain the specific temperature in a large-capacity water bath. The heat loss depends on the surrounding air temperature and air velocity. Nevertheless, heat loss is directly proportional to the open surface area exposed to the atmosphere, which depends on the capacity of the water bath. The energy required to process 1 m^3 of Stevia extract at different atmospheric conditions and with water baths of different capacity is presented in Table 10.1. It has been considered that air velocity does not exceed more than 10–15 cm/s as these processes are conducted in a closed environment. The energy requirement corresponding to different air temperatures provides an insight into extraction in different geographical locations: energy requirement increases when one operates in a cold environment. The available surface area increases with bath volume, which relates to increased heat loss to the atmosphere, but the energy required to process unit m^3 of Stevia extract decreases as the capacity of the bath increases.

Stevioside: Technology, Applications and Health, First Edition.
Sirshendu De, Sourav Mondal and Suvrajit Banerjee.

Table 10.1 Summary of the total energy required for hot water extraction (air velocity in the range 0–15 cm/s)

Bath capacity (L)	Area exposed to atmosphere (m^2)	Air temperature (°C)			
		4–5	15–16	25–27	36–37
10–12	0.093	61–62	57–58	52–53	43–45
24–25	0.147	37–38	34–35	31–32	26–27
45–50	0.132	18–19	17–18	16–17	13–14
90–100	0.200	13–14	12–13	11–12	9–10

Table 10.2 Energy required in the centrifugation process

Batch volume per cycle (L)	Mean radius (cm)	Power required per batch (W)	Energy (kWh/m^3)
0.2	5.5	0.2	1.8
0.4	8.7	0.8	4.5
2.0	10.5	5.6	6.5
Continuous at 10 L/h	7.8	6.7	0.7
Continuous at 25 L/h	7.8	16.7	0.7

The next step in the clarification process is centrifugation. The optimum operating conditions are 5334 g (8535 rpm) for 26 min. However, centrifugation capacity depends on the batch volume per cycle. The energy required to process unit m^3 varies with the centrifugation capacity. In continuous centrifugation, the flow rate should be adjusted so that the residence time is 26 min. Table 10.2 describes the energy requirement of the process, which increases with the batch volume. In continuous centrifugation, the energy required to process unit m^3 of feed is constant. However, the initial expense of setting up a continuous basket centrifuge is much more than that of a batch centrifuge.

The continuous cross-flow ultrafiltration in total recycle mode can be used for extraction of stevioside from the centrifuged extract. It has already been identified that when operating at a transmembrane pressure drop of 414 kPa and flow rate of 100 L/h, the yield of stevioside is maximal with a reasonable throughput of the process. Table 10.3 represents the energy needed to produce unit m^3 of ultrafiltered permeate. The operating cost significantly decreases as the surface area of the membrane increases. A high surface area module is typically achieved in spiral wound systems. The energy consumed in the process can be expressed as:

$$E_p = \frac{Q.\Delta \mathrm{P}}{v_w \mathrm{A} \eta_{pump}} \tag{10.1}$$

where Q is the cross-flow rate equal to 100 L/h (27.76×10^{-6} m^3/s), η_{pump} is the efficiency of the pump (consider it to be 70%), v_w is the average permeate flux

Table 10.3 Energy requirement to produce unit m^3 of permeate with different membrane surface areas

Effective membrane area (m^2)	Axial pressure drop ΔP (kPa)	Energy (kWh/m^3 of feed)	Energy (kWh/m^3 of permeate)
0.01	0.6	0.35	492.8
0.05	3.5	0.31	69.2
0.1	5.9	0.26	28.9
0.2	11.0	0.24	13.5
0.5	22.1	0.20	4.3
1.0	27.6	0.12	1.4
5.0	110.4	0.10	1.1
10.0	176.6	0.08	0.9

Table 10.4 Energy per unit m^3 of product for different diafiltration stages with varying areas of filtration

Area	Stage 1	Stage 2	Stage 3
0.008	743.6	856.2	925.8
0.05	654.4	753.5	814.7
0.1	545.3	627.9	679.0
0.2	511.2	588.7	636.5
0.5	409.0	470.9	509.2
1.0	255.6	294.3	318.3
5.0	204.4	235.4	254.5
10.0	163.5	188.3	203.6
Purity (%)	80–90	95–97	70–75
Concentration (kg/m^3)	8.5	2.4	0.73

(in terms of $m^3/m^2/s$), A is the effective membrane area (m^2) and ΔP is the axial pressure drop across the membrane module (Pa). The latter is estimated using the Hagen–Poiseuille equation:

$$\Delta P = \frac{128 \mu L Q}{\pi d_e^4} \tag{10.2}$$

where L is the length of the module section (m), μ is the viscosity of the fluid (Pa.s) and d_e is the hydraulic diameter of the flow cross-section (= $2h$, where h is the channel half-height). The typical magnitude of channel half-height is 1–2 mm. Variations in the energy required for the cross-flow process with with different membrane surface areas are described in Table 10.4. The energy consumption rate decreases with increase in the effective membrane area.

The purity and yield of stevioside can be further enhanced by constant volume diafiltration. Diafiltration is carried out with transmembrane drop (ΔP) at 414 kPa and a flow rate of 100 L/h with a volume concentration factor of 1.5. As described in the

Table 10.5 Energy requirement (kWh/m^3) of evaporation using multi-effect evaporators with backward feed

Final TDS (%)	Steam economy	$n=1.5$	$n=1.75$	$n=2.0$	$n=3.0$	$n=5$	$n=8$
5	Stage 2	414.7	355.5	311	207.3	124.4	77.8
	Stage 1	484.5	415.3	362.4	241.6	145.0	90.6
25		506.2	433.9	379.6	253.1	151.8	94.9
35		507.8	435.2	380.8	253.9	152.3	95.2
50		508.8	436.1	381.6	254.4	152.6	95.4
75		509.6	436.8	382.2	254.8	152.9	95.6

TDS, total dissolved solids.

previous chapter, the average permeate flux is 0.8×10^{-6} m^3/m^2/s for stage 1, 5.5×10^{-6} m^3/m^2/s for stage 2 and 9.0×10^{-6} m^3/m^2/s for stage 3. As observed from Table 10.4, the energy requirement decreases with the effective membrane area. The total energy requirement for the second and third stages increases, as the cost of processing in the previous stages is added. The purity of the permeate is maximised at the second stage.

Concentration of the processed ultrafiltered extract can be performed by using a multiple effect evaporator. The mode of evaporator operation is backward feeding to increase the efficiency of the process. This should be operated in a vacuum, with pressure in the feed side not exceeding 40 kPa. This is necessary so that the evaporation temperature will not exceed 70 °C. Although stevioside is thermally stable upto 110 °C, and does not degrade with heat, it is not recommended to concentrate food products at higher temperatures. The steam economy of the process can be substantially increased if the vapour generated during concentration of the liquor can be recycled. The steam used in the tube side flow is saturated at 150 psig.

Considering the optimum fuel to energy combustion efficiency, the energy required to produce saturated steam is 0.767 kWh/kg of steam. The ultrafiltered liquor has a total dissolved solids content of 0.9% and 0.25% for the first and second stages, respectively. The energy requirement of evaporators with varying steam economy is presented in Table 10.5. Typically, the steam economy is $0.8\times$*number of effects* (Dutta 2004). The energy required for evaporation reduces drastically if a greater number of effects is used. However, beyond 10% of the final total dissolved solids (TDS) content, the increase in evaporator energy is marginal for further concentrating the liquor. The feed to the evaporator is the stage 1 or stage 2 permeate of diafiltration, operated at 414 kPa and 100 L/h. Since the average total solids content in the permeate of both the stages is small (<1%), the energy required for evaporation to attain the specified level of TDS (greater than 10%) is similar. However, with lower TDS content after evaporation, the energy required is different for different initial TDS levels. The values in the first row of Table 10.5 show the energy required to achieve a 5% final TDS level, for both the first- and second-stage permeate of diafiltration.

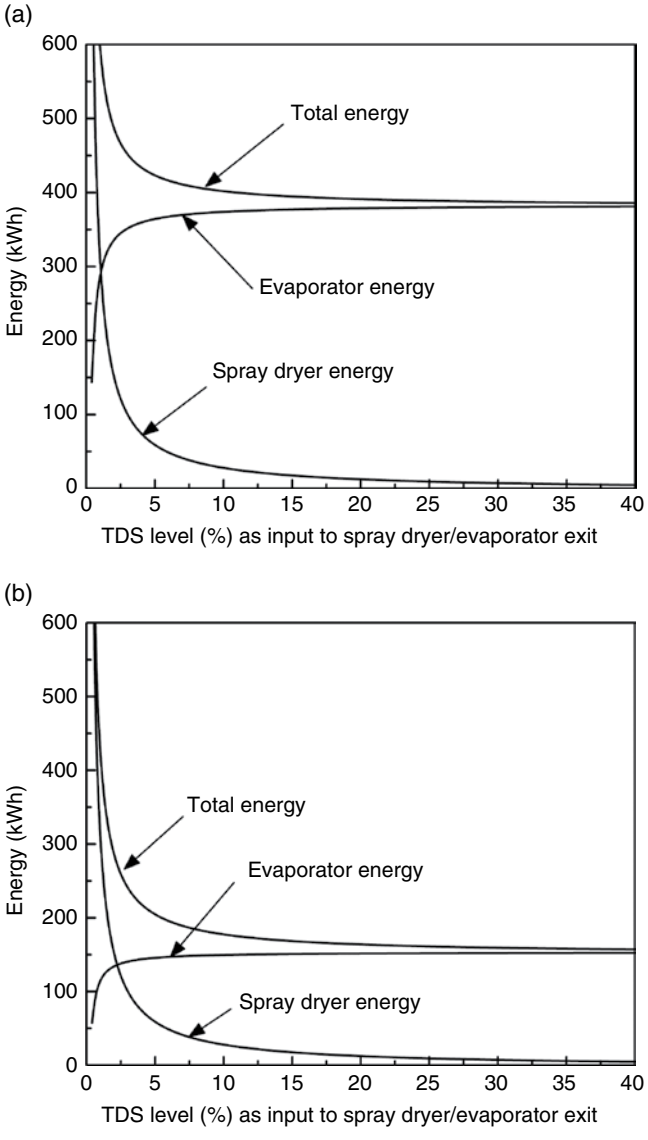

Figure 10.1 Total energy requirement in the process of final drying of the stevioside-enriched permeate. Evaporator steam economy, for (a) $n=2$ and (b) $n=5$.

The final stage of stevioside powder production involves drying the concentrated liquor, typically using a spray dryer. The energy requirement of a spray dryer typically follows the equation (Baker and McKenzie 2005):

$$\text{Energy}\left(\text{MJ/h}\right) = 4.47 \times \text{evaporation rate}\left(\text{kg/h}\right) \tag{10.3}$$

Table 10.6 Operating cost estimation of stevioside processing

Steps of processing	Energy requirement (kWh)	Cost in $ (0.1 USD/kWh)
Hot water extraction at 100 L bath capacity, air temp. 25–27 °C	17.0	2.0
Centrifugation at 400 mL/batch	6.0	0.6
Diafiltration at TMP 414 kPa, cross-flow rate 100 L/h, VCF 1.5, 2nd stage permeate, membrane area 1 m^2	118.0 (75.0 for 10 m^2 membrane area)	12.0 (7.5 for 10 m^2 membrane area)
60.0	59.8	6.0
Spray drying Feed TDS level 10%	11.0	1.0
Total (per kg of stevioside produced)	211.6 (169.0 for 10 m^2 membrane area)	21.0 (17.0 for 10 m^2 membrane area)

TDS, total dissolved solids; TMP, transmembrane pressure; VCF, volume concentration factor.

The efficiency of the spray dryer is maximised when the solid content in the feed is around 20–25%. However, the diafiltration permeate typically contains 0.25% TDS (stage 2 permeate, 414 kPa and 100 L/h). Thus, achieving a minimum 20% TDS level by evaporation for feeding to the spray dryer leads to much higher evaporator costs. Figure 10.1 shows the relative energy required for evaporation and spray drying for different TDS levels of concentration by evaporation. It is recommended that the final TDS level of concentration by evaporator should be 8–10%, so that the evaporator load is reduced significantly, as the solution viscosity is not high enough and the effect of boiling point elevation due to concentrated liquor is minimised. As expected, the total energy required in the combined process of evaporation followed by spray drying is dominated by evaporator energy and it decreases with increasing number of effects (or steam economy).

Considering the overall energy requirement in processing Stevia leaf extract to achieve pure stevioside powder, the total cost is related to energy consumption in each of the individual processes. Excluding all investment costs for setting up the equipment, the total energy required to produce a unit kilogram of 95% stevioside powder, at the optimum operating conditions, can be calculated as shown in Table 10.6.

References

Baker, C.G.J., McKenzie, K.A. (2005) Energy consumption of industrial spray dryers. Dry Technol 23, 365–386.

Dutta, B.K. (2004) *Heat Transfer: Principles and Applications*. New Delhi: Prentice-Hall.

Index

Note: Page numbers in *italics* refer to Figures; those in **bold** to Tables.

Stevioside: Technology, Applications and Health, First Edition.
Sirshendu De, Sourav Mondal and Suvrajit Banerjee.

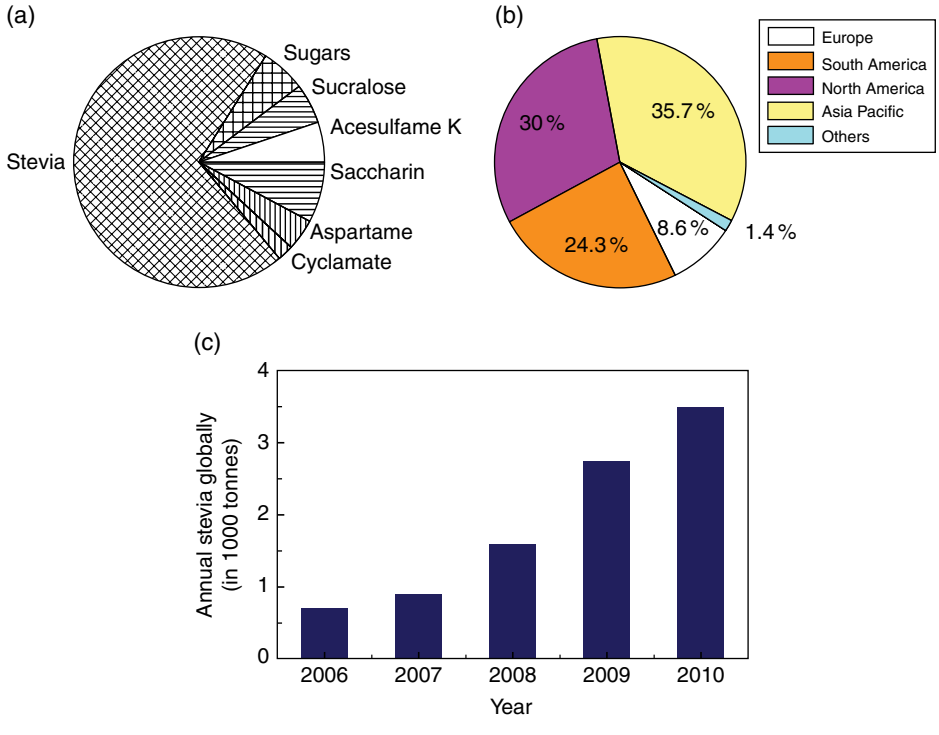

Plate 1.1 Market potential of Stevia and related products in the world. (a) Percentage compound annual growth rate (CAGR) of different sweeteners in the projected years 2011–15. (b) Global Stevia market in different regions of the world in 2010. (c) Annual global Stevia production in the last 5 years.

Stevioside: Technology, Applications and Health, First Edition.
Sirshendu De, Sourav Mondal and Suvrajit Banerjee.

Plate 1.2 *Stevia rebaudiana* Bertoni plant.

Plate 7.1 Stirred batch cell set-up.